



Stress Signalling and Fungal Pathogenesis in

***Candida* Species**

Iaroslava Kos

Thesis submitted in accordance with the regulations of Newcastle
University for the degree of Doctor of Philosophy

Faculty of Medical Sciences
Institute for Cell and Molecular Biosciences
Newcastle University

October 2016

Declaration

I certify that this thesis contains my own work, except where acknowledged, and that no part of this material has been previously submitted for a degree or any other qualification at this or any other university.

Some of the work in this thesis has been presented in the following publications:

Iaroslava Kos , Miranda Patterson , Sadri Znaidi , Despoina Kaloriti , Alessandra da Silva Dantas , Carmen Herrero-de-Dios , Christophe d'Enfert , Alistair J.P. Brown. Mechanisms underlying the delayed activation of the Cap1 transcription factor in *Candida albicans* following combinatorial oxidative and cationic stress important for phagocytic potency. *MBio*. 2016 Mar 29;7(2):e00331. doi: 10.1128/mBio.00331-16.

Dantas A*, Day A*, Ikeh M*, Kos I*, Achan B*, Quinn J. Oxidative stress responses in the human fungal pathogen, *Candida albicans*. *Biomolecules*. 25; 5(1):142-65. doi: 10.3390/biom5010142. * These authors made equal contributions.

Acknowledgements

First of all, I would like to thank my supervisor, Professor Jan Quinn, who believed in me from the first time we met far away in San Francisco, who made me a life-changing offer to join her research team, and who was my best advisor and friend thereafter. Thank you for sharing with me all the wealth of your knowledge, for the massive support and simultaneously for letting me make independent decisions, thank you for teaching me not only the excellent science, but also valuable life skills, such as critical thinking, effective time management, prioritising and hard working. You told once “There is no shortcut to success, and your success critically depends on how hard you work”, and many-many times I witnessed how true these words are. I’m also very thankful to my co-supervisor Liz Veal for her wise feedbacks and insightful discussions. Jan and Liz, they were the most demanding panel to convince, but I always knew that my ideas are truly worth expanding if they can withstand their criticism. Thank you for that! I am also very thankful to my review panel members – Professor Brian Morgan and Professor David Lydall, your thoughtful comments, great advice and support helped me a lot in making the right priorities during my PhD.

I am thankful to all members of Yeast group, especially to Dr. Simon Whitehall, Dr. Jeremy Brown and Dr. Julian Rutherford for their help and advice, Dr. Alessandra Dantas, Dr. Deborah Smith, Dr. Melanie Ikeh, Dr. Alison Day and Dr. Jonathon Brown for their massive support. I thank to all lovely fellows from the PhD cohort, past and present – Alex, Johnny, Faye M., Faye C., Zoe, Clare, Heather, Emma, Csenge, Ellen and Lewis. I am also thankful to Dr David McDonald and Andrew Fuller from Medical School Flow Cytometry Core Facility Laboratory for sharing their mastership in FACS analysis. Huge thanks to all our collaborators from the Aberdeen Fungal Group, University of Exeter and Institute Pasteur, especially to Prof. Al Brown, Prof. Christophe d’Enfert and Dr. Sadri Znaidi for all your kind help, thoughtful advice and help to promote an excellence in scientific research of human fungal pathogens.

I thank to my funding bodies – BRC and NIHR – for allowing me to conduct a research in such an excellent scientific environment at Newcastle Medical School. There are far too many wonderful people to mention to whom I experience a deep gratitude, and this work would have never been completed without your intentional or unintentional help.

Special thanks to my dear husband Roman for being such a supportive partner and friend, for your compassion, support and love that made me believe in myself when life was hard. To my daughter Katerina for being so good and understanding child, and to my newborn son Marco for doing his nights and letting me finish my thesis writing. Kids, you are my major source of energy and inspiration.

Finally, massive thanks goes to my parents, Andriy and Viola Kos, who always believed in myself, even when I didn't; for their continuous love and support, for all the sacrifices they made to nurture the best version of me. This thesis is dedicated to you.

Abstract

Candida albicans and *Candida glabrata* are major pathogens of humans, causing 8% of all hospital acquired systemic infections worldwide. Moreover, such systemic infections are associated with alarmingly high morbidity and mortality rates. One of the major immune defence mechanisms mounted by the host against fungal infections involves phagocytosis by innate immune cells. Phagocytic immune cells employ a suite of antimicrobial mechanisms in order to kill invading pathogens, such as the generation of reactive oxygen species (ROS), cationic fluxes, nutrient deprivation, extremes of pH, and the release of antimicrobial peptides. Being successful pathogens, *C. albicans* and *C. glabrata* have acquired multiple defence strategies to allow survival in the host, and *in vitro* demonstrate high levels of resistance to many of the stresses likely to be encountered following phagocytosis. However, these fungi can only cause systemic infections when host immune responses are compromised. A major question, therefore, is what underlies the potency of innate immune defences in healthy individuals to prevent fungal infections? I address this question in this thesis, and investigate the interplay between fungal stress responses and immune defences of the host.

Recent studies have indicated that it is exposure to combinations of stresses encountered following phagocytosis that effectively kills *C. albicans*. Specifically, the combination of oxidative and cationic stresses leads to a dramatic increase in intracellular ROS levels, which kills this fungus much more effectively than the corresponding single stresses *in vitro*. In this work I show that combinatorial oxidative and cationic stresses, or high concentrations of ROS, delay the activation of the oxidative stress-responsive Cap1 transcription factor in *C. albicans*. Cap1 is oxidised in response to H₂O₂, which masks the nuclear export sequence from the Crm1 nuclear export factor. This allows for the nuclear accumulation of the transcriptional factor and induction of Cap1-dependent antioxidant genes. In this work I demonstrate that combinatorial stress, or high ROS levels, trigger the generation of a transcriptionally inactive, partially oxidised, Cap1^{OX-1} form. However, whilst Cap1^{OX-1} readily accumulates in the nucleus and binds to target genes following high H₂O₂ stress, the nuclear accumulation of Cap1^{OX-1} following combinatorial H₂O₂ and NaCl stress is delayed due to a cationic stress-enhanced interaction with the Crm1 nuclear

export factor. These findings define novel mechanisms that delay activation of the Cap1 transcription factor, thus preventing the rapid activation of stress responses vital for the survival of *C. albicans* within the host, and which probably underlines the potency of the innate immune cells in immunocompetent hosts.

C. glabrata is more resistant to ROS than *C. albicans*, and recent work from the Haynes laboratory has identified four ORFs (designated *CRI-1-4*) which contribute to this enhanced ROS resistance. Orthologues of *CRI1-4* are seemingly not present in other fungal species, and their expression can confer oxidative and combinatorial stress resistance in the model yeast *Saccharomyces cerevisiae*. In this work I show that the antioxidant properties of *CRI* genes are not due to their role in reducing intracellular ROS levels in *C. glabrata* and that, in contrast to *S. cerevisiae*, ectopic expression in *C. albicans* has no impact on stress resistance. This suggests that the mechanism behind the *CRI1-4* stress protection is restricted to *C. glabrata* and closely related fungi.

To further explore the relationship between fungal stress resistance and virulence, the *Caenorhabditis elegans* infection model was employed. Previous unpublished work from J. Quinn laboratory revealed that key fungal stress regulators were only needed for *C. albicans* virulence in immunocompetent but not immunocompromised worms. This fits with the concept that survival of the pathogen against robust immune responses requires activation of key signalling pathways. *C. elegans* is also a well-established model used to study the process of aging. Here I use the *C. elegans* model of infection to study age-dependent increases in susceptibility to *C. albicans*-mediated killing. Significantly, as seen with immunocompromised worms, robust stress responses are only needed for *C. albicans* to cause infection in young but not old animals. These results indicate that age-dependent susceptibility to fungal infections is related to the immune status of the host, and that *C. albicans* stress responses are only important for virulence in young, immunocompetent animals.

Taken together, the findings presented in this thesis provide insight into the mechanisms underlying the differential ability of *C. albicans* and *C. glabrata* to survive combinations of stresses encountered following phagocytosis, and that age-

dependent effect on host immune function may determine the importance of stress responses in mediating the virulence of *C. albicans*.

Abbreviations

AIDS	Acquired Immune Deficiency Syndrome
Amp	Ampicillin
AMS	4-acetamido-4 ((iodoacetyl)amino)stilbene-2,2-disulfonic acid
AP-1	Activating protein 1
APCs	Antigen presenting cells
ARE	Antioxidant responsive element
Arg	Arginine
<i>A. fumigatus</i>	<i>Aspergillus fumigatus</i>
BCA	Bicinchoninic acid
Bp(s)	Base pair(s)
BPB	Bromophenol blue (3',3",5',5"-Tetrabromophenolsulfonphthalein)
BSA	Bovine serum albumin
BSI	Bloodstream infection
bZip	Basic leucine zipper
C	Carbon
C•	Carbonyl radical
CaCl ₂	Calcium chloride
<i>C. albicans</i>	<i>Candida albicans</i>
cAMP	Cyclic adenosine monophosphate
CDC	Centres for Disease Control and Prevention
CdSO ₄	Cadmium sulphate
CGC	<i>Caenorhabditis</i> Genetics Center
CGD ¹	<i>Candida</i> Genome Database
CGD ²	Chronic granulomatous disease
<i>C. glabrata</i>	<i>Candida glabrata</i>
CIP	Calf intestinal alkaline phosphatase
Cl ⁻	Chloride ion
cm	Centimetre

<i>C. neoformans</i>	<i>Cryptococcus neoformans</i>
CO ₂	Carbon dioxide
<i>C. parapsilosis</i>	<i>Candida parapsilosis</i>
cps	counts per second
CRD	Cysteine rich domain
CRE	cAMP-responsive element
DAPI	4'-6-diamidino-2-phenylindole
DAR	Deformed anal region
dATP	Deoxyadenosine triphosphate
DC	Dendritic cell
dCTP	Deoxycytidine triphosphate
DEM	Diethyl maleate
DEPC	Diethylpyrocarbonate
dGTP	Deoxyguanosine triphosphate
DIC	Differential interference contrast
<i>D. melanogaster</i>	<i>Drosophila melanogaster</i>
DMSO	Dimethyl sulphoxide
DNA	Deoxyribonucleic acid
dNTP	Deoxyribonucleotide triphosphate
dsDNA	Double-stranded DNA
DTT	Dithiothreitol
dTTP	Deoxythymidine triphosphate
<i>E.coli</i>	<i>Escherichia coli</i>
EDTA	Ethylenediaminetetraacetic acid
EGTA	Ethylene glycol tetraacetic acid
FACS	Fluorescence-activated cell sorting
g	Gram
GI	Gastrointestinal
GM-CSF	Granulocyte-Macrophage Colony-Stimulating Factor
Gpx	Glutathione peroxidase

GSH	Glutathione
HEPES	4-(2-hydroxyethyl)-1-piperazineethanesulfonic acid
HIV	Human Immunodeficiency Virus
H_2O	Water
H_2O_2	Hydrogen peroxide
HOCl	Hypochlorous Acid
HRP	Horseradish Peroxidase
Hz	Hertz
IC	Invasive candidiasis
ICUs	Intensive care units
IFNy	Interferon gamma
IL	Interleukin
iNOS	Inducible nitric oxide synthase
IP	Immunoprecipitation
K^+	Potassium cation
Kb	Kilobase
KCl	Potassium chloride
kDa	Kilodalton
KH_2PO_4	Monopotassium phosphate
KOH	Potassium hydroxide
L	Litre
LAD1	Leukocyte adhesion deficiency type 1
LB	Luria-Bertani broth
LiAc	Lithium acetate
m	Mass
M	Molar
MAPK	Mitogen-activated protein kinase
MAPKK	Mitogen-activated protein kinase kinase
MAPKKK	Mitogen-activated protein kinase kinase kinase
M-CSF	Macrophage-colony stimulating factor

MDMs	Monocyte-Derived Macrophages
Mg	Milligram
MgCl ₂	Magnesium chloride
MgSO ₄	Magnesium sulphate
Min(s)	Minute(s)
ML	Millilitre
Mm	Millimetre
Mmol	Millimol
mPEG-Mal	Methoxy PEG maleimide
MPO	Myeloperoxidase
mRNA	Messenger RNA
MW	Molecular Weight
Mφ	Macrophage
N	Nitrogen
Na ⁺	Sodium cation
NaCl	Sodium chloride
NADP ⁺	Nicotinamide adenine dinucleotide phosphate
NADPH	Reduced form of NADP ⁺
NaF	Sodium fluoride
NaH ₂ PO ₄	Monosodium phosphate
Na ₂ HPO ₄	Disodium phosphate
Na ₃ VO ₄	Sodium orthovanadate
NEM	N-Ethylmaleimide
NES	Nuclear Export Signal
Ng	Nanogram
NK	Natural killer
NLS	Nuclear Localisation Sequence
Nm	Nanometre
NO	Nitric Oxide
NO ₂ ⁻	Nitrite Anion

NO_3^-	Nitrate Anion
NORE	Nitric Oxide Responsive Element
NPC	Nuclear pore complex
O_2^-	Superoxide anion
OC	Oral candidiasis
OD	Optical density
OH^-	Hydroxyl Anion
$\cdot\text{OH}$	Hydroxyl Radical
ONOO^-	Peroxynitrite
OPC	Oropharyngeal candidiasis
ORF	Open reading frame
OSR	Oxidative stress response
^{32}P	Phosphorus-32
<i>P. aeruginosa</i>	<i>Pseudomonas aeruginosa</i>
PAMPs	Pathogen-associated molecular patterns
PBS	Phosphate-buffered saline
PCR	Polymerase chain reaction
PEG	Polyethylene glycol
pg	Picogram
PIPES	Piperazine-N,N'-bis(2-ethanesulfonic acid)
PKA	Protein kinase A
PMNs	Polymorphonuclear neutrophils
PMSF	Phenylmethylsulfonyl fluoride
PRRs	Pattern recognition receptors
PUFAs	Polyunsaturated fatty acids
qPCR	Quantitative PCR
RE	Restriction endonuclease
RES	Reactive electrophilic species
RNA	Ribonucleic acid
RNA Pol II	RNA Polymerase II

RNase	Ribonuclease
RNS	Reactive nitrogen species
ROS	Reactive oxygen species
RPM	Revolutions per minute
SAP(s)	Secreted aspartyl protease(s)
SAPK	Stress-activated protein kinase
<i>S. aureus</i>	<i>Staphylococcus aureus</i>
<i>S. cerevisiae</i>	<i>Saccharomyces cerevisiae</i>
SDS	Sodium dodecyl sulphate
SDS-PAGE	SDS-polyacrylamide gel electrophoresis
Sec	Second
Ser	Serine
SNPs	Single nucleotide polymorphisms
SOD	Superoxide dismutase
<i>S. pombe</i>	<i>Schizosaccharomyces pombe</i>
SSPE buffer	Saline-Sodium Phosphate-EDTA Hybridization Buffer
STRE	Stress response element
<i>t</i> -BOOH	Tert-butyl hydroperoxide
TCA	Trichloroacetic acid
TEMED	<i>N,N,N',N'</i> -tetramethylethylenediamine
Th	T helper cell
Thr	Threonine
TLRs	Toll-like receptors
TNF α	Tumor necrosis factor alpha
Tpx	Thiol peroxidase
Trr	Thioredoxin reductase
Trx	Thioredoxin
TSA	Thichostatin
Txl	Thioredoxin-like protein
Ura	Uracil

uri	Uridine
UV	Ultraviolet
V	Volume
V	Volt
V-ATPase	Vacuolar-type ATPase
VVC	Vulvovaginal candidiasis
YPD	Yeast extract peptone dextrose
YRE	Yeast responsive element
°C	Degrees Celsius
Δ	Gene deletion
µl	Microliter
µM	Micromoles
8-oxoG	7,8-dihydro-8-oxo-2'-deoxyguanosine

Table of Contents

Chapter 1. Introduction	1
1.1 <i>Candida</i> species as major pathogens of humans	1
1.2 Impaired immune defences result in increased susceptibility to <i>C. albicans</i> infection.....	4
1.2.1 Immunocompromised increases	4
1.2.2 Age-associated increases	6
1.3 Host immune defences against <i>Candida</i> species	7
1.3.1 Innate immune defences as a first line of combatting fungal infection ...	8
1.3.2 Immune recognition.....	10
1.3.3 Phagocytosis.....	11
1.3.4 Stresses encountered during phagocytosis.....	12
1.3.4.1 Nutrient deprivation	12
1.3.4.2 Acidification	14
1.3.4.3 Cationic fluxes	14
1.3.4.4 ROS and RNS	15
1.3.4.4.1 Cellular effects of ROS	17
1.3.4.5 Degranulation	19
1.4 <i>Candida</i> spp. virulence determinants that allow survival in the host	19
1.4.1 <i>Candida albicans</i> virulence determinants that allow survival following phagocytosis.....	20
1.4.1.1 Morphological switch	21
1.4.1.2 Metabolic flexibility.....	22
1.4.1.3 Stress responses.....	24
1.4.1.3.1 pH adaptation	24
1.4.1.3.2 Cationic stress response.....	25
1.4.1.3.3 Nitrosative stress response.....	29
1.4.1.3.4 Oxidative stress response.....	29
1.4.2 <i>Candida glabrata</i> virulence determinants	30
1.5 Oxidative stress responses	32
1.5.1 ROS detoxification systems employed by <i>C. albicans</i>	32

1.5.1.1	Non-enzymatic detoxification of reactive oxygen species	33
1.5.1.2	Enzyme-mediated detoxification of reactive oxygen species	34
1.5.1.2.1	Superoxide dismutases	34
1.5.1.2.2	Peroxidases	35
1.5.2	Oxidative stress-responsive signalling pathways in <i>C. albicans</i>	37
1.5.2.1	The Stress Activated Protein Kinase Hog1	37
1.5.2.2	The Rad53 DNA damage checkpoint kinase	39
1.5.2.3	Fungal AP-1 like transcription factors	40
1.5.2.3.1	<i>S. cerevisiae</i> Yap1	40
1.5.2.3.2	<i>S. pombe</i> Pap1.....	46
1.5.2.3.3	<i>C. albicans</i> Cap1	47
1.5.2.4	Skn7.....	51
1.6	Oxidative stress-responsive signalling pathways in <i>C. glabrata</i>	51
1.7	Response of <i>C. albicans</i> and <i>C. glabrata</i> to combinatorial oxidative and cationic stresses	53
1.7.1	Synergistic killing of <i>C. albicans</i> by combinatorial stress is due to impaired activation of Cap1 transcriptional factor.....	54
1.7.2	<i>C. glabrata</i> resistance to combinatorial stress is mediated by the uncharacterised <i>CRI</i> genes.....	55
1.8	Project Aims	55
1.8.1	Investigation into the molecular basis underlying innate immune defence mediated killing of <i>Candida</i> species	55
1.8.2	Investigation into the importance of fungal stress responses in mediating virulence in hosts with defective immune defences	56
Chapter 2. Materials and methods	57
2.1	Microbiological techniques	57
2.1.1	Yeast strains and growth conditions	57
2.1.2	<i>C. albicans</i> strain construction.....	59
2.1.2.1	Tagging of Crm1, Cap1 and Txl1	59
2.1.2.2	Heterologous expression of <i>Candida glabrata</i> <i>CRI</i> genes in <i>C. albicans</i>	61
2.1.3	DNA transformation	64

2.1.3.1	Transformation of <i>E. coli</i>	64
2.1.3.2	Transformation of <i>C. albicans</i>	64
2.2	Cell biology techniques	65
2.2.1	Spot tests	65
2.2.2	Yeast flow cytometry	65
2.3	Molecular biology techniques.....	66
2.3.1	DNA isolation	66
2.3.1.1	Plasmid isolation from <i>E. coli</i>	66
2.3.1.2	Isolation of <i>C. albicans</i> and <i>C. glabrata</i> total DNA.....	66
2.3.2	DNA manipulation and analysis	67
2.3.2.1	<u>P</u> olymerase <u>c</u> hain <u>r</u> eaction (PCR)	67
2.3.2.2	Restriction endonuclease digestion, phosphatase treatment and DNA ligation reactions.....	69
2.3.2.3	Analysis of DNA by agarose gel electrophoresis	70
2.3.2.4	DNA sequencing.....	70
2.3.3	Cap1 chromatin immunoprecipitation (ChIP).....	70
2.3.3.1	Harvesting the cells	71
2.3.3.2	Preparing the beads	71
2.3.3.3	Breaking the cells	72
2.3.3.4	Sonication of the chromatin	72
2.3.3.5	Immunoprecipitation	72
2.3.3.6	DNA purification.....	73
2.3.3.7	Quantification of DNA	73
2.3.3.8	Selection of the targets and qPCR primers design	74
2.3.3.9	Q-PCR	75
2.3.4	RNA extraction, manipulation and analysis	75
2.3.4.1	RNA extraction	75
2.3.4.2	Northern blotting.....	76
2.4	Protein analysis.....	78
2.4.1	Preparation of native protein extracts.....	78
2.4.2	SDS-PAGE and western blotting.....	79
2.4.3	Cap1 phosphorylation assay	81

2.4.4 Determination of RNA polymerase II phosphorylation.....	81
2.4.5 Cap1-Crm1 co-immunoprecipitation	82
2.4.6 Acid lysis protein extraction	83
2.4.7 Determination of Cap1, Trx1 and Txl1 oxidation.....	84
2.4.8 Determination of histone H3 modifications	86
2.5 Imaging techniques	87
2.5.1 Differential interference contrast (DIC) microscopy	87
2.5.2 Fluorescence microscopy to detect Cap1 localisation	87
2.6 <i>Caenorhabditis elegans</i> virulence assays	88
2.6.1 <i>Caenorhabditis elegans</i> strains and growth conditions.....	88
2.6.2 <i>C. elegans</i> synchronisation techniques	88
2.6.3 Solid plate <i>C. elegans</i> infection assay	89
2.6.4 Fluorescent microscopy of <i>C. elegans</i> infected with <i>C. albicans</i>	89
2.6.5 Statistical analysis	90
2.7 General laboratory suppliers	90
Chapter 3. Investigation of the responses of <i>Candida</i> species to combinatorial stress	91
3.1 Introduction.....	91
3.2 Results	92
3.2.1 Cap1 activation is prevented following exposure to combinatorial oxidative and cationic stress	92
3.2.2 The inactivation of Cap1 following combinatorial stress is transient ..	101
3.2.3 The formation of Cap1 ^{OX-1} is dependent on Gpx3 and Ybp1.	108
3.2.4 Combinatorial stress-induced delay in Cap1 activation is specific to the combination of H ₂ O ₂ and cationic stresses.....	108
3.2.5 Combinatorial stress-mediated inhibition of Cap1 is maintained in hyphal <i>C. albicans</i> cells.....	112
3.2.6 Cationic stress promotes the interaction of Cap1 with the Crm1 nuclear exportin	112
3.2.7 Combinatorial stress triggers a dramatic increase in intracellular ROS levels in <i>Candida</i> species.....	121

3.2.8 <i>CRI</i> genes are essential for <i>C. glabrata</i> combinatorial stress resistance.....	123
3.3 Discussion	130
Chapter 4. Mechanisms underlying the delayed activation of Cap1 in response to high levels of ROS	135
4.1 Introduction	135
4.2 Results.....	135
4.2.1 Cap1 activation, but not nuclear accumulation, is delayed in response to high doses of H ₂ O ₂	135
4.2.2 The oxidation profile of Cap1 is similar following exposure to high H ₂ O ₂ and combinatorial H ₂ O ₂ and cationic stresses	141
4.2.3 Comparison of the Cap1 ^{OX-1} form generated following high H ₂ O ₂ and combinatorial stress.....	141
4.2.4 Investigation into whether the impaired oxidation of Cap1 following high ROS is due to the increased activity of the thioredoxin proteins Trx1 and Txl1	145
4.2.5 Investigation into Cap1 promoter occupancy following exposure to high H ₂ O ₂ concentrations	150
4.2.6 High ROS levels and combinatorial stress cause the global inhibition of antioxidant gene expression	154
4.2.7 Impact of high ROS levels on global regulation of transcription	156
4.3 Discussion	158
Chapter 5. The Requirement for Stress Responses in Mediating <i>C. albicans</i> Virulence is Dependent on the Immune Status of the Host.....	166
5.1 Introduction	166
5.2 Results.....	169
5.2.1 <i>C. elegans</i> is more susceptible to <i>C. albicans</i> infection with ageing ..	169
5.2.2 Is the age-associated decline in resistance to <i>C. albicans</i> mediated due to a decline in PMK-1 function in <i>C. elegans</i> ?	172
5.2.3 <i>C. albicans</i> does not need to mount a Hog1-mediated stress response during infection of old nematodes	177
5.2.4 <i>C. albicans</i> colonisation of <i>C. elegans</i>	179

5.3 Discussion	184
Chapter 6. Final Discussion	187
6.1 Summary	187
6.2 Inhibition of Cap1-dependant oxidative stress response – a major antifungal defence mechanism?.....	188
6.3 <i>C. glabrata CRI</i> genes as a novel mechanism of combinatorial stress resistance	191
6.4 <i>C. elegans</i> age-dependant susceptibility to <i>C. albicans</i> infection	193
6.5 Concluding remarks	195
Chapter 7. References	197

List of Figures

Chapter 1

Figure 1.1	Pathogenic <i>Candida</i> species colonise different niches in the host, but promote the infection only in susceptible host.....	3
Figure 1.2	The hostile environment of the phagosome.	13
Figure 1.3	Hog1 SAPK signalling in response to osmotic and oxidative stress in <i>C. albicans</i>	27
Figure 1.4	Schematic diagram of thioredoxin/ peroxiredoxin system in <i>C. albicans</i>	36
Figure 1.5	Generation of reactive oxygen species (ROS) in the phagosome and the pathways that respond to ROS in <i>Candida albicans</i>	38
Figure 1.6	AP-1like transcriptional factors.....	41
Figure 1.7	Schematic representation of Yap1 oxidation in response to H ₂ O ₂	44
Figure 1.8	Schematic representation of Yap1 oxidation in response to diamide.	45
Figure 1.9	Mechanism of Cap1 activation in response to oxidative stress.	49

Chapter 2

Figure 2.1	Schematic diagram illustrating a strategy used to myc-HIS tag CRM1 in <i>C. albicans</i>	61
Figure 2.2	Schematic diagram illustrating a strategy used to express <i>C. glabrata</i> <i>CRI1</i> in <i>C. albicans</i>	63

Chapter 3

Figure 3.1	The lack of antioxidant gene expression following combinatorial stress is due to the inhibition of Cap1 activation.	93
Figure 3.2	Cap1 is differentially oxidised in response to combinatorial stress.....	95
Figure 3.3	Quantification of Cap1 protein levels pre- and post-stress treatment.	97
Figure 3.4	Cap1 oxidation following oxidative and combinatorial stress.....	98

Figure 3.5 Cap1 forms multiple differentially oxidised intermediates following combinatorial stress treatment.....	100
Figure 3.6 Cap1 nuclear accumulation is delayed following combinatorial stress.	102
Figure 3.7 Cap1 phosphorylation is delayed following combinatorial stress treatment.	103
Figure 3.8 The inhibition of Cap1-dependent gene expression following combinatorial stress is transient.....	104
Figure 3.9 The differential oxidation of Cap1 following combinatorial stress is not sustained.	106
Figure 3.10 Cap1 activation profile in response to combinatorial stress in cells expressing <i>CAP1</i> under the control of its own or constitutive <i>ACT1</i> promoter.....	107
Figure 3.11 Gpx3 and Ybp1 regulate the formation of the combinatorial stress-induced Cap1 ^{OX-1} form.	109
Figure 3.12 Cap1-GFP nuclear accumulation in response to different stresses and their combinations.....	111
Figure 3.13 Combinatorial stress-mediated Cap1 inactivation is maintained in hyphal cells.	113
Figure 3.14 Cationic stress stimulates the interaction of Cap1 with the Crm1 nuclear export factor.....	115
Figure 3.15 The increased interaction of Cap1 with Crm1 following combinatorial stress is transient.....	116
Figure 3.16 The NaCl-enhanced interaction between Cap1 and Crm1 is Hog1-independent and cationic stress specific.....	119
Figure 3.17 Cationic stress fails to promote the interaction of the diamide-induced oxidised form of Cap1 with Crm1.....	120
Figure 3.18 FACS analysis of intracellular ROS levels in response to oxidative stress and the combination of the oxidative and cationic stresses in <i>C. albicans</i> ..	122
Figure 3.19 FACS analysis of intracellular ROS levels in response to oxidative stress and the combinatorial oxidative and cationic stresses in <i>C. glabrata</i>	124
Figure 3.20 The sensitivity of <i>C. glabrata</i> <i>CR1</i> mutants in response to oxidative, osmotic and combinatorial stresses.....	126

Figure 3.21 FACS analysis of intracellular ROS levels in <i>C. glabrata</i> <i>CRI1</i> mutants following combinatorial oxidative and osmotic stress.	127
Figure 3.22 Impact of ectopic expression of <i>C. glabrata</i> <i>CRI1-4</i> genes on <i>C. albicans</i> stress resistance.	129
Figure 3.23 A model of combinatorial stress-mediated Cap1 inactivation.	133

Chapter 4

Figure 4.1 Cap1 nuclear accumulation in response to different doses of H ₂ O ₂ ...	137
Figure 4.2 Cap1 phosphorylation in response to increasing H ₂ O ₂ concentrations.	138
Figure 4.3 Cap1-dependent gene expression is delayed in response to high H ₂ O ₂ concentrations.	140
Figure 4.4 High levels of H ₂ O ₂ result in sustained Cap1 ^{OX-1} formation.	142
Figure 4.5 Differential Cap1 oxidation in response to high ROS.	144
Figure 4.6 The oxidation profile of <i>C. albicans</i> thioredoxins Trx1 and Txl1 in response to oxidative and combinatorial stress.	147
Figure 4.7 The formation of Cap1 ^{OX-1} following combinatorial stress and high H ₂ O ₂ stress is independent of Trx1 and Txl1.	149
Figure 4.8 Analysis of Cap1-CSE binding to the selected gene promoters.	152
Figure 4.9 ChIP analysis of Cap1 binding to the promoters of its target genes in response to different H ₂ O ₂ concentrations.	153
Figure 4.10 Cap1-independent antioxidant gene expression is inhibited in response to high H ₂ O ₂ levels.	155
Figure 4.11 Impact of different stress conditions on histone acetylation.	157
Figure 4.12 RNA Pol II phosphorylation is maintained following high H ₂ O ₂ exposure and combinatorial stress.	159
Figure 4.13 A model depicting the deregulation of Cap1 activation in response to high H ₂ O ₂ levels and combinatorial oxidative plus cationic stress.	161
Figure 4.14 A model of Cap1 inactivation following high ROS.	165

Chapter 5

Figure 5.1	<i>C. elegans</i> are more susceptible to <i>C. albicans</i> infection with age	171
Figure 5.2	Immunocompromised <i>sek-1</i> mutants are more susceptible to <i>C. albicans</i> killing compare to the immunocompetent nematodes.....	173
Figure 5.3	The increased susceptibility of <i>C. elegans sek1</i> mutants to <i>C. albicans</i> infection with age.....	175
Figure 5.4	Age-associated decline in resistance may be related to impaired p38 (PMK-1) responses in <i>C. elegans</i>	176
Figure 5.5	<i>C. albicans</i> SAPK Hog1 is required for virulence in young but not old nematodes.	178
Figure 5.6	Kinetics of <i>C. albicans</i> intestinal colonisation of young <i>C. elegans</i>	180
Figure 5.7	Kinetics of <i>C. albicans</i> intestinal colonisation of mature <i>C. elegans</i> .	182
Figure 5.8	Kinetics of <i>C. albicans</i> intestinal colonisation of aged <i>C. elegans</i>	183

Chapter 6

Figure 6.1	Impact of combinatorial stress and high H ₂ O ₂ levels on Cap1 activation.	189
------------	---	-----

List of Tables

Chapter 2

Table 2.1 Yeast strains used in this study.....	59
Table 2.2 Oligonucleotide primers used in the study.....	68
Table 2.3 Primer sequences used for Q-PCR binding assays.....	74
Table 2.4 Oligonucleotide primers used in the study to amplify probes for northern blot.....	77
Table 2.5 Antibodies used in this study.....	81
Table 2.6 Chemicals and reaction conditions used to determine Cap1 oxidation status.....	86
Table 2.7 <i>C.elegans</i> strains used in this study.....	88

Chapter 4

Table 4.1 Relative levels of induction of the selected Cap1 targets in response to oxidative and combinatorial stresses.....	152
--	-----

Chapter 1. Introduction

1.1 *Candida* species as major pathogens of humans

Fungal infections are a major, but often overlooked, medical problem. Due to the dramatic increase in fungi-attributed human deaths over recent years, there is a striking need to better understand the biology of these 'hidden killers' and to develop novel mechanisms to combat pathogenic fungi.

The increase in fungi-attributed deaths is mainly attributed to three species – *Cryptococcus neoformans*, *Aspergillus fumigatus* and *Candida albicans* (Pfaller and Diekema, 2007). Recent studies showed that about 8% of hospital-acquired nosocomial infections are caused by *Candida* species, and among the most frequently isolated species are *Candida albicans* and *Candida glabrata* (Pfaller and Diekema, 2007, Pappas, 2006, Wisplinghoff et al., 2004, Morgan, 2005). Both these *Candida* species are ubiquitous inhabitants of the human microbiome (Cole et al., 1996, Fidel et al., 1999), and 30-70% of healthy individuals carry *Candida* spp. as a commensals, where they exist as part of the normal healthy microbiota of human gastrointestinal, oropharyngeal and urogenital tracts (Naglik et al., 2011, Luo et al., 2013b). Robust immunity and healthy microbiome are key factors in preventing *C. albicans* transition from benign commensal to an aggressive pathogen (Romani, 2011). *Candida* spp. can cause systemic infections associated with high morbidity and mortality when the immune system of the host is compromised (Perlroth et al., 2007, Pfaller and Diekema, 2007), or when the host is encountering the perturbations of the gut microbiome (Underhill and Pearlman, 2015). In addition to the defects in innate and adaptive immunity, numerous other factors contribute to *C. albicans* switching from the benign commensal to the pathogen. The major prerequisites of *Candida* infection are impaired barrier functions of the mucosal surfaces, misbalanced microflora, metabolic disorders, extremes of age, use of the immunosuppressive therapies during organ transplantation or cancer treatment, and HIV-AIDS (Luo et al., 2013b, Koh et al., 2008, Segal et al., 2006, Davies et al., 2006).

C. albicans can cause superficial or more severe systemic infections, depending on the immune status of the host. As a commensal, this fungus can occupy the skin, oral cavity, gastrointestinal tract and genitalia of healthy people. However, as an opportunistic pathogen, *C. albicans* can overgrow in such environments causing

superficial infections, termed oral candidiasis (OC) or vulvovaginal candidiasis (VVC), which more commonly referred as a thrush. For instance, OC affects 80-90% of all HIV-positive individuals (Elias et al., 2009, Wu et al., 2012), whereas VVC affects nearly 80% of the female population of childbearing age (Sobel, 2007).

More serious is the situation in individuals with immune system defects, who are susceptible to fatal systemic infections (Figure 1.1). Clinical descriptions of different stages of infection caused by *Candida* species distinguish candidemia, invasive candidiasis and disseminated candidiasis. Candidemia occurs when the pathogen enters the bloodstream, whereas invasive candidiasis (IC) refers to the colonisation of specific organs by *Candida* spp. Nowadays IC is a persistent public health problem with a mortality rate of 30-50%, which has remained unchanged during the past decade, despite antifungal drug development (Pfaller and Diekema, 2007, Eggimann et al., 2003, Dimopoulos et al., 2013). When the pathogen affects multiple sites and colonises diverse organs, the disease is named disseminated candidiasis. Candidiasis usually affects such sites as the brain, liver, kidney, heart and spleen of susceptible hosts. For instance, *C. albicans* is responsible for 24% of all cases of fungal endocarditis with over 70% mortality rate (Ellis et al., 2001).

According to a recent NIH report, 80% of human chronic infections are biofilm-associated (Dongari-Bagtzoglou et al., 2009), and *Candida* spp. are among the most frequently found components of mixed microbial biofilms, that are formed on both biotic and abiotic surfaces within a host (Harriott and Noverr, 2011). A population study in the US, performed in 1998-2000, suggested that 78% of those patients diagnosed with *Candida* spp. BSI, had an implanted central catheter, which was a surface for biofilm formation, and therefore the biofilm was a source of the pathogenic *Candida* spp. (Hajjeh et al., 2004).

C. glabrata is the second most common pathogenic *Candida* isolate, according to the ARTEMIS DISK Global Antifungal Surveillance Study (Pfaller et al., 2010). The number of life-threatening infections caused by *C. glabrata* has tremendously increased during recent decades. *C. glabrata* is responsible for at least 20-24% of hospital-acquired bloodstream *Candida* infections (Trick et al., 2002).

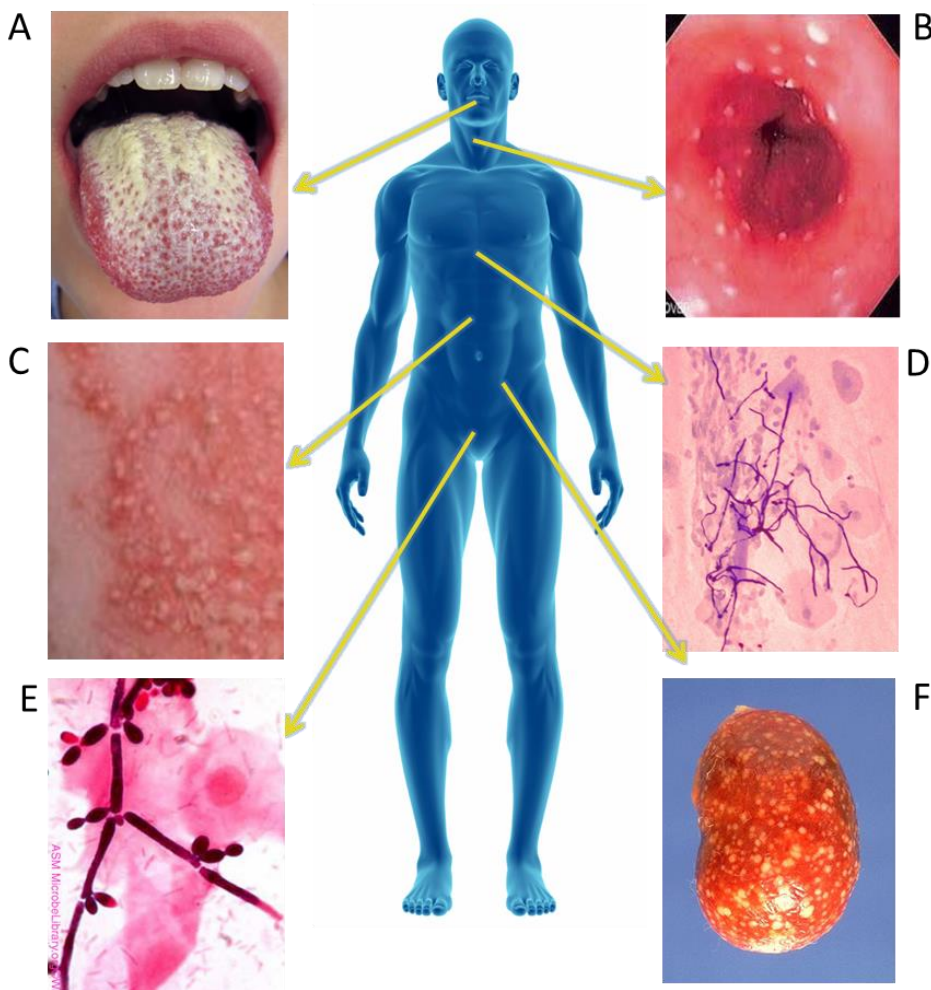


Figure 1.1 Pathogenic *Candida* species colonise different niches in the host, but promote the infection only in susceptible host.

(A) Infection of the oral mucosa (oral thrush) (<http://www.medicinenet.com/thrush/page5.htm>). (B) Oesophageal candidiasis (gastrointestinal tract infection). An endoscopic image illustrating oesophageal candidiasis in a patient undergoing chemotherapy (http://link.springer.com/chapter/10.1007/978-81-322-2419-8_8?no-access=true). (C) Cutaneous congenital candidiasis (<http://emedicine.medscape.com/article/1090632-clinical#b4>). (D) Sputum smear from patient with pulmonary candidiasis, gram stain, LM X100. © Dr. John D. Cunningham/Visuals Unlimited, Inc. (<http://visualsunlimited.photoshelter.com/image/I00001vJWoWd9ne0>) (E) Gram stain of vaginal smear showing *C. albicans* epithelial cells (1,000X oil) © Danny L. Wiedbrauk, Warde Medical Laboratories, Ann Arbor, Michigan and The MicrobeLibrary (<http://www.microbiologybook.org/mycology/mycology-3.htm>) (F) Systemic kidney infection, CDC (https://phil.cdc.gov/phil/details_linked.asp?pid=1213).

It is suggested that this increase is due to the inherent resistance of *C. glabrata* to fluconazole and other azole drugs (Pfaller et al., 1998), a widely used prophylactic antifungal treatment.

The increasing number of life-threatening fungal infections by *Candida* spp. (Richardson, 2005) demonstrates a clear and urgent need to understand what makes these fungi such successful pathogens.

1.2 Impaired immune defences result in increased susceptibility to *C. albicans* infection

Robust innate immune defences are vital for pathogen clearance; hence, any defect in such defences is associated with increased susceptibility to infection, and this is seen in both immunocompromised and elderly hosts. In the following section, two major groups of the susceptible hosts – immunocompromised and elderly, and the risk factors associated with each condition, will be considered.

1.2.1 Immunocompromised increases

“Immunotherapy must be tailored to specific immunocompromised states”
(Segal et al., 2006)

The dissemination of *Candida* species into the bloodstream is only possible when both innate and adaptive immunity are affected (Romani, 2004). In patients with impaired immunity *C. albicans* can enter and disseminate throughout the bloodstream, colonise internal organs and cause life-threatening systemic infections (Odds, 1979). For example, oropharyngeal candidiasis (OPC) – *Candida*-associated medical condition that develops in the mouth or throat – affects nearly 90% of HIV-positive individuals (de Repentigny et al., 2004). Susceptible hosts include patients with genetic predisposition that favour the progression of *Candida* infection, and treatment-induced immunocompromised individuals.

Genetic factors that increase susceptibility to systemic candidiasis include human disorders such as chronic mucocutaneous candidiasis (CMC) and chronic granulomatous disease (CGD). CMC occurs in the absence of proper immune recognition of the pathogen due to inborn errors in cytokines (interleukin IL-17A/F) immunity, resulting in fungal colonisation of the mucosal surfaces (Kirkpatrick, 1994, Okada et al., 2015). CMC often accompanies a primary immunodeficiency disorder, such as autoimmune disease or endocrinopathy, and is mainly linked to a deficiency in the Th17 response (Puel et al., 2011, Eyerich et al., 2008, Ng et al., 2010, Okada et al., 2015). CGD is an inherited X-linked genetic disorder, where defects in the phagocytic NADPH oxidase complex result in impaired production of reactive oxygen species (ROS) via the respiratory burst, and thus less efficient killing of microbial pathogens, including *Candida* spp. (Holland, 2010, Diamond et al., 1978).

Additionally, many other neutrophil disorders are shown to increase predisposition to disseminated candidiasis (Mansour and Levitz, 2002), with an alarming increase in systemic candidiasis rates among the patients with impaired neutrophils function or neutropenia (Vazquez-Torres and Balish, 1997, Andrews and Sullivan, 2003). Neutrophil-mediated *C. albicans* killing is also impaired in patients with a defective myeloperoxidase enzyme, which is essential for the phagocytic respiratory burst (Andrews and Sullivan, 2003, Diamond et al., 1980). Another example of neutrophil dysfunction that leads to increased susceptibility to candidiasis is a leukocyte adhesion deficiency type 1 (LAD1), due to the deficiency in β - integrins expression. Patients with LAD1 suffer from recurrent infections due to the defects in neutrophil adhesion and their poor chemotaxis.

The rising numbers of clinical case reports about systemic candidiasis in patients with compromised leukocyte function illustrate the importance of innate immunity for an effective pathogen clearance (Shoham and Levitz, 2005, Pasqualotto et al., 2006). The first emergence of systemic candidiasis coincided with HIV infection and among cancer patients undergoing chemotherapy. However, nowadays medical interventions such as organ transplantations and use of catheters and implants are among the leading factors to induce predisposition to candidiasis.

1.2.2 Age-associated increases

Rising numbers of clinical case reports highlight that the aged population is at particular risk and is highly susceptible to bacterial and fungal infections (Bradley and Kauffman, 1990). Multiple reports highlight that the highest rate of IC occurs between very young children (less than 1 year old) or in advanced age groups (over 65 years old) (Pfaller and Diekema, 2007). Thus, the susceptibility to infectious diseases has been described as a “U” shaped function of age, with the highest risk of infection among premature infants and elderly groups (Miller and Gay, 1997). Consistent with this, recent clinical reports indicate that those two groups experience much higher frequency of OC due to defects in immunity of such individuals (Flevani et al., 2013, Healy et al., 2008). An Extended Prevalence of Infection in Intensive Care (EPIC) II study involving 1,246 intensive care units (ICUs) from 75 countries reported that, whereas the susceptibility to infections between the patients of different age groups remained unchanged, the mortality rates as a result of nosocomial infection were much higher in the individuals of advanced age (Dimopoulos et al., 2013).

An increase in morbidity and mortality caused by infectious diseases in elderly is a reflection of functional and metabolic alterations in cells and tissues, together with the process of immunosenescence – a complex deterioration of the immune system with age (Panda et al., 2009). This decline in immune function in elderly individuals is conserved among almost all vertebrates (Shanley et al., 2009). The process of immunosenescence includes both innate and adaptive immune responses, mainly due to the decline in the activity and selectivity of the receptors of different immune cells, as well as defects in signalling in the downstream regulatory pathways (Panda et al., 2009). Impairment of the innate immune system in the elderly population is mainly associated with inflammo-ageing, a phenomenon linked to increase in the production of pro-inflammatory cytokines that contribute to further tissue damage (Franceschi et al., 2007).

There are many other reasons that make the aged population so vulnerable to fungal infections, such as inevitable physiological changes, comorbidity and an increase use of different drugs (Flevani et al., 2013). In fact, one of the most widely used antifungals, Amphotericin B, is not an ideal treatment for elderly patients, due to

the high levels of nephrotoxicity, that is associated with renal failure, and resulting in comorbidity (Kauffman, 2001).

Taken together, multiple reasons promote the higher susceptibility to fungal infections in aged population, but the mechanism behind it that will aid to target the treatment of age-associated mycoses remains unclear. A wealth of data illustrates that a robust immune system is pivotal in preventing and combatting fungal infections. In the next section, the mechanisms employed by the immune system of a healthy host to counteract *Candida* infections will be briefly considered.

1.3 Host immune defences against *Candida* species

The immune defence mechanisms in mammals are evolutionarily advanced to protect against bacterial and fungal onslaught. In healthy individuals, mucosal surfaces successfully mount the first mechanical and immunological barrier against the invading pathogens, enabling their recognition and triggering the cascade of signalling events, leading to the activation of immune response, thus preventing the bloodstream entry of the pathogen.

Traditionally, protective mechanisms that emerged very early through evolution are referred to as innate immune mechanisms, whereas more advanced and complicated mechanisms are referred to as adaptive. The latter possess high specificity and evolve after the contact with the potential threat (Romani, 2011). Adaptive immunity is responsible for the generation of the long-lasting pathogen-specific memory (Medzhitov and Janeway, 1997). The interplay between innate and acquired immune defences is highly effective, and therefore systemic fungal infections are very unusual in the immunocompetent host (Mansour and Levitz, 2002, Steinman, 1991, Farah et al., 2001).

The key stages and processes involved in effective innate immune defence mechanisms against *Candida* species discussed in this section.

1.3.1 Innate immune defences as a first line of combatting fungal infection

Innate immune defences are traditionally divided into humoral (complement and cytokines) and cellular (phagocytic immune cells) responses.

The phagocytic immune cells are the major players in innate immune defences. Their primary role is recognition, binding and destruction of the xenobiotic bodies, including pathogens. The mechanisms of phagocytic attack and detoxification of the pathogen include chemotaxis to the site of infection, activation of Toll-like receptors (TLRs) signalling, binding of complement, activation of the granules containing a cocktail of the antimicrobial substances with a subsequent degranulation, as well as other non-oxidative mechanisms, such as defensins (Chauhan et al., 2006). Furthermore, innate immune cells produce different cytokines and play a prominent role in antigen presentation to T cells, along with the further initiation of adaptive immune response via Th priming and education, thus enabling a link between innate and adaptive immunity (Lorenz et al., 2004, Mansour and Levitz, 2002).

There are three major groups of the phagocytic cells: monocytes/ macrophages, polymorphonuclear leukocytes (PMNs, also known as neutrophils), and dendritic cells (DCs) (Mansour and Levitz, 2002, Miramon et al., 2013).

Macrophages are involved in the recognition of the pathogen-associated molecular patterns (PAMPs) located on the fungal cell wall (section 1.3.2). The primary role of a macrophage is to kill the pathogen through oxidative phagocytic mechanisms, but also functions in antigen presentation to T cells. Stimulation of human macrophages by macrophage colony-stimulating factor (M-CSF) increases their fungicidal potency via the induction of the oxidative burst (Gioulekas et al., 2001). Macrophages also produce a range of immunomodulatory molecules, such as cytokines and chemokines, and therefore are important for the engagement of the entire network of the immune defences (Major et al., 2002). But *C. albicans*, being a successful pathogen, can proliferate and form hyphae within the macrophages, and eventually escape (Lo et al., 1997).

Neutrophils, or polymorphonuclear neutrophils (PMNs) are the most abundant group of phagocytic immune cells (Segal, 2005). Their major function is phagocytosis

and pathogen killing, and they are not involved in antigen presentation to T cells (Oehler et al., 1998). PMNs possess both complement and Fc receptors, and therefore act to destroy the opsonised microorganisms (Mansour and Levitz, 2002). Neutrophils employ both non-oxidative (defensins) and oxidative (ROS production) mechanisms in order to kill the invading microbes. PMNs are highly reactive and possess the receptors for cytokines and chemokines on their surface, so they can be rapidly and effectively recruited to the site of invasion (Mansour and Levitz, 2002). Neutrophils are the major players in killing *C. albicans* hyphae, as these immune cells are recruited more efficiently to hyphal cells compared to yeast cells due to the activation of the MEK/ERK MAPK signalling pathway (Wozniok et al., 2008, Gow et al., 2011). Importantly, *C. albicans* cannot proliferate within neutrophils, as the neutrophilic environment is too harsh and therefore inhibiting fungal proliferation (Fradin et al., 2005).

Dendritic cells (DCs) are the group of highly specialised antigen presenting cells (APCs), whose primary function is to bridge innate and adaptive immunity via aiding antigen presentation to T cells (Steinman, 1991, Mansour and Levitz, 2002, Romagnoli et al., 2004). However, their function is not limited to the presentation of the antigens to T cells: dendritic cells also take part in *C. albicans* inactivation. Similarly to macrophages, they recognise *C. albicans* cells via mannose-fucose receptors and kill them (Newman and Holly, 2001, d'Ostiani et al., 2000), albeit less effectively than macrophages or neutrophils (Netea et al., 2004). DCs discriminate between *C. albicans* yeast and hyphal morphology (section 1.4.1.1) by switching the pattern of cytokine production (d'Ostiani et al., 2000, Mansour and Levitz, 2002). Both yeast and hyphal forms of *C. albicans* are phagocytosed by DCs, but the yeast form is killed more effectively (Jacobsen et al., 2012).

Natural killer (NK) cells are cytotoxic lymphocytes that form part of the innate immune defence system. A recent report indicates that these cells play an important role in *C. albicans* clearance in immunosuppressed organisms, but can cause hyper-inflammation in healthy immunocompetent hosts (Quintin et al., 2014).

1.3.2 Immune recognition

Initially, the recognition of non-opsonised pathogens is mediated via specific pattern recognition receptors (PRRs) on the surface of the antigen presenting immune cells (APCs) (macrophages and dendritic cells), which can sense both external and internal stimuli, thus playing a leading role in the immune homeostasis of the host (Netea et al., 2008, Medzhitov and Janeway, 1997, Gordon, 2002, Erwig and Gow, 2016).

Multifarious types of receptors are implicated in *C. albicans* recognition, such as Toll-like receptors (TLR), Nod-like receptors (NLR) and C-type lectin receptors (CLR) (Gow et al., 2011). These receptors recognise specific components of the fungal cell wall and transmit the proinflammatory signal, leading to cytokine production and the stimulation of the adaptive immune response (Netea et al., 2008, Mora-Montes et al., 2012, Hall, 2015, Underhill and Ozinsky, 2002).

The cell wall of *C. albicans* is a complex structure consisting of three major layers: an inner chitin layer, median β -glucan and outer mannan layers (Netea et al., 2008). Mannose residues from fungal cell wall are recognised by surface mannose receptors of the macrophages and dendritic cells (MR) and C-type lectin Receptors (CLR), whereas Toll-like receptors TLR2 and TLR4 are responsible for the recognition of mannan (Netea et al., 2008, Netea et al., 2006, Tada et al., 2002). Dectin-1 receptor is involved in the recognition of the β -glucan, whereas dectin-2 is responsible for the recognition of *C. albicans* hyphae (Brown et al., 2002, Sato et al., 2006).

To prevent host recognition of fungal antigens such as β -1,3-glucan and chitin by immune PAMPs, *C. albicans* cells are coated with mannoprotein, resulting in the lessening of phagocytosis by the neutrophils (Chai et al., 2009). Some components of the cell wall, such as Pra1, Gpm1 and Gpd2, can actively prevent the complement binding and subsequent opsonisation (Poltermann et al., 2007, Luo et al., 2009, Luo et al., 2013a). Recently the role of Pra1 antigen in *C. albicans* recognition has been described. Pra1 is recognised by the integrin CD11b/CD18 complement receptor 3 and modulates the neutrophils migration and adherence, thus plays an important role in pathogen's recognition by innate immune system (Soloviev et al., 2011). However,

C. albicans is able to release a soluble Pra1 protein and diminish neutrophils function – the production of ROS, myeloperoxidase and cytokines (Losse et al., 2011).

In conclusion, PAMPs are responsible for immune recognition of *C. albicans* and stimulation of cytokine production by immune cells. Mannan and β -glucan form the majority of the pathogen's cell wall and are the main antigenic components on its cell surface (Netea et al., 2006). Distinct phagocytic immune cells subsets exhibit the preference to certain fungal morphology and the composition of the fungal cell wall (Lohse and Johnson, 2008, Quintin et al., 2012). Efficient recognition of fungal PAMPs by phagocytic cells is vital for the subsequent pathogen's clearance (Erwig and Gow, 2016).

1.3.3 *Phagocytosis*

Immune recognition of *C. albicans* leads to engulfment of the fungus with the subsequent killing of the internalised pathogen within the mature phagolysosome (Underhill and Ozinsky, 2002). Phagosomal maturation involves several RAB GTPases that trigger the fusion of vesicles, containing ROS and other toxic chemicals, with the phagosome to form the mature phagolysosome (Romani, 2011).

Transcript profiling of phagocytised *C. albicans* cells illustrates that fungus undergoes rapid responses to this stressful environment and drastic changes in gene expression take place. Transcriptional changes lead to stress adaptation and stimulate the morphological transition from yeast to hyphal cells, resulting in macrophage killing and escape of the pathogen from immune attack (Lorenz et al., 2004, Lorenz and Fink, 2001, Fradin et al., 2005, Fradin et al., 2003). In contrast, *C. albicans* is unable to proliferate while phagocytised by neutrophils, and neutrophils strongly inhibit germ tube formation (Fradin et al., 2005).

Taken together, two major subsets of the phagocytes, PMNs and macrophages, equally contribute to *C. albicans* clearance. In the presence of both PMNs and macrophages in the culture, *C. albicans* yeast cells are predominantly cleared by PMNs, whereas majority of hyphal cells are phagocytosed by macrophages (Rudkin

et al., 2013). In the next section, I describe the key antimicrobial mechanisms employed by phagocytes to kill *C. albicans*.

1.3.4 Stresses encountered during phagocytosis

There are numerous stress factors engendered by host phagocytes to kill the invading pathogen, both intra- and extracellular, acting via oxidative and non-oxidative mechanisms (Miramon et al., 2013). The phagocytic armoury includes the generation of reactive oxygen species (ROS), reactive nitrogen species (RNS), and reactive chloride species (RCS), ambient pH changes, nutrient poor conditions, cationic fluxes, degradative enzymes and antimicrobial peptides. Altogether, these stresses form a strong barrier against the colonisation and proliferation of the pathogen (Figure 1.2).

1.3.4.1 Nutrient deprivation

According to microarray analysis, the *C. albicans* gene expression profile observed upon internalisation by innate immune cells is highly similar to that induced during carbon and nitrogen starvation conditions. For instance, *C. albicans* genes, which encode the enzymes of the glyoxylate cycle, one of the main ways of the metabolic response to C and N starvation, are also upregulated following phagocytosis (Fradin et al., 2005, Rubin-Bejerano et al., 2003, Lorenz et al., 2004). In addition to the nutrient limitation inside the phagosome, the pathogen experiences lack of vital microelements, such as iron, zinc, and copper (Lorenz et al., 2004, Miramon et al., 2013), and has to employ additional mechanisms of acquisition and sequestration of these chemicals in order to survive. The neutrophils use the extrusion of the chromatin decorated with antimicrobial peptides – neutrophils extracellular traps (NETs), which are responsible for the binding of divalent cations, such as Mn^{2+} and Zn^{2+} , thus restricting their availability for the pathogen (Urban et al., 2006, Urban et al., 2009). The formation of the extracellular traps is induced in many effector cells by pathogens or cytokines (Dühring et al., 2015). NETs are proposed to play an additional level of immune defence against invading microbes,

since in addition to the chromatin and histones they contain granules of the bioactive antimicrobials, such as myeloperoxidase, proteolytic enzymes such as cathepsin G, lysozyme and elastase (Dühring et al., 2015).

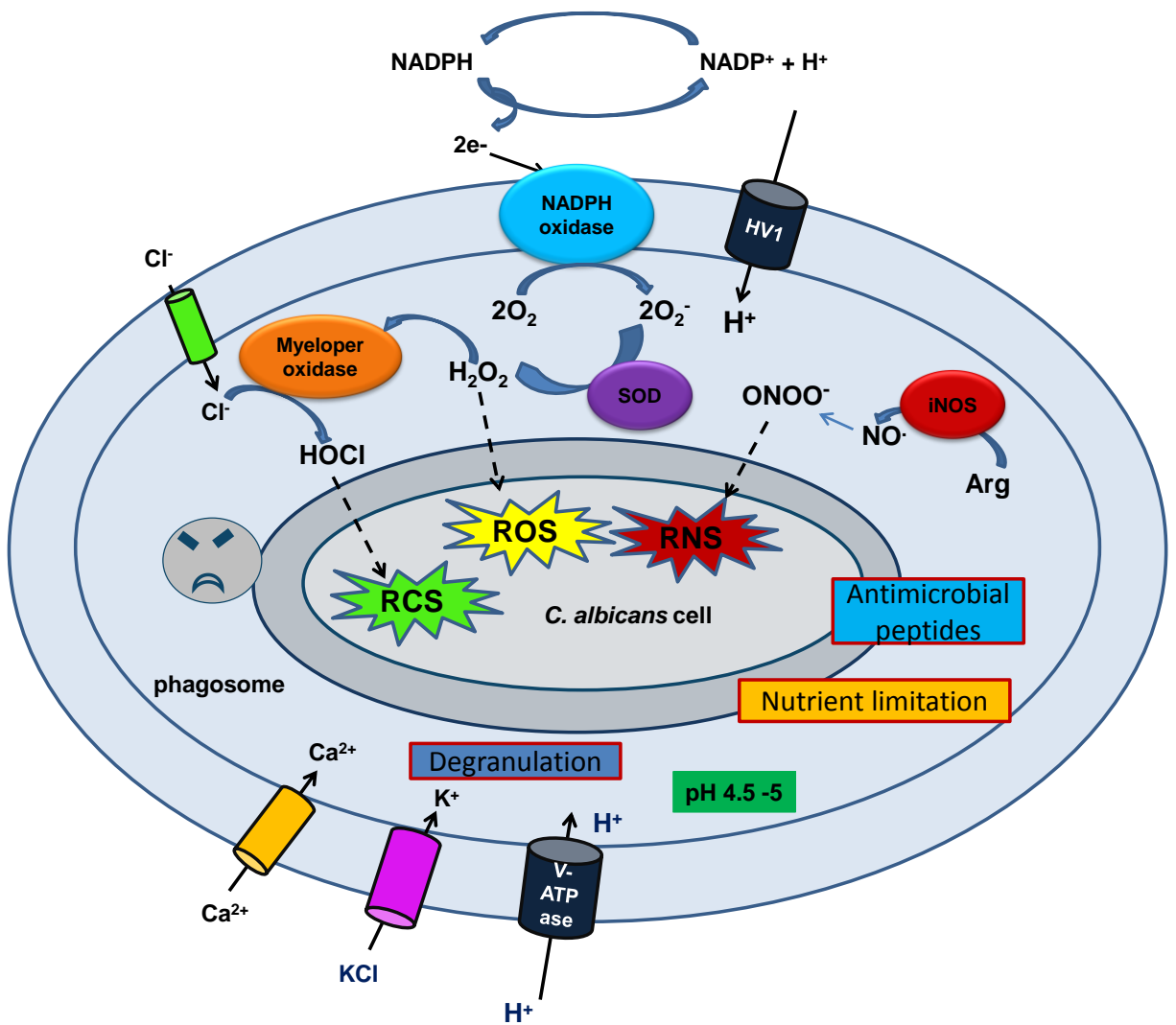


Figure 1.2 The hostile environment of the phagosome.

Mechanisms employed by innate immune cells in order to kill *C. albicans* include the generation of reactive oxygen, nitrogen and chloride species, cationic fluxes, acidification, antimicrobial peptides, degranulation and nutrient limitation. Adapted from (Brown et al., 2009, El Chemaly and Demaurex, 2012, Vazquez-Torres and Balish, 1997, Brechard et al., 2013).

In addition, nutritional stress is a prominent fungistatic host defence mechanism that leads to the global repression of all biosynthetic translational machinery of the pathogen (Lorenz et al., 2004).

1.3.4.2 Acidification

Acidification of the phagocytic lumen occurs due to the pH gradient and membrane potential mounted on the phagocytic membrane (Steinberg et al., 2007). This process is an essential prerequisite of successful pathogen killing and determines the maturation of the phagolysosome (Steinberg et al., 2007).

Following pathogen engulfment, the intraphagosomal pH rapidly decreases due to an active vacuolar-type ATPase transporter (Lukacs et al., 1990). V-ATPase pumps protons into the lumen of the mature phagosome, enabling the action of proteases and hydrolases involved in pathogen killing (El Chemaly and Demaurex, 2012). Such acidification of the phagosome is also essential for the activity of the NADPH oxidase and inducible NO-synthase (iNOS) enzymes, facilitating the generation of Reactive Oxygen Species (ROS) and Reactive Nitrogen Species (RNS) (section 1.3.4.4), and provides a suitable microenvironment for the activity of cationic antimicrobial peptides. In human PMNs, the process of acidification does not start immediately after pathogen engulfment, but instead initially arises from pH 4-6 to pH 8 following phagocytosis as a result of ROS production and high levels of H^+ consumption (Segal et al., 1981, Reeves et al., 2002) (detailed in the next sections).

1.3.4.3 Cationic fluxes

The major cationic flux into the phagosome is generated by a potent K^+ influx to counteract the anionic charge generated through superoxide production (Reeves et al., 2002). The estimate intraphagosomal concentration of K^+ is between 200 – 300 mM (Reeves et al., 2002). This cationic counterflux supports the acidification of the phagosome, as well as engendering a cationic stress against indwelling pathogens, and contributes to the antimicrobial capacities of the phagocytes (Steinberg et al.,

2010). Importantly, the addition of a K^+ ionophore causes the acceleration of ROS production, whereas blocking of the cationic channels has an opposite effect on the phagocytic burst (Reeves et al., 2002). Additionally, recent report indicates that the active import of other cations, such as Ca^{2+} , also takes place during phagocytosis (Brechard et al., 2013). Ca^{2+} influx is essential for NADPH oxidase activation, and therefore for an efficient ROS production by phagocytes (Brechard et al., 2013).

When cationic fluxes are impaired, the performance of the phagocytic cells is very poor. This is due to increased H^+ influx to compensate for the anionic charge generated by oxidative burst, and thus the pH inside the phagosomal vacuole becomes very low, far below the optimal pH range for the action of key antimicrobial peptides and proteases. For example, lactoferrin, which is an antimicrobial peptide from the neutrophilic granules, can cause its candidacidal effect by the induction of apoptosis only in the presence of K^+ efflux (Miramon et al., 2013, Andrés et al., 2008). In addition, osmotic stress that is generated by cationic influx leads to the shrinking of the pathogen which makes further proteolytic digestion more effective (Reeves et al., 2002).

1.3.4.4 ROS and RNS

Upon activation, phagocytic cells generate ROS, a major player in antimicrobial defence mechanisms employed by innate immune cells (Murphy, 1991, Diamond et al., 1978). The process of ROS generation by phagocytic immune cells is called the oxidative burst. Chemically, ROS are intermediate reduction products of O_2 (Nathan and Shiloh, 2000). The membrane-associated NADPH oxidase complex within phagocytes is responsible for the generation of the superoxide anion (O_2^-) by the one-electron reduction of oxygen, using NADPH as the electron donor in the following reaction:



The NADPH oxidase complex consists of six independent subunits. The assembly of the active enzyme complex at the phagosomal membrane only takes place upon cell activation, as a result of the membrane translocation of the $p67^{phox}$

cytosolic subunit triggered by phagocytic stimuli (Burg and Pillinger, 2001, Bedard and Krause, 2007). Importantly, the generation of ROS by NADPH oxidase also harbors a signaling function that promotes chemotaxis of the phagocytic cells to the site of infection, as well as limiting the ability of *C. albicans* to form hyphae (Brothers et al., 2013).

Superoxide anion radicals O_2^- themselves possess very low antimicrobial activity, but they are precursors in the production of a variety of toxic reactive oxygen, nitrogen and chloride species. The concentration of the superoxide radicals in the phagosome can reach $5-10 \times 10^{-9}$ Mol per second (Hampton et al., 1998), with an approximately 4 Mol L^{-1} generated per microorganism engulfed in the phagocytic vacuole (Reeves et al., 2002). Inside the phagosome, the superoxide anion is rapidly dismutated into hydrogen peroxide (H_2O_2) by superoxide dismutases (SODs) or to hydroxyl anions (OH^-) and hydroxyl radicals ($\cdot OH$) via the Haber–Weiss reaction (Babior, 1999, Brechard et al., 2013). The NADPH-dependent oxidative burst is an essential function of innate immunity, which is impaired in patients with CGD (Thrasher et al., 1994). Patients with CGD are highly susceptible to life-threatening bacterial and fungal infections, including *C. albicans* (Holland, 2010, Cohen et al., 1981, Thrasher et al., 1994).

Myeloperoxidase (MPO) is an enzyme highly abundant inside the neutrophilic granules and lysosomes of the neutrophils, which catalyzes the reaction of halogenation between H_2O_2 and chloride ions (Cl^-), resulting in the generation of hypochlorous acid (HOCl) (Nordenfelt et al., 2009, Dühring et al., 2015). This highly oxidative molecule can react with organic amines to form chloramines, which have further antimicrobial properties (Winterbourn et al., 2006). MPO is highly important for *C. albicans* clearance by phagocytes – cells lacking this enzyme or those with insufficient MPO system were shown to be much less active in clearing fungal infections *in vitro*, especially the hyphal form of the fungus (Diamond et al., 1980).

Reactive nitrogen species (RNS) are the products of the inducible nitric oxide synthase (NO-synthase, iNOS or NOS2), which is involved in the synthesis of a nitric oxide (NO) (Nathan and Shiloh, 2000, Miramon et al., 2013, Andrews and Sullivan, 2003). Nitrosative stress mounted by immune cells within the phagosome is due to

an oxidative deamination of L-arginine by nitric oxide synthase. NO itself is not harmful, but it can react with superoxide anion and form a very potent toxin – peroxynitrite (ONOO⁻), an unstable structural isomer of nitrate (NO³⁻) known for its fungicidal activity, and nitrite combines hypochlorous acid to form nitrile chloride (Fang, 2004). Although RNS are highly unstable, peroxynitrite production is important for *C. albicans* killing by macrophages (Vazquez-Torres et al., 1996, Cheng et al., 2012). Importantly, despite of the fact that the invading pathogen stimulates phagocytic NO-synthase, a recent report indicates that *C. albicans* can actively repress NO production by macrophages *in vivo* (Fernández-Arenas et al., 2009). iNOS is more active in acid conditions (Abaitua et al., 1999), and inhibition of the phagosomal acidification by the pathogen can inhibit RNS production. Notably, •NO radicals are inhibitors of mitochondrial oxidative phosphorylation, resulting in production of superoxide anion, peroxynitrite and hydrogen peroxide. Hence, the exposure of *C. albicans* to nitrosative stress leads to the expression of antioxidant genes in order to prevent the formation of reactive oxygen intermediates (Hromatka et al., 2005).

Therefore, phagocytic cells generate a toxic cocktail of reactive oxygen, nitrogen and chlorine species that can promote killing of the invading pathogens. I discuss the toxic effects of ROS and oxidative damage at the cellular level in the next section.

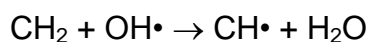
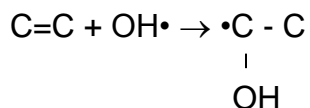
1.3.4.4.1 Cellular effects of ROS

ROS cause fungal cell damage by reacting with proteins, lipids and DNA, causing protein oxidation, lipid peroxidation and DNA damage, with the subsequent changes of cellular function and promoting the apoptosis (Brown et al., 2009, Phillips et al., 2003).

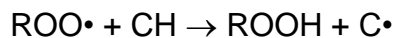
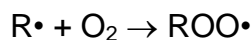
Reaction between ROS and cellular proteins could impact proteins stability resulting in their decreased or altered functionality (Lu et al., 1999). ROS can react with different amino acids, but in particular sulphur-containing cysteine and methionine residues that are prone to oxidation. Cysteine oxidation may provoke the formation of intra- or intermolecular disulphide bonds and reversible or non-reversible

protein cross-linking. Additionally, ROS may react with metal cofactors of enzymes, resulting in their inactivation (Imlay, 2003).

ROS can also affect the stability of cellular membranes by interfering with the phospholipid bilayer and polyunsaturated fatty acids (PUFAs) of the cell membranes, causing lipid peroxidation and loss of membrane integrity (Halliwell, 2006). Lipid peroxidation is initiated by removal of a hydrogen atom from the methylene group of the lipid, resulting in the formation of a carbonyl radical (C[•]):



Following the oxidation of PUFAs, carbonyl radical reacts with molecular O₂, resulting in the formation of the fatty acid hydroperoxyl radical (ROO[•]). ROO[•] is extremely reactive and can continuously react with the adjacent fatty acids:



The result of such chain reaction is the production of multiple fatty acid hydroperoxide molecules, that cause significant damage to the cell membrane (Halliwell, 2006).

DNA damage caused by ROS results in the formation of single and double strand breaks or nucleotide changes in the genetic code. For instance, the reaction of •OH radical with the C8 of purine bases cause a formation of 7,8-dihydro-8-oxo-2'-deoxyguanosine (8-oxoG), which subsequently leads to the alterations of the genetic code due to GC→TA transversion (Olinski et al., 2002). Oxidant-induced changes cause replication errors, mutations, genome instability and can lead to cell death (Klaunig et al., 2010). Fungal cells respond to ROS-induced DNA damage via the activation of the Rad53 checkpoint kinase and cell cycle arrest.

1.3.4.5 Degranulation

The respiratory burst generated by neutrophils in response to the pathogen recognition leads to the release of ROS and formation of the primary phagosome. The differential charge generated in this process provokes degranulation – a formation of secretory vesicles and the release of microbicidal compounds into the phagosome (Andrews and Sullivan, 2003). Antimicrobial peptides, such as defensins and lysosomal hydrolases, mediate non-oxidative fungal killing by intercalation into the membrane bilayer, resulting in osmotic perturbation (Mansour and Levitz, 2002). Two main types of antimicrobial peptides are α -defensins and β -defensins, with the prevalence of α -defensins in neutrophilic granules. The mechanism of defensins' action include non-lytic perturbation of the pathogen's membrane with a subsequent release of ATP (Dühring et al., 2015). Cathepsins G and B, protease-3 and phagosomal elastase are cationic serine proteases that are stored in the neutrophilic granules and essential for *C. albicans* killing in a murine model of systemic candidiasis (Reeves et al., 2002, Dühring et al., 2015). At the later stages of phagocytosis, *C. albicans* live cells can inhibit phagolysosome maturation, evading its own trafficking to lytic compartments and therefore supporting survival (Fernández-Arenas et al., 2009).

Altogether, the phagocytic cells employ a wide range of elegant mechanisms in order to recognise, uptake and kill the invading pathogen.

1.4 *Candida* spp. virulence determinants that allow survival in the host

Virulence is a complex phenomenon that underlines a cross-talk between the pathogen and the host, and both sides are important for such an interaction (Casadevall and Pirofski, 2001).

C. albicans and *C. glabrata* possess different virulence strategies (Brunke and Hube, 2013). In immunocompromised hosts, *C. albicans* behaves as an aggressive invader, actively suppressing the host immune machinery and acquiring nutrients important for survival from the host, without a regard for the survival of the host itself. This strategy ultimately, and very often, leads to the lethal infections. In contrast, *C.*

glabrata often behaves as a more ‘mild’ pathogen, avoiding serious harm to the host, resulting in its persistence and chronic nature of the infection (Brunke and Hube, 2013). The mechanisms of *Candida* spp. response to phagocytosis have been extensively studied in transcriptional and translational levels (Fernandez-Arenas et al., 2007, Fradin et al., 2003, Rubin-Bejerano et al., 2003, Fukuda et al., 2013), highlighting that these pathogenic fungi response to the state of the host by changing physiology.

In this section, I describe the main virulence traits of *C. albicans* and *C. glabrata*.

1.4.1 *Candida albicans* virulence determinants that allow survival following phagocytosis

Upon internalisation by phagocytic immune cells, the pathogen will face the combination of different stresses, and disease establishment requires the ability to survive within different host niches and being exposed to all armoury of host defences (Brown et al., 2014) (section 1.3.4). *C. albicans* possesses a wide repertoire of virulence factors and fitness attributes that promotes its pathogenicity (Brown et al., 2014).

The cohort of *C. albicans* virulence factors include: morphological flexibility (ability to switch between yeast and hyphal forms), adhesion molecules expressed on the cell surface, that facilitate fungal binding and penetration of host tissues, biofilm formation, extracellular lipolytic and proteolytic activity, and a range of fitness attributes (Jacobsen et al., 2012, Hube and Naglik, 2001, Mitchell, 1998).

The fitness attributes include the ability of the pathogen to adapt to the range of diverse environments encountered during infection. These include an ability to adapt to a wide range of pH environments, metabolic flexibility, powerful nutrient acquisition systems and robust stress response machineries (Mayer et al., 2013, Gow et al., 2011, Jacobsen et al., 2012).

In the following sections, the major virulence mechanisms of *C. albicans*, which specifically promote the pathogen’s survival during phagocytosis, are described in detail.

1.4.1.1 **Morphological switch**

Being a polymorphic fungus, *C. albicans* can exist in different morphological states: budding yeast, hyphae, pseudohyphae, hyperpolarised buds and chlamydospores (Whiteway and Bachewich, 2007, Sudbery et al., 2004). True hyphae are comprised of elongated cells with parallel-sided walls. Pseudohyphae consist of elongated cells with constrictions at the septa (Sudbery et al., 2004). Hyperpolarised buds are another form of *C. albicans* filamentous morphology, which have constrictions at the septa similar to pseudohyphae, but the nucleus moves from the mother cell to the polarized bud instead of nuclear division (da Silva Dantas et al., 2010). Clamydospores are thick-walled cells that are formed in response to suboptimal environments (Fabry et al., 2003). The host environment possesses multiple triggers of filamentation, such as serum, neutral pH, temperatures of 37 °C and elevated CO₂ concentrations, that all together enable the pathogen to switch from yeast form to hyphal or pseudohyphal morphology (Sudbery, 2011). Different environmental stimuli trigger *C. albicans* morphogenesis via distinct pathways. Both yeast and hyphal form promote the virulence of *C. albicans* via their specific roles in adhesion, invasion, damage, dissemination, immune evasion and host responses (Jacobsen et al., 2012). In this section, only *C. albicans* signalling pathways implicated in hyphal formation during phagocytosis are described.

Key signalling pathways that regulate morphological switching during phagocytosis include the cAMP-dependent protein kinase A (PKA) pathway that responds to serum, and the MAPK kinase Cek1 pathway that responds to nutrient limitation (Leberer et al., 2001, Feng et al., 1999, Csank et al., 1998). Ras1-mediated increases in cytosolic cAMP levels promote the activation of PKA and its downstream target, Efg1 transcriptional factor. Ras1 signalling also activates the Cek1 MAPK pathway, which in turn activates the transcription factor Cph1. Cek1, together with Efg1 and Cph2, regulates the expression of hyphae-specific genes (Rocha et al., 2001).

Morphogenesis is important for the pathogenicity of *C. albicans*. Successfully phagocytosed *C. albicans* cells can escape macrophage-mediated killing by switching to the hyphal form (Tavanti et al., 2006), with the subsequent piercing of

the phagosomal membrane and pathogen's escape (Lorenz et al., 2004). *C. albicans* mutant cells that are 'locked' in either yeast or hyphal form exhibit dramatically decreased virulence, indicating that morphological switch is important for virulence (Lo et al., 1997). Mutants lacking key transcriptional factors important for hyphal formation, Efg1 and Cph1, are avirulent in murine model of infection (Lo et al., 1997).

Recent studies provide compelling evidences that *C. albicans*-mediated macrophage killing is more than a result of the hyphae physically rupturing the macrophage. Hyphae have a distinct mechanism in surviving phagocytosis – pyroptosis, which is a host cell programmed macrophage death in the presence of fungal hyphae (Krysan et al., 2014). Pyroptosis is a lytic cell death pathway, which is dependent of the activation of caspase 1 following by the formation of the NLRP3 inflammasome.

1.4.1.2 *Metabolic flexibility*

C. albicans possesses a metabolic plasticity that helps the pathogen to survive in nitrogen and carbohydrate poor conditions. Facing a nutrient deprivation inside the phagosome, *C. albicans* rapidly switches its metabolism to a starvation mode. This includes upregulation of the enzymes responsible for energy acquisition by alternative catabolic processes, such as glyoxylate and tricarboxylic acid cycles, and the use of available lipids and fatty acids as an alternative energy source (Fernandez-Arenas et al., 2007). The induction of the glyoxylate cycle genes, isocitrate lyase (*ICL1*) and malate synthase (*MLS1*), within the phagosomal environment enables *C. albicans* to utilize two-carbon compounds in the absence of glucose. *C. albicans* mutants lacking *ICL1* are less virulent *in vivo* (Lorenz and Fink, 2001), demonstrating the importance of this nutrient adaptation for virulence.

Robust regulation of metabolic pathways is highly important for *C. albicans* virulence (Barelle et al., 2006). *C. albicans* is a Crabtree-negative fungus, which provides a metabolic advantage in phagosomal microenvironment: when glucose is available, the pathogen continues to assimilate alternative carbon sources alongside

the glucose, as the enzymes responsible for assimilation of the alternative energy sources are not subjected to catabolite repression (Childers et al., 2016).

Not only are genes responsible for catabolism of alternative energy sources induced, there is also a need to overexpress the transporters for non-fermentable energy sources such as mono- and dicarboxylic acids. Carbon source utilised by the fungus can promote the changes in the fungal cell wall composition, and therefore influence pathogen's recognition by innate immune cells. *C. albicans* cells that were grown on lactate as a major energy source were found to be less susceptible to phagocytosis by murine macrophages *in vitro* (Ene et al., 2013).

Other adaptations include up-regulation of the genes responsible for amino acids biosynthesis and transport (Fradin et al., 2005). In particular, genes responsible for amino acids biosynthesis, such as arginine, are upregulated following phagocytosis (Rubin-Bejerano et al., 2003, Fradin et al., 2005). The induction of arginine biosynthesis helps the fungus to generate extra quantities of CO₂ and urea, and this may contribute to the auto-induction of the hyphae via upregulation of the Rim101 pathway, as well as coping with the acidification of the phagosome (Miramon et al., 2013, Vylkova et al., 2011, Jiménez-López et al., 2013). Numerous other uptake systems are induced upon phagocytosis, including various permeases and transporters, to sequester available nutrients from the host cell and to maintain the pathogen's homeostasis (Lorenz et al., 2004).

Additionally, *C. albicans* is faced to the limitation of highly important microelements, such as iron, zinc and cooper. The pathogen response to such limitation includes an overexpression of the genes responsible for the uptake of trace elements, such as zinc scavengers (*PRA1*, *ZRT1*, *ZRT2*), ferric reductases (*FRE3*, *FRE7*) and cooper (*CTR1*, *SLF1*) uptake systems (Lorenz et al., 2004, Mayer et al., 2013, Fernandez-Arenas et al., 2007, Citiulo et al., 2012). The phenomenon of the active sequestration of the required metals has been referred to 'nutritional immunity' (Brunke and Hube, 2013).

Overall, the transcriptomic data provide compelling evidences of a substantial metabolic shift in phagocytosed *C. albicans* cells, suggesting that nutritional stress responses form a prominent part of the early response to phagocytosis (Lorenz et al.,

2004). Metabolic flexibility promotes *C. albicans* resistance to macrophage killing, host colonisation and virulence (Childers et al., 2016).

1.4.1.3 Stress responses

In *C. albicans* the stress response mechanisms evolved in concordance with the adaptation to the host, resulting in greater stress resistance of the pathogen compared to non-pathogenic yeast *S. cerevisiae* and *S. pombe* (Nikolaou et al., 2009). Yeasts respond to oxidative and osmotic stress by the induction of similar groups of genes, and key regulatory factors are conserved throughout pathogenic and non-pathogenic fungal species (Enjalbert et al., 2006, Enjalbert et al., 2003). However, the mechanisms underlying the regulation of the stress-responsive transcriptomes in some cases have diverged between *C. albicans* and the benign model yeasts *S. cerevisiae* and *S. pombe*. In this section, the mechanisms of *C. albicans* stress responses that are relevant to the phagocytic microenvironment will be discussed, with particular emphasis on oxidative stress responses, as this is the focus of this thesis.

1.4.1.3.1 pH adaptation

C. albicans adaptations to phagosomal pH include the alkalinisation of the microenvironment through the release of ammonia via amino acid breakdown, which promotes the yeast-hyphal transition and thus virulence of the fungus (Vylkova et al., 2011). Stp2 is required for the modulation of the pH in the phagosome (Vylkova and Lorenz, 2014). Stp2 is a transcription factor that is involved in the regulation of genes that control amino acid permeases (Martínez and Ljungdahl, 2005). These data support the fact that for active alkalinisation of the media *C. albicans* requires exogenous amino acids (Vylkova and Lorenz, 2014). *C. albicans* mutants lacking *STP2* are unable to induce hyphal transition under alkaline pH and therefore cannot escape from phagocytosis, resulting in their attenuated virulence (Vylkova and Lorenz, 2014). Δ *stp2* mutant strains are also more sensitive to the killing by innate immune cells and unable to alkalinise the acidic pH within the phagosome, but at the

same time, they are not more sensitive to other phagosome-induced stresses, such as oxidative or nitrosative stress (Vylkova and Lorenz, 2014).

The induction of amino acid biosynthetic pathways as a result of nutrient starvation might be also a mechanism of neutralisation of the acidic pH via breakdown products, carbon dioxide and urea, enabling the filamentation and escape from the macrophages (Vylkova et al., 2011, Miramon et al., 2013). Recent reports indicate that *C. albicans* can actively raise the pH of the media *in vitro* from pH=4 to pH=7 in less than 12 hours, leading to the auto induction of hyphae and expulsion from the macrophage cell (Vylkova et al., 2011, Bain et al., 2012). This phenomenon is the case for both solid and liquid culture. Importantly, carbon depletion is needed to trigger alkalinisation of the milieu, as the presence of glucose inhibits alkalinisation (Vylkova et al., 2011).

Exogenous pH changes influence the gene expression profile in *C. albicans*, and the pathogen has acquired different strategies to cope with pH fluctuations within the host. Rim101 is a key transcriptional factor that is responsible for pH adaptation in *C. albicans* under alkaline conditions, including alkaline-induced filamentous growth, and is vital for *C. albicans* virulence (Davis et al., 2000a, Davis et al., 2000b). Taking into consideration the fact that phagosomal pH is not maintained low, but rapidly arise to pH=8 following phagocytosis (Reeves et al., 2002), the Rim101-dependent pH response downstream of the Stp2-mediated alkalinisation of the media is vital for *C. albicans* to escape the phagocytic attack.

1.4.1.3.2 Cationic stress response

The influx of K⁺ ions into the phagosome generates both cationic and osmotic stresses. An important regulator of the cationic/ osmotic stress response in *C. albicans* is the Hog1 stress activated protein kinase (SAPK). Hog1 belongs to a family of mitogen activated protein kinases (MAPKs). First described in *S. cerevisiae*, the Hog1 (High Osmolality Glycerol) MAPK pathway plays a central role in the osmotic stress response and is a conserved eukaryotic signal transduction module (Hohmann, 2002, Gustin et al., 1998).

The MAPK is activated by a cascade of kinases, which includes a MAP kinase kinase kinase (MAPKKK), which activates the downstream MAP kinase kinase (MAPKK) by phosphorylation of conserved Ser and Thr residues, which in turn activates the MAPK by phosphorylation of Tyr and Thr residues within the kinase domain. The activated MAPK then phosphorylates target substrates including transcription factors, leading to the activation of the downstream responses (Figure 1.3) (Smith et al., 2004).

SAPKs are MAPKs that are specifically activated in response to stress stimuli (Nguyen and Shiozaki, 1999). Examples of SAPKs are Hog1 in *S. cerevisiae* and *C. albicans*, Sty1 in *S. pombe*, and p38 in mammalian cells. Despite the conservation of the SAPK pathways, their components and regulators have diverged in different organisms. For example, the *S. cerevisiae* MAPK pathway consist of a single MAPKK Pbs2 and three MAPKKKs – Ssk2, Ssk22 and Ste11 (Smith et al., 2010). In contrast, in *C. albicans* MAPK pathway comprises of a single MAPKKK Ssk2, which drives the activation of the MAPKK Pbs2, which in turn phosphorylates Hog1, leading to its nuclear accumulation and the induction of osmoprotective genes such as *GPD1* and *GPP1* (Cheetham et al., 2011, Arana et al., 2005, Cheetham et al., 2007) (Figure 1.3). In fungi two-component related signal transduction pathways play an important role in stress sensing and signalling (Fassler and West, 2013, Stock et al., 2000).

Fungal two-component signalling pathway is a multi-step system that comprises of three classes of proteins, a histidine protein kinase, an intermediary phosphorelay protein, and a response regulator. When stimulated, the bipartite histidine kinase autophosphorylates itself on a histidine residue, leading to the formation of high energy phosphohistidine intermediate, which in turn is transferred to an aspartate residue on an adjacent receiver domain (Moye-Rowley, 2003). This is then transferred to a histidine on the phosphorelay protein and the finally to an aspartate on the receiver domain of the terminal response regulator. In *C. albicans* Hog1-mediated osmotic stress signalling requires Sln1 histidine kinase, Ypd1 phosphorelay protein, and the response regulator Ssk1 (Yamada-Okabe et al., 1999, Calera et al., 2000, Chauhan et al., 2003, Bruce et al., 2011).

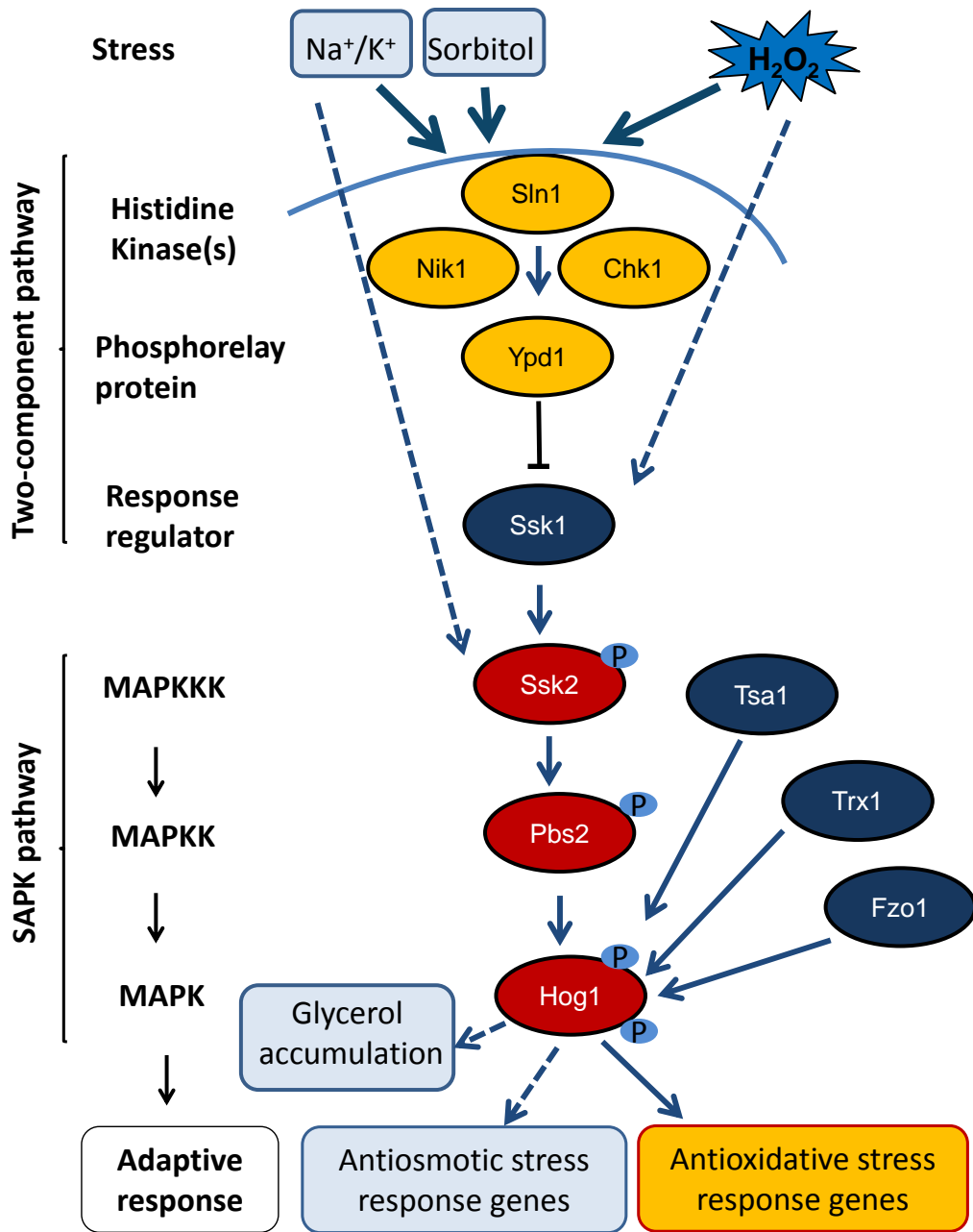


Figure 1.3 Hog1 SAPK signalling in response to osmotic and oxidative stress in *C. albicans*.

The core components of the SAPK pathway are shown in red, whereas two-component signalling proteins are shown in yellow. Proteins that are required specifically for H_2O_2 -induced Hog1 activation are shown in navy, including the response regulator Ssk1, and redox sensitive components of the peroxiredoxin/ thioredoxin system Tsa1 and Trx1, as well as mitochondria biogenesis factor Fzo1. Dashed lines indicate that the pathways are not fully characterised. Adapted from (Smith et al., 2010, Dantas et al., 2015, Chauhan et al., 2006).

The Sln1-Ypd1-Ssk1 phosphorelay has been extensively characterised in *S. cerevisiae*: it is halted upon osmotic stress, resulting in accumulation of unphosphorylated Ssk1, which is a potent activator of the Ssk2/ Ssk22 MAPKKs (Posas and Saito, 1998, Posas et al., 1996). When *S. cerevisiae* is exposed to osmotic stress, Hog1 is activated via a cascade of upstream kinases, Sln1 and Pbs2 MAPKK (Posas et al., 2000). Phosphorylation of *S. cerevisiae* Hog1 on two conserved sites – Thr174 and Tyr176 – is essential for the activation and the nuclear translocation of the kinase (Brewster et al., 1993). Similarly in *C. albicans*: in response to osmotic stress, the conserved TGY motif within Hog1 becomes phosphorylated, resulting in translocation to the nucleus (Smith et al., 2004, Dantas et al., 2015, Bellon et al., 1999). The activated SAPK then triggers the induction of osmoprotective genes and accumulation of an intracellular osmolite glycerol (Enjalbert et al., 2006). Hog1 activation also leads to the downstream activation of Sko1, resulting in induction of the genes that encode the ionic transporters, such as Eno1 (Na^+ importin) (Marotta et al., 2013).

In addition to osmotic response, the *C. albicans* Hog1 SAPK is activated in response to other physiologically relevant stress stimuli, such as oxidative stress and antimicrobial peptides (Smith et al., 2004, Alonso-Monge et al., 2003). The function of *C. albicans* Hog1 in oxidative stress responses is expanded in the section 1.5.2.1.

Hog1 signalling is essential for *C. albicans* virulence in a diverse range of infection models, including the murine model of systemic infection (Alonso-Monge et al., 1999, Román et al., 2007) and commensal model (Prieto et al., 2014). In addition, cells lacking Hog1 or any upstream components of the Hog1 signalling pathway are more susceptible to the killing by neutrophils (Arana et al., 2007, Herrero-de-Dios et al., 2014, Alonso-Monge et al., 1999) and macrophages (Patterson et al., 2013).

Another SAPK, Cek1 has been mainly described for its role in cell wall biogenesis of *C. albicans* (Román et al., 2005), although a recent study has shown that it is also involved in the osmotic stress response and cooperates with Hog1 (Herrero-de-Dios et al., 2014).

1.4.1.3.3 Nitrosative stress response

C. albicans possesses a rapid mechanism to sense and respond to •NO radicals, produced by neutrophils. Flavohemoglobins are known to counteract RNS in many fungi. The *C. albicans* genome encodes three different flavohemoglobins –Yhb1, Yhb4 and Yhb5, but only one – Yhb1 – is important for •NO scavenging (Hromatka et al., 2005, Ullmann et al., 2004). Yhb1 acts as nitric oxide dioxygenase, and detoxifies harmful •NO radicals by aerobic binding to the heme cofactor with a formation of harmless nitrate and ferric flavohemoglobin, and subsequent reduction of the enzymes via electron transfer between NADPH and its FAD-oxidoreductase domain (Hromatka et al., 2005). *C. albicans* *yhb1* null mutants are sensitive to RNS and exhibit an attenuated virulence in the murine model of disseminated candidiasis (Ullmann et al., 2004, Hromatka et al., 2005).

The regulation of the transcriptional responses to RNS is mediated by the opposing action of two transcriptional factors – Cta4 and Cwt1. Cta4 is a positive regulator that triggers •NO sensing *in vivo* through the binding to the nitric oxide responsive element (NORE) within the *YHB1* promoter that results in *YHB1* expression (Chiranand et al., 2008). Cwt1 is responsible for the negative regulation of the nitrosative stress transcriptome (Sellam et al., 2012, Miramon et al., 2013).

1.4.1.3.4 Oxidative stress response

In the host, *C. albicans* is exposed to exogenous ROS generated by the oxidative burst by the phagocytic NADPH oxidase complex. In addition, some bacteria that are common inhabitants of the polymicrobial community of the human GI tract actively produce exogenous ROS in their surroundings. For instance, *Enterococcus faecalis* and *Lactobacillus acidophilus* use the generation and excretion of the ROS to combat competing species (Fitzsimmons and Berry, 1994, Huycke et al., 2002). Therefore, antioxidant responses are vital for *C. albicans* to shield itself not only from the phagocytes, but also from other competing species (Cruz et al., 2013, Fitzsimmons and Berry, 1994).

Analysis of *C. albicans* proteome and transcriptome during co-cultivation *in vitro* with human serum (Aoki et al., 2013) and *ex vivo* with neutrophils (Fradin et al., 2005) revealed, that pathogen expresses a large set of genes that have the potential to detoxify ROS. Subsequently, major protein pools that are induced during phagocytosis tightly associated with oxidative stress responses. A detailed description of the mechanisms underlying these responses described in section 1.5.

1.4.2 *Candida glabrata* virulence determinants

C. glabrata does not belong to the CUG clade (the members of CUG clade translate the CUG codon to Ser instead of Leu) in contrast to other pathogenic *Candida* species, such as *C. albicans*, *C. dubliniensis*, *C. tropicalis* or *C. parapsilosis*, and shares high genetic similarity to *S. cerevisiae* (Dujon et al., 2004). Consistently, the mechanisms employed by *C. glabrata* to withstand the phagocytic attack and promote its virulence differ from those of *C. albicans*.

Examination of the transcriptional responses of *C. glabrata* in response to phagocytosis illustrate that similar groups of genes are up regulated as those seen in *C. albicans* – including genes involved in nutrient acquisition, metal homeostasis, cell wall biosynthesis and stress responses (Rai et al., 2012, Kaur et al., 2007, Seider et al., 2011). Similarly to *C. albicans* (Bain et al., 2014), while engulfed by the phagocyte, *C. glabrata* actively inhibits phagosomal maturation, preventing its acidification and ROS production, perturbing cytokine signalling, which together enable fungal persistence within the macrophage (Seider et al., 2011). A recent report indicates a prominent role of autophagy, especially pexophagy, in *C. glabrata* survival following phagocytosis (Roetzer et al., 2010). This phenomenon could be explained as an alternative way to acquire amino acids as an energy source in the nutrient-poor environment of the phagosome, whereas for *C. albicans* such auto-recycling systems are not essential for survival (Palmer et al., 2007). *C. glabrata* also experiences glucose starvation following phagocytosis (Roetzer et al., 2010, Fukuda et al., 2013), leading to its metabolic adaptation by switching to alternative energy

acquisition strategies, such as the glyoxylate cycle, gluconeogenesis and lipid β -oxidation (Kaur et al., 2007).

Similar to *C. albicans*, *C. glabrata* is also able to alter the phagosomal pH, but the mechanism differs from that for *C. albicans* (Vylkova and Lorenz, 2014, Seider et al., 2011). Phagolysosomes that contain *C. glabrata* cells fail to recruit cathepsin D and are only weakly acidified, causing the inhibition of the phagolysosomal fusion and maturation (Seider et al., 2011).

In contrast to the diploid polymorphic *C. albicans*, *C. glabrata* does not undergo yeast to hyphal transition following phagocytosis, and usually exists in the haploid yeast form (Kaur et al., 2005). Also *C. glabrata* does not secrete the proteolytic enzymes that are the characteristic trait of *C. albicans* virulence (Kaur et al., 2005). Although *C. glabrata* is able to successfully counteract the attack of immune cells, unlike *C. albicans* this fungus can proliferate within macrophages, but not neutrophils (Seider et al., 2014). These findings suggest that the neutrophil environment is too harsh for the pathogen and although ROS do not seem to play a major role in *C. glabrata* clearance following the phagocytosis by macrophages, the efficiency of neutrophil-mediated phagocytosis is largely determined by the NADPH-oxidase driven ROS attack (Seider et al., 2014). *C. glabrata* does not kill the macrophages, but persists intracellularly and can undergo major microevolutional events. When *C. glabrata* co-existed with murine macrophages for a prolonged time, a point nucleotide mutation occurred in the chitin synthase-encoding *CHS2* gene. This new SNP led to global changes in cellular morphology from typical yeasts to pseudohyphae-like structures, and had a large impact on cell wall composition. The new strain was hypervirulent in a murine model of infection and more able to escape from immune attack (Brunke et al., 2014).

C. glabrata is still able to survive in the hostile phagosomal environment due to the potent antioxidant mechanisms, and is extremely resistant to high doses of oxidative stress (Roetzer et al., 2011). The mechanisms of *C. glabrata* oxidative stress resistance will be discussed in more detail in the section 1.6.1.

Robust chromatin remodelling and modification strategies are crucial for *C. glabrata* survival upon phagocytosis to withstand ROS-mediated DNA damage and

adapt to the nutrient poor environment of the phagosome. Impairment of chromatin organisation and DNA repair mechanisms cause fungal avirulence in a murine model of infection and *ex vivo* internalisation by human MDMs (Rai et al., 2012).

1.5 Oxidative stress responses

ROS generation by phagocytic NADPH oxidase promotes the activation of key fungal protective responses aiding the pathogen to survive. Although the oxidative stress response mechanisms employed by *C. albicans* are similar to those found in non-pathogenic fungi, such as *S.cerevisiae* and *S. pombe* (Nikolaou et al., 2009), it has also tuned its stress responses to promote its survival within the host. Extensive transcriptomic and proteomic profiling *in vitro* revealed that large numbers of antioxidant genes are upregulated during the contact with the host (Enjalbert et al., 2006, Kusch et al., 2007, Yin et al., 2009). The mechanisms of the oxidative stress response in *C. albicans* are niche-specific: some of the key antioxidant genes, such as *CTA1*, *TRX1* and *TTR1* are only upregulated following the contact with neutrophils, but not macrophages (Enjalbert et al., 2007, Lorenz et al., 2004). At the initial stages of bloodstream infection, the oxidative stress response machinery is rapidly induced, largely as a response to the phagocytic oxidative burst. At the later stages, when the infection is already established (for example when *C. albicans* colonises the kidney), only minor incitement of antioxidant gene expression is observed (Enjalbert et al., 2007, Walker et al., 2009, Thewes et al., 2007). These findings highlight the physiological importance of ROS-mediated fungal killing by innate immune cells. In turn, *C. albicans* possesses wide repertoire of the antioxidant mechanisms to counteract ROS attack. Key mechanisms employed by the pathogen to withstand oxidative stress will be considered in the following sections.

1.5.1 ROS detoxification systems employed by *C. albicans*

C. albicans employs different mechanisms to survive the oxidative burst generated by the innate immune cells. ROS scavenging systems present as non-enzymatic and enzyme-mediated detoxification mechanisms. Non-enzymatic

detoxification involves ROS scavenging molecules that are able to bind directly to ROS and detoxify harmful free radicals. These include the tripeptide glutathione (GSH), the disaccharide trehalose, tocopherols, and ascorbic acid. Enzyme-mediated defences against free radicals require the function of the specific enzymes, such as catalase, different superoxide dismutases (SODs), and peroxidases.

1.5.1.1 *Non-enzymatic detoxification of reactive oxygen species*

A number of small bioactive molecules are widely employed to detoxify ROS, such as glutathione and trehalose.

Glutathione is a ubiquitous redox buffer that plays a pivotal role in ROS detoxification and oxidative stress protection of the eukaryotic cells (Ayer et al., 2010). In living cells glutathione exists in both oxidised (GSHG) and reduced (GSH) forms, and the conversion between different oxidation states is controlled by glutathione reductase in an NADPH-dependent manner (Tillmann et al., 2015). Reduced GSH is an active donor of electrons that can directly scavenge ROS or prevent irreversible protein oxidation by S-thiolation (Garcerá et al., 2010). *Candida* cells with depleted levels of GSH are highly susceptible to oxidative killing and show attenuated virulence (Yadav et al., 2011, Chaves et al., 2007).

Similar to other fungi, *C. albicans* accumulates reserve sugars, such as disaccharide trehalose, in response to oxidative and heat shock stresses. Trehalose prevents the fungus from ROS-induced apoptosis (Lu et al., 2011, Alvarez-Peral et al., 2002). Notably, the induction of the genes that are involved in stress-induced trehalose biosynthesis and accumulation in *C. albicans* is much lower than for example in *S. cerevisiae* (Enjalbert et al., 2003). Mutants deficient in trehalose production display attenuated virulence (Zaragoza et al., 1998) and decreased resistance to killing by macrophages or neutrophils (Martínez-Esparza et al., 2007, Mayer et al., 2012).

1.5.1.2 Enzyme-mediated detoxification of reactive oxygen species

1.5.1.2.1 Superoxide dismutases

Superoxide dismutases (SODs) act by dismutating the superoxide anion (O_2^-) into molecular oxygen (O_2) and hydrogen peroxide (H_2O_2) (Frohner et al., 2009). The evolutionarily expansion of the SOD family has been suggested to explain the enhanced resistance of *C. albicans* to ROS compare to other non-pathogenic fungi (Dantas et al., 2015).

The genome of *C. albicans* encodes six SODs. SODs 1-3 are intracellular and SODs 4-6 are extracellular (Miramon et al., 2013, Mayer et al., 2013, Frohner et al., 2009, Dühring et al., 2015). SODs are metalloproteins by biochemical nature, and all have metal ions incorporated into their catalytic centre: SOD1 and cell surface SODs 4-6 contain cooper and zinc or copper, whereas SOD2 and SOD3 are manganese-dependant (Martchenko et al., 2004, Frohner et al., 2009, Lamarre et al., 2001). A recent study revealed that SOD5 lacks an active zinc-binding domain and is solely copper-dependent: this appears to be an adaptation to the poor availability of zinc but not copper. Macrophages liberate high levels of copper as an antimicrobial defence mechanism. Thus in *C. albicans*, which have extracellular SODs that can accept Cu without a copper chaperone, it appears to be a specific adaptation to promote pathogenicity (Gleason et al., 2014). The expression of SODs is morphology-specific: while SOD4 is expressed predominantly in yeast form, SOD5 is usually associated with hyphal morphology (Heilmann et al., 2011). SOD1 is cytosolic and essential to survive phagocytosis by macrophages (Hwang et al., 2002). SOD2 is mitochondrial and its induced expression is observed following contact with neutrophils (Chaves et al., 2007). SOD2 does not appear inducible in response to low levels of the hydrogen peroxide *in vitro* (Enjalbert et al., 2003). Due to the ability of the innate immune cells to excrete ROS into the outer milieu (Miramon et al., 2012), the primary function of the extracellular SODs is detoxification of the extracellular ROS (Dühring et al., 2015, Frohner et al., 2009). Following co-culture with either macrophages or dendritic cells, *C. albicans* mutants lacking SOD4 or SOD5 show a dramatic increase in the levels of extracellular ROS, but not when co-cultured with mutant macrophages cell line lacking an active NADPH oxidase (Frohner et al., 2009). SOD1, SOD4 and SOD5 are

required for full virulence in murine model of systemic candidiasis (Hwang et al., 2002, Wysong et al., 1998, Martchenko et al., 2004).

1.5.1.2.2 Peroxidases

Catalase is one of the key antioxidant enzymes in aerobic organisms, and shown to be highly important for antioxidant defence in various fungi (Wysong et al., 1998, Cohen et al., 1988, Kawasaki et al., 1997, Ueda et al., 1990). It works by the conversion of hydrogen peroxide (H_2O_2) into water (H_2O) and oxygen (O_2). *C. albicans* possesses a single *CAT1* gene encoding catalase, which is essential for pathogen's survival following the attack by human neutrophils *in vitro*, as well as in systemic model of murine candidiasis (Wysong et al., 1998, Chauhan et al., 2006, Nakagawa et al., 2003, Enjalbert et al., 2007, Fradin et al., 2005).

Two other families of peroxidases with additional roles in stress signalling, besides the ROS detoxification, are the components of the glutaredoxin and thioredoxin systems.

The glutaredoxin system comprises of glutathione peroxidases (Gpxs) and glutathione reductases (Grxs). Glutathione peroxidases are enzymes involved in the detoxification of H_2O_2 , resulting in a formation of the oxidised glutathione, with its further reduction by glutathione reductases via electron transfer from NADPH (Miramon et al., 2013). *C. albicans* genome encodes four ORFs with hypothetical glutathione peroxidase activity (Patterson et al., 2013). In addition to a direct role in ROS scavenging, Gpxs are also involved in oxidative stress signalling: for instance, Gpx3 is essential for the ROS-mediated oxidation and activation of the key oxidative stress responsive transcription factor Cap1 (Patterson et al., 2013). *C. albicans* Gpxs and Grxs are found to be essential for the pathogen's survival upon exposure to phagocytes (Patterson et al., 2013).

An additional antioxidant mechanism in *C. albicans* is a thioredoxin system (da Silva Dantas et al., 2010). *C. albicans* thioredoxins act in system composed of thioredoxin (Trx1), thioredoxin reductase (Trr1) and the thioredoxin peroxidase (peroxiredoxin) Tsa1 (Figure 1.4). The function of Trx1 and Trr1 is to reduce

disulphide bonds of the oxidised protein substrates in NADPH-dependant manner, as well as to reduce Tsa1, which becomes oxidised upon reducing of H_2O_2 . Peroxiredoxins (Prxs) possess peroxidase activity and are directly oxidised upon reduction of H_2O_2 , and their reduction and reactivation is dependent on the thioredoxin Trx1. The Tsa1 is a 2-cys peroxiredoxin in *C. albicans*, associated with the cell wall in hyphal cells (Urban et al., 2005), but dispensable for *C. albicans* virulence (Urban et al., 2005). Prx1 is a 1-cys peroxiredoxin that accumulates in the nucleus of the cells in hyphal morphology (Srinivasa et al., 2012). The genes that encode the components of peroxiredoxin-thioredoxin system *TSA1*, *TRX1* and *TRR1* are up-regulated following the contact with phagocytes (Fradin et al., 2005, Fernandez-Arenas et al., 2007, Enjalbert et al., 2007) and essential for *C. albicans* oxidative stress resistance *in vitro* as a part of oxidative signal transduction mechanisms (da Silva Dantas et al., 2010).

In summary, a dramatic induction of *C. albicans* genes that encode ROS detoxifying enzymes is seen in certain host niches. The generation of such antioxidants as peroxidases, SODs, thioredoxins and glutaredoxins enable the fungus to detoxify the ROS and survive the ROS attack. Many of the antioxidant genes, discussed in this section, are important for *C. albicans* virulence *in vivo*.

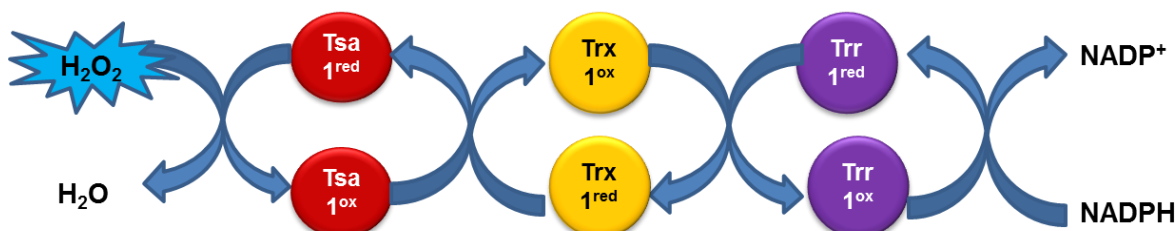


Figure 1.4 Schematic diagram of thioredoxin / peroxiredoxin system in *C. albicans*.

H_2O_2 is directly detoxified by peroxiredoxin Tsa1 (Tsa1^{red}), which becomes oxidised (Tsa1^{ox}). Thioredoxin Trx1 reduces Tsa1^{ox} and becomes oxidised (Trx1^{ox}). Oxidised thioredoxin is reduced by thioredoxin reductase (Trr1^{red}), which in turn becomes oxidised (Trr1^{ox}). NADPH is a terminal electron donor that promotes the reduction of the oxidised Trr1^{ox} with the formation of Trr1^{red} . Adapted from (da Silva Dantas et al., 2010).

1.5.2 Oxidative stress-responsive signalling pathways in *C. albicans*

In *C. albicans* there are three major signalling pathways activated by ROS. These include the Hog1 SAPK pathway (Smith et al., 2004), the Rad53 DNA damage checkpoint pathway (Shi et al., 2007, da Silva Dantas et al., 2010), and the Cap1 AP-1 like transcription factor (Wang et al., 2006). The activation of these pathways in response to the phagocytic oxidative burst aids the pathogen to sense and adapt to ROS (Figure 1.5) (detailed in the following sections).

In addition, there are other mechanisms that play role in ROS sensing and response of this fungal pathogen, such as cAMP/PKA signalling and various checkpoint kinases (Dantas et al., 2015). While the adenylyl cyclase pathway is known to decrease fungal resistance to the oxidants (Deveau et al., 2010), *C. albicans* cells lacking certain spindle checkpoint kinases such as Mps1 are hypersensitive to ROS (Kamthan et al., 2014). Two members of Hsp70 family – Ssa1 and Ssa2 – are also involved in oxidative stress protection in *C. albicans* (Cuéllar-Cruz et al., 2014).

1.5.2.1 The Stress Activated Protein Kinase Hog1

In addition to the role in cationic stress response (section 1.4.1.3.2), the Hog1 SAPK is activated in response to ROS. Hog1 is rapidly phosphorylated and accumulates in the nucleus following the exposure of *C. albicans* to H₂O₂ (Smith et al., 2004). Hog1 activation in response to oxidative stress requires the upstream Pbs2 MAPKK, and the Ssk2 MAPKKK (section 1.4.1.3.2 and Figure 1.3).

Although Hog1 is activated in response to oxidative stress (Smith et al., 2004, Enjalbert et al., 2006), the precise role of Hog1 signalling in *C. albicans* oxidative stress response remains unknown. In contrast to *S. pombe* SAPK Sty1, Hog1 is only activated following exposure of *C. albicans* cells to relatively high levels of H₂O₂ (Smith et al., 2004). In the model yeast *S. pombe*, Sty1 is essential for the transcription of key antioxidant genes encoding catalase and glutathione peroxidase (Chen et al., 2003). This is not the case in *C. albicans*, as Hog1 is dispensable for antioxidant gene expression (Enjalbert et al., 2006).

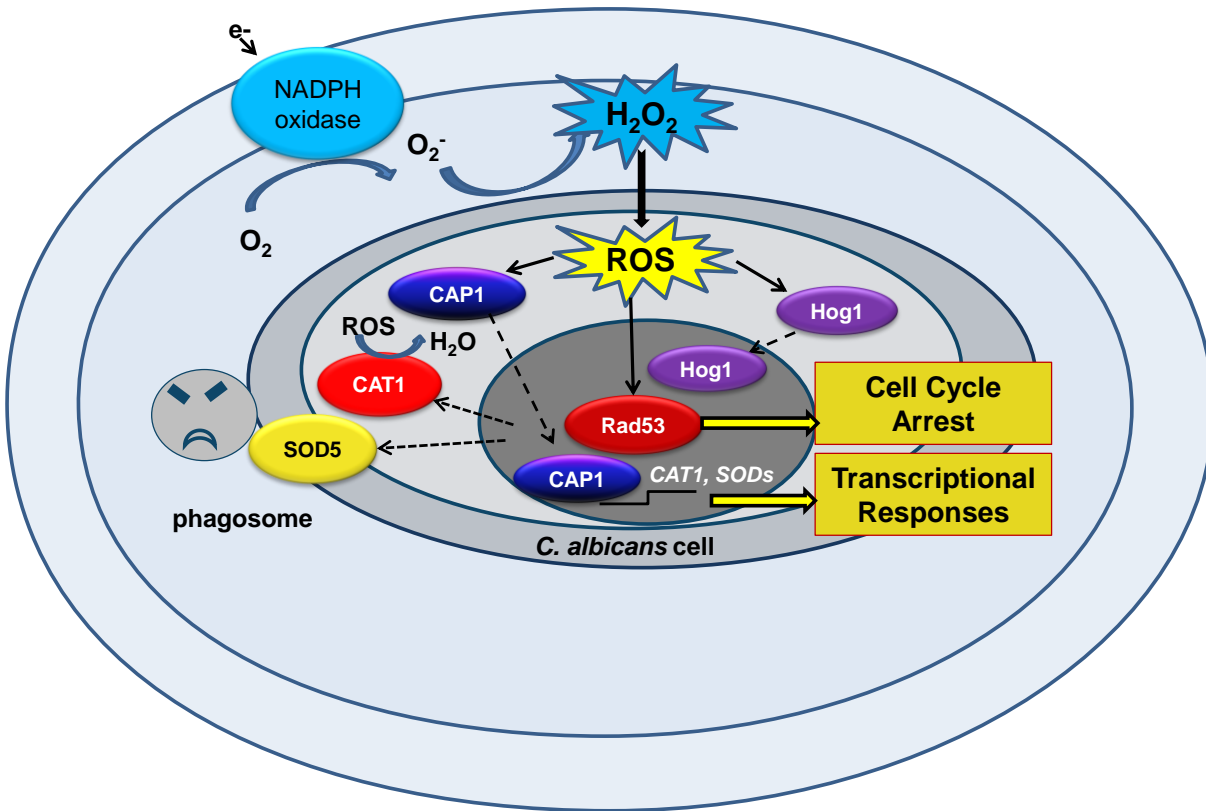


Figure 1.5 Generation of reactive oxygen species (ROS) in the phagosome and the pathways that respond to ROS in *Candida albicans*.

Activation of the phagocyte triggers the assembly of the NADPH oxidase complex, which generates high levels of superoxide within the phagosome. Superoxide is rapidly converted to H_2O_2 and other ROS. Three key signalling pathways activated in response to oxidative stress in *C. albicans* are Cap1, Hog1 and Rad53. Adapted from (Brown et al., 2009, da Silva Dantas et al., 2010).

Two-component regulation of Hog1 in response to H₂O₂ requires the Ssk1 response regulator (Chauhan et al., 2003). However, there are no reports of Hog1 activation in response to H₂O₂ requiring the upstream histidine kinases. *C. albicans* possess three histidine kinases – Chk1, Sln1 and Nik1, but their deletion does not impair Hog1 activation in response to the oxidative stress (Román et al., 2005, Menon et al., 2006). The activation of *C. albicans* Hog1 in response to ROS does require the thioredoxin peroxidase Tsa1, the thioredoxin Trx1, and the mitochondria biogenesis factor Fzo1 (Veal et al., 2004, da Silva Dantas et al., 2010, Thomas et al., 2013). In *S. pombe*, H₂O₂-induced activation of Sty1 requires the Tsa1 orthologue Tpx1 (Veal et al., 2004). The role of thioredoxin Trx1 in ROS-induced Hog1 activation is not fully understood: Trx1 regulates the redox status of Tsa1, and mutants lacking *TRX1* experience impaired H₂O₂-induced Hog1 activation, however, the catalytic cysteine residues of Tsa1, which are reduced by Trx1, are dispensable for Hog1 activation (da Silva Dantas et al., 2010). Interestingly, mitochondrial mutants are defective in Hog1 activation (Alonso-Monge et al., 2009), suggesting that oxidative stress-induced activation of Hog1 could be related to its role in respiratory function.

1.5.2.2 The Rad53 DNA damage checkpoint kinase

The Rad53 DNA damage checkpoint kinase pathway is activated in response to ROS. When *C. albicans* senses H₂O₂, Rad53 is rapidly phosphorylated on conserved threonine-glutamine or serine-glutamine sites, leading to the formation of hyperpolarised buds (section 1.4.1.1) (da Silva Dantas et al., 2010). Formation of hyperpolarised buds is linked to the cell cycle arrest (Shi et al., 2007). As a consequence of sustained cell cycle arrest, polarized growth progress in a dose-dependent manner with the higher level of induction upon treatment with higher H₂O₂ concentrations (Nasution et al., 2008).

The activators of Rad53 are not described in *C. albicans*, although the negative regulation of this checkpoint kinase by the thioredoxin Trx1, suggests a role of protein oxidation in the activation of the pathway (da Silva Dantas et al., 2010). *C. albicans* mutants with the deletion of Rad53, or with impaired function of its kinase

domain, are unable to form hyperpolarized buds in response to oxidative stress (Shi et al., 2007, Loll-Krippleber et al., 2014, da Silva Dantas et al., 2010).

1.5.2.3 Fungal AP-1 like transcription factors

The bZip protein superfamily includes transcription factors that have a specific highly conserved basic region (BZ) responsible for DNA binding and a leucine zipper (LZ) domain with a key role in protein dimerization (Amoutzias et al., 2006). bZip proteins are known to be regulated by oxidation and phosphorylation of conserved cysteine and serine residues respectively (Amoutzias et al., 2006). Posttranslational modification of transcriptional factors via oxidation is a widely accepted common mechanism of transcriptional regulation in response to external stimuli in a variety of organisms – from OxyR and SoxRS in *E.coli*, to human regulators such as AP-1, p53 and NF- κ B. Redox changes then cause an alteration in gene expression and subsequently – inhibition or activation of the signal transduction pathways (Marshall et al., 2000).

The AP-1 like transcription factors are conserved throughout the fungal kingdom with key roles in the oxidative stress response. AP-1 like proteins share a similar domain structure with an N-terminal domain involved in DNA binding to its target sequences, a leucine zipper motif (bZip) that is important for dimerization, and a C-terminus regulatory acidic domain (Figure 1.6). Within this C-terminal domain are two cysteine-rich domains that are indispensable for the H_2O_2 -driven activation of the protein (Alarco et al., 1997).

Representatives of AP-1 like factors are *S. cerevisiae* Yap1, *S. pombe* Pap1 and *C. albicans* Cap1. Their regulation and function in oxidative stress responses will be further discussed in detail below.

1.5.2.3.1 *S. cerevisiae* Yap1

S. cerevisiae Yap1 involves in pleiotropic drug resistance and plays a key role in mediating oxidative and heavy metal stress responses (Fernandes et al., 1997).

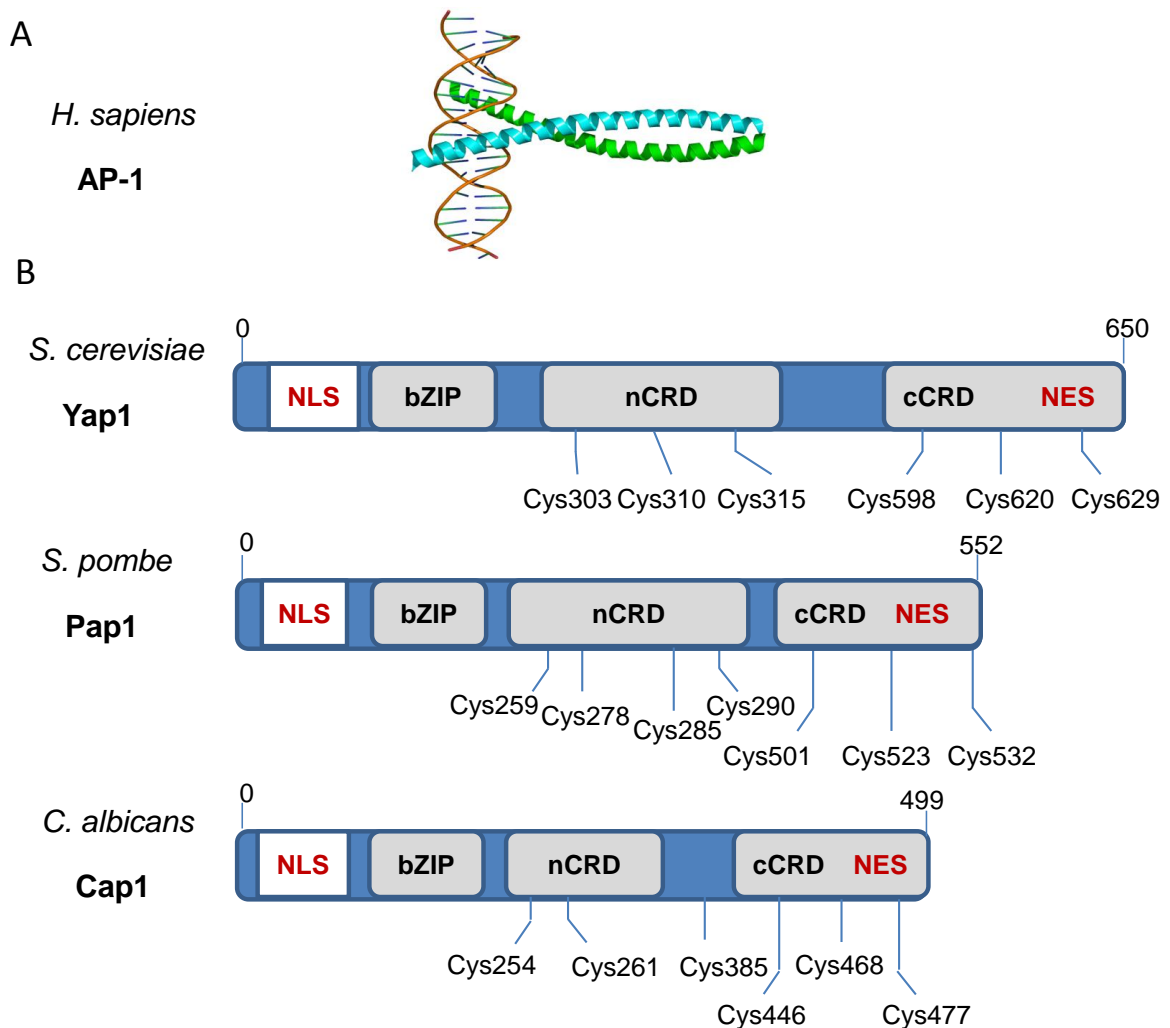


Figure 1.6 AP-1like transcriptional factors.

(A) Crystal structure of human AP-1 transcriptional factor heterodimer, comprising of c-Fos and c-Jun (Glover and Harrison, 1995).

(B) Yeast AP1-like transcriptional factors have three conserved domains: bZip DNA binding domain and two cysteine-rich domains (c-CRD and n-CRD), containing redox-sensitive cysteine residues. A nuclear export sequence (NES) is located within c-CRD, whereas a nuclear localisation sequence (NLS) is found at the N-terminus of a protein. Adapted from (Wood et al., 2003, Calvo et al., 2013, Alarco et al., 1997).

To date, Yap1 is perhaps the best characterised fungal AP-1 like transcription factor. Yap1 was firstly described by its homology to human AP-1 (Moye-Rowley et al., 1988) (Figure 1.6). The studies of Yap1 regulation in response to oxidative stress have provided a paradigm for redox regulation of fungal AP-1 like transcriptional factors.

The activation of Yap1 is determined by its nuclear localisation with the subsequent posttranslational modifications via oxidation and phosphorylation, and the activation of the Yap1-dependent transcriptome. Under non-stressed conditions Yap1 freely shuttles between the cytoplasm and the nucleus due to the interaction of the nuclear export sequence (NES), located at the C-terminus of Yap1, with the b-karyopherin-like nuclear exporter Crm1 (Delaunay et al., 2000, Yan et al., 1998). H₂O₂-induced oxidation triggers a conformational change within Yap1 by the formation of reversible interdomain disulphide bonds between the carboxyl-terminal cysteine-rich domain (c-CRD) and amino-terminal cysteine-rich domain (n-CRD). This structural change masks the NES sequence and prevents Yap1 export from the nucleus. Mutations within the NES sequence, or of certain redox sensitive cysteine residues, or the removal of the c-CRD are prerequisites for constitutively nuclear Yap1 (Kuge et al., 1997, Kuge et al., 1998, Yan et al., 1998), supporting the key role of this region in mediating Yap1-Crm1 interaction via the oxidation of cysteine residues. In contrast, the nuclear import of Yap1 is not dependent on oxidative stress stimulus, and mediated via the recognition of the nuclear localisation sequence (NLS) by Pse1 and Kap123 importins (Isoyama et al., 2001). The reduction of active Yap1 is dependent on the redundant action of two cytosolic thioredoxins Trx1 and Trx2 (Kuge and Jones, 1994, Izawa et al., 1999). *S. cerevisiae* *trx1Δ* *trx2Δ* mutant cells display increased levels of oxidised Yap1, which then accumulates in the nucleus under non-stress conditions (Delaunay et al., 2002, Izawa et al., 1999).

H₂O₂-induced oxidation of Yap1 is not direct, but requires glutathione peroxidase Gpx3 and Yap1 binding protein (Ybp1) (Delaunay et al., 2002). Gpx3 is a peroxide sensor directly oxidised by H₂O₂. Upon exposure to H₂O₂, the catalytic site cysteine Cys36 of Gpx3 is oxidised to a reactive sulphenic acid (Cys36-SOH) with the subsequent formation of the intramolecular disulphide between Cys36 and Cys82

(Delaunay et al., 2002). Oxidised Gpx3 then reacts with Cys598 of Yap1 c-CRD to form a transient intermolecular Yap1-Gpx3 disulphide intermediate. These events trigger a multistep transmission of the oxidation within Yap1 with the subsequent activation of the transcriptional factor (Delaunay et al., 2002). The subsequent multiple disulphide bonds formation between different cysteine residues determines the level and duration of the activity of Yap1 (Okazaki et al., 2007, Okazaki et al., 2005, Tachibana et al., 2009). Initially the disulphide bond is formed between Cys310 and Cys315 of nCRD, resulting in the formation of Yap1^{OXI} . The next step involves, in addition to Cys310-Cys315 linkage, the formation of a disulphide between Cys303 and Cys598 ($\text{Yap1}^{\text{OXII-1a}}$), with the further resolution to $\text{Yap1}^{\text{OXII-1b}}$ that contains two disulfides between Cys303-Cys598 and Cys310–Cys629. Fully oxidised active $\text{Yap1}^{\text{OXII-2}}$ emerges from $\text{Yap1}^{\text{OXII-1b}}$ as a result of the formation of an additional disulphide between Cys315 and Cys620 (Okazaki et al., 2007) (Figure 1.7). Full oxidation of Yap1 is essential for its function and only Yap1 that contains correct interdomain disulphide linkage can effectively recruit Rox3 subunit of RNA polymerase II mediator complex to the promoters of its targets (Gulshan et al., 2005).

In contrast to ROS-mediated interdomain disulphide bond formation, in response to glutathione depleting agents such as diamide, the disulphide linkage is formed between two reactive cysteines within the c-CRD of Yap1 (Kuge et al., 2001, Gulshan et al., 2011). The functional differences in Yap1 activation in response to diamide and H_2O_2 support the findings of mutational analysis, where the intact cCRD was shown to be sufficient for diamide-induced oxidation and activation of Yap1 (Wemmie et al., 1997). In contrast, for H_2O_2 -induced activation of Yap1, both the cCRD and nCRD are important (Coleman et al., 1999). In response to diamide, disulphide bonds between reactive cysteines within the cCRD are formed – Cys598-Cys620, Cys598-Cys629 and Cys620-Cys629 (Delaunay et al., 2000, Wood et al., 2004, Kuge et al., 2001) (Figure 1.8). Important, that both Gpx3 and Ybp1 are essential only for H_2O_2 -induced Yap1 activation and dispensable for diamide-induced oxidation of the transcriptional factor (Veal et al., 2003, Delaunay et al., 2002, Gulshan et al., 2004).

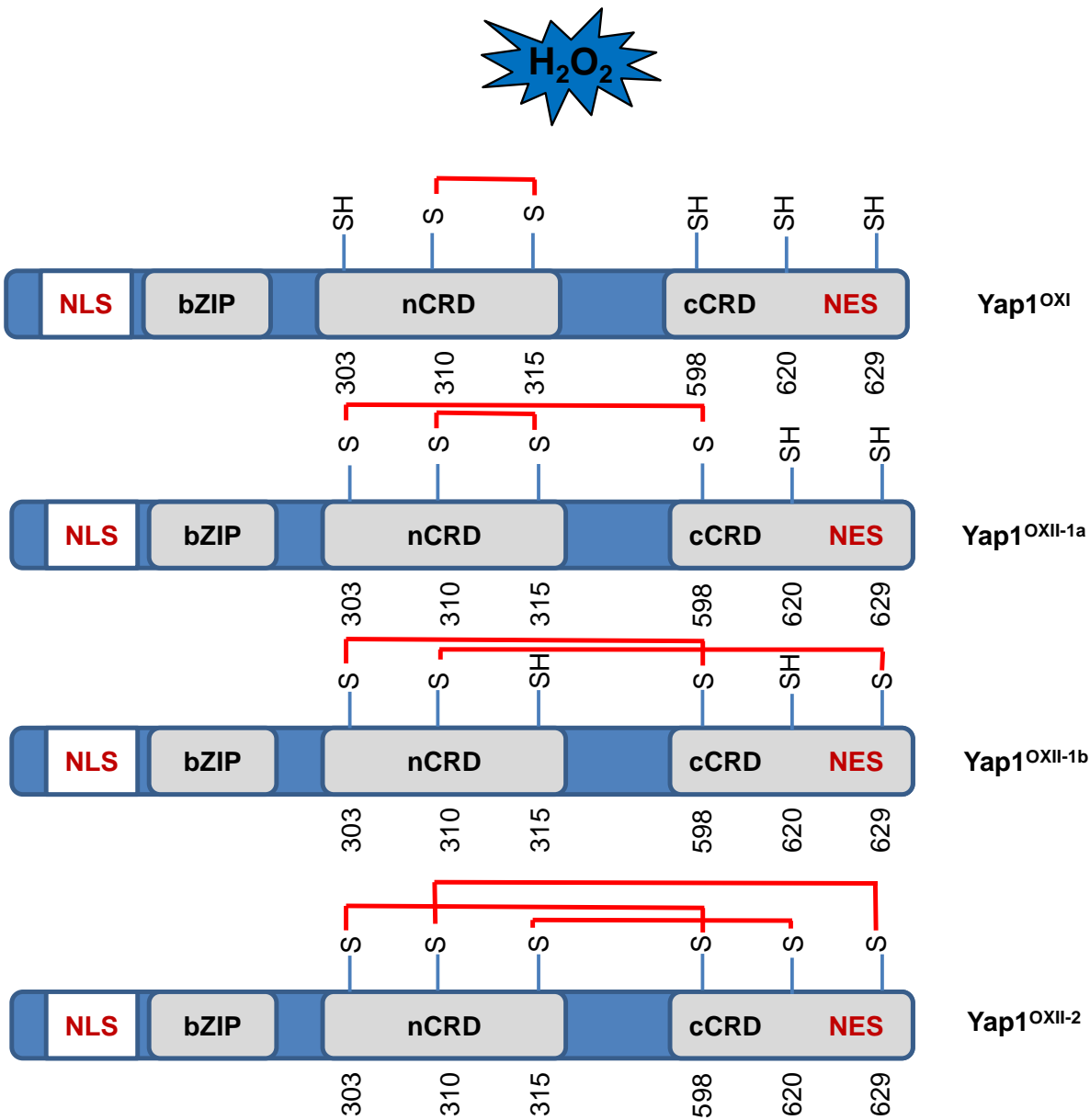


Figure 1.7 Schematic representation of Yap1 oxidation in response to H_2O_2 .

The oxidation of Yap1 in response to H_2O_2 involves the formation of multiple disulphide bonds between redox reactive cysteines of cCRD and nCRD. Detailed description at p. 43. Adapted from (Okazaki et al., 2007)

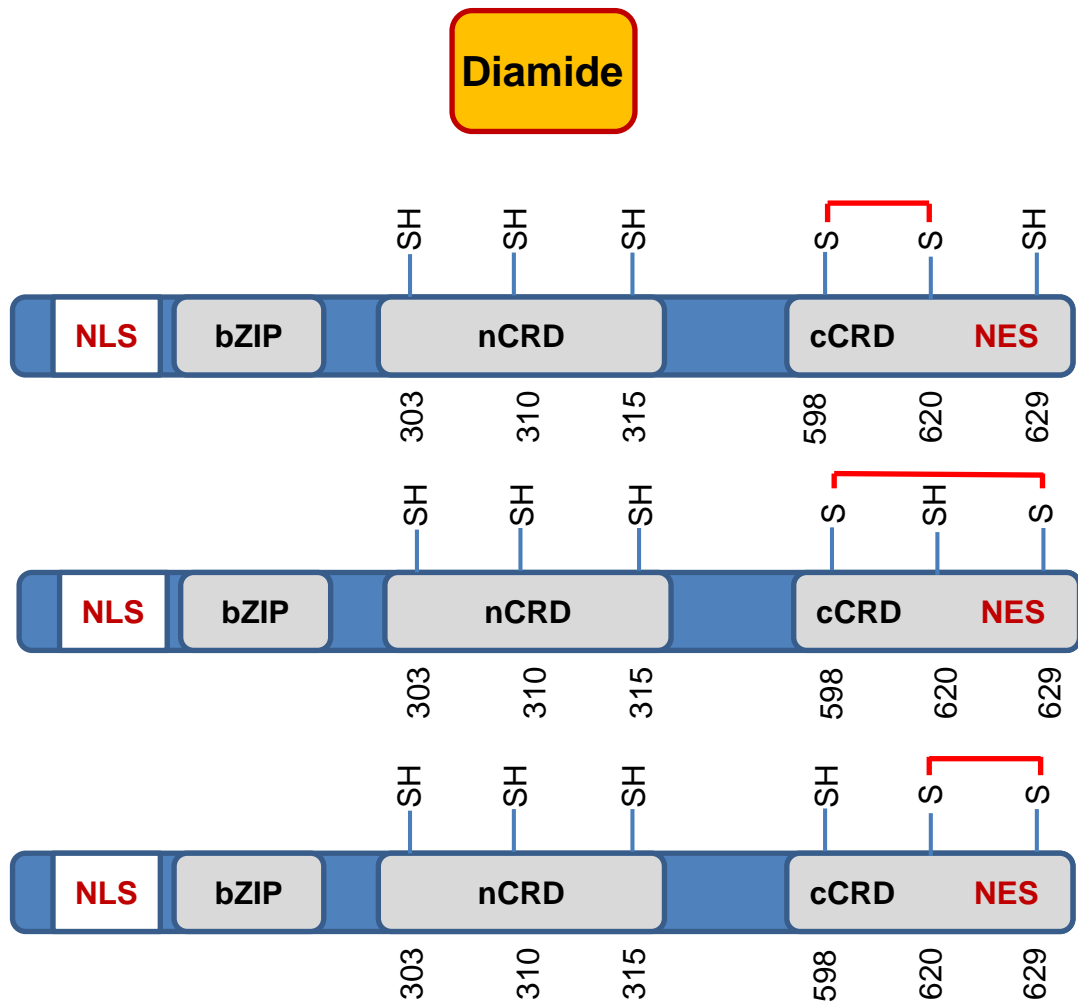


Figure 1.8 Schematic representation of Yap1 oxidation in response to diamide.

Following diamide treatment, the disulphide bonds in Yap1 are formed between the reactive cysteines within the cCRD. Detailed description at p. 43.

Recent report indicates that Ybp1 is also vital for Yap1 stability, the levels of Yap1 protein is considerably lessened in $\Delta ybp1$ cells (Patterson et al., 2013). Oxidised Yap1 undergoes ubiquitin-mediated degradation (Gulshan et al., 2011), and Ybp1 binding to the reduced cytoplasmic pools of Yap1 prevents the proteasomal degradation of the transcriptional factor (Patterson et al., 2013, Gulshan et al., 2011).

Transcriptional profiling revealed that majority of the genes that are essential to withstand oxidative stress in *S. cerevisiae* are Yap1-dependant (Gasch et al., 2000). Among Yap1 targets are important antioxidants such as Trr1, Trx2 and Glr1 (Kuge and Jones, 1994, Grant et al., 1996). Upon activation, Yap1 binds to the specific TTA(C/G)T(A/C)A sequence located in the promoter region of the target genes (yap recognition element, YRE) (Nguyen et al., 2001). Additionally, another transcriptional regulator Skn7 cooperates with Yap1 to induce antioxidant genes (Lee et al., 1999).

1.5.2.3.2 *S. pombe* Pap1

S. pombe Pap1 has a similar function to Yap1 and other yeast AP-1 like transcriptional factors in regulating oxidative stress responses (Toda et al., 1991). Similar to Yap1, Pap1 contains two cysteine-rich domains – cCRD and nCRD, and three redox cysteins in cCRD (Cys501, Cys523 and Cys532), but four in nCRD (Cys259, Cys278, Cys285, Cys290; Figure 1.6). Both the cCRD and nCRD are important for H_2O_2 -induced oxidation of Pap1 (Vivancos et al., 2004). As with Yap1, the activation of Pap1 is regulated by oxidation, which promotes the nuclear accumulation of the transcription factor, leading to the induction of antioxidant genes (Toone et al., 1998). Pap1 accumulates in the nucleus due to the inability of the Crm1 exporter to recognise NES, which is masked by oxidation as seen with Yap1 (Toone et al., 1998). The degradation of active Pap1 in the nucleus is mediated by Ubr1 ubiquitin ligase (Kitamura et al., 2011).

The striking difference of Pap1 activation compared to Yap1 is the H_2O_2 concentration dependence, as Pap1 activation is significantly delayed following high doses of H_2O_2 (Quinn et al., 2002). In addition, while Yap1 activation requires Gpx3 and Ybp1, there is no close Ybp1 homologue in fission yeasts. In return, Pap1

activation requires the thioredoxin peroxidase Tpx1 (Bozonet et al., 2005). Similar to Yap1, the reduction of active Pap1 is mediated by thioredoxin Trx1, and a thioredoxin like protein Txl1. Low levels of H_2O_2 promote the oxidation of Tpx1 to the sulphenic form, which acts as a peroxide sensor (Bozonet et al., 2005): the sulphenic form of Tpx1 forms a disulphide with a second Tsa1 molecule. This disulphide-bonded dimer is reduced by Trx1 and Txl1, thus promoting their oxidation and inactivation. High levels of H_2O_2 cause the hyperoxidation of Tpx1 to the sulphinic form. Once Tpx1 is trapped in the sulphinic form, this is no longer a substrate for Txl1 and Trx1, which are now free to reduce other substrates, such as Pap1 (Koo et al., 2002, Bozonet et al., 2005, Vivancos et al., 2004). The inactive sulphinic form of Tpx1 is reversible and can be reduced by sulfiredoxin Srx1, leading to a subsequent activation of Pap1 (Bozonet et al., 2005). Oxidised Tpx1 is a major substrate for the thioredoxin Trx1, and inactive oxidised thioredoxin is no longer available to reduce the proteins (Brown et al., 2013).

1.5.2.3.3 *C. albicans* Cap1

Cap1, for *C. albicans* AP-1, is a homolog of the *S. cerevisiae* Yap1 and *S. pombe* Pap1 transcription factors (Alarco and Raymond, 1999, Bozonet et al., 2005, Toda et al., 1991, Moye-Rowley et al., 1989). Cap1 was initially shown to be able to partially complement a *S. cerevisiae* *yap1Δ* mutant, since Cap1 can recognize Yap1-binding sites at the promoters of target genes and thus partially rescue the sensitivity of *yap1Δ* cells to H_2O_2 , Cd^{2+} and multiple drugs (Zhang et al., 2000, Alarco et al., 1997). Structurally Cap1 is similar to Yap1 (Alarco and Raymond, 1999). Cap1 contains six redox sensitive cysteine residues: Cys254 and Cys261 in the nCRD, Cys385, which is located between the two CRDs, and Cys466, Cys468, Cys477 in the cCRD (Figure 1.6). The primary functions of Cap1 are to regulate the oxidative stress response and promote multidrug resistance (Alarco and Raymond, 1999). Oxidative stress-mediated changes in the *C. albicans* transcriptome and proteome are largely Cap1-dependent (Znaidi et al., 2009, Kusch et al., 2007). Additionally, this transcriptional factor is also involved in energy metabolism, substance transport and the

maintenance of a cell redox homeostasis under basal non-stress conditions (Wang et al., 2007).

In response to ROS, both *in vitro* and *ex vivo*, Cap1 signalling is essential for *C. albicans* survival and for macrophage killing, enabling the pathogen to escape from the macrophages (Patterson et al., 2013, Fradin et al., 2005). ChIP-sequencing analysis identified Cap1 binding to 89 target genes (Znaidi et al., 2009). Among these Cap1 targets are well known antioxidant enzymes such as catalase (Cat1) and thioredoxin reductase (Trr1), as well as the proteins essential for drug resistance (Mdr1) (Znaidi et al., 2009). Cap1 binding element can be located not only in the promoter region, but also within the open reading frame of its target genes, and may therefore recruit the transcriptional and chromatin remodelling machinery to mount its function (Znaidi et al., 2009). The mechanism of Cap1 action as a facilitator of transcription includes the recruitment of the Ada2 component of the ADA/SAGA complex; a conserved chromatin remodelling transcriptional coactivator (Baker and Grant, 2007). Cap1-dependent recruitment of the ADA/SAGA complex is required for oxidative stress resistance in *C. albicans* (Ramírez-Zavala et al., 2014, Sellam et al., 2009).

Similar to Yap1 and Pap1, Cap1 is regulated at the level of nuclear localization post-translationally by oxidation (da Silva Dantas et al., 2010). Oxidative stress-induced nuclear accumulation of Cap1 is essential for its function and is, analogously to Yap1, c-CRD-dependent (Zhang et al., 2000). Based on structural studies in *S. cerevisiae*, it is predicted that Cap1 oxidation masks the NES from the Crm1 nuclear export factor, which leads to its nuclear accumulation. Once in the nucleus, Cap1 is phosphorylated, and Cap1-dependent genes are induced, promoting the resistance of the pathogen to oxidative stress (Zhang et al., 2000, Patterson et al., 2013; Figure 1.9). The nuclear localisation of Cap1 is essential, but not sufficient to activate Cap1, as a truncated mutant form of Cap1, which is constitutively nuclear, unable to recover wild type levels of H₂O₂ tolerance (Alarco and Raymond, 1999). As seen with Yap1 regulation (Delaunay et al., 2002, Wood et al., 2004), Cap1 is not directly oxidised by peroxide, which instead is dependent on both the Gpx3 thiol peroxidase enzyme and Ybp1 (Patterson et al., 2013).

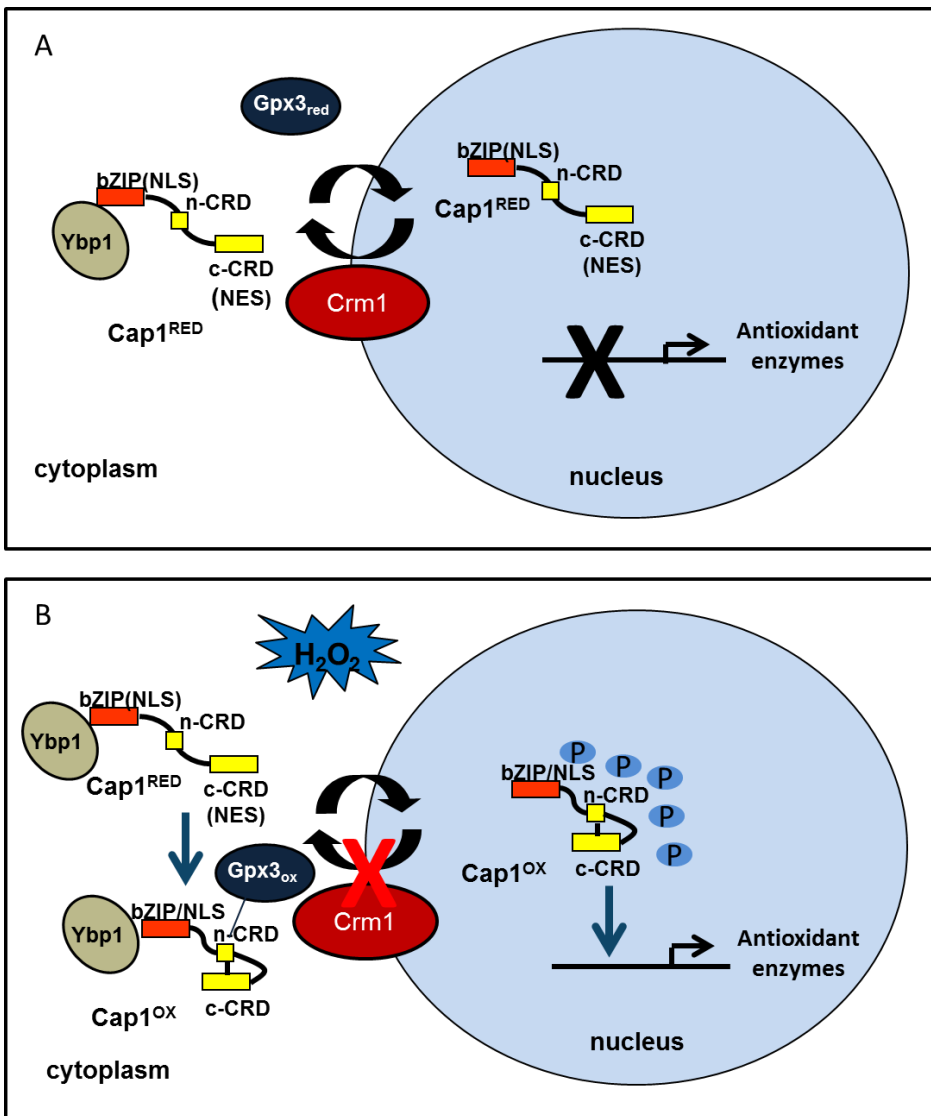


Figure 1.9 Mechanism of Cap1 activation in response to oxidative stress.

(A) Under non-stress conditions, Cap1 is reduced and shuttles between the cytoplasm and the nucleus due to the opposing actions of Cap1 nuclear import and export. Reduced Cap1 does not accumulate in the nucleus and therefore does not stimulate antioxidant gene expression. (B) In response to H_2O_2 , Cap1 forms a complex with Ybp1 when in the cytoplasm, which functions to prevent degradation of Cap1 and to facilitate H_2O_2 -induced oxidation of Cap1 by the Gpx3 peroxidase. Based on studies in *S. cerevisiae*, it is predicted that the Crm1 nuclear exporter can no longer recognise Cap1^{OX} due to the masking of the NES; this leads to the nuclear accumulation and subsequent phosphorylation of the transcriptional factor, which in turn facilitates Cap1 binding to the promoters of its targets, enabling antioxidant gene expression. Adapted from (Patterson et al., 2013, Dantas et al., 2015).

In addition to mediating Cap1 oxidation, Ybp1 also prevents the proteasome-mediated degradation of Cap1. Ubiquitin-dependant proteasomal degradation of transcription factors is a common regulatory mechanism to maintain cellular homeostasis, and here Ybp1 forms a cytosolic complex with reduced Cap1 (similar to what is seen for Yap1) possibly to prevent Cap1 getting targeted for degradation (Patterson et al., 2013, Gulshan et al., 2012, Gulshan et al., 2011). Gpx3-initiated oxidation of Cap1 triggers the subsequent formation of disulphide bonds. The oxidised transcriptional factor accumulates in the nucleus and triggers the expression of antioxidant genes, enabling stress response and survival of the pathogen.

Similar to Yap1, oxidised Cap1 is reduced by the thioredoxin Trx1 when the activation of the transcription factor is no longer needed. Loss of Trx1 prolongs H₂O₂-induced Cap1 oxidation, nuclear accumulation, and Cap1-dependent gene expression (da Silva Dantas et al., 2010). However, in mutant *trx1Δ* cells Cap1 is not constitutively nuclear, suggesting that Trx1-independent mechanisms of Cap1 regulation may exist. In contrast to *S. pombe*, where Pap1 requires an active SAPK Sty1 for its activation, the mechanisms underlying an oxidative stress response in *C. albicans* via Cap1 pathway are independent on Hog1 SAPK (Alonso-Monge et al., 2003).

Cap1 signalling is important for *C. albicans* to withstand ROS-mediated killing, and cells lacking Cap1 and its regulators Ybp1 and Gpx3 are more susceptible to killing by neutrophils and macrophages (Patterson et al., 2013, Fradin et al., 2005, Jain et al., 2013). While Cap1 is essential for full fungal virulence in *Caenorhabditis elegans* and *Galleria mellonella* models of infection, it is dispensable for *C. albicans* virulence in a murine model of systemic candidiasis (Jain et al., 2013, Patterson et al., 2013). The infection model dependent requirement for Cap1 in *C. albicans* virulence may indicate that the levels of ROS encountered vary in different host niches.

1.5.2.4 *Skn7*

In *S. cerevisiae* oxidative stress-induced gene expression also requires the transcription factor Skn7 (Morgan et al., 1997). Skn7 is important for both oxidative and osmotic stress responses, but the mechanism of its activation differs: while osmotic stress-induced activation of Skn7 depends on phosphorylation at D427 aspartate by the upstream Sln1 two-component phosphorelay system, the regulation of this response regulator following oxidative stress is independent of the phosphoaspartate D427 (He et al., 2009). However, the receiver domain of Skn7 is required for the oxidative stress-induced phosphorylation of the transcriptional factor and the formation of the ternary structure that is required for promoter binding and the interaction with Yap1 (He et al., 2009). *S. cerevisiae* Skn7 co-operates with Yap1 to regulate antioxidant genes expression, and the targets of both transcriptional factors largely overlap (Lee et al., 1999).

A similar situation is seen in *S. pombe*, where the analogous Pap1 and Prr1 transcriptional factors co-operate to regulate H₂O₂-responsive genes (Calvo et al., 2012). The homolog of Skn7/ Prr1 is present in the *C. albicans* genome, and mutants lacking *SKN7* are sensitive to ROS and showed slightly attenuated virulence in a mouse model of systemic disease (Singh et al., 2004). However, the precise role of Skn7 in antioxidant gene expression, and its putative co-operation with Cap1, has not been investigated.

1.6 Oxidative stress-responsive signalling pathways in *C. glabrata*

C. glabrata possesses a very high tolerance to ROS *in vitro* (Seider et al., 2014), and some studies attribute this high tolerance to the activity of the single catalase-peroxidase, regulated by multiple transcriptional factors, including CgYap1, CgSkn7, and CgMsn2/4 (Cuéllar-Cruz et al., 2008). Recent findings suggest that despite the existence of well-known antioxidant genes that are crucial for *C. albicans* survival following phagocytosis, such as catalase, SODs, thioredoxins and peroxiredoxins, none of these genes are essential for *C. glabrata* survival during co-culture with human macrophages (Seider et al., 2014). In addition, *C. glabrata* strains lacking

catalase do not show a significant decrease in virulence in immunodeficient mice, whereas for other pathogenic fungi such as *C. albicans* and *A. fumigatus*, catalase is pivotal for the virulence in murine model of infection (Cuéllar-Cruz et al., 2008, Paris et al., 2003, Nakagawa et al., 2003). It appears that reactive oxygen species do not play a major role in the host-mediated clearance of this pathogen, possibly because of the high tolerance to ROS exhibited by *C. glabrata* compared to other fungi (Seider et al., 2014). The catalase gene, however, is upregulated in response to oxidative stress and nutrient depletion in *C. glabrata* following phagocytosis (Roetzer et al., 2010) and is essential to withstand ROS attack *in vitro* (Cuéllar-Cruz et al., 2008). ChIP analysis revealed that the components of the thioredoxin and glutaredoxin systems, such as CgTsa1, CgTsa2, CgTrr1, CgTrr2, CgTrx2, CgGpx2 are induced *in vitro* in response to various oxidative stimuli, suggesting that these systems are involved in the oxidative stress response of the pathogen (He et al., 2009).

C. glabrata resistance to oxidative stress *in vitro* is mediated by Cgap1, Skn7, and Msn2/ Msn4 transcriptional factors (Cuéllar-Cruz et al., 2008).

Cgap1 is an orthologue of *S. cerevisiae* Yap1 and *C. albicans* Cap1, and has similar functions to control oxidative stress responses and multidrug resistance in *C. glabrata* (Chen et al., 2007). The cooperation of Cgap1 and Skn7 is essential to withstand oxidative stress, and the interaction of these two transcriptional factors is important for the activation of key antioxidants, such as *TSA1* both *in vivo* and *in vitro* following the oxidative stress (He et al., 2009). The Cgap1/ Skn7 complex was found to bind upstream to the promoters of core stress response genes in *C. glabrata* (He et al., 2009). Interestingly, Sod1 that is essential to resist oxidative burst mounted by phagocytes and controlled by Cap1 in *C. albicans*, is not dependent on Cgap1 in *C. glabrata* (Roetzer et al., 2011). *C. glabrata* Skn7 plays a pivotal role in oxidative stress response of this pathogen (Saijo et al., 2010). In *C. glabrata* Skn7 shares more similarity with ScSkn7 compare to CaSkn7, and co-operates with CgYap1 to induce antioxidant transcriptome. *C. glabrata* strains lacking *SKN7* display an attenuated virulence (Saijo et al., 2010).

Msn2 and Msn4 are Cys2His2 zinc finger proteins that bind to the stress response element (STRE) (Görner et al., 1998). They are essential for *C. glabrata* to

withstand various environmental stresses (Roetzer et al., 2008). *C. glabrata* Msn2/4 share high similarity with Msn2/4 transcriptional factors in *S. cerevisiae*, where their activation is determined at the level of nuclear localisation with the subsequent chromatin recruitment. *CgMSN2* and *CgMSN4* are dispensable for virulence in *Drosophila melanogaster* model of infection (Roetzer et al., 2008); however, this model might not reflect different host niches.

1.7 Response of *C. albicans* and *C. glabrata* to combinatorial oxidative and cationic stresses

Whilst the responses of *C. albicans* to single physiologically relevant stresses have been extensively studied (Brown et al., 2009), the response of this pathogen to combinations of such stresses is less understood. However, in the host *Candida* spp. will undoubtedly be simultaneously exposed to a range of stresses (Kaloriti et al., 2012). *C. albicans* has successfully adapted to survive in the presence of relatively high levels of osmotic and oxidative stresses *in vitro* – the pathogen can survive 10 mM H₂O₂, 3 M sorbitol or 2 M NaCl (Nikolaou et al., 2009). So why can this pathogen not evade phagocyte killing in healthy hosts? Significantly, the combination of stresses can kill pathogenic *Candida* species much more effectively than the corresponding single stresses, this phenomenon has been called ‘stress pathway interference’ (Kaloriti et al., 2014). Moreover, such mechanism of the synergistic killing is more likely highly conserved through the evolution, since other pathogenic and nonpathogenic yeast species such as *S. pombe*, *S. cerevisiae* and *C. glabrata* also exhibit an increased killing by combinatorial stress (Kaloriti et al., 2012).

Specifically, the combination of two physiologically relevant stresses – oxidative and cationic – is very potent in killing *C. albicans* *in vitro* (Kaloriti et al., 2012), and the potency of the phagocytic immune cells to kill the pathogen is a result of the synergy of oxidative burst (Sasada and Johnston, 1980) and cationic influxes (Reeves et al., 2002, Kaloriti et al., 2014). The molecular basis of this phenomenon was explored by genome-wide expression profiling. This revealed significant differences in the genes upregulated following exposure of *C. albicans* to oxidative, cationic, or both stresses. Significantly, key antioxidant genes, such as *CAT1*

encoding catalase, and *TRR1* encoding thioredoxin reductase, were not induced in response to combinatorial cationic and oxidative stress treatments, and both the oxidative stress Cap1 regulon and cationic stress Hog1 regulon are not induced following combinatorial stress. However, the Hog1 pathway is active, whereas the Cap1 pathway is not due to the lack of nuclear accumulation of the transcriptional factor. Specifically, the combination of H_2O_2 and NaCl causes the synergistic effect and the adaptation of the pathogen to these stresses is delayed *in vitro* due to the inhibition of ROS detoxification systems by cations (Kaloriti et al., 2012, Kaloriti et al., 2014). Specifically, cations inhibit catalase function, which results in high levels of intracellular ROS, and ectopic expression of the catalase gene *CAT1*, which is Cap1-dependant, partially rescues the hypersensitivity to the combinatorial stress (Kaloriti et al., 2014). However, the mechanism behind the combinatorial stress-mediated inactivation of Cap1 remains unknown.

1.7.1 Synergistic killing of *C. albicans* by combinatorial stress is due to impaired activation of Cap1 transcriptional factor

As discussed in section 1.5.2.3.3, the key regulator of antioxidant gene expression in *C. albicans* is the AP-1-like transcription factor Cap1. In response to combinatorial oxidative and cationic stresses, Cap1 does not accumulate in the nucleus, explaining the lack of Cap1-dependent gene expression. As combinatorial oxidative and cationic stresses contribute to the potency of neutrophils in *C. albicans* killing (Kaloriti et al., 2014), it is likely that the lack of Cap1 activation following such combinatorial stress treatment prevents the rapid adaptive response to H_2O_2 , leading to the death of the pathogen. These observations are supported by the fact that ectopic expression of the Cap1 target catalase gene (*CAT1*) in *C. albicans* partially rescues the hypersensitivity to combinatorial oxidative and cationic stresses and promotes fungal survival following phagocytosis (Kaloriti et al., 2014).

It is a prominent question to understand the signalling mechanisms underlying *C. albicans* susceptibility to combinatorial stress killing, as this reflects a physiologically relevant mechanism of pathogen clearance employed by innate immune cells.

1.7.2 *C. glabrata* resistance to combinatorial stress is mediated by the uncharacterised *CRI* genes

C. glabrata can persist in the human host for long periods of time, causing chronic infection (Brunke and Hube, 2013). Although this fungus is also susceptible to combinatorial oxidative and cationic stress-mediated killing *in vitro*, about 20% of the *C. glabrata* population can survive macrophage attack and proliferate within the phagocyte, causing the progress of infection (Jacobsen et al., 2010, Seider et al., 2014). Being continually exposed to the host' immune defences, this pathogen appears very successful in adapting to stresses encountered following phagocytosis. However, the molecular mechanisms of *C. glabrata* adaptation remain unknown. To understand the mechanism underlying the *C. glabrata* resistance to combinatorial stresses, Professor K. Haynes group based at Exeter University initiated a screen for *C. glabrata*-specific genes that promote stress resistance. Their recent unpublished findings suggest that four uncharacterised ORFs, which encode proteins with unknown function and have no apparent orthologues in other organisms, are essential for combinatorial stress resistance. The uncharacterised ORFs were designated as *CRI1-4* for Combinatorial stress Resistance Increased. When expressed in *S. cerevisiae*, which is extremely sensitive to combinatorial stress (Kalogriti et al., 2012), these genes were able to rescue sensitivity and promote survival. Further investigation of the mechanism of action of these proteins will allow a better understanding for what allows *C. glabrata* to combat host defenses.

1.8 Project Aims

1.8.1 *Investigation into the molecular basis underlying innate immune defence mediated killing of Candida species*

To better understand how life-threatening fungal infections caused by *Candida* spp. can be prevented, it is important to understand how innate immune defences in healthy host co-operate to kill invading pathogenic fungi. Specifically, we build on data that innate immune defences employ a combination of oxidative and cationic stresses to kill pathogenic *Candida* spp., with the specific aims to:

- (1) Decipher the molecular mechanisms underlying the combinatorial stress-mediated inhibition of the Cap1 transcription factor in *C. albicans* (Kalogriti et al., 2014), and
- (2) Investigate the mechanisms that promote combinatorial stress resistance in *C. glabrata* (J. Usher and K. Haynes, unpublished).

1.8.2 Investigation into the importance of fungal stress responses in mediating virulence in hosts with defective immune defences

Whilst it is well established that fungal stress responses are vital for virulence in immunocompetent hosts, less is known about the importance of such responses in mediating fungal virulence in hosts with defective innate defence mechanisms. To investigate the importance of stress responses in fungal pathogenesis in immunodeficient hosts, such as immunocompromised and elderly populations, a *Caenorhabditis elegans* infection model is employed. Several studies have established nematodes as a useful model to study pathogenesis and innate immunity (Kurz and Tan, 2004, Kim et al., 2002, Mallo et al., 2002). In addition, *C. elegans* is a well-established model at the forefront of ageing research (Finch and Ruvkun, 2001). Recently, *C. elegans* was shown to display a decline in immune function with age, thus resulting in age-dependent susceptibility to bacterial infections (Evans et al., 2008b, Komura et al., 2012). Thus, *C. elegans* is an ideal model to explore the impact of the immune status of the host in dictating the requirement of fungal stress responses in mediating virulence.

Chapter 2. Materials and methods

2.1 Microbiological techniques

2.1.1 Yeast strains and growth conditions

Yeast strains used in this study are listed in Table 2.1. Yeasts were grown either in YPD rich media (1% w/v yeast extract, 2% w/v bacto-peptone, 2% w/v glucose) or SD minimal media (0.67% w/v yeast nitrogen base without amino acids, 2% w/v glucose) supplemented with required amino acids for selective growth (L-histidine-HCl [20mg/ml], L-tryptophan [20 mg/ml], L-arginine-HCl [40 mg/ml], L-leucine [60 mg/ml], uridine [20 mg/ml], L-methionine [20 mg/ml]) in liquid media, or supplemented with 2% bacto-agar for solid media (Sherman, 1991) and maintained at 30 °C, unless stated otherwise.

To investigate combinatorial stress response, *Candida* cells were cultured in YPDT (YPD as described above supplemented with 100 mM Tris-HCl pH 7.4) liquid media or with the addition of 2% bacto-agar for solid media. When cationic stress was applied, the cell culture was supplemented with pre-warmed 4 M NaCl made in YPDT to give a final concentration of 1 M. Oxidative stress was generated by the addition of H₂O₂ from a 8.82 M stock to give the desired concentration either directly to the media, or pre-diluted in YPDT immediately before use.

For hyphal induction, *C. albicans* cells were incubated in YPD media supplemented with 10% human serum and incubated for 4 hours at 37 °C in order to induce hyphae prior to stress treatment.

Strain	Genotype	Reference
<i>Candida albicans</i> strains		
SN148	<i>arg4Δ/arg4Δ leu2Δ/leu2Δ his1Δ/his1Δ</i> <i>ura3Δ::imm434/ura3Δ::imm434</i> <i>iro1Δ::imm434/iro1Δ::imm434</i>	(Noble and Johnson, 2005)
JC52	<i>ura3:: λ imm434/ura3::λimm434, his1::hisG/his1::hisG,</i> <i>hog1::LoxP-ura3-LoxP, hog1::LoxP-HIS1-LoxP Clp20-HOG1</i>	(Smith et al., 2004)

Strain	Genotype	Reference
JC50	<i>ura3::λ imm434/ura3::λimm434, his1::hisG/his1::hisG, hog1::LoxP-ura3-LoxP, hog1::LoxP-HIS1-LoxP</i> Clp20	(Smith et al., 2004)
JC45 (324)	<i>ura3::λ imm434/ura3::λimm434, his1::hisG/his1::hisG, hog1::LoxP-ura3-LoxP/hog1::LoxP-HIS1-LoxP</i>	(Enjalbert et al., 2006)
JC710	SN148 <i>cap1::loxP-HIS1-loxP/cap1::loxP-ARG4-loxP</i>	(da Silva Dantas et al., 2010)
JC747	SN148 Clp30	(da Silva Dantas et al., 2010)
JC807	SN148 <i>cap1::loxP-HIS1-loxP/cap1::loxP-ARG4-loxP, Clp20-CAP1</i>	(Patterson et al., 2013)
JC930	SN148 <i>TRX1-MH-URA3</i>	(da Silva Dantas et al., 2010)
JC948	SN148 <i>CAP1-MH-URA3</i>	(da Silva Dantas et al., 2010)
JC954	SN148 <i>ybp1::loxP-HIS1-loxP/ybp1::loxP-ARG4-loxP, CAP1-MH-URA3</i>	(Patterson et al., 2013)
JC983	SN148 <i>trx1Δ::loxP-HIS1-loxP/trx1Δ::loxP-ARG4-loxP, CAP1-MH-URA3</i>	(da Silva Dantas et al., 2010)
JC1060	SN148 <i>CAP1-GFP-URA3</i>	(da Silva Dantas et al., 2010)
JC1253	SN148 <i>txl1Δ::loxP-HIS1-loxP</i>	Dr. A. Dantas
JC1311	SN148 <i>gpx3::loxP-HIS1-loxP/gpx3::loxP-ARG4-loxP, CAP1-MH-URA3</i>	(Patterson et al., 2013)
JC1388	SN148 <i>cap1::loxP-HIS1-loxP/cap1::loxP-ARG4-loxP, pACT1-CAP1</i>	(Patterson et al., 2013)
JC1732	SN148 <i>pACT-GFP</i>	Dr. M. Ikeh
JC1925	SN148 <i>CRM1-MH-URA3</i>	This work
JC1940	JC45 <i>CRM1-MH-URA3</i>	This work
JC1291	SN148 <i>txl1Δ::loxP-HIS1-loxP/txl1Δ::loxP-ARG4-loxP</i>	Dr. A. Dantas
JC2092	JC1291 <i>CAP1-MH-URA3</i>	This work

Strain	Genotype	Reference
JC2101	JC1253 <i>TXL1-MH-URA3</i>	This work
JC2123	SN148 <i>pPGK</i>	This work
JC2124	SN148 <i>Clp20_pPGK_CRI1</i>	This work
<i>Candida glabrata</i> strains		
G2001HTU	<i>his3Δ trp1Δ ura3Δ</i>	(Kitada et al., 1995)
<i>Cg Cri1 O/E-GFP</i>	G2001HTU MAT α <i>his3 trp1::ScURA3 p423-GPDp-ccdB (CgCRI1 HIS)</i>	Dr. J. Usher, University of Exeter
<i>Cg cri1Δ</i>	G2001HTU <i>cri1Δ::CgTRP1</i>	Dr. J. Usher, University of Exeter

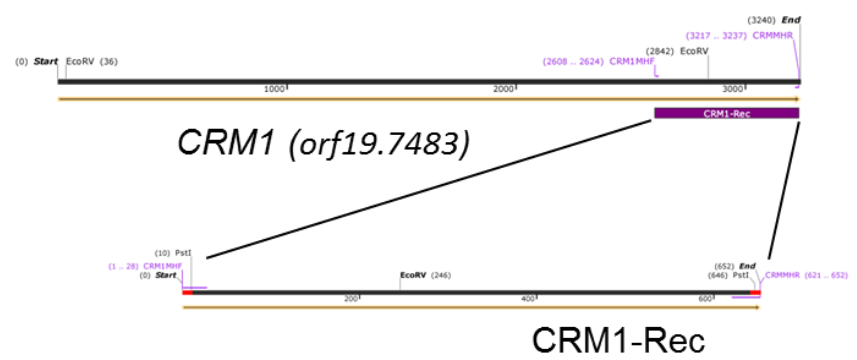
Table 2.1 Yeast strains used in this study.

2.1.2 *C. albicans* strain construction

2.1.2.1 Tagging of *Crm1*, *Cap1* and *Txl1*

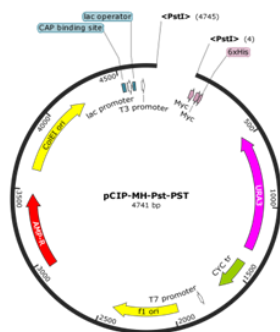
To C-terminally tag *Crm1*, expressed from its native chromosomal locus (*orf19.7483*), with 2 copies of the myc epitope and 6-His residues, the 3'-region of *CRM1* (630 bp) was amplified by PCR using the oligonucleotide primers *Crm1MHPstF* and *Crm1MHPstR* from *C. albicans* SN148 genomic DNA template. The resulting PCR product with flanking *PstI* sites was digested with *PstI* and ligated into the same site of *Clp-MH-PstI* plasmid (4744 bp) (da Silva Dantas et al., 2010) to generate *pCRM1-MH*. *pCRM1-MH* was linearized by digestion with *EcoRV*, to target the integration at the *CRM1* locus in SN148 wild-type cells (Noble and Johnson, 2005), or *hog1Δ* cells (JC45) (Smith et al., 2004) to generate strains JC1925 and JC1940, respectively (Figure 2.1). Chromosomal integration and tagging of *CRM1* was verified by PCR from total DNA as a template using the oligonucleotide primers *Crm1MH_F* and *CycTR_R* and DNA sequencing.

1. PCR amplification of CRM1 insert

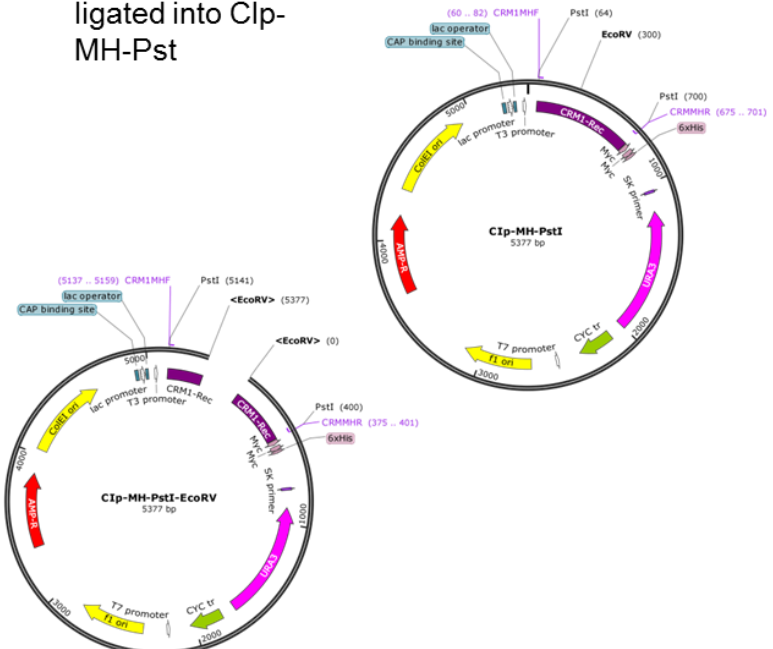


2. Preparative restriction of PCR product with *PstI*

3. Vector digested with *PstI* and dephosphorylated



4. CRM1 fragment ligated into Clp-MH-Pst



5. Plasmid linearized with *EcoRV*

<EcoRV> <EcoRV>

6. Transformation of *C. albicans* to Myc-tag CRM1

2000 4000
CRM1-Rec URA3 CYC tr AMP-R f1 ori ColE1 ori CRM1-Rec

Homologous recombination

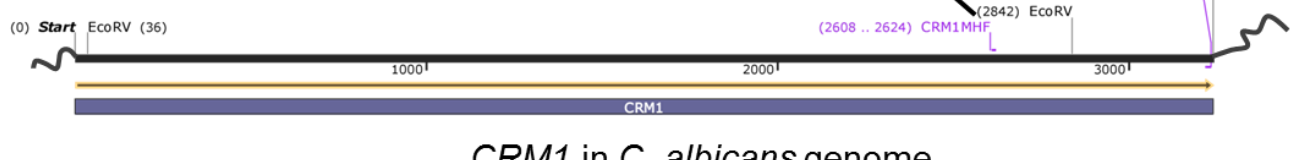


Figure 2.1 Schematic diagrams illustrating a strategy used to myc-HIS tag *CRM1* in *C. albicans*.

A fragment of *CRM1* gene (630 bp) was amplified from *C. albicans* genomic DNA and ligated into *PstI* site of Clp-C-MH-PstI. The resulting construct was linearized by *EcoRV* to target its integration into *CRM1* locus to tag *CRM1* at C-terminus with 2Myc 6His epitope. The same strategy was employed to construct *C. albicans* strains expressing 6His 2Myc-tagged *TXL1*. Plasmid maps were created using SnapGene software (from GSL Biotech; available at snapgene.com). To tag *Cap1* with 2 myc epitopes and 6 His residues in *txl1Δ* cells (JC1291), Clp20-Cap1MH (da Silva Dantas et al., 2010) was linearized with *SphI* to target integration into the native *CAP1* locus, and transformed into *txl1Δ* cells to generate the strain JC2092.

To tag *Txl1* with 2 myc epitopes and 6-His residues, *TXL1* (*orf19.3319*) (984 bp) was amplified from *C. albicans* SN148 chromosomal DNA using the primers *Txl1_MH-Pst_F* and *Txl1_MH-Pst_R*, digested with *PstI* and ligated into the *PstI* site of Clp-MH-PstI, generating pTXL1-MH (5725 bp). Correct plasmid construction was verified by PCR and DNA sequencing. The plasmid was linearized with *SalI* to target its integration into the native *TXL1* locus and transformed into *txl1/TXL1* heterozygous cells (JC1253) to generate JC2101. Chromosomal integration of *TXL1-MH* was confirmed by PCR using the primers *Txl1_MH-Pst_F* and *CycTR_R*.

2.1.2.2 Heterologous expression of *Candida glabrata CRI* genes in *C. albicans*

CRI1-CRI4 genes were amplified from *C. glabrata* G2001 genomic DNA as a template using oligonucleotide primers that are listed in Table 2.2. For the constitutive expression of *C. glabrata CRI* genes under the control of the *ACT1* promoter, *CRI1* (CAGL0G06710g, 252bp) was amplified using the primers CRI1pACT_SallF and CRI1pACT_SallR. The resulting PCR product was digested with *SalI* and ligated into *SalI* site between the *C. albicans ACT1* promoter and *S. cerevisiae CYC1* terminator in pACT (6351 bp) (Tripathi et al., 2002), resulting in the generation of pACT1-CRI1 (Figure 2.2).

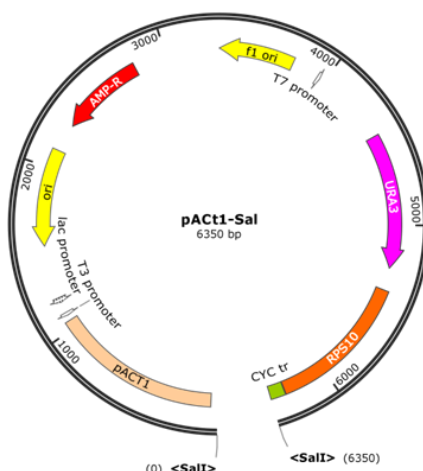


CRI1 (CAGL0G06710g) (252 bp)

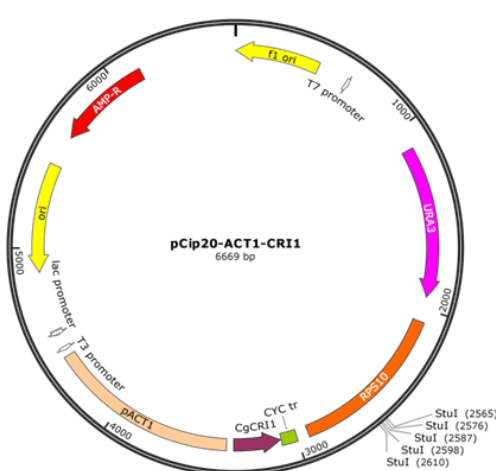


CRI1 + CRI1 terminator (537 bp)

2. Cloning into *Sall* site of pACT1



3. *CRI1* gene ligated into pACT1

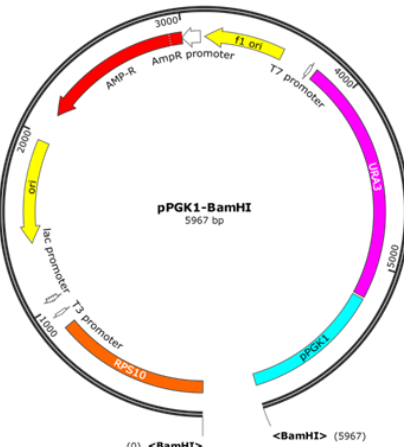


4. Integration into *C. albicans* *RPS10* locus



1. PCR amplification of *CgCRI1* and *CgCRI1 + CRI1 tr*

2. Cloning into *BamH1* site of pPGK1



3. *CRI1* gene and its terminator ligated into pPGK1

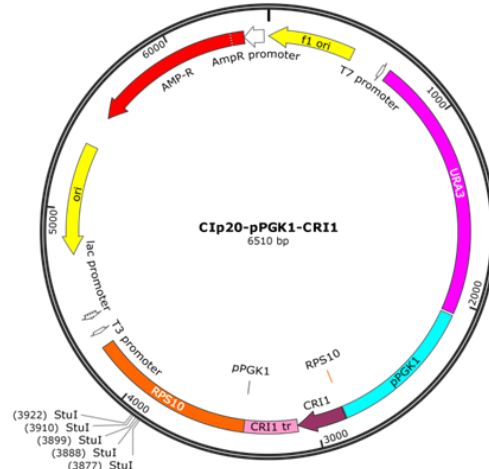


Figure 2.2 Schematic diagram illustrating a strategy used to express *C. glabrata CRI1* in *C. albicans*.

To constitutively express *CgCRI1* in *C. albicans*, *CRI1* ORF (252bp) was cloned into *Sall* site of pACT1 plasmid (da Silva Dantas et al., 2010) to generate Clp20-pACT1-CRI1. In order to overexpress *CgCRI1*, *CRI1* and 285 bp of its own terminator sequence were ligated into *BamHI* site of pPGK1 (Cheetham et al., 2007) to generate Clp20-pPGK-CRI1. Both constructs were digested with *Stu*I to target their integration into *RPS10* locus of *C. albicans* genome. Similar strategy was employed to create *C. albicans* strains expressing *CgCRI2*, *CgCRI3* and *CgCRI4*.

Similarly, *CRI2* (CAGL0E06094g, 174 bp), *CRI3* (CAGL0H04059g, 444 bp) and *CRI4* (CAGL0A00649g, 384 bp) were amplified from *C. glabrata* genomic DNA using the corresponding primers (CRI2pACT_SallF, CRI2pACT_SallR, CRI3pACT_SallF, CRI3pACT_SallR CRI4pACT_SallF, CRI4pACT_SallR). The resulting PCR products were linearized with *Sall* and cloned into *Sall* site of pACT, resulting in the construction of plasmids pACT1-CRI2, pACT1-CRI3 and pACT1-CRI4.

To overexpress *CRI1* in *C. albicans*, *CRI1* orf with its own terminator region [0; +537] was amplified from *C. glabrata* G2001 chromosomal DNA using the primers CRI1pPGK1_BamH1F and CRI1pPGK_BamH1R. The resulting PCR product was digested with *BamHI* and subcloned into *BamHI* site adjacent to the *PGK1* promoter of pPGK1 to generate pPGK1-CRI1 (Cheetham et al., 2011, Murad et al., 2000). All plasmids were linearized with *Stu*I prior to *C. albicans* transformation in order to target their integration into *RPS10* locus of *C. albicans* SN148 (Figure 2.2). The successful transformation was confirmed by PCR using *C. albicans* chromosomal DNA as a template and the pair of oligonucleotide primers, with a forward primer to either *ACT1* or *PGK1* promoter and reverse primer to *CYC1* terminator for pACT1 constructs (CYC_TR_R) or CRI1_OE_PGK_R for pPGK construct. The resulting synthetic gene was amplified using the oligonucleotide primers CRI1pPGK_BamH1F and CRI1_TERM_pPGK_BamHIR, and subcloned into the *BamHI* site of pPGK1. This plasmid, which expresses a codon optimised version of *CRI1* under the control of the strong *PGK1* promoter, was digested by *Stu*I and integrated into the *RPS10* locus of *C. albicans* SN148 cells to generate the strain JC2124.

2.1.3 DNA transformation

2.1.3.1 Transformation of *E. coli*

Escherichia coli SURE competent cells {e14⁻(McrA⁻) Δ(*mcrCB-hsdSMR-mrr*)171 *endA1* *gyrA96* *thi-1* *supE44* *relA1* *lac* *recB* *recJ* *sbcC* *umuC*::Tn5 (Kan^r) *uvrC* [F' *proAB* *lacI*^qZΔM15 Tn10 (Tet^r)]} (Stratagene, UK) were thawed on ice. 5-10 µl of DNA was added to 50 µl of competent cells and gently mixed by several inversions, following by incubation on ice for 20 minutes. Cells were heat-shocked for 45 seconds at 42 °C and placed on ice for 1-2 minutes. 500 µL of pre-warmed to 37 °C liquid LB media (2% w/v bacto tryptone, 1% w/v bacto yeast extract, 1% w/v NaCl, pH 7.2) was added to each sample and incubated at 30 °C for 45 minutes to allow cells recovery. For selection of the positive transformants, cells were spread onto LB agar plates supplemented with 100 µg/ mL ampicillin (Sigma, Dorset, UK) and incubated at 37 °C overnight. The colonies were patched onto fresh LB+Amp plates, following by plasmid extraction and PCR verification. For long term maintenance of *E. coli* stocks, 70 µl of DMSO was added to 930 µl of overnight *E.coli* liquid culture in LB+Amp and stored at -80 °C.

2.1.3.2 Transformation of *C. albicans*

C. albicans cells were transformed with exogenous DNA using an optimised lithium acetate protocol (Walther and Wendland, 2003). Single yeast colony was subcultured in 10 ml YPD and incubated overnight at 30 °C with shaking. The following morning, pre-cultures were diluted in 50 ml of fresh YPD to the OD₆₆₀=0.2 and incubated 3-4 hours at 30 °C with agitation till the exponential phase of growth (OD₆₆₀=0.6). Cells were placed on ice and collected by centrifugation for 5 minutes at 3500 rpm, 4 °C. The pellet was washed with 10 ml of cold 1 x TE buffer (10 mM Tris-HCl pH7.5, 1 mM EDTA pH8.0) and centrifugation was repeated at 3000 rpm for 5 minutes. Washed cells were resuspended in 1 ml of LiAc/ TE (100 mM LiAc, 1 x TE) and incubated overnight on ice at 4 °C. The following day, 20 µl of DNA for transformation was mixed with 5 µl of the salmon sperm carrier DNA (10 mg/ml) and incubated on ice for 5 minutes. 50 µl of *C. albicans* competent cells and 300 µl of

freshly prepared Plate Mix (1 ml 10 x TE, 1 ml 1 M LiAc, 8 ml 50% PEG 3350) were added to the DNA, mixed gently by several inversions and incubated 2-3 hours at 30 °C. Cells were then heat shocked by incubating at 44 °C for 15 minutes. 1 ml of sterile H₂O was added to the cells to dilute the PEG, following by the centrifugation for 2 minutes at 3000 rpm. Approximately 1 ml of the supernatant was eliminated and cells were resuspended in the remaining volume. Cell suspension was spread on selective SD media and incubated 2-3 days at 30 °C. Colonies were patched onto an appropriate selective media and the genotype was confirmed by PCR. Positive clones were streaked for single colonies and stored as 15% glycerol stock in YPD at -80 °C.

2.2 Cell biology techniques

2.2.1 Spot tests

Overnight cultures of *C. albicans* and *C. glabrata* strains were grown in YPD (*C. albicans*) or SD (*C. glabrata*) media and diluted in fresh media to OD₆₆₀=0.2, followed by incubation for 3-4 hours with agitation at 30 °C till mid-exponential phase (OD₆₆₀=0.6-0.8). The cultures were diluted in YPD or SD and serial dilutions were spotted onto YPD or SD agar plates containing the indicated stress compounds using 48-well replica plater (Sigma). Strains were incubated at 30 °C for 24 - 48 hours.

Oxidative stress was induced using stocks of 30% v/v H₂O₂, 100 mM *t*-BOOH, 100 mM diamide or 100 mM menadione. Osmotic stress was induced using stocks of 4 M NaCl or 8 M sorbitol. Combinatorial stress induction was achieved by using the combination of certain oxidative and osmotic stress agents of defined concentration.

2.2.2 Yeast flow cytometry

For intracellular ROS detection, *C. albicans* or *C. glabrata* cells were grown in YPD pH 7.4 until mid-exponential phase (OD₆₆₀= 0.6-0.8). Cells were treated with the indicated stresses simultaneously with the fluorescent probe dihydroethidium (DHE, Sigma) to a final concentration of 20 µM from a 100 mM stock in DMSO.

Control samples were supplemented with an equal amount of solvent. The cultures were incubated at 30 °C for 45 minutes in the dark with agitation. Cells were collected by centrifugation at 3500 rpm for 2 minutes and an excess of dye was removed by washing the cells in 5 ml of 1 x PBS (Phosphate Buffered Saline pH 7.4; 137 mM NaCl, 2.7 mM KCl, 10 mM Na₂HPO₄, 1.8 mM K₂HPO₄). To avoid cell clumps, the suspension was sonicated at 35 kHz for 15 seconds and the homogeneity of cell suspension was accessed by microscope prior to the FACS. Cells were subjected to Fluorescence-Activated Cell Sorting (FACS) using a FACSAria Fusion (BD Biosciences, Sydney, Australia) with an argon 488 nm laser emitting at 595 nm. Data were analysed from three independent biological replicates using FlowJo software (TreeStar, Inc., Ashland, OR, USA).

2.3 Molecular biology techniques

2.3.1 DNA isolation

2.3.1.1 Plasmid isolation from *E. coli*

E. coli strains carrying plasmid DNA were cultured for 12-18 hours in LB media supplemented with 100 µg/mL ampicillin. The cells from 2-5 ml of culture were harvested by centrifugation at 3500 rpm for 10 minutes and subjected to the plasmid DNA extraction using GenEluteTM Plasmid Miniprep Kit (Sigma, Dorset, UK) according to the manufacturer's instructions.

2.3.1.2 Isolation of *C. albicans* and *C. glabrata* total DNA

For the isolation of total chromosomal DNA, *C. albicans* or *C. glabrata* strains were taken from a fresh patch on solid YPD agar, resuspended in 1 ml of sterile H₂O and centrifuged at 13000 rpm for 2 minutes. Cells were resuspended in chromosomal DNA breakage buffer (10 mM Tris-HCl pH 8, 1 mM EDTA, 100 mM NaCl, 1% w/v SDS, 2% v/v TritonX-100), transferred to a 2 ml screw-capped tube, followed by the addition of 200 µl of glass beads and 200 µl of phenol/ chloroform. Cells were disrupted using a bead beater (Biospec Products) for 20 seconds. The samples were centrifuged at maximum speed for 5 minutes and the supernatant containing

chromosomal DNA was transferred into a new tube. To precipitate DNA, 1/ 10th volume of 3 M sodium acetate and 2 volumes of 100% ethanol were added to each sample, mixed by several inversions and centrifuged for 15 minutes at 13000 rpm. Samples were washed with 400 µl of 70% ethanol and centrifuged for 5 minutes at 13000 rpm. Air-dried DNA pellets were dissolved in 100 µl of H₂O and stored at -20 °C.

2.3.2 DNA manipulation and analysis

2.3.2.1 Polymerase chain reaction (PCR)

All PCR reactions were carried on T3000 thermocycler (Biometra). In order to amplify DNA for cloning, DNA fragments were obtained using Pfusion PCR System (New England Biolabs). Each reaction mix contained:

H ₂ O	37 µl
5 x GC Buffer	10 µl
dNTPs 10 mM	1 µl
Forward primer 100 mM	0.5 µl
Reverse primer 100 mM	0.5 µl
DNA template	0.5 µl
Pfusion Polymerase	0.5 µl (10 units)

The DNA fragments generated by PCR were purified using QIAquick Nucleotide Removal Kit (QIAGEN) prior to cloning. The oligonucleotide primers for PCR reactions were synthesized by Eurogenetec (Southampton, UK; Table 2.2).

Oligonucleotide	Sequence 5' – 3'	Restriction site
CRM1MHF	AATGTCTGCAGCAATTATCTGGAGAAGC	<i>Pst</i> I
CRM1MHR	AATGTCTGCAGTTCGTCATCCATTCAAGAAGG	<i>Pst</i> I
TXL1MHF_PstI	AATGTCTGCAGATGTCAATTAAATTG	<i>Pst</i> I
TXL1MHR_PstI	AATGTCTGCAGTTCATCATCTATTG	<i>Pst</i> I

CRI1pACT_SalI F	AGGCAGGGTCGACATGCGTTCCCTCTTCC	SalI
CRI1pACT_SalI R	AGGCAGGGTCGACTTAGCAAGATATTAC	SalI
ACT1prom_F	GATGAAGCCAATCCAAAG	
PGK1prom_F	CCAGATGAGCGCGACATTAATACG	
CYC_TR_R	CGACAGCCATGTTGTAC	
CRI1pPGK_BamH1F	GCGCGGATCCATGCGTTCCCTCTTCC	BamH1
CRI1pPGK_BamH1R	GCGCGGATCCCTTGTATGTGCAAACGGATA	BamH1
CRI1_TERM_pPGK_Ba mH1-R	GCGCGGATCCCTTGTATGTGCAAACGGATA	BamH1
CRI2pACT_SalI F	AGGCAGGGTCGACATGCGTGCAAACAGC	SalI
CRI2pACT_SalI R	AGGCAGGGTCGACCTATGTACGTTG	SalI
CRI3pACT_SalI F	AGGCAGGGTCGACATGTACAAACCCCTTCC	SalI
CRI3pACT_SalI R	AGGCAGGGTCGACTCCAGTTGTTGC	SalI
CRI4pACT_SalI F	AGGCAGGGTCGACATGAAATTATTAAATTACT ATTAG	SalI
CRI4pACT_SalI R	AGGCAGGGTCGACCTAGTTACGTACAC	SalI

Table 2.2 Oligonucleotide primers used in the study

The reactions were performed using the following conditions:

98 °C – 10 min

98 °C – 30 sec

50 °C – 30 sec

72 °C – 1 min/ kb

} 35 cycles

72 °C – 10 min

4 °C – Hold

To check for correct strain construction, analytical PCR was performed using yeast genomic DNA as a template and Simple Red *Taq* polymerase system (Thermo Scientific, UK). Each 50 µl of reaction mix contained:

H ₂ O	42 µl
Buffer (0.5 M KCl, 100 mM Tris pH8, 1% Triton-X, 15 mM MgCl ₂)	5 µl
dNTPs 10 mM	1 µl
Forward primer 100 mM	0.5 µl
Reverse primer 100 mM	0.5 µl
DNA template	0.5 µl
<i>Taq</i> Polymerase	0.5 µl

Analytical PCR reactions were performed using the following conditions:

94 °C – 5 min
 94 °C – 1 min
 50 °C – 30 sec
 72 °C – 1 min/kb
 72 °C – 10 min
 4 °C – Hold

} 35 cycles

2.3.2.2 *Restriction endonuclease digestion, phosphatase treatment and DNA ligation reactions*

Restriction endonucleases were supplied by either Promega (Southampton, UK), or New England Biolabs (Herts, UK). Restriction endonuclease digestion was carried out according to the specific manufacturer's instructions. Reactions were terminated by the addition of 2-3 µl of 6 x DNA loading buffer (30% v/v glycerol, 0.25% w/v bromophenol blue, 0.25% w/v xylene cyanol FF) prior to analysis by agarose gel electrophoresis.

Phosphatase treatment was carried out using calf intestinal alkaline phosphatase supplied by New England Biolabs (Herts, UK). The reactions were set up according to manufacturer's instructions and incubated at 37 °C for 15-30 minutes.

DNA ligation reactions were carried out using T4 DNA Ligase (Promega, Southampton, UK), reactions contained a molar ratio of approximately 1 vector (50 ng): 3 insert fragment and incubated at 16 °C for 12-16 hours prior to the transformation into *E. coli* competent cells.

2.3.2.3 Analysis of DNA by agarose gel electrophoresis

DNA samples were analysed by gel electrophoresis on 0.8% w/v agarose/ TAE (40 mM Tris-acetate, 1 mM EDTA, pH 8.4) gels containing 0.02% ethidium bromide. Gels were run in TAE buffer at 100 V for 30-60 minutes. DNA fragments were visualized by UV light emission using a Gel Doc 1000 transilluminator system and analysed by Quantity One software (Bio-Rad Laboratories, Inc., California, USA). In order to purify DNA fragments for cloning, fragments were isolated from the gel using QIAquick® Gel Extraction Kit (Qiagen, UK) according to manufacturer's protocol.

2.3.2.4 DNA sequencing

DNA sequencing was carried by GATC Biotech (GATC Biotech Ltd, London, UK). The sequencing files were analysed using Chromas 2.4 software (Technelysium Pty Ltd).

2.3.3 Cap1 chromatin immunoprecipitation (ChIP)

To investigate Cap1 binding to the promoters of its target genes, chromatin immunoprecipitation assays were performed essentially as described by Liu et al (Liu et al., 2007).

2.3.3.1 Harvesting the cells

C. albicans cells expressing Myc-tagged Cap1 (JC948), and an untagged control strain (JC465), were inoculated into YPD media and allowed to grow overnight at 30 °C with agitation. Overnight cultures were diluted to an OD₆₆₀=0.2 in fresh YPD and incubated until exponential growth was obtained (OD₆₆₀ =0.8-1). Three independent cultures were subjected to different doses of oxidative stress (0.4 mM, 5 mM and 25 mM H₂O₂) and 50 ml of each culture was collected 5, 10, 30 and 60 minutes post stress addition. Proteins to the DNA were crosslinked by the addition of 37% formaldehyde (final 1% v/v) and incubated at room temperature for 30 minutes with agitation at 20 rpm. The crosslinking was quenched by the addition of 125 mM glycine and further agitation at 20 rpm, room temperature, for 10 minutes. In order to remove all of the formaldehyde, samples were centrifuged and washed twice with 40 ml of ice-cold TBS buffer (20 mM Tris-HCl, pH 7.5, 150 mM NaCl), spinning each time for 5 minutes at 4000 rpm at 4 °C. Pellets were resuspended in the remaining liquid and transferred into 1.5 ml screw-capped tubes, and centrifuged again for 1 minute at 14000 rpm. The remaining supernatant was removed, and cellular pellets were snap-frozen in liquid nitrogen.

2.3.3.2 Preparing the magnetic beads

To prepare the magnetic beads (Dynabeads, Invitrogen Life Technologies), 50 µl of beads per sample (2.5 ml total) were washed twice with 5 ml of freshly prepared 0.5% w/v BSA in PBS and collected by pulse-spin each time. After washing, 5 ml of 0.5% BSA in PBS was added to the beads, following by the addition of 500 µl of monoclonal mouse c-Myc Antibody (9E10, Santa Cruz Biotech) (10 µl per IP), gently resuspended and incubated overnight on rotary wheel at 4 °C. The following day, the beads coupled to the antibodies were washed twice for 5 minutes on a rotating wheel with 10 ml of lysis buffer (50 mM HEPES-KOH pH 7.5, 140 mM NaCl, 1 mM EDTA, 1% v/v Triton X-100, 0.1% w/v sodium deoxycholate) plus protease inhibitors (1 mM PMSF, 1 mM benzamidine, 10 µg/ ml aprotinin, 1 µg/ ml leupeptine, 1 µg/ ml

pepstatin), and resuspended in 30 μ l per IP of the lysis buffer plus protease inhibitors.

2.3.3.3 *Breaking the cells*

To break the cells, the samples were thawed on ice and resuspended in 700 μ l of lysis buffer plus protease inhibitors and 0.5 ml of glass beads. Cells were disrupted using a bead beater (Biospec Products) at 4 °C for 5 minutes, 3 times. Cell breakage was confirmed by examining cell suspensions under a light microscope. To collect the cell lysate, a hole was punched into the bottom of the screw-capped tube containing the lysed cells. This was placed on top of a fresh Eppendorf tube, and the lysate recovered by centrifugation for 2 minutes at 2000 rpm.

2.3.3.4 *Sonication of the chromatin*

Each sample was sonicated using a Sonic Dismembrator 100 (BioLogics, Inc.) four times for 20 seconds at output power level 8-9 Watts using the “Constant Power” setting. The tubes were kept on ice at all times between rounds of sonication. Samples were centrifuged at 14000 rpm for 10 minutes, 4 °C and the soluble fraction containing sheared chromatin (~400 bp DNA fragments) was transferred into a fresh tube and stored at -20 °C until required. The pellet generated after centrifugation was kept to use it as a control for qPCR and to check the primer efficiency curves.

2.3.3.5 *Immunoprecipitation*

For the immunoprecipitation, 30 μ l of washed beads were added to the soluble chromatin extracts and immunoprecipitated overnight at 4 °C. The following day, the beads were washed twice with 1 ml of lysis buffer plus protease inhibitors, twice with 1 ml of lysis buffer containing 360 mM NaCl, and once with 1 ml of TE buffer. Samples were centrifuged for 2 minutes at 4000 rpm at 4 °C and the supernatant was discarded.

2.3.3.6 *DNA purification*

For reverse crosslinking of the DNA, 100 μ l of freshly made TE/SDS (10 mM Tris pH 8.0, 1 mM EDTA, 1% w/v SDS) was added to the beads, vortexed and incubated overnight at 65 °C. Then samples were centrifuged at 14000 rpm for 2 minutes and the supernatant was transferred into a fresh tube. All samples were supplemented with a mixture of 295 μ l of TE buffer, 3 μ l of RNase A (10 mg/ ml), 2 μ l of glycogen and incubated for 2 hours at 37 °C in dry incubator, following by the addition of 15 μ l of 10% w/v SDS and 7.5 μ l of proteinase K, and incubated at 37 °C for another 2 hours. Proteins were removed by the addition of 400 μ l of phenol/ chlorophorm/ isoamyl alcohol (25:24:1), vortexing each time for 1 minute at maximum speed and centrifuging for 10 minutes at 14000 rpm, room temperature. Chromatin was precipitated by the addition of 16 μ l of 5 M NaCl and 2.5 volumes of ice-cold 100% ethanol to the 350 μ l aqueous layer and incubating overnight at -80 °C. The following day, the samples were centrifuged at 14000 rpm for 40 minutes at 4 °C and washed with 1 ml of 70% ethanol. Precipitated DNA was pelleted by centrifugation at 14000 rpm for 15 minutes at 4 °C and dried at 37 °C for 5 minutes. The pellet containing purified chromatin was solubilized in 50 μ l of TE buffer and stored at -20 °C until required.

2.3.3.7 *Quantification of DNA*

DNA concentrations were quantified using Quant-iT PicoGreen double-stranded DNA assay kit (Molecular Probes/ Invitrogen). Samples were diluted 1:50 in TE buffer (10 mM Tris-HCl pH 8.0, 1 mM EDTA), and PicoGreen mix was prepared following manufacturer's instructions. The measurement of dsDNA content was performed in 96-well black plate measuring the intensity of fluorescence of the substrate using TECAN fluorescent reader. The measurements were scored in triplicate for each sample, and DNA concentration was calculated related to a lambda phage standard curve control. The DNA concentrations ranged [0.03 - 0.69 ng/ μ l] for the tagged strain and [0.49 - 0.72 ng/ μ l] for the untagged strain.

2.3.3.8 Selection of the targets and qPCR primers design

To select the targets for Cap1 binding analysis, the candidate genes were shortlisted based on (i) Cap1 enrichment at their promoters (Znaidi et al., 2009) and (ii) the Cap1-dependent induction of these genes by H₂O₂ (Enjalbert et al., 2006, Wang et al., 2006, Urban et al., 2005). Q-PCR primers used in this study (Table 2.3) were optimized using Primer3 Web software (version 4.0.0) and synthesized by Invitrogen (Life Technologies).

Promoter	ChIP qPCR Primers (5'-3') SYBR Green Method	Amplon location relative to translation start site (ATG codon) – Assembly 19
CAT1	F: CACCACTTATAACCACCCATTAG R: GGTACAGAAATATGGTAGAAGTGAA	-990 to -773 (218 bp)
TSA1	F: GTCTGTTATGCCAATAGGTAAGAT R: ATTGGTGAGTGAGAGCTACAATATG	-522 to -317 (206 bp)
GLR1	F: TATATTGTCCGTCTGTGTATGC R: CGCTCCACAGTATAACTTATCAAAG	-261 to -126 (136 bp)
ACT1	F: TATGAAAGTTAAGATTATTGCTCCACC AGAAA R: GGAAAGTAGACAATGAAGCCAAGATA GAAC	+927 to +1,012 (86 bp)
TEF3	F: GATCACAAATTGGGTCCAAGG R: AGCAGCGGCAATCTTGTAC	+2,938 to +3,042 (105 bp)

Table 2.3 Primer sequences used for Q-PCR binding assays.

2.3.3.9 Q-PCR

To check the efficiency of the primers, serial dilutions of the whole cell extract sample fractions reserved after step 2.3.3.4 were used as a template for the reaction. All PCR products had melting curves indicating the presence of a single amplicon.

For quantitative PCR reactions, DNA samples obtained after 2.3.3.6 were diluted 1:10 to 1:100 depending on their concentrations and used as a template. Q-PCR reactions were performed in duplicates for each sample on Mastercycler® ep realplex (Eppendorf) qPCR system using the Takyon™ ROX Probe MasterMix (Eurogentec). Each qPCR reaction contained 10 µl of Takyon x SYBR® Green Universal PCR Master mix, 0.05 µl of 100 µM forward or reverse primer, 6 pg of DNA, and H₂O in a final volume of 20 µl. The reactions were carried with 1 cycle at 95 °C for 10 minutes, 40 cycles at 95 °C for 15 seconds, and 60 °C for 1 minute. Data analysis and threshold cycle (CT) values determination was performed using Realplex software (Eppendorf). The relative signal enrichment of the targets (*CAT1*, *TSA1* and *GLR1*) were calculated using 2(-Delta Delta C(T)) method (Livak and Schmittgen, 2001). *ACT1* promoter was used as a control for statistical analyses by t-test, and *TEF1* (orf19.1435) as a reference for normalization. Statistical analysis was performed using R software (version 3.2.2) using double sided T-test and equal variance assumption. Statistical significance was determined using Welsh's two-sample t-test (p<0.05 - *, p<0.01 - **, p<0.001 - ***).

2.3.4 RNA extraction, manipulation and analysis

2.3.4.1 RNA extraction

To collect the samples for RNA extraction, cells were grown until mid-exponential phase, treated or untreated with the required stresses, and 25-50 ml of cell culture was collected by centrifugation at 3500 rpm for 2 minutes. Cells were washed with 1 ml of sterile DEPC-treated H₂O, transferred to 2 ml screw-capped tubes and snap-frozen in liquid nitrogen. The samples were stored at -80 °C until required. Pellets were thawed on ice and resuspended in 200 µl of cold RNA buffer (100 mM EDTA pH 8.0, 100 mM NaCl, 50 mM Tris-HCl pH8.0) and 5 µl of 20% w/v SDS was added

to each sample, following by the addition of 200 μ l of phenol/ chloroform and ~500 μ l of baked glass beads. The samples were disrupted in a bead beater (Biospec Products) for 20 seconds. 800 μ l of RNA buffer was added to each sample, then the samples were vortexed and centrifuged at 6000 rpm for 10 minutes. The supernatant containing RNA was transferred into a new Eppendorf tube and phenol/ chloroform extraction was repeated twice. The aqueous layer was transferred to a fresh tube to which 1/10 volume of 3 M sodium acetate (pH 5.2) and 0.6 volumes of isopropanol was added. RNA was precipitated overnight at -80 °C. Samples were centrifuged for 15 minutes at 13000 rpm and washed with 300 μ l of 70% ethanol, following by centrifugation for 5 minutes at 13000 rpm. The RNA samples were air-dried and resuspended in 30-50 μ l of DEPC-treated sterile H₂O. RNA was dissolved by freezing the samples at -80 °C for 30 minutes following by thawing, vigorous vortexing and incubation for 30 minutes at 50 °C. The freezing-thawing cycles were repeated twice and RNA concentration was measured by absorbance at 260 nm using a nanodrop spectrophotometer (NanoDrop1000). The samples were diluted to a concentration of 10-30 μ g/ ml and kept at -80 °C until required.

2.3.4.2 Northern blotting

5 μ l of each RNA sample at a final concentration of 10-30 μ g/ ml was mixed with 12 μ l of denaturing buffer (2.5 μ l of 40% glyoxal [6.6 M], 8 μ l of DMSO in 10 mM NaPO₄ buffer pH6.5) and incubated 15 minutes at 50 °C. The samples were immediately chilled on ice and 4 μ l of RNA loading dye (50% v/v glycerol, 10 mM NaPO₄, 0.4% w/v bromophenol blue) was added. Denatured RNA samples were separated on 1.2% agarose gel prepared with 15 mM NaPO₄ buffer pH 6.5 at 4V/ cm with buffer recirculation for 2.5-3.5 hours.

Glyoxylated RNA was transferred immediately after electrophoresis from the gel onto a GeneScreen membrane (Dupont NEN Research Products, Boston MA) by capillary elution with 25 mM NaPO₄ buffer pH 6.5. The transfer was allowed to proceed for 12-16 hours, following by crosslinking of the membrane using a UV Stratalinker

2400 with auto cross link settings. Cross-linked membranes were wrapped in saran and stored at -20 °C until required.

Prior to radioactive labelling of RNA, the membranes were soaked in 2 x SSPE buffer (0.002 M EDTA, 0.298 M NaCl, 0.02 M phosphate buffer, pH 7.4) and pre-incubated with 5 ml of QuickHyb solution (Agilent Technologies, Inc.) for 20 minutes at 68 °C on rotary wheel. Gene-specific probes were amplified by PCR from *C. albicans* SN148 genomic DNA as a template and oligonucleotide primers specific for the required probe listed in the Table 2.4 using Pfusion DNA polymerase and the protocol described in 2.3.2.1.

Target gene	PCR primers (5' – 3')
<i>ACT1</i>	F: GATGAAGCCAATCCAAAAG R: GGAGTTGAAAGTGGTTGGT
<i>CTA1</i>	F: GAGTTGTCCACGCTAAAGGTTCCG R: CTCATGGGTATTCTTGTGTGGC
<i>TRR1</i>	F: CGAAGGTATGTTGGCTAATGG R: GGTTTGAATGTAACCAGCTTC
<i>IPF20401</i>	F: ATTGCTGTTGGTGATAAAGTCACC R: AGAACAGTTTCTTCACTGAGTGG
<i>NPR1</i>	F: TTTGACTGCGACGGTGTCTTATGG R: AACTAGCAATGTGTCCAAACCACC
<i>GPD2</i>	F: TGTATTGTCGGTCCGGTAAGTGG R: CTTAACATTCTACCAACCTGAGC

Table 2.4 Oligonucleotide primers used in the study to amplify probes for northern blot.

Adapted from (Enjalbert et al., 2006).

For radioactive labelling, 100 ng of amplified DNA in 33 µl of DEPC-treated H₂O was denatured by boiling for 5 minutes at 98-100 °C. Samples were immediately placed on ice, following by the addition of 10 µl of 5 x labelling buffer, 2 µl of dNTP mix (dGTP, dATP, dTTP [final concentration of 20 µM each]), 2 µl of BSA (400µg/ ml) and 1 µl of DNA Polymerase I Large (Klenow) Fragment (100u/ ml) from the Prime-a-

Gene labelling kit (Promega, Southampton, UK, Madison WI). The tubes were transferred to the radiation area and 2 μ l of α -³²P- labelled dCTP was added to each sample. Reactions were performed at 37 °C for 1 hour. Probes were denatured by boiling at 100 °C for 5 minutes and 200 μ l of salmon sperm carrier DNA (10 mg/ ml) was added to each sample. Radioactive content of the tubes was diluted in 1 ml of Quick-Hyb and transferred into glass tubes containing the membranes to be labelled. The membranes were incubated with the radioactive probes for 1 hour at 68 °C on the rotary wheel. The radioactive probes were then discarded and the membranes washed twice with 2 x SSPE buffer plus 0.1% w/v SDS at 60 °C for 10 minutes, followed by one wash with 0.1 x SSPE plus 0.1% w/v SDS for 10 minutes at 60 °C. The blot was wrapped in cling film and checked using Geiger counter. The washes were repeated until radioactive background counts were less than 20 counts per second (cps). Visualization of the northern blot was performed by exposing the membrane to a phosphoimaging screen for 30 minutes – 4 hours and RNA levels were observed using the phosphorimaging system (Typhoon, Amersham Biosciences) and quantified using Image Quant software (GE Healthcare Life sciences). Additionally, autoradiographs were obtained following exposure to X-ray film (Fuji Medical X-ray film - SuperRX) overnight at -80 °C.

Northern membranes were stripped by incubation with 50-100 ml of boiling stripping solution (0.1% SDS w/v, 0.1 x SSC [15 mM NaCl, 1.5 mM sodium citrate pH7.0], 40 mM Tris pH7.5) for 15 minutes at 68 °C in a glass tube with agitation. The procedure was repeated, then the solution was discarded and the membrane was checked using Geiger counter to ensure the successful removal of the radioactive probe.

2.4 Protein analysis

2.4.1 Preparation of native protein extracts

25-30 ml of mid-exponentially growing *C. albicans* cells were untreated or treated with the required stresses, collected by centrifugation at 3500 rpm for 2 minutes and immediately snap-frozen in liquid nitrogen. Thawed pellets were resuspended in 750

μ L of ice-cold lysis buffer (50 mM Tris-HCl pH7.5, 150 mM NaCl, 0.5% NP40, 10 mM imidazole) supplemented with a cocktail of protease inhibitors (10 μ g/ ml leupeptin, 10 μ g/ ml pepstatin, 0.07 trypsin inhibitor units/ ml aprotinin, 1 mM phenylmethanesulfonyl fluoride [PMSF] and phosphatase inhibitors [2 mM Na₃VO₄ and 50 mM NaF]). For samples that required the subsequent treatment with phosphatase, Na₃VO₄ and NaF were omitted. Samples were centrifuged at 13000 rpm for 2 minutes and the supernatant was discarded. Cell pellets were resuspended in 200 μ l of lysis buffer and transferred into 2 ml screw-capped tubes. An equivalent of 1 ml of glass beads was added to each tube and cells were disrupted using a bead beater for 2 x 30 sec. The protein extract was clarified by centrifugation at 13000 rpm for 10 minutes at 4 °C and protein concentration was measured using the Bradford method (Bradford, 1976).

2.4.2 SDS-PAGE and Western blotting

4 x SDS loading sample buffer (50 mM Tris-HCl pH 6.8, 2% w/v SDS, 10% v/v glycerol, 1% v/v β -mercaptoethanol, 12.5 mM EDTA, 0.02 % w/v bromophenol blue) was added to the protein extracts, and denaturing was completed by incubating at 100 °C for 5 minutes. Samples were then subjected to SDS-PAGE on 8-15% polyacrylamide gels depending on the size of the protein to be detected. 5 μ l of pre-stained molecular weight markers (Page Ruler, Thermo Scientific) was loaded and used to monitor running of the gel and efficient transfer. Gel preparation was performed using the protocol described by Laemmli et al. (Laemmli, 1970). Gels were run at 200 V in SDS-PAGE electrophoresis running buffer (2.5 mM Tris-HCl, 19.2 mM glycine, 0.01% SDS pH 8.3) for the required time and transferred onto nitrocellulose membrane (Protran®, Schleicher & Schuell Bioscience, DE) at 100 V for 1 hour. Transfer buffer contained 2.5 mM Tris-HCl, 19.2 mM glycine, 0.01% SDS, pH 8.3 and 20% v/v methanol.

The membrane was incubated with 10% BSA made in TBST (15 mM NaCl, 1 mM Tris-HCl pH 8.0, 0.1% Tween 20 v/v) and supplemented with 0.2% Na₃VO₄ v/v and 5% NaF, to block non-specific sites, for 30 minutes with agitation. Following blocking,

the membrane was incubated with the required primary antibody solution (Table 2.5) made in 5% BSA in TBST, and incubated at 4 °C overnight with agitation. Membranes were rinsed five times for 5 minutes in TBST following by incubation with the secondary antibody for 45 minutes at room temperature. Membranes were washed three times with TBST again and manually developed using ECL™ Western blotting detection system (Amersham Pharma Biotech) and Fuji Medical X-ray film.

Membranes were stripped by agitation at 50 °C for 30 minutes with stripping buffer (100 mM 2-Mercaptoethanol, 2% SDS w/v, 62.5 mM Tris-HCl pH 6.7), followed by two washes with TBST for 10 minutes with agitation at room temperature. Stripped membranes were blocked with 10% BSA in TBST and re-probed with the required primary antibody at 4 °C overnight.

Antibody	Description	Working dilution in 5% (w/v) BSA	Supplier
c-Myc 9E10: (SC40)	IgG mouse monoclonal	1:1000	Santa Cruz Biotech., Inc.
Anti-Cap1	IgG rabbit polyclonal	1:1500	Professor Scott Moyer-Rowley, University of Iowa
Anti-Histone H3,pan, clone A3S	IgG rabbit monoclonal	1:2000	EMD Millipore Corporation, Temecula, CA
Anti-acetyl-Histone H3 (Lys9)	IgG rabbit polyclonal	1:2000	EMD Millipore Corporation, Temecula, CA
Anti-acetyl-Histone H3 (Lys14)	IgG rabbit polyclonal	1:2000	EMD Millipore Corporation, Temecula, CA
anti-Phospho RNA Polymerase II (S2), ab5095	IgG rabbit polyclonal	1:2000	Abcam, Cambridge, UK
anti-Phospho RNA	IgG mouse monoclonal	1:2000	Abcam, Cambridge,

Antibody	Description	Working dilution in 5% (w/v) BSA	Supplier
Polymerase II (S5), ab5408			UK
anti-RNA Pol II CTD repeat YSPTSPS, ab817	IgG2a mouse monoclonal	1:2000	Abcam, Cambridge, UK

Table 2.5 Antibodies used in this study.

2.4.3 Cap1 phosphorylation assay

Cap1 phosphorylation assay was performed by adaptation of the protocol used by (Smith et al., 2004). Exponentially growing yeast cells expressing Myc-tagged Cap1 (JC948) were collected following exposure to oxidative, osmotic, or combinatorial stresses. 25-30 ml of the culture was harvested by centrifugation at 3500 rpm for 2 minutes and pellets were immediately snap-frozen in liquid nitrogen. Protein extracts were prepared as described in 2.4.1, with the lysis buffer supplemented with phosphatase inhibitors. 30 – 50 µg of total protein extract was subjected to SDS-PAGE on 8% polyacrylamide gels (4.6 ml of H₂O, 2.6 ml of acrylamide/ bis-acrylamide [30%/0.8% w/v], 2.6 ml of 1.5 M Tris-HCl pH8.8, 0.1 ml of 10% w/v SDS, 100 µl of 10% w/v ammonium persulfate, 10 µl of TEMED for 10 ml of separating gel). Phosphorylation of Cap1-Myc was detected by western blotting as described at 2.4.2. The membranes were blocked with 10% BSA and incubated overnight with anti-Myc primary antibodies at 4 °C, followed by the secondary horse radish peroxidase (HRP) conjugated anti-Mouse IgG antibody (1/2000 in 5% BSA; Sigma) with the subsequent manual development.

2.4.4 Determination of RNA polymerase II phosphorylation

C. albicans cells were collected and processed as described in section 2.4.1, with the exception that one extra time “zero” sample was collected and processed to allow

protein dephosphorylation. Essentially cells were lysed in buffer lacking the phosphatase inhibitors Na_3VO_4 and NaF and subsequently incubated with 200 units of Lambda protein phosphatase (New England Biolabs) for 30 min at 30 °C. All samples at the final concentration of 15 μg of the total protein extract were resuspended in 4 x SDS reducing sample loading buffer and subjected to SDS-PAGE on 8% polyacrylamide gels. SDS-PAGE was performed as described in section 2.4.2 and RNA Pol II phosphorylation was detected using anti-RNA Pol II phospho S2 (ab5095 [Abcam]) and anti-RNA Pol II phospho S5 (ab5408 [Abcam]) antibodies. Total levels of RNA Pol II were detected using an anti-RNA Pol II CTD repeat antibody (ab817 [Abcam]). Blots were stripped, and Cap1-MH was detected using anti-Myc antibodies (9E10 [Sigma]).

2.4.5 *Cap1-Crm1 co-immunoprecipitation*

Exponentially growing wild-type (JC1925), Δcap1 (JC710) or Δhog1 (JC1940) cells expressing 2-myc 6-His tagged Crm1 were harvested before and after stress treatments. Total protein extracts were prepared as described at 2.4.1, and 25 μg of each sample was supplemented with 4-5 μl of 4 x SDS loading dye and reserved as the 5% protein input sample. To precipitate Crm1-Myc, 20 μl of anti-myc (9E10) antibody-coupled agarose beads (Santa Cruz Biotechnologies) were added to 500 μg of total protein extract and incubated at 4 °C for 1 hour at rotary wheel. Then samples were spun at 6000 rpm for 1 minute and the beads were extensively washed with lysis buffer without NaF and Na_3VO_4 (7-10 times). The lysis buffer was removed and the beads were incubated in the residual buffer with 200 units of Lambda protein phosphatase (New England Biolabs) for 30 min at 30 °C. Finally, the beads were resuspended in 5-10 μl of 4 x SDS loading dye. To dissociate bound proteins from the beads, samples were boiled for 5 minutes at 98 °C, and the beads were removed by centrifugation at 13000 rpm for 1 minute. The supernatant containing proteins was immediately subjected to SDS-PAGE on 8% polyacrylamide gels, and co-precipitation of Cap1 was monitored by western blotting using anti-Cap1 polyclonal antibodies (kindly provided by Professor Scott Moye-Rowley, University of Iowa).

Membranes were subsequently probed with anti-myc antibodies (9E10 [Sigma]) to determine the precipitated Crm1 levels.

2.4.6 Acid lysis protein extraction

For the extraction of proteins under acid conditions, 1 ml of mid-exponentially growing *C. albicans* cells were rapidly added to 1 ml of 20% w/v trichloroacetic acid (TCA), harvested by centrifugation for 2 minutes at 3500 rpm and immediately snap-frozen in liquid nitrogen. The thawed pellets were resuspended in 1 ml of ice-cold 10% TCA and transferred into screw-capped tubes containing an equivalent of 1 ml cold glass beads. Cells were disrupted using a bead beater (30 seconds, ice 2 minutes, 30 seconds) and the lysate was transferred into 1.5 ml Eppendorf tubes. Samples then were centrifuged for 10 minutes at 13000 rpm, 4 °C and the TCA removed. Remaining TCA was removed by washing protein pellets three times with 500 µl of ice-cold acetone, spinning each time at 6000 rpm for 1 minute. Acetone was removed and samples were air-dried at room temperature. The sample pellet was resuspended in 20 µl of TCA buffer (200 mM Tris-HCl pH8, 1 mM EDTA, 1% w/v SDS) supplemented with 1 mM PMSF with or without 25 mM 4-acetamido-4'-((iodoacetyl)amino)stilbene-2,2-disulphonic acid (AMS, Invitrogen, Paisley, UK). Samples were incubated at 25 °C for 30 minutes with further incubation at 37 °C for 5 minutes to allow AMS binding. Soluble fractions were obtained after centrifugation for 3 minutes at 13000 rpm and treated with 5 units of calf intestinal alkaline phosphatase (CIP [New England Biolabs]) for 1 h at 37 °C. Protein concentrations were quantified using Pierce™ BCA Protein Assay Kit (Fisher Scientific UK Ltd, Loughborough, UK) according to the manufacturer's protocol. 4-5 µl of 4 x SDS sample loading buffer (50 mM Tris-HCl pH 6.8, 2% w/v SDS, 10% v/v glycerol, 1% v/v β-mercaptoethanol, 12.5 mM EDTA, 0.02 % w/v bromophenol blue) was added to each sample and samples were stored at -20 °C until required. Proteins were separated by SDS-PAGE, following by the western blotting as described in section 2.4.2.

2.4.7 Determination of Cap1, Trx1 and Txl1 oxidation

To determine the oxidation status of Cap1, protein extracts were prepared under acid lysis conditions and treated with the thiol alkylating agent AMS, as described previously (da Silva Dantas et al., 2010). Briefly, 2 ml of *C. albicans* cells expressing myc-tagged Cap1 (JC948) untreated or treated with the required stresses were collected and proteins extracted as described in section 2.4.5. The TCA buffer was supplemented with 1 mM PMSF and 25 mM of the thiol binding reagent AMS (Invitrogen Paisley, UK) to monitor the shift in oxidised Cap1-Myc mobility. For control samples, AMS was omitted. All samples were resuspended in 5 µl of non-reducing 4 x SDS loading buffer (50 mM Tris-HCl pH 6.8, 2% w/v SDS, 10% v/v glycerol, 12.5 mM EDTA, 0.02 % w/v bromophenol blue) and separated for 3-4 hours by SDS-PAGE under non-reducing conditions on 8% polyacrylamide gels (width 15 cm, length 12 cm). The oxidation of Cap1-Myc was analysed by western blotting using anti-Myc antibodies (9E10 [Sigma]).

In order to determine the nature of Cap1 oxidation following different doses of oxidative stress and combinatorial stress, acid extracted protein pellets were subjected to rounds of alkylation and reduction using various chemicals that are listed in the Table 2.6. Protein extracts were incubated with *N*-ethylmaleimide (NEM [Thermo Scientific, Paisley, United Kingdom]) at a final concentration of 10 mM at 30 °C for 30 min in order to block free thiols, following by precipitation with 1 V of 20% trichloroacetic acid (TCA) on ice for 30 min, and washed extensively three times with acetone. NEM-labelled samples were resuspended in sample buffer (200 mM Tris-HCl pH 8, 1% SDS, 1 mM EDTA) supplemented with 20 mM DTT and incubated at 37 °C for 60 minutes in order to reduce the existing disulfides. Soluble fraction was separated by centrifugation at 13000 rpm for 3 minutes. An equal volume of 20% TCA was added to each tube and protein samples were precipitated on ice for 30 minutes or at -20 °C for 10 minutes. Then samples were spun for 15 minutes at 13000 rpm at 4 °C and supernatant was discarded. Protein pellets were resuspended in the sample buffer (100 mM Tris-HCl pH 6.7, 1 mM EDTA, 1% SDS) containing methoxy PEG-maleimide (mPEG-Mal; PEG-maleimide with a molecular weight of 2,000 [Nanocs, Inc., Boston, MA]) at a final concentration of 10 mM at 30 °C for 45

minutes (Okazaki et al., 2007) in order to label free thiols that were involved in the formation of disulfides. Acid precipitation and acetone washes were repeated, and samples were treated with 5 U of alkaline phosphatase (New England Biolabs) at 37 °C for 1 h to prevent phosphorylation from having an impact on AMS/PEG-maleimide-dependent mobility shifts (Patterson et al., 2013). Soluble fraction was separated by centrifugation at 13000 rpm for 3 minutes and the protein concentration was determined using BCA protein assay kit (PierceTM, Thermo Scientific). Required amount of protein extract was mixed with 4 x non-reducing SDS loading dye and stored at -20 °C. Samples were subjected to SDS-PAGE on 8% gels under non-reducing conditions, and Cap1-MH was detected as described above for AMS-treated Cap1 samples.

To monitor Trx1-Myc oxidation, *C. albicans* JC930 cells were treated or untreated with the required stresses and 1 ml of cell culture was collected per time point. Samples were extracted and AMS-labelled as described for Cap1-Myc, but the phosphatase treatment step was omitted. Protein extracts were ran on 15% polyacrylamide gels for 1-1.5 hours with the subsequent western blotting using anti-Myc antibodies for Trx1-Myc detection.

To examine the oxidation of Txl1-Myc, *C. albicans* JC2101 cells were treated and processed as described above for Cap1, with the only difference that the samples were ran on 10% polyacrylamide gels for 1.5-2.5 hours, following by the western blotting using anti-Myc antibodies to detect Txl1-Myc.

Agent	Stock concentration, mM	Working concentration, mM	Incubation temperature, °C	Incubation time, min	Source
NEM	200 (250 mg in 10 ml ethanol)	10	25 +Inactivation at 37	30 +Inactivation 5	Thermo Scientific, UK

Agent	Stock concentration, mM	Working concentration, mM	Incubation temperature, °C	Incubation time, min	Source
AMS	25 (25 µg of AMS in 1.6 ml TCA buffer)	25	25 + Inactivation at 37	30 +Inactivation 5	Invitrogen, UK
DTT	1 M in H ₂ O	10	37	60	Sigma, UK
mPEG-Maleimide	0.03 g in 250 µl of TCA buffer, pH 6.7	10	30	45	NANOCS Inc., Boston, USA

Table 2.6 Chemicals and reaction conditions used to determine Cap1 oxidation status.

2.4.8 Determination of histone H3 modifications

To examine histone modifications following treatment with different doses of H₂O₂ and combinatorial stress, *C. albicans* cells were treated with H₂O₂ (5 and 25 mM), 1 M NaCl and 5 mM H₂O₂ + 1 M NaCl for 10 and 60 minutes. Samples were collected and proteins extracted using the acid lysis protocol as described in section 2.4.6. 10 µg of total protein extract was subjected to SDS-PAGE on 15% polyacrylamide gels. Total levels of histone H3 and levels of H3 carrying H3K9 and H3K14 modifications were monitored using the antibodies from EMD Millipore Corporation (Temecula, CA) listed in the Table 2.5. Due to unmodified and modified versions of histone H3 having a very similar molecular mass, triplicate gels were ran and probed in parallel.

2.5 Imaging techniques

2.5.1 Differential interference contrast (DIC) microscopy

C. albicans cells were grown to mid-exponential phase ($\sim OD_{660} = 0.6$) and 10 ml collected before or after treatment with required stresses. Cells were fixed by the addition of 1/10 volume of freshly prepared 3.7% para-formaldehyde solution made in PEM (100 mM piperazine-1, 4-bis (2-ethanesulfonic acid) (PIPES) pH 6.8, 1 mM EGTA pH 8.0, 1 mM MgSO₄) and agitated for 30 minutes at room temperature. Fixed cells were washed three times in PEM and resuspended in 100 μ l of PEM. For microscopy, 5 μ l of cells were spread onto Poly-L-lysine coated glass slides and air-dried. The fixation was performed by incubating in ice-cold methanol for 6 minutes, following by the incubation in ice-cold acetone for 30 seconds. 3-5 μ l of Vectashield[®] mounting medium with 1.5 mg/ml DAPI (4', 6-diamidino-2-phenylindole) was added on top of each sample, to which a glass coverslip was added and sealed with nail varnish. Differential interference contrast (DIC) images were captured using Zeiss Axioscope with a 63 x oil immersion objective, and AxioVision digital imaging system.

2.5.2 Fluorescence microscopy to detect Cap1 localisation

To detect the localization of Cap1-GFP, the cells were prepared as described by (Enjalbert et al., 2006, Barelle et al., 2004). *C. albicans* cells expressing GFP-tagged Cap1 (JC1060) were grown in YPDT media to mid-exponential phase ($\sim OD_{660} = 0.6$), treated or untreated with required stresses for the indicated times, and immediately fixed in 3.7% paraformaldehyde made in PEM as described in section 2.5.1. Samples were mounted using 3-5 μ l of Vectashield[®] mounting medium, a glass coverslip was applied and sealed with nail varnish. DAPI and GFP fluorescence were captured by exciting cells with 365- and 450- to 490-nm wavelengths, respectively, by using a Zeiss Axioscope with a 63 x oil immersion objective, and AxioVision digital imaging system.

2.6 *Caenorhabditis elegans* virulence assays

2.6.1 *Caenorhabditis elegans* strains and growth conditions

C. elegans strains listed in Table 2.7 were maintained on Nematode Growth Medium (NGM; 50 mM NaCl, 1.7% w/v agar, 0.25% w/v peptone, 1 mM CaCl₂, 25 mM KH₂PO₄, 1 mM MgSO₄), supplemented with 1 ml/L cholesterol (5 mg/ml stock in 95% ethanol) and streptomycin (300 ng/ml); 7ml of media was poured into small Petri dishes and seeded with 300 µl of an overnight culture of *Escherichia coli* OP50 (uracil auxotroph derived from *E. coli* B [Berkeley strain]) as a standard food source (Brenner, 1974) and allowed to grow for 48 hours. 20-40 worms at L4 stage were transferred into each plate and stocks were maintained at 15 °C.

Strain	Genotype	Reference
glp-4	glp-4(bn2)	<i>Caenorhabditis</i> Genetics Center (CGC)
glp-4 sek-1	glp-4(bn2)1;sek-1(km4)	CGC

Table 2.7 *C.elegans* strains used in this study

2.6.2 *C. elegans* synchronisation techniques

Age-synchronised young adult worms were generated by placing young adults at L4 stage onto NGML plates seeded with *E. coli* and incubating for 7-10 days at 15 °C. All animals were washed off from agar media with M9 buffer (6% w/v Na₂HPO₄ [BDH], 3% w/v KH₂PO₄ [BioChemika], 5% w/v NaCl [Sigma], 0.25% w/v MgSO₄ x 7 H₂O [BDH]; Brenner, 1974), and young larvae were separated from the adult population by centrifugation at 1000 rpm for 1 minute. The supernatant containing young larvae was transferred to fresh NGML plates seeded with *E.coli* and incubated for an additional 2 days at 25 °C to induce sterility: the glp-4(bn2) mutant strain is severely depleted in germ cells, and unable to give progeny while raised at the restrictive temperature due to the cell cycle arrest (Beanan and Strome, 1992).

2.6.3 Solid plate *C. elegans* infection assay

An overnight culture of *C. albicans* cells expressing GFP reporter (JC1732) in 10 ml of YPD was diluted to an $OD_{660}=0.2$ and 10 μ l of cells spotted onto the centre of a Brain Heart Infusion (BHI, Scientific Laboratory Suppliers, Nottingham, UK) plates supplemented with kanamycin (45 μ g/ml from 10 mg/ml stock), and kept at room temperature overnight.

100-200 age-synchronised young adult worms (L4 stage) were transferred from NGML plates with *E. coli* as a standard food source to an organism-free NGML plate for 1 hour and then transferred to the experimental plates seeded with *C. albicans*. This prevented cross-contamination of the *C. albicans* plates with *E. coli*. For control plates, an equal number of worms were transferred to a fresh NGML plate seeded with *E. coli*. To examine the age-dependent susceptibility to infection, worms of three age groups were placed onto *C. albicans* plates – young adults (L4), mature adults (three days after L4 stage, L4+3 days), and worms of advanced age (L4+6 days). Experimental and control plates were incubated at 25 °C and the viability of worms was checked daily. Death was confirmed when the animal did not respond to touch with a platinum wire and there was no pharynx contraction observed. At the same time, the control group was maintained on non-pathogenic *E. coli* OP50 as a food source in order to subtract the animals dead due to age, rather than infection.

2.6.4 Fluorescent microscopy of *C. elegans* infected with *C. albicans*

Populations of 100-200 age-synchronised *glp-4* or *glp-4 sek-1* animals were infected as described in section 2.6.2 with a *C. albicans* GFP-fluorescent strain (JC1732) and maintained at 25 °C. In order to visualise the progression of accumulation of *C. albicans* cells in the worm intestine, 10-20 animals per time point were gently taken using a platinum wire and placed into a drop of 0.06% levamisole positioned on top of a patch of 3% agarose on a microscopy slide. When the animals were anaesthetised via the levamisole treatment, coverslips were applied and samples taken for immediate DIC and GFP fluorescence microscopy using a Zeiss Axioscope with 40 x and 63 x oil immersion objectives for DIC and GFP (at 450-490-nm

wavelengths) Axiovision imaging system. 40 x objective was used to image whole animals, whereas 63 x objective was used to visualise *C. albicans* cells.

2.6.5 Statistical analysis

C. elegans survival was examined by the Kaplan-Meier method and differences were determined by log-rank test (Minitab 16, State College, PA). A *P* value of <0.05 in 3 replicate experiments was considered statistically significant.

2.7 General laboratory suppliers

All commonly used laboratory reagents and media were supplied by Sigma (Dorset, UK), Thermo Fisher Scientific, Invitrogen Life Technologies or New England Biolabs, unless stated otherwise.

Chapter 3. Investigation of the responses of *Candida* species to combinatorial stress

3.1 Introduction

Phagocytes employ multiple strategies to kill pathogens, such as the generation of reactive oxygen, nitrogen and chloride species, cationic fluxes, acidification of the phagosome, and nutrient deprivation. *C. albicans* can successfully adapt to all of these stresses *in vitro*, and numerous reports provide compelling evidences that stress responses are essential for *C. albicans* virulence (Smith et al., 2004, Wysong et al., 1998, Alonso-Monge et al., 1999, Hwang et al., 2002, Lorenz et al., 2004, Fradin et al., 2005, Hromatka et al., 2005, Barelle et al., 2006, Wilson et al., 2009, Patterson et al., 2013). The majority of these studies have examined *C. albicans* responses to a single stress stimulus, and comparative studies have illustrated that *C. albicans* is more resistant to many stress conditions compared to other pathogenic and non-pathogenic fungi (Nikolaou et al., 2009, Jamieson et al., 1996). This begs the question of why is *C. albicans* sensitive to phagocyte-mediated killing in the immunocompetent host, when this pathogen displays high levels of resistance to phagocyte-imposed stress conditions *in vitro*?

Recent studies have provided some insight into what underlies the potency of phagocytes in the killing of *C. albicans*. Specifically, it has been observed that combinations of the physiologically relevant oxidative and cationic stresses is much more potent in killing *C. albicans* than the corresponding single stresses (Kaloriti et al., 2012). Furthermore, transcript profiling analysis revealed that the classical oxidative and osmotic stress-responsive transcriptomes fail to be induced following combinatorial cationic and oxidative stress treatment (Kaloriti et al., 2014). The AP-1 like transcription factor, Cap1, is the major regulator of the oxidative stress-induced transcriptome. Thus, a major aim of this Chapter is to delineate the mechanism(s) underlying the inhibition of Cap1 activation following treatment of *C. albicans* cells with combinations of cationic (NaCl) and oxidative (H₂O₂) stresses (Kaloriti et al., 2014). Such findings should provide insight into how phagocytes employ combinations of stresses to prevent activation of key stress-responsive regulators, a

phenomenon which has been referred to as ‘stress-pathway interference’ (Kalariti et al., 2014).

Compared to *C. albicans*, *C. glabrata* is more resistant to combinatorial cationic and oxidative stress-mediated killing (Kalariti et al., 2012). In this Chapter, potential mechanisms that may underlie this increased resistance of *C. glabrata* to combinatorial stress are also explored.

3.2 Results

3.2.1 *Cap1 activation is prevented following exposure to combinatorial oxidative and cationic stress*

The increased sensitivity of *C. albicans* to combinatorial oxidative and cationic stress is largely attributed to the lack of activation of the Cap1 transcription factor (Kalariti et al., 2014). However, the mechanisms behind combinatorial stress-induced inactivation of Cap1 remain unknown. As previously described in the introduction (section 1.5.2.3.3), one of the key events in the activation of Cap1 is the oxidation of conserved cysteine residues resulting in interdomain disulphide bond formation between two cysteine rich domains, the n-CRD and c-CRD. The oxidised form of Cap1 accumulates in the nucleus, as the NES located within the c-CRD is now masked and thus cannot be recognised by the Crm1 nuclear exporter. Therefore, the oxidation status of Cap1 was examined following treatment with combinations of oxidative (5 mM H₂O₂) and osmotic (1 M NaCl) stresses, alongside other readouts of Cap1 activation. *C. albicans* cells expressing myc-His tagged Cap1 and GFP-tagged Cap1 were subjected to the combinatorial stress treatment, or treatment with H₂O₂ alone, for 10 minutes and Cap1 activation compared. No nuclear accumulation of Cap1-GFP was evident following a 10 minute combinatorial stress treatment, in contrast to the clear nuclear accumulation seen following H₂O₂ treatment alone (Figure 3.1A). Consistent with phosphorylation of Cap1 being a nuclear-mediated event (Patterson et al., 2013), Cap1 phosphorylation was observed following H₂O₂ treatment but not following combinatorial stress (Figure 3.1B).

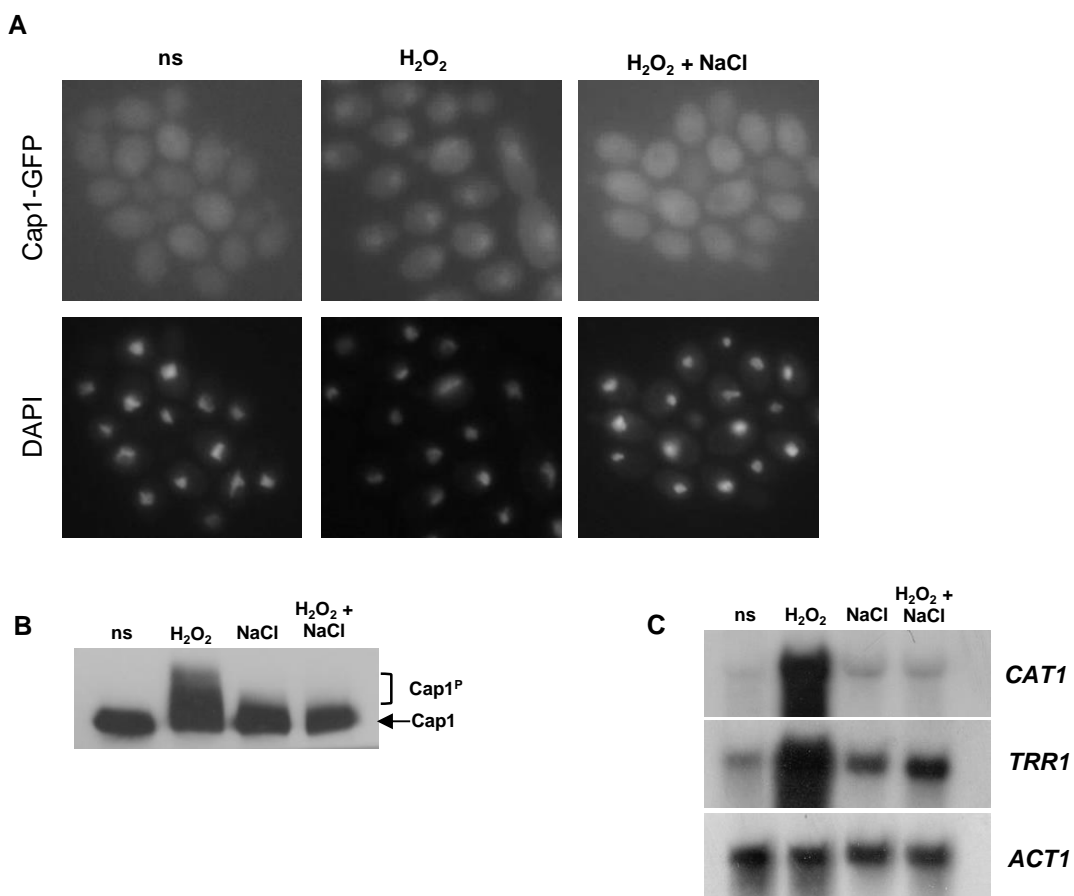


Figure 3.1 The lack of antioxidant gene expression following combinatorial stress is due to the inhibition of Cap1 activation.

(A) Cap1 does not accumulate in the nucleus following combinatorial stress. Localisation of Cap1 was detected by fluorescence microscopy of cells expressing Cap1-GFP (JC1060) under non-stress conditions (ns) and after exposure to 5 mM H_2O_2 or 5 mM H_2O_2 plus 1 M NaCl for 10 min. The position of the nuclei is shown by DAPI staining. (B) Cap1 is phosphorylated following H_2O_2 exposure, but not combinatorial stress. Lysates from cells expressing 2Myc- and 6His-tagged Cap1 (Cap1-MH-JC948), before (ns) and after the indicated stress treatments, were analysed by western blotting using an anti-Myc antibody. The positions of unphosphorylated (Cap1) and phosphorylated (Cap1^P) Cap1 are indicated. (C) Combinatorial stress inhibits H_2O_2 -induced antioxidant gene expression. Northern blot analysis of RNA isolated from wild-type (JC747) cells before (ns) and following a 10 min treatment with 5 mM H_2O_2 , 1 M NaCl, or 5 mM H_2O_2 plus 1 M NaCl. Blots were analysed with probes specific for the catalase (*CAT1*) and thioredoxin reductase (*TRR1*) genes. A probe against *ACT1* was used as a loading control.

Furthermore, in line with previous microarray data (Kaloriti et al., 2014), northern analysis confirmed that key antioxidant genes regulated by Cap1 – *CAT1* encoding catalase and *TRR1* encoding thioredoxin reductase – were not induced in response to combinatorial oxidative and cationic stress (Figure 3.1C). Based on these findings, that combinatorial stress prevents Cap1 activation and that Cap1 oxidation is essential for the activation of this transcriptional factor, we predicted that Cap1 oxidation was prevented by the combinatorial stress treatment.

To detect the status of Cap1 oxidation, cell extracts were prepared using acid lysis (which prevents spurious oxidation events) and treated with the alkylating agent 4-aceto-4'-maleimidylstilbene-2,2'-disulfonic acid (AMS) (Delaunay et al., 2002). AMS binds specifically to reduced cysteines residues, increasing the size of the protein by 0.64 kDa per modified cysteine residue (Figure 3.2A). The H_2O_2 -induced oxidation of thiols prevents AMS binding, and consequently oxidised proteins have a lower molecular mass and faster mobility on non-reducing PAGE compared to the corresponding reduced proteins. *C. albicans* cells expressing Cap1-Myc were treated with the indicated stresses and oxidation followed by western blotting of AMS-treated samples. Cap1 oxidation was seen in response to H_2O_2 , but not NaCl (Figure 3.2B), as detected by a faster AMS-dependent mobility on SDS-PAGE (designated as $Cap1^{OX}$). The anti-Hog1 signal was used as a loading control. However, in contrast to the prediction that Cap1 oxidation would be inhibited by combinatorial stress treatment, Cap1 exhibited a faster AMS-dependent mobility than seen following H_2O_2 -treatment alone (designated as $Cap1^{OX-1}$). The faster mobility of $Cap1^{OX-1}$ indicates that Cap1 is more oxidised following combinatorial stress than H_2O_2 treatment alone. Although the faster mobility form of Cap1 observed following combinatorial stress was AMS-dependent, indicating that this was due to increased oxidation, experiments were performed to exclude the possibility that this faster mobility of Cap1 was due to protein degradation. *C. albicans* cells expressing Myc-tagged Cap1 were treated with oxidative (5 mM H_2O_2), cationic (1 M NaCl) stresses and their combination, and native protein extracts were analysed by SDS-PAGE and western blotting.

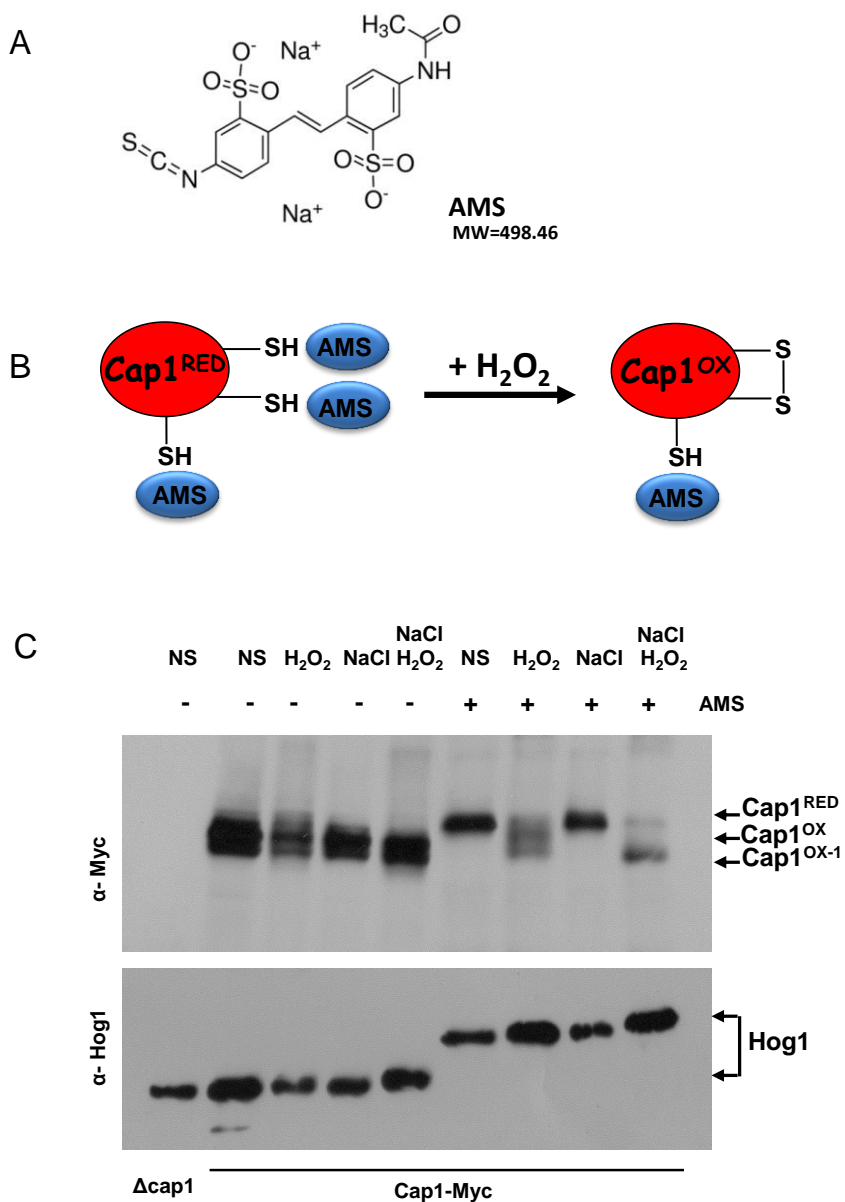


Figure 3.2 Cap1 is differentially oxidised in response to combinatorial stress.

(A) Chemical structure of AMS (4-Acetamido-4'-isothiocyanato-2,2'-stilbenedisulfonic acid disodium salt hydrate). (B) Cartoon illustrating the detection of protein oxidation by AMS binding to reduced thiols. (C) Cap1 is differentially oxidised following combinatorial stress. Cap1 oxidation was analysed by non-reducing SDS-PAGE and western blotting of AMS-modified or untreated proteins prepared from the cells expressing Cap1-MH, before (NS) and following 10 minutes of 5 mM H_2O_2 , 1 M NaCl and 5 mM H_2O_2 + 1 M NaCl stress treatments. Extracts from *cap1Δ* cells were included as a control. The positions of reduced (Cap1^{RED}), oxidised (Cap1^{OX}), and differentially oxidised (Cap1^{OX-1}) Cap1 are indicated. The blot was subsequently reprobed with anti-Hog1 antibodies as a loading control.

This revealed no impact of the stresses examined on Cap1 stability (Figure 3.3A). Densitometric quantification of Cap1 protein levels showed no statistically significant difference before or after the stresses tested.

The increased mobility of Cap1^{OX-1} generated in response to combinatorial stress indicated that Cap1 is more oxidised following this treatment. To explore the nature of this oxidised form, the presence of redox-sensitive disulfides was investigated. To detect redox-sensitive disulfides, protein extracts were treated with the small molecular weight thiol-binding agent *N*-Ethylmaleimide (NEM), which binds to reduced, but not oxidised cysteine residues. Any oxidised disulfides present in the protein are then reduced with dithiothreitol (DTT), and the newly released reduced thiols then bound with AMS (Figure 3.4A). Thus, in this experiment, increasing numbers of disulfides is reflected by a reduced mobility on SDS-PAGE. Cells expressing Cap1-MH were exposed to 5 mM H₂O₂ or combinations of 5 mM H₂O₂ and 1 M NaCl for 10 minutes, and the subsequent acid lysis-derived extracts were treated with NEM, DTT and AMS and different combinations of these chemicals. The appearance of the double band of Cap1 seen before stress was investigated and the fact that it disappears when cell extracts are immediately treated with NEM (which protects thiols from oxidation) suggests that this is due to some spurious oxidation during the preparation of the protein extracts. However, more importantly, Cap1 displayed a reduced mobility following the sequential NEM-DTT-AMS treatment following both H₂O₂ and combinatorial stress treatment. This illustrates that both Cap^{OX} and Cap^{OX-1} forms, generated following H₂O₂ and combinatorial stress treatments respectively, contain disulphide bonds (Figure 3.4B). Samples treated with NEM-DTT-AMS showed Cap1-MH increased mobility compare to DTT-AMS treated samples following both oxidative and combinatorial stresses, suggesting that Cap1 may not be fully oxidised in these conditions; similarly, stress untreated DTT-AMS sample also exhibited increased relative mobility compare to NEM-DTT-AMS treated sample, indicating that Cap1 may potentially contain disulfides in non-stress conditions.

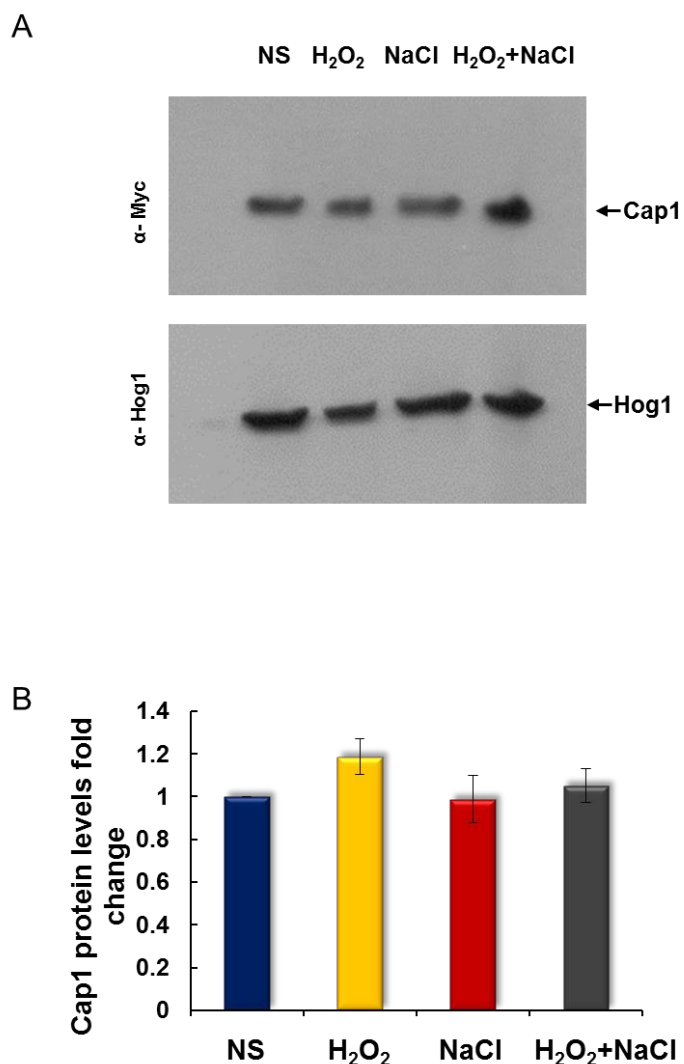


Figure 3.3 Quantification of Cap1 protein levels pre- and post-stress treatment.

(A) Cap1 protein levels were analysed by SDS-PAGE and western blotting of native extracts prepared from cells expressing Cap1-MH before (NS) and following a 10 min exposure to 5 mM H_2O_2 , 1 M NaCl, or combinations of these stresses. Blots were stripped and reprobed with an anti-Hog1 antibody as a loading control. (B) Quantification of Cap1 levels. Quantitative densitometric analysis of western blots from five biological replicates was conducted to determine the relative levels of Cap1 following the stress treatments described above, compared to non-stress (NS) levels. Mean values (\pm SEM) are shown and ANOVA was used to determine statistically significant differences in Cap1 levels. (Figure 3.3B). These results indicate that the differential mobility of Cap1 observed following combinatorial stress is not a result of protein degradation. No significant differences were observed; $p>0.05$.

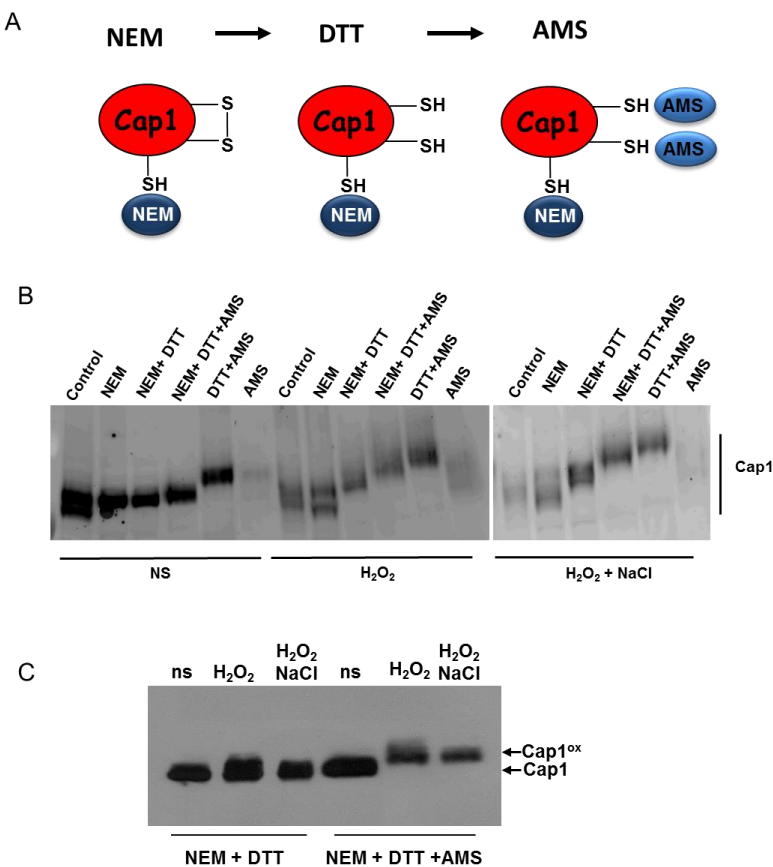


Figure 3.4 Cap1 oxidation following oxidative and combinatorial stress.

(A) Cartoon showing the sequential NEM-DTT-AMS treatments employed to allow for the detection of disulphide bonds. (B) Cap1 mobility was monitored by non-reducing SDS-PAGE and western blotting of proteins prepared from cells expressing Cap1-HM exposed to 5 mM H₂O₂, or to 5 mM H₂O₂ plus 1 M NaCl, for 10 min. Disulphide bonds are indicated by a retarded mobility of Cap1 due to AMS binding to DTT-resolved disulfides (compare NEM-DTT with NEM-DTT-AMS treated lanes). (C) The oxidised forms generated following both oxidative and combinatorial stress contain disulphide bonds. Cap1 mobility was monitored by non-reducing SDS-PAGE and western blotting of proteins prepared from cells expressing Cap1-HM, under non-stress conditions (ns, Cap1) or following treatment with the indicated compounds. The presence of disulphide bonds is indicated by a retarded mobility of Cap1 due to AMS binding to DTT-resolved disulfides. Slower mobility of Cap1 following oxidative stress could be due to residual phosphorylation seen following oxidative but not combinatorial stress (Figure 3.1B). To circumvent this issue, samples were phosphatase treated prior to loading. Data are shown as representative of three experiments.

To be able to better compare the mobility of Cap1 following H_2O_2 and combinatorial stress treatments, the NEM-DTT-AMS samples were ran together. As illustrated in Figure 3.4C, Cap1 has a slightly slower mobility following H_2O_2 treatment than combinatorial stress, indicating that Cap1^{OX} may have more disulfides than $\text{Cap1}^{\text{OX-1}}$. However, it was possible that the decreased mobility of Cap1 could be due to residual phosphorylation seen following oxidative stress, but not combinatorial stress (Figure 3.1B). To circumvent this issue, the experiment was repeated in which a higher molecular weight thiol binding agent, PEG-maleimide, was used instead of AMS (Figure 3.5A). Upon binding to free thiols, PEG-maleimide (PEG-M), results in a mobility shift of ~ 2 kDa per cysteine residue compared to ~ 0.64 kDa when treated with AMS (Okazaki et al., 2007). As shown in Figure 3.5B, a predominantly single oxidised form of Cap1 is seen following H_2O_2 treatment, whereas multiple differentially oxidised forms are detected following combinatorial stress.

The slow mobility of the single form of Cap1^{OX} generated post- H_2O_2 treatment indicates the presence of multiple disulfides. This may reflect the situation observed for Yap1 in *S. cerevisiae* in which three disulfides are formed between the six redox active cysteine residues (Figure 1.7, Okazaki et al., 2007). In contrast the multiple, faster mobility, bands seen with the combinatorial stress treatment are, most likely, intermediates that are less oxidised compared to Cap1^{OX} . These findings are reminiscent of the multistep oxidation mechanism of Yap1 (Okazaki et al., 2007), and that following combinatorial stress Cap1 is trapped in intermediate, partially oxidised, forms of the transcriptional factor. These data conflict with our previous AMS-binding experiments, where $\text{Cap1}^{\text{OX-1}}$ was more oxidised than Cap1^{OX} (Figure 3.2B). This seemingly contradictory observation could be explained by the hyperoxidation of cysteine thiols to sulphenic or sulfonic acid derivatives in the $\text{Cap1}^{\text{OX-1}}$ form (see discussion).

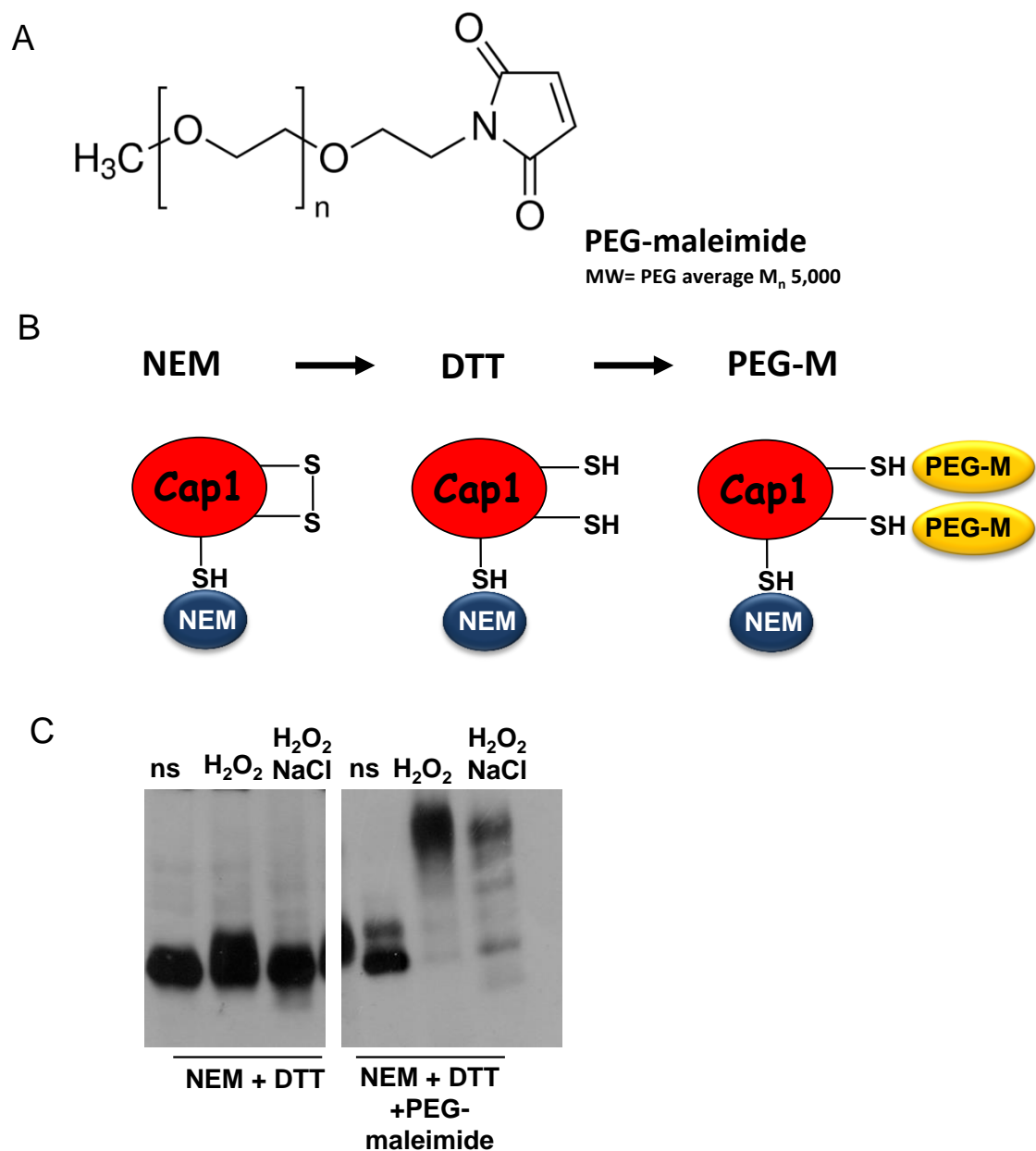


Figure 3.5 Cap1 forms multiple differentially oxidised intermediates following combinatorial stress treatment.

(A) Chemical structure of PEG-maleimide. (B) Cartoon showing the sequential NEM-DTT-PEG-maleimide (PEG-M) treatments which allow for the detection of disulphide bonds. (C) Comparison of Cap1 oxidation before (ns) and following oxidative and combinatorial stress by PEG-maleimide binding to DTT-resolved thiols. Samples were phosphatase treated prior to loading. This shows that different oxidised forms of Cap1 are present following combinatorial stress, whereas a single form containing multiple disulfides is prevalent following oxidative stress. Data are shown as representative of three experiments.

3.2.2 The inactivation of Cap1 following combinatorial stress is transient

According to the findings above, Cap1^{OX-1} has less disulfides than Cap1^{OX} and thus may be an intermediate form of fully active Cap1. This prompted the question as to whether combinatorial stress-mediated inactivation of Cap1 was irreversible or transient. To examine this, *C. albicans* cells were exposed to H₂O₂ stress alone, combinatorial H₂O₂ and cationic stress, and different readouts of Cap1 activation – nuclear accumulation, phosphorylation and Cap1-dependent gene expression - were examined over time. The nuclear accumulation of Cap1-GFP in response to the oxidative and combinatorial stresses indicated that following both stress treatments Cap1 accumulates in the nucleus (Figure 3.6). However, Cap1 nuclear accumulation was significantly delayed following H₂O₂ + NaCl treatment and Cap1 was not seen in the nucleus until 60 minutes post stress treatment. This contrasts to the rapid H₂O₂-induced nuclear accumulation of the transcriptional factor observed 10 minutes post stress treatment.

The kinetics of Cap1 phosphorylation in response to H₂O₂ and H₂O₂ + NaCl were next compared, as this post translational modification is associated with the nuclear accumulation of yeast AP-1 like transcriptional factors (Delaunay et al., 2000). Consistent with the delayed nuclear accumulation of Cap1, combinatorial stress caused a dramatic delay in Cap1 phosphorylation compared to H₂O₂ treatment alone (Figure 3.7), with the phosphorylated form of Cap1 (Cap1^P) not seen until 60 minutes post combinatorial stress treatment. In addition, northern blot analysis of two Cap1 target genes – *CAT1* and *TRR1* – revealed, that the combination of the oxidative and cationic stresses cause a significant delay in Cap1-dependent gene expression (Figure 3.8). The delay in the induction of Cap1 gene targets coincided with the delayed Cap1 nuclear accumulation and phosphorylation. Therefore, combinatorial stress-induced Cap1 inactivation is transient.

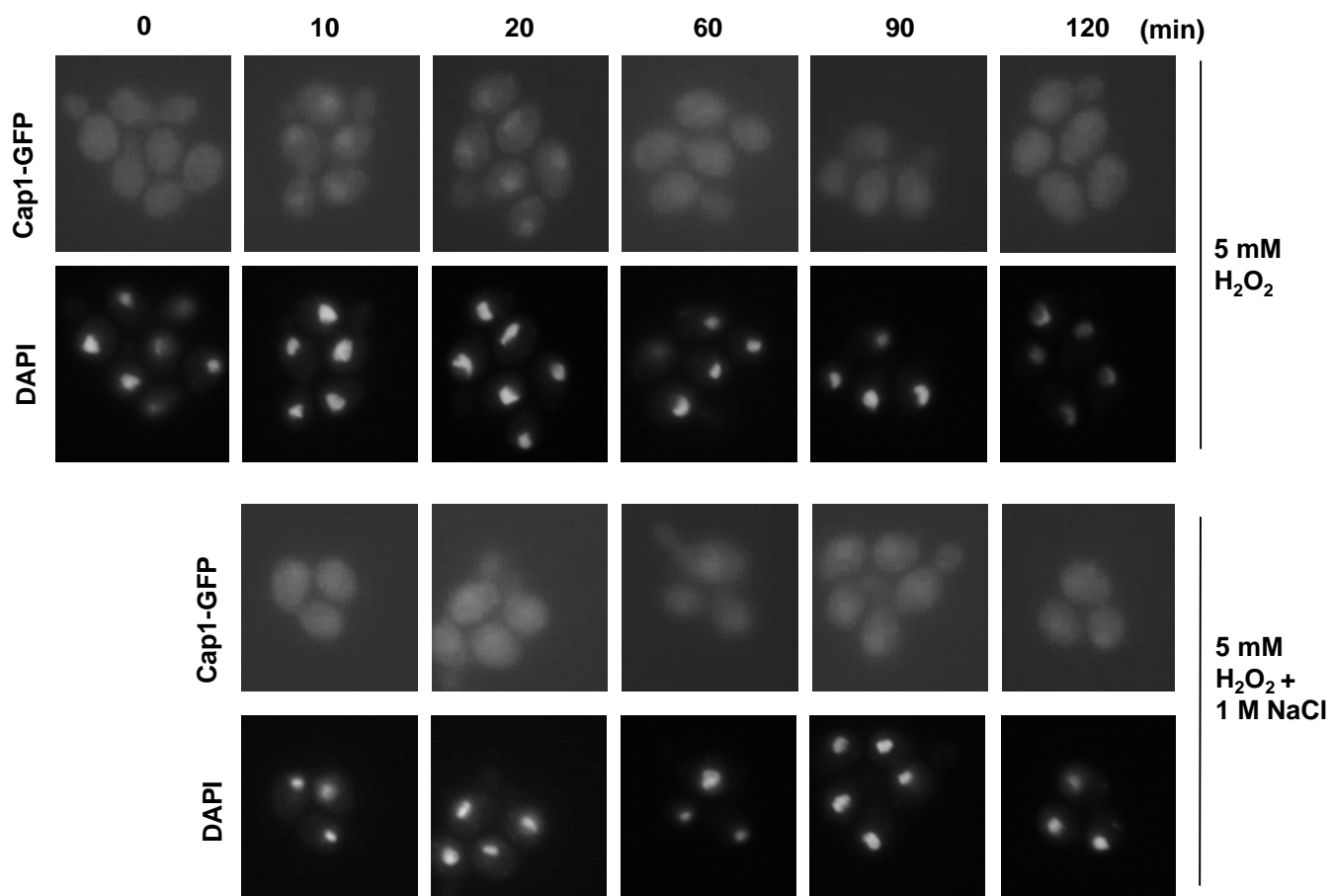


Figure 3.6 Cap1 nuclear accumulation is delayed following combinatorial stress.

Localisation of Cap1 was detected by fluorescence microscopy of cells expressing Cap1-GFP (JC1060) under non-stress conditions (ns) and after exposure to 5 mM H_2O_2 or 5 mM H_2O_2 plus 1 M NaCl for the indicated times. The position of the nuclei is shown by DAPI staining.

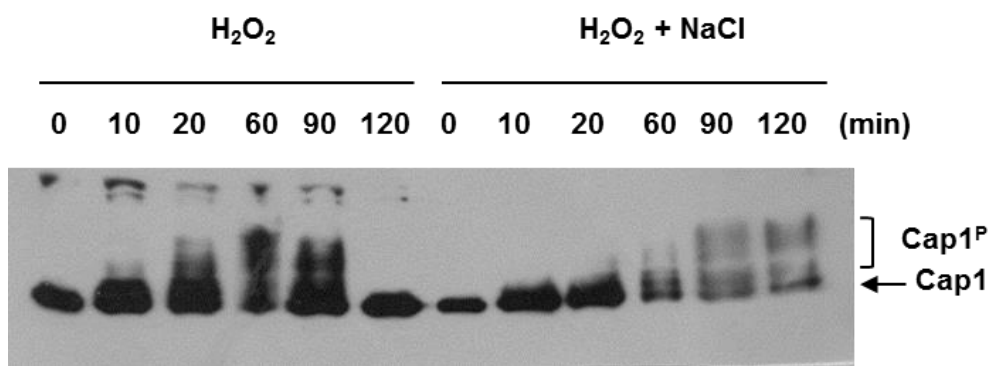
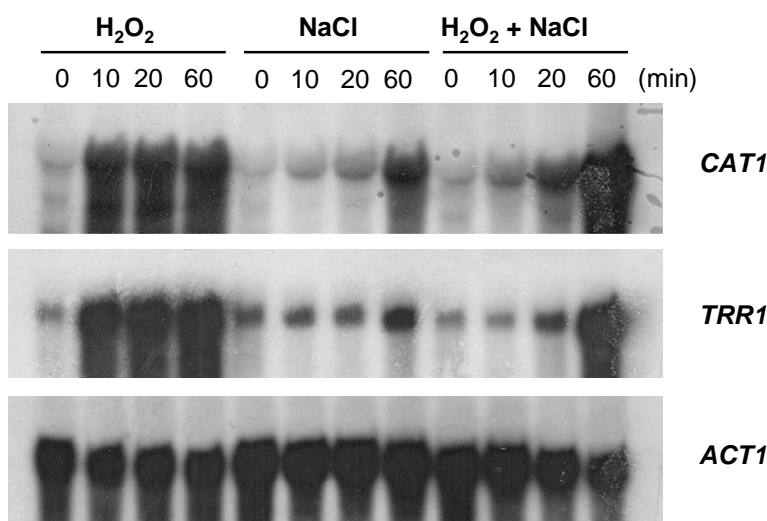


Figure 3.7 Cap1 phosphorylation is delayed following combinatorial stress treatment.

Lysates from cells expressing 2Myc- and 6His-tagged Cap1 (Cap1-MH, JC948), before (0) and after the exposure to oxidative (5 mM H₂O₂) or combinatorial (5 mM H₂O₂ + 1 M NaCl) stresses for the indicated times were analysed by western blotting using an anti-Myc antibody. The positions of unphosphorylated (Cap1) and phosphorylated (Cap1^P) Cap1 are indicated. Data are shown as representative of five experiments.

A



B

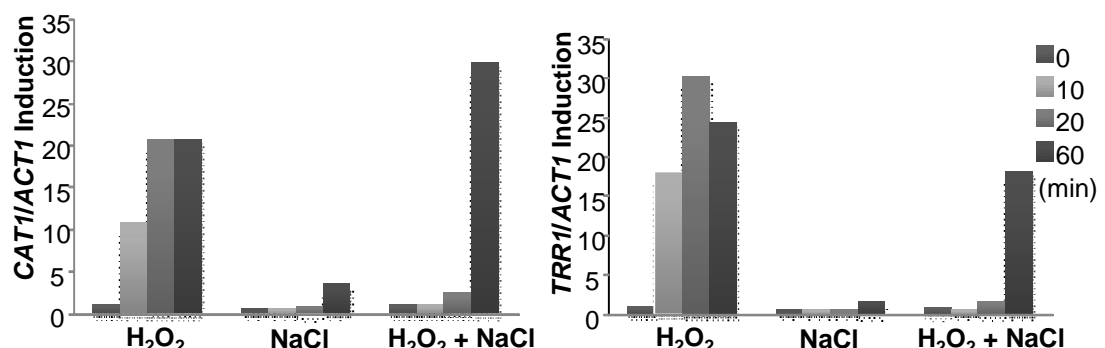


Figure 3.8 The inhibition of Cap1-dependent gene expression following combinatorial stress is transient.

(A) Northern blot analysis of RNA isolated from wild-type (JC747) cells before (ns) and following treatment with 5 mM H_2O_2 , 1 M NaCl, or 5 mM H_2O_2 plus 1 M NaCl for the indicated times. Blots were analysed with probes specific for the catalase (*CAT1*) and thioredoxin reductase (*TRR1*) genes. A probe against *ACT1* was used as a loading control. (B) The levels of *CAT1* and *TRR1* mRNA were quantified relative to the *ACT1* loading control.

As Cap1 activation was delayed following combinatorial stress, the kinetics of Cap1^{OX-1} formation was examined to investigate whether the restoration of Cap1 activity coincided with the resolution of the Cap1^{OX-1} to the Cap1^{OX} form. AMS-binding experiments revealed that, consistent with previous findings, Cap1^{OX} was quickly generated post H₂O₂ treatment and resolved back to the reduced form within 60 minutes (Figure 3.9). Treatment with combinatorial stress led to the initial generation of Cap1^{OX-1}, which was resolved to a form with mobility similar to that of Cap1^{OX} by 60 minutes post stress, demonstrating the transient nature of Cap1^{OX-1}. The differentially oxidised form of Cap1, generated post combinatorial stress, may therefore represent a transient intermediate in the generation of an active oxidised Cap1. Furthermore, the appearance and resolution of Cap1^{OX-1} coincides with both the delayed phosphorylation, nuclear accumulation of Cap1 and the expression of Cap1 target genes. Collectively, these results indicate that the differentially oxidised form of Cap1 generated following combinatorial stress can be resolved to an active oxidised form of this transcription factor, and combinatorial stress-induced Cap1^{OX-1} is inactive and unable to trigger the transcription of Cap1-dependent genes.

The *CAP1* gene itself is induced following oxidative stress (Fradin et al., 2005). Therefore, it was possible that new Cap1 synthesis was needed for the restoration of active Cap1 post combinatorial stress treatment. To test this hypothesis, the oxidation and phosphorylation profile of Cap1 was examined in *C. albicans* cells expressing *CAP1* under the control of heterologous *ACT1* promoter from its native locus. Cap1 phosphorylation in response to H₂O₂ and to the combination of H₂O₂ and NaCl was similar irrespective whether *CAP1* was expressed from its own or the *ACT1* promoter. In both strains, Cap1 was phosphorylated 10 minutes post H₂O₂ stress treatment, and Cap1 phosphorylation was delayed until 60 minutes following combinatorial stress (Figure 3.10A). Similarly, the oxidation profile of Cap1 in *pACT1-CAP1* cells was similar to that observed in wild-type cells (Figure 3.10B), suggesting that *CAP1* promoter-driven Cap1 synthesis is not required for the restoration of Cap1^{OX-1} to Cap1^{OX}. These findings indicate that new Cap1 synthesis is not required to restore Cap1 function post combinatorial stress, and support our hypothesis regarding the intermediate nature of Cap1^{OX-1} in the formation of an active Cap1^{OX}.

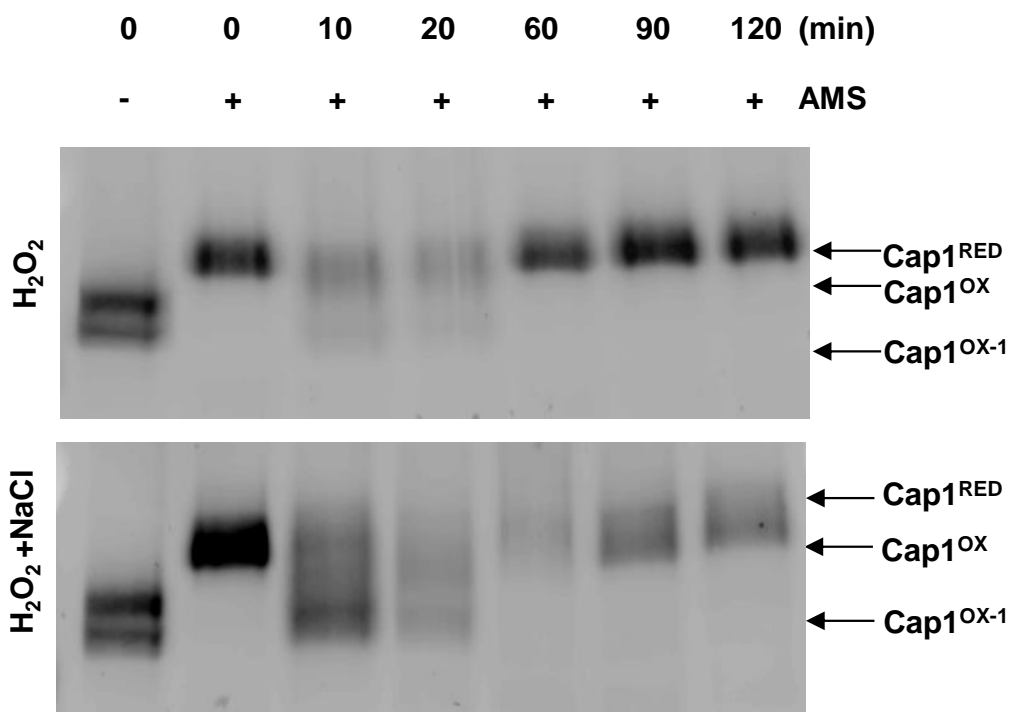


Figure 3.9 The differential oxidation of Cap1 following combinatorial stress is not sustained.

Cap1 oxidation was analysed by non-reducing SDS-PAGE and western blotting of AMS-modified or untreated proteins prepared from the cells expressing Cap1-MH, before (NS) and following exposure of Cap1-MH cells to 5 mM H_2O_2 or 5 mM H_2O_2 + 1 M NaCl for the indicated times. The positions of reduced (Cap1^{RED}), oxidised (Cap1^{OX}), and differentially oxidised (Cap1^{OX-1}) Cap1 are indicated. Data are shown as representative of five experiments.

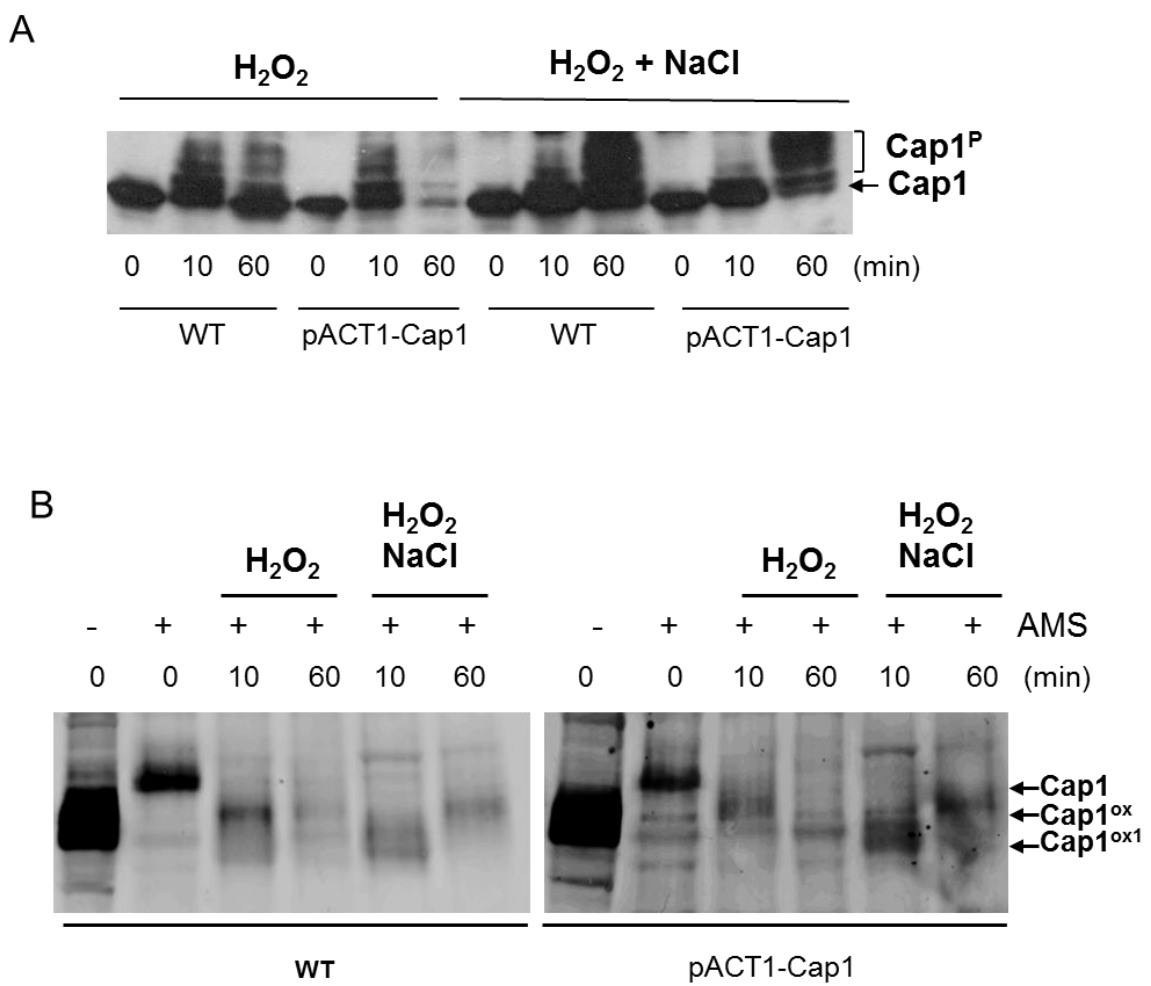


Figure 3.10 Cap1 activation profile in response to combinatorial stress in cells expressing *CAP1* under the control of its own or constitutive *ACT1* promoter.

(A) Cap1 phosphorylation in response to oxidative and combinatorial stress. Lysates were prepared from WT (JC747) or pACT1-CAP1 (JC1388) cells following treatment with oxidative (5 mM H_2O_2) or combinatorial (5 mM $\text{H}_2\text{O}_2 + 1 \text{ M NaCl}$) stresses for the indicated times. Cap1 phosphorylation was detected by western blotting using anti-Cap1 antibodies. The positions of unphosphorylated (Cap1) and phosphorylated (Cap1^{P}) Cap1 are indicated. (B) Cap1 oxidation profile in WT cells compared to cells in which *CAP1* is under the control of the *ACT1* promoter. The oxidation of Cap1 was measured by non-reducing SDS-PAGE and western blotting of AMS-modified or untreated proteins following exposure of WT (JC747) or pACT1-Cap1 (JC1388) cells to 5 mM H_2O_2 or 5 mM $\text{H}_2\text{O}_2 + 1 \text{ M NaCl}$ for the indicated times. Western blots were probed with anti-Cap1 antibodies. Data are shown as representative of three experiments.

3.2.3 The formation of $\text{Cap1}^{\text{OX-1}}$ is dependent on *Gpx3* and *Ybp1*

As discussed in the introduction (section 1.5.2.3.3), two proteins, Gpx3 and Ybp1, are required for the H_2O_2 -induced Cap1 oxidation (Patterson et al., 2013). Hence, the role of these two proteins in the generation of the combinatorial-stress induced $\text{Cap1}^{\text{OX-1}}$ form was investigated. Cap1 oxidation was followed using the thiol binding agent, AMS, as described previously. As illustrated in Figure 3.11A, no AMS-dependent formation of $\text{Cap1}^{\text{OX-1}}$ was observed in either *gpx3Δ* or *ybp1Δ* mutant cells following combinatorial stress. Consistent with previous findings (Patterson et al., 2013), there was also no formation of Cap1^{OX} following oxidative stress in cells lacking either Gpx3 or Ybp1. In addition, Cap1 levels were noticeably reduced in *ybp1Δ* cells due to previously established role of Ybp1 in maintaining Cap1 stability (Patterson et al., 2013). In addition, no Cap1 phosphorylation was observed following exposure to oxidative or combinatorial stress in $\Delta ybp1$ and $\Delta gpx3$ mutants (Figure 3.11B). These results illustrate that the generation of $\text{Cap1}^{\text{OX-1}}$ following combinatorial oxidative and cationic stress is dependent on both the Gpx3 thiol peroxidase and the Ybp1 protein. This is suggestive that the differentially oxidised Cap1^{OX} and $\text{Cap1}^{\text{OX-1}}$ forms emerge from the same oxidation pathway.

3.2.4 Combinatorial stress-induced delay in Cap1 activation is specific to the combination of H_2O_2 and cationic stresses

To examine whether combinatorial stress-induced Cap1 inactivation was specific for the combination of NaCl and H_2O_2 stresses, we investigated the potential of other combinations of related stresses to prevent Cap1 activation. For instance, to explore whether it is cationic, or osmotic, stress generated by NaCl that prevents the H_2O_2 -induced Cap1 activation, combinations of sorbitol and H_2O_2 were tested. Sorbitol is a commonly employed inducer of osmotic stress (section 1.4.1.3.2). *C. albicans* cells expressing Cap1-GFP were treated or untreated with 2 M sorbitol, 5 mM H_2O_2 , and the combination of these stresses (Figure 3.12A). 2 M sorbitol was used as the stressor, as this has the same osmolarity as 1 M NaCl.

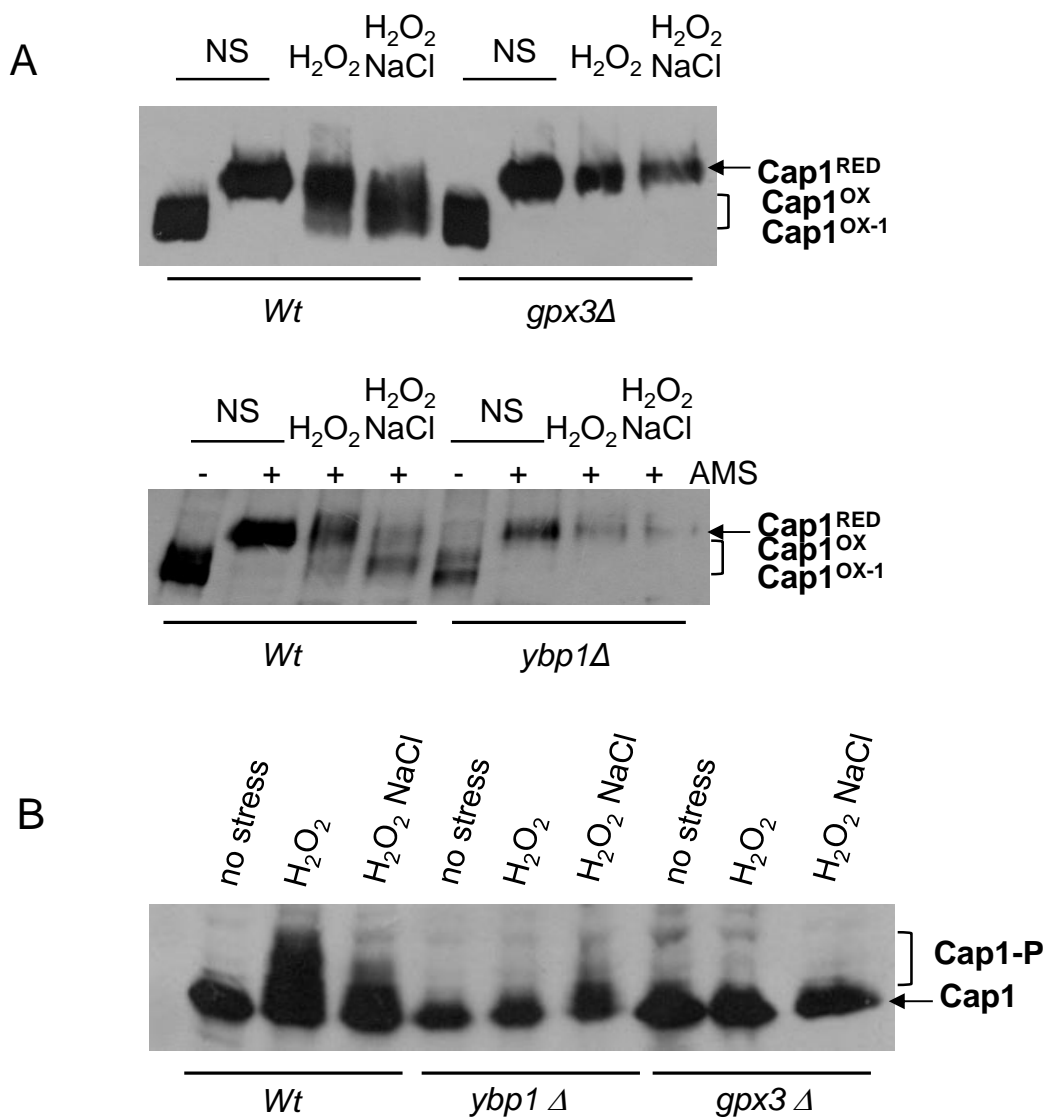


Figure 3.11 Gpx3 and Ybp1 regulate the formation of the combinatorial stress-induced $\text{Cap1}^{\text{OX-1}}$ form.

(A) Cap1 oxidation in cells lacking *YBP1* or *GPX3*. Cap1 oxidation was determined by western blotting of AMS-modified protein extracts from wild-type (*Wt*, JC948), *gpx3Δ* (JC1311) and *ybp1Δ* (JC954) cells expressing Cap1-MH before (ns) and following 10 minutes post stress treatments (5 mM H_2O_2 or 5 mM H_2O_2 plus 1 M NaCl). (B) Cap1 is unphosphorylated following combinatorial stress in *ybp1Δ* and *gpx3Δ* mutants. Cap1 phosphorylation was accessed by western blotting of native protein extracts from wild-type (*Wt*, JC948), *gpx3Δ* (JC1311) and *ybp1Δ* (JC954) cells expressing Cap1-MH 10 minutes post stress treatments. Cap1 was detected using anti-Myc antibodies. Data are shown as representative of three experiments.

Consistent with previous findings, Cap1-GFP localised to the nucleus in response to 5 mM H₂O₂, but not following the treatment with sorbitol. However, in contrast to the NaCl-mediated inhibition of Cap1 nuclear accumulation following H₂O₂ stress, the addition of sorbitol failed to prevent H₂O₂-induced Cap1 nuclear accumulation. These results indicate that cationic stress, and not osmotic stress, is vital for the combinatorial stress-induced Cap1 inactivation.

We also explored whether the cationic stress-mediated inhibition of Cap1 was specific to the ROS (H₂O₂), or whether this extended to other redox active compounds that activate Cap1. For instance, diamide induces oxidative stress by depleting cells of glutathione (Obin et al., 1998), and this triggers *S. cerevisiae* Yap1 nuclear accumulation via a different mechanism to what is reported to H₂O₂-driven response (Delaunay et al., 2000; Figure 1.8). As described in the introduction (section 1.5.2.3.1), studies of Yap1 oxidation revealed that the formation of interdomain disulphide bonds between the c-CRD and n-CRD occur upon oxidation of Yap1 in response to H₂O₂, whereas diamide triggers the formation of an intra-domain disulphide within the c-CRD. To investigate whether cationic stress could similarly inhibit diamide-mediated Cap1 activation, *C. albicans* cells expressing Cap1-GFP were exposed to 100 mM diamide in the presence or absence of 1 M NaCl, and Cap1 nuclear accumulation monitored. Cap1 rapidly accumulated in the nucleus following diamide treatment, illustrating that as with *S. cerevisiae* Yap1, this glutathione-depleting agent can trigger activation of Cap1 in *C. albicans*. However, in contrast to that seen with H₂O₂-induced Cap1 nuclear accumulation, cationic stress treatment did not inhibit diamide-stimulated Cap1 nuclear accumulation (Figure 3.12B).

Taking together the results of Cap1-GFP nuclear accumulation in response to different combinations of stress stimuli we can summarise that: (i) it is the cationic and not osmotic stress imposed by 1 M NaCl that inhibits the H₂O₂-induced activation of Cap1 and, (ii) NaCl-mediated inhibition of Cap1 activation only occurs when interdomain disulfides are generated within Cap1, as seen following H₂O₂ treatment.

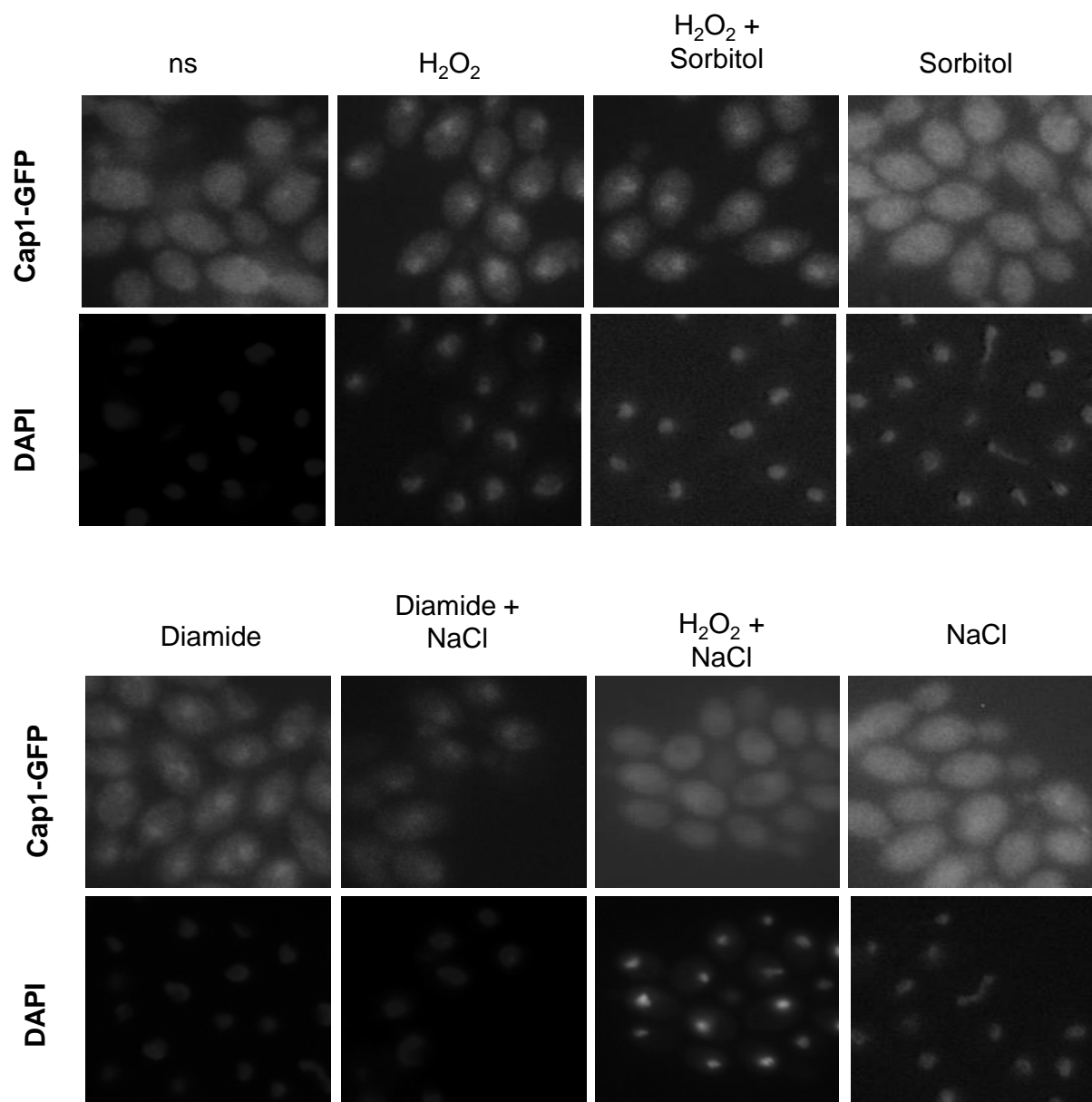


Figure 3.12 Cap1-GFP nuclear accumulation in response to different stresses and their combinations.

Localisation of Cap1 was detected by fluorescence microscopy of cells expressing Cap1-GFP (JC1060) under non-stress conditions (ns) and after exposure to (A) 5 mM H_2O_2 , 5 mM $\text{H}_2\text{O}_2 + 2$ M sorbitol and 2 M sorbitol, or (B) 100 mM diamide, 100 mM diamide + 1 M NaCl, $\text{H}_2\text{O}_2 + 1$ M NaCl, or 1 M NaCl for 10 min. The position of the nuclei is shown with DAPI staining.

Thus, the phenomenon of Cap1 stress pathway interference is exquisitely attributed to the combination of cationic stress and H₂O₂, which is of physiological relevance, as both stresses are found in the phagosomal microenvironment.

3.2.5 Combinatorial stress-mediated inhibition of Cap1 is maintained in hyphal *C. albicans* cells

C. albicans is a dimorphic fungus and can rapidly switch from budding to hyphal morphology in response to various environmental cues within the human host. This pathogen can successfully undergo hyphal transitions inside monocytes, resulting in the penetration of the phagosome membrane, macrophage killing and pathogen escape (detailed in section 1.4.1.1). Thus, we asked whether combinatorial stress-driven Cap1 inactivation is maintained when the fungus is in the hyphal form. To examine this, the nuclear accumulation of Cap1 was monitored under non-hyphae inducing conditions (YPD media, 30 °C), and under hyphae-inducing conditions (YPD media plus 10% fetal calf serum, 37 °C). As illustrated in the Figure 3.13, whilst Cap1 readily localised to the nucleus in both budding and hyphal cells following H₂O₂ treatment, no Cap1 nuclear accumulation was observed in either yeast or hyphal forms after combinatorial stress treatment until 60 minutes post stress. Thus, the mechanism of combinatorial stress-mediated inactivation of Cap1 occurs in different morphological forms of *C. albicans*.

3.2.6 Cationic stress promotes the interaction of Cap1 with the Crm1 nuclear exportin

Previous experiments revealed that cationic, and not osmotic, stress specifically impaired the H₂O₂-induced Cap1 nuclear accumulation. The mechanism of Cap1 nuclear accumulation is predicted to be similar to that reported for *S. cerevisiae* Yap1 and *S. pombe* Pap1, and is based on the oxidation-dependent masking of the nuclear export sequence, which inhibits the recognition of the protein by the Crm1 exportin (Wood et al., 2004, Yan et al., 1998, Kuge et al., 1998) (detailed description in section 1.5.2.3.1).

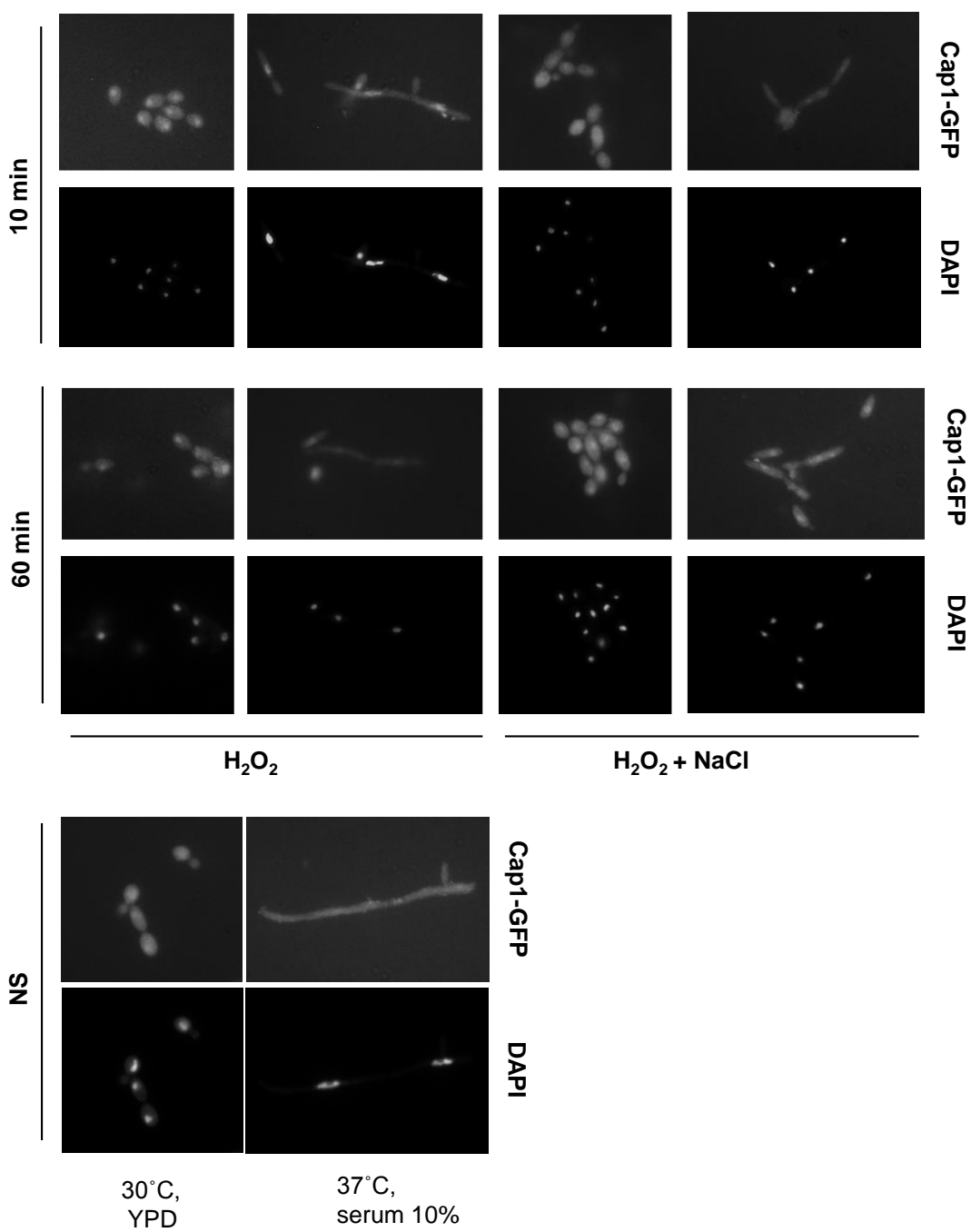


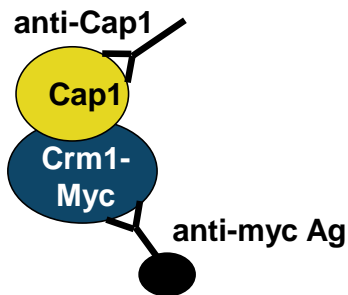
Figure 3.13 Combinatorial stress-mediated Cap1 inactivation is maintained in hyphal cells.

Cells expressing GFP-tagged Cap1 (JC1060) were incubated in YPD at 30 °C, or YPD supplemented with 10% human serum at 37 °C prior to stress. Localisation of Cap1-GFP was detected after exposure to 5 mM H₂O₂ or 5 mM H₂O₂ plus 1 M NaCl for the indicated times by fluorescence microscopy. Nuclei were detected by DAPI staining.

What, therefore, is the mechanism underlying the delay in Cap1 nuclear accumulation following combinatorial oxidative and cationic stress? Possibly, Cap1^{OX-1} forms a structure in which the NES is still accessible resulting in Crm1-mediated export. Alternatively, the cationic stress may have a more direct effect on the Cap1-Crm1 interaction. To test this latter hypothesis, a *C. albicans* strain was created in which Crm1 was tagged with 6 His residues and 2 Myc epitopes (Crm1-MH) and expressed from its native chromosomal locus. Crm1-MH was immunoprecipitated from extracts prepared from cells before and after exposure to 5 mM H₂O₂, 1 M NaCl, and 5 mM H₂O₂ + 1 M NaCl. The interaction between Cap1 and Crm1 was then examined by western blot analysis of these co-immunoprecipitates (Figure 3.14). In this assay, anti-Myc-agarose was used to precipitate Myc-tagged Crm1, and following SDS-PAGE co-precipitation of Cap1 was detected using anti-Cap1 antibodies (Figure 3.14A). Consistent with previous findings in *S. cerevisiae* (Kuge et al., 1998), Cap1 interacted with Crm1 *in vivo*, and this interaction was lessened in the presence of the oxidative stress (5 mM H₂O₂) (Figure 3.14B). However, both combinatorial stress and cationic stress alone led to the stabilisation of the Cap1-Crm1 complex, as more Cap1 co-precipitated with Crm1 following NaCl or NaCl plus H₂O₂ stress treatments. Similar amounts of myc-tagged Crm1 were immunoprecipitated in each sample, and the input controls confirmed that cationic stress-induced increased levels of Cap1 immunoprecipitation were not due to increases in Cap1 protein levels (Figure 3.14B). The diffused mobility of Cap1 following H₂O₂ treatment in the input sample (Figure 3.14B) is likely due to phosphorylation as these samples were not phosphatase treated.

Next, the kinetics of the cationic stress-induced increase in the Cap1-Crm1 interaction was examined to explore whether this was a transient effect or whether the enhanced interaction persisted over time. The interaction between Cap1 and Crm1 was detected as described above. More Cap1 co-precipitated with Crm1 following 10 minutes post combinatorial stress treatment compared to that observed after 60 minutes (Figure 3.15A).

A



B

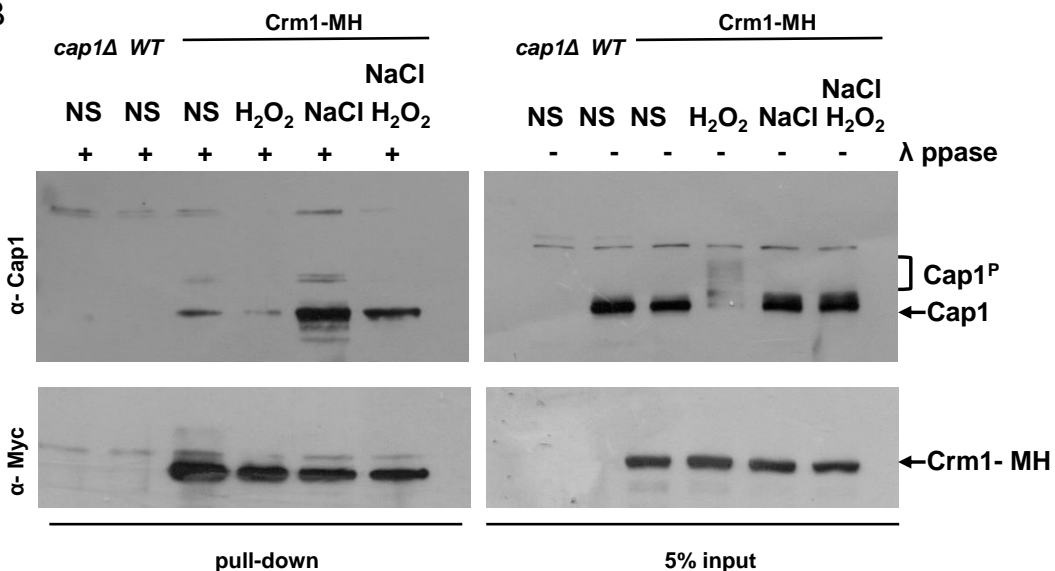


Figure 3.14 Cationic stress stimulates the interaction of Cap1 with the Crm1 nuclear export factor.

(A) A strategy used to examine Cap1 association with Crm1. (B) Stress effects on Cap1 interaction with Crm1. Extracts were prepared from wild-type (*Wt*, JC747), *cap1Δ* (JC842), and wild-type cells expressing 2Myc-6His tagged Crm1 (Crm1-MH, JC1925) before (NS) and following exposure to 5 mM H₂O₂, 1 M NaCl, or combinations of these stresses for 10 min. Crm1-MH was immunoprecipitated using anti-myc agarose. Precipitated proteins and 5% input were subjected to SDS-PAGE. Co-precipitation of Cap1 was assayed by western blotting using an anti-Cap1 antibody (top panel) and precipitation of Crm1-MH assayed using anti-Myc antibodies (bottom panel). Data are shown as representative of five experiments.

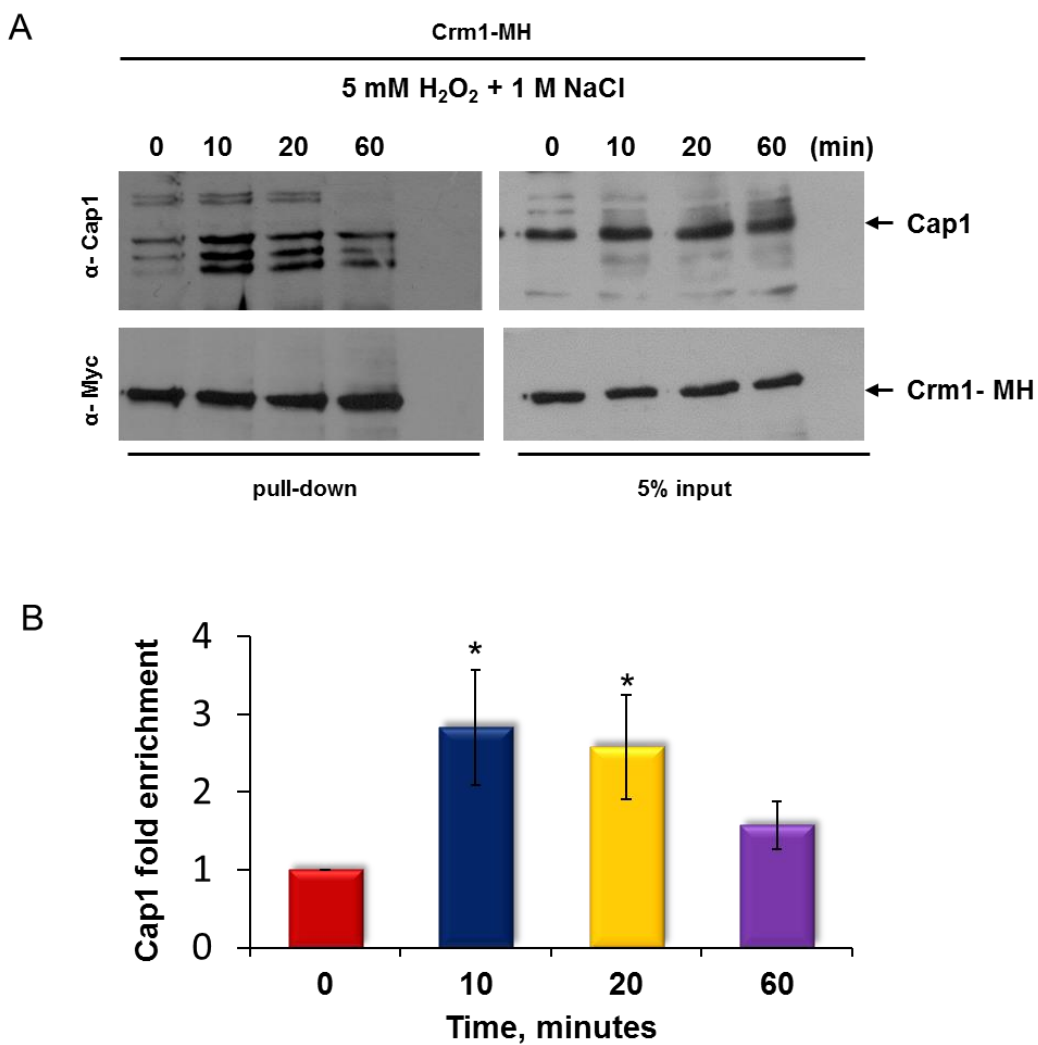


Figure 3.15 The increased interaction of Cap1 with Crm1 following combinatorial stress is transient.

(A) Kinetics of Cap1-Crm1 immunoprecipitation following the treatment with combinatorial oxidative and cationic stress. Cap1 interaction with Crm1 was analysed as described in Figure 3.14 legend, before (0) and following treatment of Crm1-MH cells with $5\text{ mM H}_2\text{O}_2 + 1\text{ M NaCl}$ for the times indicated. (B) Quantification of the increased interaction of Cap1 with Crm1 following combinatorial stress. Quantitative densitometric analysis of western blots from four biological replicates was conducted to determine the fold enrichment of Cap1 interaction with Crm1 relative to time “0”. Mean values (\pm SEM) are shown and ANOVA was used to determine statistically significant differences in Cap1 enrichment levels: *, $p < 0.01$.

The appearance of multiple Cap1 species in the immunoprecipitates may indicate that some protein degradation occurs during the precipitation procedure (Figure 3.15A). The levels of Cap1 enrichment were quantified from four biological replicates, and statistical analysis revealed a significant increase in Cap1 binding to Crm1 at both 10 and 20 minutes after the combinatorial stress, but not after 60 minutes (Figure 3.15B). Thus, the cation-induced Cap1-Crm1 interaction is transient and this effect is weakened 1 h post stress. The kinetics of the enhanced Cap1 interaction with Crm1 coincides with the delayed kinetics of Cap1 nuclear accumulation, phosphorylation and Cap1-dependent gene expression, observed following the combinatorial cationic and oxidative stress. Only when the cationic stress-mediated Cap1-Crm1 interaction is lessened after 60 minutes, is Cap1 activity restored. Thus, the kinetics of the Cap1-Crm1 interaction largely matches the kinetics of Cap1 inactivation following combinatorial stress. Taken together, these results, demonstrating a cationic stress-enhanced interaction of Cap1 with Crm1, likely underlie the combinatorial stress-mediated inhibition of Cap1 nuclear accumulation. Importantly, the salt-induced Cap1-Crm1 interaction is seemingly independent of the oxidation status of Cap1, as this is seen following cationic stress alone.

Previous experiments examining *C. albicans* responses to combinatorial oxidative and cationic stresses revealed that, in contrast to Cap1, the Hog1 SAPK was rapidly phosphorylated and localised to the nucleus (Kalogeriti et al., 2014). As cationic stress stimulates the Cap1-Crm1 interaction, it was possible that a specific cationic stress response such as Hog1-mediated glycerol production was important for this enhanced interaction. To examine whether Hog1 function contributed to the enhanced Cap1-Crm1 interaction following combinatorial stress, a strain was constructed in which Myc-tagged Crm1 was expressed in *hog1Δ* cells. This strain was subjected to H₂O₂ and NaCl stress treatments and their combination for 10 minutes and Cap1 precipitation with Crm1 was determined as described above. As shown in Figure 3.16A, the cationic-stress mediated enrichment of the Cap1-Crm1 interaction was maintained in *hog1Δ* cells. These results clearly demonstrate that NaCl-enhanced interaction between Cap1 and Crm1 is Hog1-independent.

Previously we found that the osmotic stress inducer, sorbitol, was unable to prevent the H₂O₂-induced nuclear accumulation of Cap1 (Figure 3.12). As Hog1 is activated in response to sorbitol, this observation is also consistent with the finding above (Figure 3.16A) that the cationic stress-mediated Cap1-Crm1 interaction is Hog1-independent. Nonetheless, for completeness, the impact of sorbitol treatment on the Cap1-Crm1 interaction was examined. Protein extracts were prepared from wild-type cells expressing 2Myc- and 6His tagged Crm1 before and following the exposure to 1 M NaCl for 10 minutes or 2 M sorbitol for 10, 30 and 60 minutes, and the co-precipitation between Cap1 and Crm1 was determined as described above. Consistent with previous findings, NaCl treatment clearly enhanced the Cap1-Crm1 interaction. However, sorbitol treatment failed to stimulate Cap1 binding to Crm1 (Figure 3.16B), thus confirming that the increased Cap1-Crm1 co-precipitation is cationic stress specific.

In addition to the cation specificity in preventing Cap1 activation, previous experiments revealed that this was also specific to H₂O₂, as cationic stress did not prevent the diamide-mediated nuclear accumulation of Cap1 (Figure 3.12B). Therefore, the impact of NaCl on the Cap1-Crm1 interaction in the presence of diamide stress was examined. *C. albicans* wild-type cells expressing Crm1-MH were incubated with 1 M NaCl, 100 mM diamide and the combination of 1 M NaCl and 100 mM diamide for 10 minutes. Protein extracts were then subjected to the Cap1-Crm1 pulldown assays as described previously. Significantly, the addition of NaCl did not promote the interaction between Cap1 and Crm1 when cells were treated with diamide (Figure 3.17). This is consistent with the observation that cations fail to impair diamide-induced Cap1 nuclear accumulation, indicating that diamide-mediated structural changes in Cap1 (oxidation in c-CRD) are dominant to the cationic stress effects on the Cap1-Crm1 interaction.

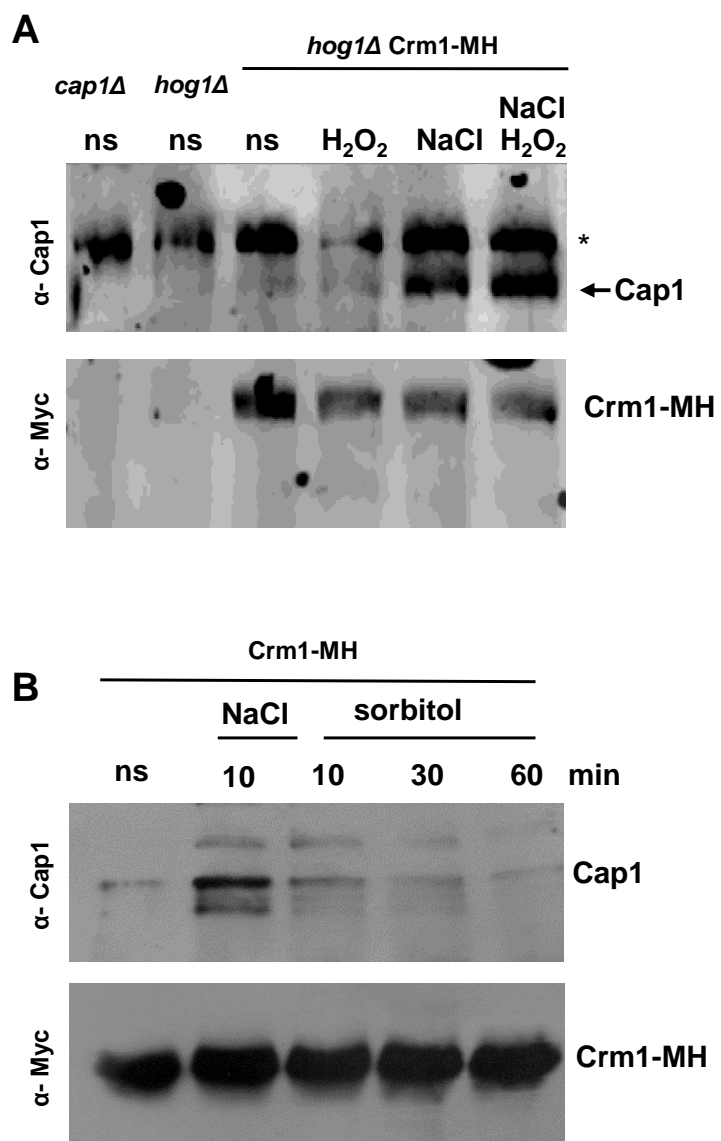


Figure 3.16 The NaCl-enhanced interaction between Cap1 and Crm1 is Hog1-independent and cationic stress specific.

(A) Hog1 is dispensable for the NaCl-induced Cap1-Crm1 interaction. Extracts were prepared from *hog1Δ* (JC45), and *hog1Δ* cells expressing 2Myc-6His tagged Crm1 (JC1940) before and following exposure to 5 mM H_2O_2 , 1 M NaCl, or combinations of these stresses for 10 min. Co-precipitation of Cap1 was detected as described in Figure 3.14 legend. * designates a non-specific band as this is seen in *cap1Δ* cells. (B) Sorbitol fails to promote the Cap1 interaction with Crm1. Extracts were prepared from wild-type cells expressing 2Myc-6His tagged Crm1 (Crm1-MH, JC1925) before and following exposure to 1 M NaCl for 10 min, or 2 M sorbitol for the indicated times. Co-precipitation of Cap1 was detected as described in Figure 3.14 legend.

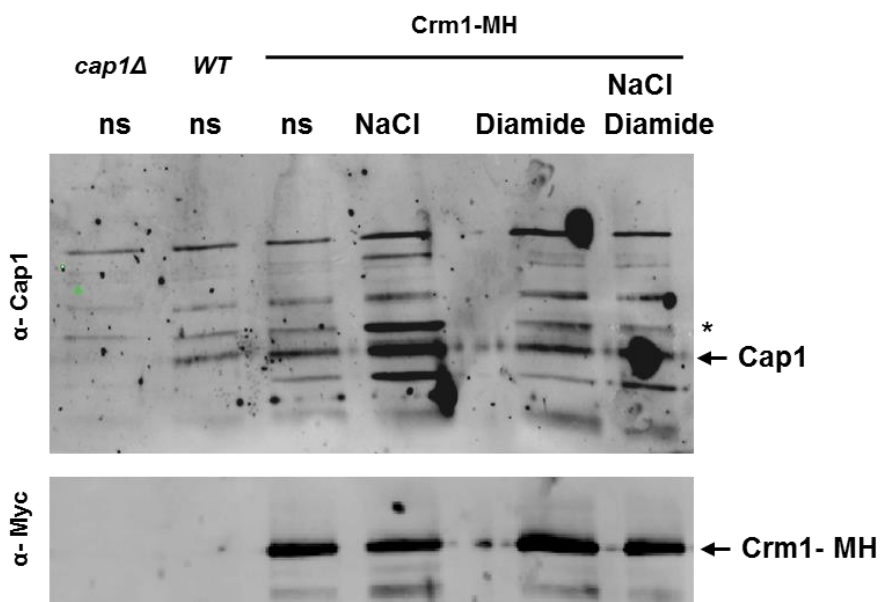


Figure 3.17 Cationic stress fails to promote the interaction of the diamide-induced oxidised form of Cap1 with Crm1.

Extracts were prepared from *cap1Δ* cells (JC710), untagged WT cells (JC747), and WT cells expressing 2Myc-6His tagged Crm1 (JC1925) before and following exposure to 1 M NaCl, 100 mM diamide or combination of these stresses for 10 min. Co-precipitation of Cap1 was detected as described in Figure 3.14 legend. * designates a non-specific band as this is seen in *cap1Δ* cells.

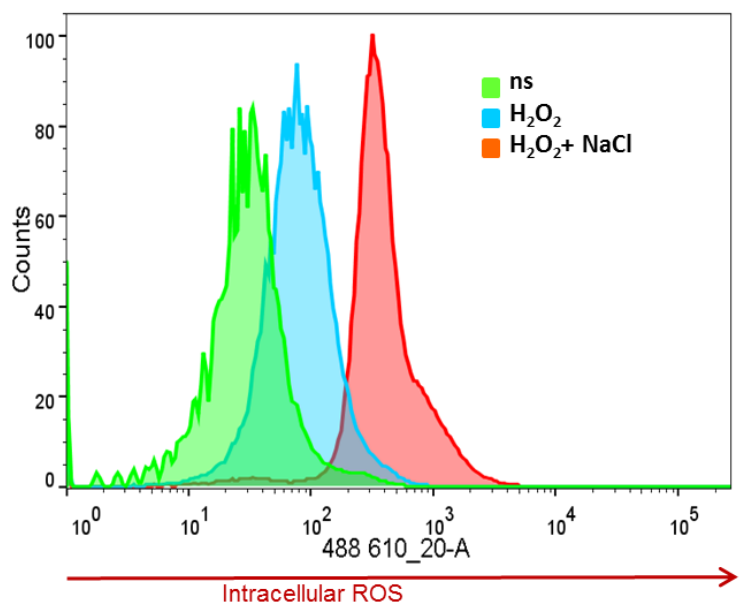
3.2.7 Combinatorial stress triggers a dramatic increase in intracellular ROS levels in *Candida* species

Whilst the experiments detailed above provide some mechanistic advances as to why the NaCl and H₂O₂ combinatorial stress treatment prevents the nuclear accumulation of Cap1, it remains unclear as to why the combinatorial stress-mediated oxidation of Cap1 is different to that observed with H₂O₂ treatment alone. Previous work indicated that the combination of 5 mM H₂O₂ and 1 M NaCl cause a dramatic increase in intracellular ROS levels in *C. albicans* (Kaloriti et al., 2014). Thus, it was possible that the rise in intracellular ROS could drive the differential oxidation and inactivation of Cap1.

To quantify the increase in intracellular ROS levels following treatment of *C. albicans* cells with oxidative (5 mM H₂O₂) and combinatorial (5 mM H₂O₂ + 1 M NaCl) stresses, the redox sensitive fluorescent probe dihydroethidium (DHE) was employed. Briefly, exponentially growing wild-type *C. albicans* cells were treated with the required stresses and simultaneously 20 µM solution of the DHE was added to each sample. Samples were incubated at 30 °C for 45 min in the dark. Cells were washed, sonicated and subjected to fluorescence-activated cell sorting (FACS). Consistent with previous findings (Kaloriti et al., 2014), the combinatorial stress treatment triggered significantly higher intracellular ROS levels than oxidative stress treatment alone (Figure 3.18A). Approximately 5-fold higher ROS levels were observed following the exposure of cells to 5 mM H₂O₂ in the presence of 1 M NaCl, compared to 5 mM H₂O₂ alone (Figure 3.18B). These results indicate that the differential oxidation of Cap1 following combinatorial stress treatment could be attributed to the dramatic increase in intracellular ROS levels. Further experiments to explore the impact of H₂O₂ concentration on Cap1 oxidation and activation are described in Chapter 4.

C. glabrata is extremely resistant to H₂O₂ (Nikolaou et al., 2009), and yet this fungal pathogen is also susceptible to combinatorial stress-mediated killing (Kaloriti et al., 2014). Therefore, we decided to examine the impact of combinatorial oxidative and cationic stress on intracellular ROS levels in *C. glabrata*.

A



B

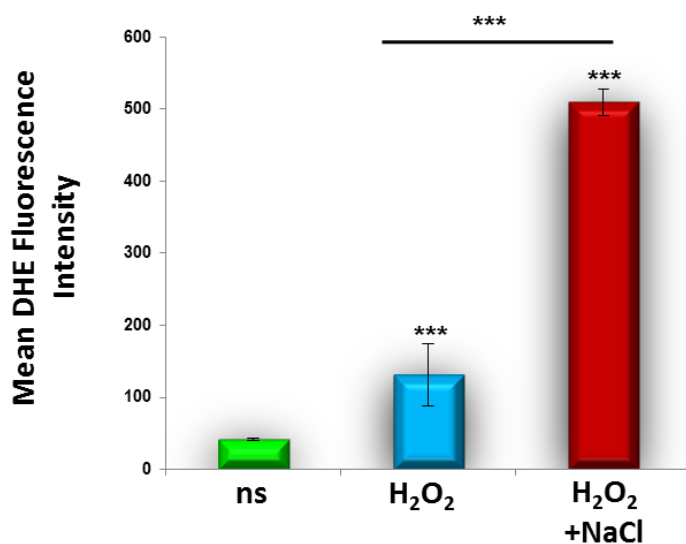


Figure 3.18 FACS analysis of intracellular ROS levels in response to the oxidative stress and the combination of oxidative and cationic stresses in *C. albicans*.

(A) FACS analysis of intracellular ROS levels in DHE-treated *C. albicans* cells before stress (ns) or following the treatment with 5 mM H₂O₂ or 5 mM H₂O₂ plus 1 M NaCl for 60 minutes (B) Quantification of intracellular ROS production before (ns) and following treatment with indicated stresses by calculating the mean DHE fluorescence intensity of the area under the curve. The mean \pm SD from three independent experiments is shown. ***, $P \leq 0.001$.

Wild-type *C. glabrata* cells (G2001HTU) were untreated or treated with 100 mM H₂O₂ or combinations of 100 mM H₂O₂ and 0.5 M NaCl, and intracellular ROS levels measured by DHE fluorescence as described above. The concentrations of the stresses were chosen as they had been used previously (Kaloriti et al., 2012). Similar to that seen in *C. albicans*, combinatorial stress caused a dramatic increase in *C. glabrata* intracellular ROS levels, compared to H₂O₂ alone (Figure 3.19). FACS analysis showed that the mean fluorescent intensity in *C. glabrata* combinatorial stress-treated samples were considerably higher compare to *C. albicans*; however, *C. glabrata* and *C. albicans* samples were not examined simultaneously, and therefore the intracellular ROS levels are not quantitatively comparable between two species. This experiment confirms that the combination of the oxidative and osmotic stresses generates elevated ROS levels in a different pathogenic *Candida* species, and could potentially explain the synergistic killing of these fungi by combinatorial stress.

3.2.8 *CRI* genes are essential for *C. glabrata* combinatorial stress resistance.

Recent unpublished work from Professor Ken Haynes' laboratory (University of Exeter) has provided insight into the mechanism by which *C. glabrata* survives and adapts to combinatorial cationic and oxidative stress. In a screen, *S. cerevisiae* cells, which are exquisitely sensitive to combinatorial stress, were transformed with a *C. glabrata* genomic library and combinatorial stress-resistant clones were isolated to identify genes that mediate resistance. This screen identified 17 genes that conferred combinatorial stress resistance to *S. cerevisiae* (J. Usher & K. Haynes unpublished). In addition to well-known stress-protective genes such as *GPD1*, *GPD2* and *TRX3*, and a number of genes encoding proteins with general roles in transcription/translation, epigenetic modification and endosomal sorting, the screen identified four ORFs that have no known orthologue in *S. cerevisiae* (*CAGL0G06710g*, *CAGL0E06094g*, *CAGL0H04059g* and *CAGL0A00649g*). These ORFs were designated as *CRI1-4* for Combinatorial stress Resistance Increased. *CRI1* was prioritised for further analysis, as this was isolated in 34/85 combinatorial stress-resistant mutants.

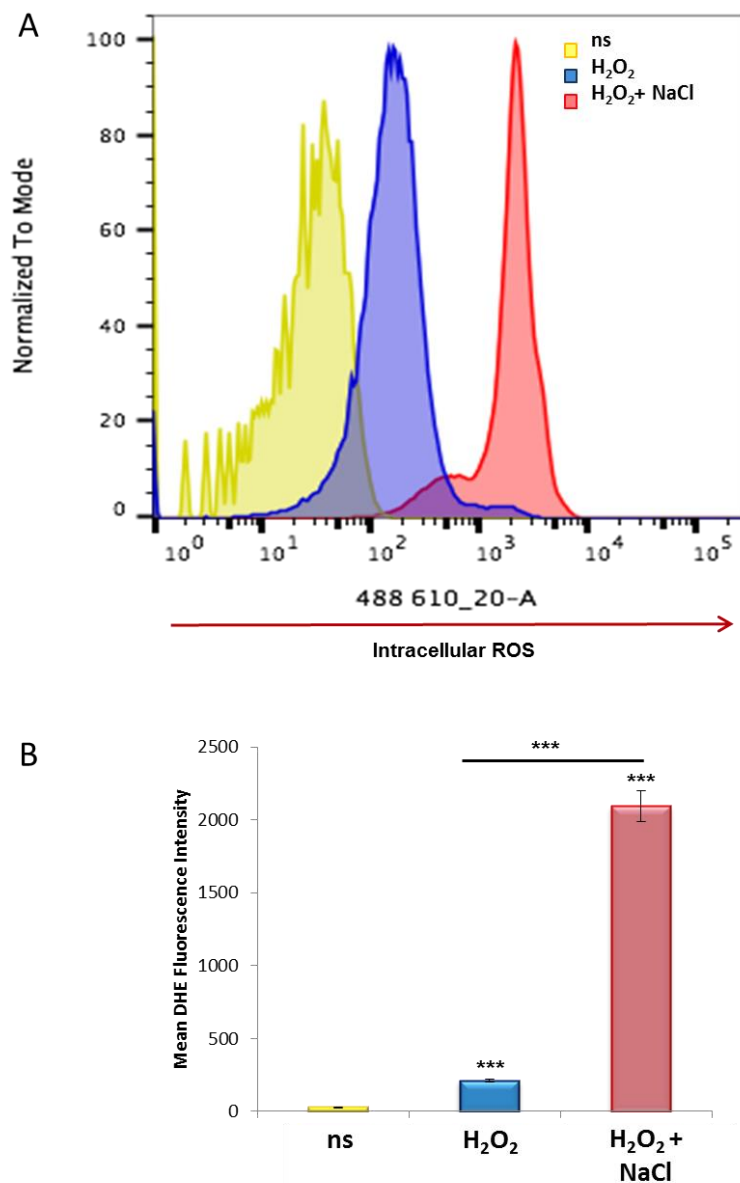


Figure 3.19 FACS analysis of intracellular ROS levels in response to oxidative stress and the combinatorial oxidative and cationic stresses in *C. glabrata*.

(A) FACS analysis of intracellular ROS levels in DHE-treated *C. glabrata* cells before stress (ns) or following the treatment with 100 mM H_2O_2 or 100 mM H_2O_2 plus 0.5 M NaCl for 60 minutes (B) Quantification of intracellular ROS production before (ns) and following treatment with indicated stresses by calculating the mean DHE fluorescence intensity of the area under the curve. The mean \pm SD from two independent experiments is shown. The following *P* values were considered: *, $P \leq 0.05$; **, $P \leq 0.01$; and ***, $P \leq 0.001$.

To validate the screen results, the resistance of *C. glabrata* wild-type (G1000) and Δ *cri1* cells together with cells over-expressing *CRI1* (*CRI1* O/E) to combinatorial stress was analysed using a standard spot test assay. Serial dilutions of exponentially growing cells were plated on selective media containing 0.5 M NaCl (cationic stress), 1.5 mM *t*-BOOH (oxidative stress), or combinations of 0.5 M NaCl + 1.5 mM *t*-BOOH (combinatorial stress) and allowed to grow for 48 hours. The organic peroxide *t*-BOOH was used in place of H₂O₂, as this stable peroxide is routinely used by the Haynes group in preference to the less stable H₂O₂. Spot test results supported the screen findings, as *C. glabrata* Δ *cri1* mutant cells were much more sensitive to both oxidative and combinatorial stresses than wild-type cells, whereas the *CRI1* over-expressing strain had an increased tolerance to both conditions (Figure 3.20). This clearly demonstrates a role for Cri1 in mediating *C. glabrata* oxidative and combinatorial stress resistance. To explore the mechanism behind the altered combinatorial stress resistance of *C. glabrata* cells lacking or over-expressing *CRI1*, we examined whether Cri1 played a role in modulating intracellular ROS levels, as it was possible that the lack of *CRI1* might cause an increase in intracellular ROS levels following combinatorial stress. *C. glabrata* wild-type, Δ *cri1* and *CRI1* O/E strains were treated with combinatorial stress and intracellular ROS levels detected using DHE fluorescence as before. Figure 3.21 illustrates an overlay histogram of the intracellular ROS levels in response to 1.5 mM *t*-BOOH plus 0.5 M NaCl in *C. glabrata* wild-type cells, Δ *cri1* strain, and cells over-expressing *CRI1* (*CRI1* O/E). No significant changes in intracellular ROS levels were detected between any of these strains. This result is indicative that the stress-protective properties of Cri1 are not due to a role in reducing intracellular ROS levels in *C. glabrata*.

Based on previous data, that the heterologous expression of *C. glabrata* *CRI* genes confers increased combinatorial stress resistance to *S. cerevisiae* (J. Usher and K. Haynes, unpublished), experiments were designed to test whether the expression of the *CRI* genes could also confer stress protection in *C. albicans*. Unlike *C. glabrata*, *C. albicans* belongs to the CTG clade (Butler et al., 2009).

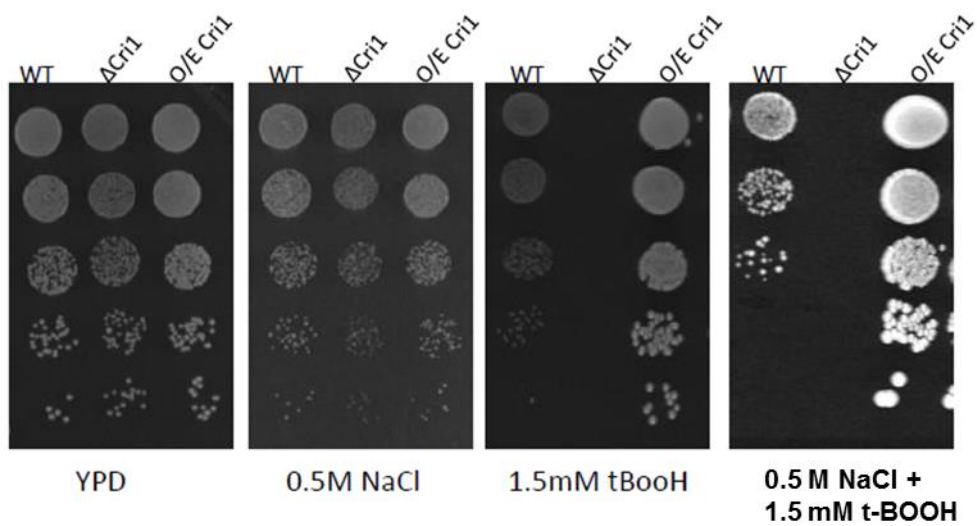


Figure 3.20 The sensitivity of *C. glabrata* *CRI1* mutants in response to oxidative, osmotic and combinatorial stresses.

Serial dilution spot assay showing the stress sensitive phenotypes of *C. glabrata* WT, Δ cri1 and *CRI1* over-expressing (O/E *CRI1*) strains to cationic (0.5 M NaCl), oxidative (1.5 mM *t*-BOOH) or combinatorial (0.5 M NaCl +1.5 mM *t*-BOOH) stresses. This sensitivity test was performed by Dr. J. Usher, University of Exeter.

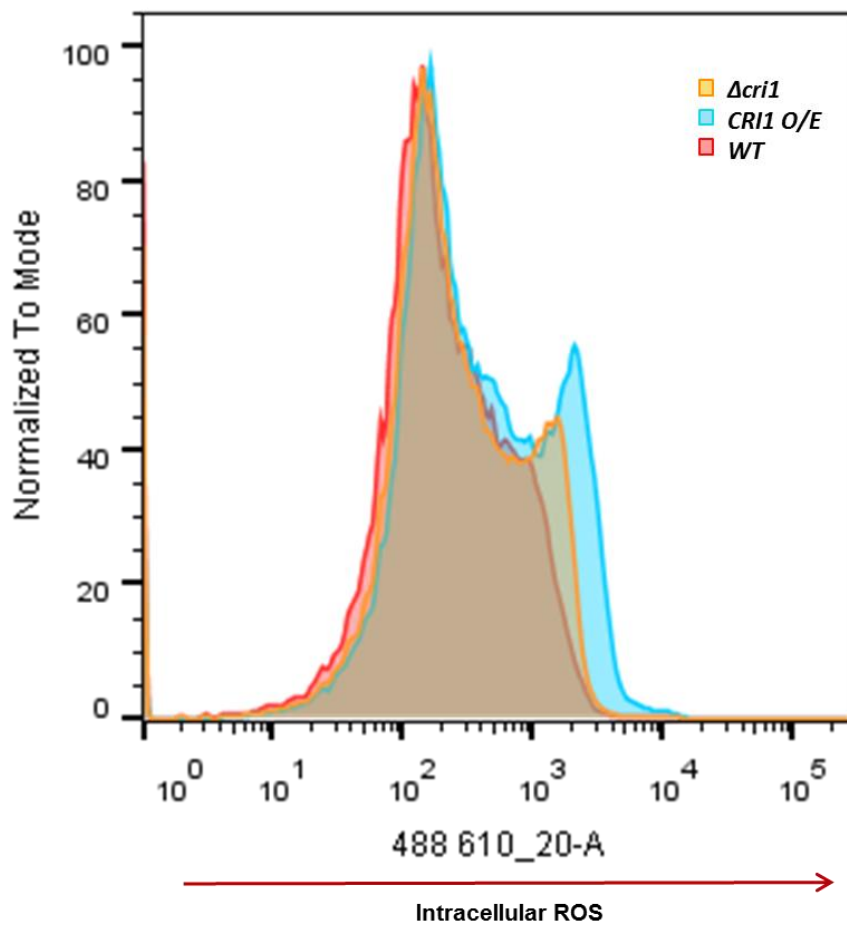


Figure 3.21 FACS analysis of intracellular ROS levels in *C. glabrata* *CRI1* mutants following combinatorial oxidative and osmotic stress.

FACS analysis of intracellular ROS levels in DHE-treated *C. glabrata* cells lacking *CRI1* ($\Delta cri1$), over-expressing *CRI1* (*CRI1 O/E*) and a wild-type (WT), following the treatment with 1.5 mM *t*-BOOH plus 0.5 M NaCl for 60 minutes.

The members of the CTG clade decode the standard leucine-CTG codon as serine (Massey et al., 2003). The *CR1/1* ORF contains two CTG codons, and therefore codon optimisation was essential prior to *CR1/1* expression in *C. albicans*. For this reason, an artificial *CR1/1* gene with two mutated codons at positions 96^{S_{32L}} and 222^{S_{74L}} and its own terminator sequence (537 bp) was synthesised by Eurofins genomics, Inc. The resulting product was then placed under the control of the constitutive *ACT1* or strong *PGK1* promoter and the construct was integrated into the *RPS10* locus of wild-type *C. albicans* cells. The *CR1/2-4* ORFs, which do not contain any CTG codons, were also expressed from the *ACT1* promoter in *C. albicans*. Stress resistant phenotypes of the *C. albicans* strains heterologously expressing the *CR1* genes were then examined by spot test analysis. The following stresses were examined: 0.5 and 1 M NaCl (cationic stress), 2.5, 5 and 10 mM H₂O₂ or 1.5 and 3 mM *t*-BOOH (oxidative stress), as well as combinations of the cationic and oxidative stresses. Consistent with combinatorial stress-mediated synergistic killing, *C. albicans* strains showed very little or no growth on plates that contained combinations of the cationic and oxidative stresses (Figure 3.22). However, the ectopic expression of *CR1/1-4* had no impact on any of the *C. albicans* stress resistance phenotypes tested. *C. albicans* strains expressing *CR1/1-4* did not exhibit an increased resistance to oxidative or combinatorial stresses: cells survived 1 M NaCl, 3 mM *t*-BOOH and 5 mM H₂O₂, but not their combinations (Figure 3.22). This is contrast to that observed in *S. cerevisiae*, and in *C. glabrata* upon overexpressing *CR1/1* (Figure 3.20). These results indicate that although the combination of oxidative and cationic stresses kills *C. albicans* synergistically, the ectopic expression of *C. glabrata* *CR1* genes in *C. albicans* is unable to promote an increased resistance to combinatorial stress.

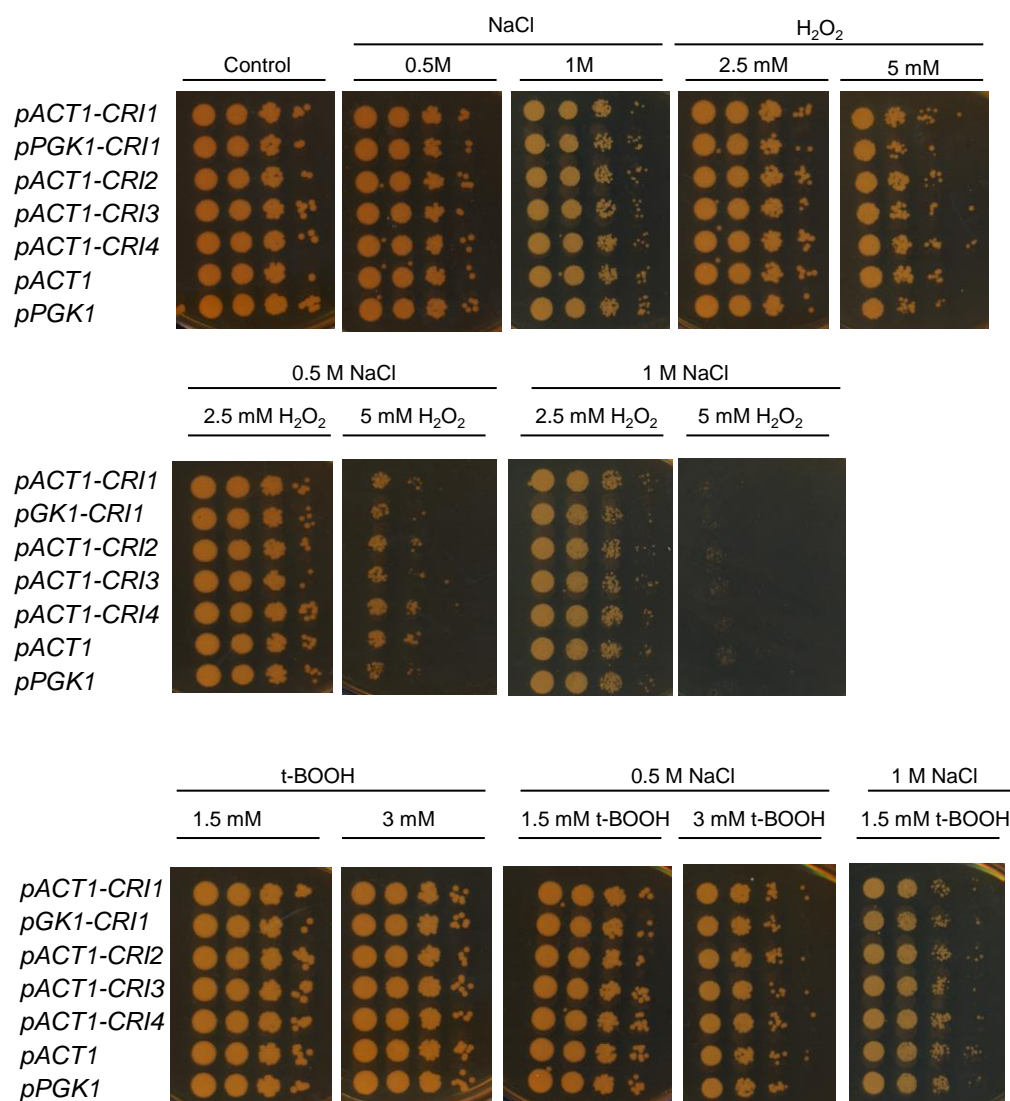


Figure 3.22 Impact of ectopic expression of *C. glabrata* *CRI1-4* genes on *C. albicans* stress resistance.

Serial dilutions of *C. albicans* wild type and the indicated strains expressing *CgCRI* genes were spotted onto agar plates containing indicated stresses or their combinations. Plates were incubated at 30 °C for 48 h. Data shown is representative of two independent biological replicates.

3.3 Discussion

In summary, this work provides mechanistic insight into the combinatorial stress-mediated deregulation of Cap1 activation in *C. albicans*. Two major findings are presented – (i) Cap1 is trapped in a differentially oxidised form, Cap1^{OX-1}, following treatment with the combination of cationic and oxidative stress and, (ii) cationic stress promotes the interaction of Cap1 with the Crm1 nuclear export factor.

Combinatorial stress drives an alternative oxidation of Cap1 and the generation of Cap1^{OX-1}, which is possibly an inactive precursor of active Cap1^{OX}. In *S. cerevisiae*, the oxidation of Yap1 in response to H₂O₂ is a multistep process, and the formation of three disulfides is vital for full activation of Yap1 (Okazaki et al., 2007). The data on Cap1 oxidation presented in this Chapter suggest that, analogously to Yap1, multiple disulfides are formed in Cap1 following oxidative, but not combinatorial stress. This result, however, seemingly conflicts with the oxidation profiles of Cap1 observed when we used the thiol binding agent AMS to detect differentially oxidised forms of this transcription factor. In such experiments, oxidation of cysteine residues precludes the binding of AMS and thus oxidised proteins run with a faster mobility. Employing such an approach we observed a faster mobility form generated immediately following H₂O₂ stress (Cap1^{OX-1}), which is then resolved into the Cap1^{OX} slower mobility state (Figures 3.2, 3.9). How can these findings be reconciled with our observations that Cap1^{OX} has more H₂O₂-induced disulfides than Cap1^{OX-1} (Figure 3.5)? Oxidation events, in addition to disulphide bond formation, such as the hyperoxidation of cysteine thiols to sulphenic or sulphonic acid derivatives would preclude AMS binding. In this regard it may be relevant that combinatorial stress triggers high levels of intracellular ROS, which may result in the hyperoxidation of specific Cap1 cysteine residues – which in turn could delay the formation of disulfides. An alternative explanation, however, is that AMS binding to the Cap^{OX-1} form may induce a conformation change that results in the observed faster mobility. Further experiments to delineate the nature of the multistep Cap1 oxidation and to understand the relationship between Cap1^{OX} and Cap1^{OX-1} are warranted. One possible way of doing this is to use mass-spectroscopy analysis to study the status of reversibly oxidised cysteines of Cap1 *in vivo* following the treatment with oxidative

and combinatorial stresses, as was described for the oxidation of *S. pombe* Pap1 (Calvo et al., 2013, García-Santamarina et al., 2011). Such approaches involve taking acid lysates to freeze the redox state of the cysteine residues, blocking free thiols with *N*-ethylmaleimide, and then the sequential reduction of the reversibly oxidised thiols and further alkylation with a larger molecular weight alkylating agent such as AMS or iodoacetamide. The denatured proteins are solubilised and the protein of interest is immunoprecipitated and analysed by LC/MS-MS. Attempts were made during this study to analyze Cap1 in this way, but problems were encountered with resolubilisation of the proteins prior to immunoprecipitation. An alternative approach could involve the construction of Cap1 mutant strains, in which each of the predicted thiol-reactive cysteines is mutated to determine which are essential for the formation of the different oxidised forms of Cap1. One possible mechanism to explain the delay in the resolution of Cap1^{OX-1} into active Cap1^{OX} could be due to the combinatorial stress-induced blocking of Cap1-Gpx3 complex. This initial complex between the peroxidase and Yap1 was described in *S. cerevisiae* and shown to be crucial for Yap1 oxidation (Wood et al., 2004).

In addition to the altered oxidation of Cap1, data from this study have found that cations promote the interaction of Cap1 with the Crm1 nuclear export factor, which is predicted to prevent the nuclear accumulation of this transcriptional factor. It is also noteworthy that cations have been demonstrated to inhibit catalase activity in *C. albicans* (Kalogeriti et al., 2014), and thus cationic stress appears to inhibit oxidative stress adaptation in this fungal pathogen in two distinct ways. Regarding the cationic stress-induced stabilisation of the Cap1-Crm1 complex, it is unknown if this involves a direct or indirect mechanism, and further structural investigation of the Cap1-Crm1 complex is needed to address this. Crm1 is a ubiquitous exportin employed in the regulated export of a plethora of proteins, and it is possible that the cationic stress has a general, rather than Cap1-specific effect on Crm1 function. Evidence against this, however, is that combinatorial cationic and oxidative stress does not prevent the nuclear accumulation of Hog1 (Kalogeriti et al., 2014), which is predicted to be Crm1-dependent based on studies with *S. cerevisiae* Hog1 (Ferrigno et al., 1998). Therefore, the enhanced stabilisation of Cap1-Crm1 complexes by cations may be specific to Cap1, and the mechanism behind it is independent of Hog1-mediated

osmotic stress responses (Figure 3.16). However, the mechanism underlying cationic stress-mediated enhancement of the interaction between Cap1 and Crm1 still remains unknown. In addition to the Hog1 SAPK pathway, there are other well-documented cationic stress responsive pathways in *C. albicans*, such as the Rim101 pathway (Homann et al., 2009). It is noteworthy that the Rim101 pathway is implicated only in response to cationic, but not osmotic stress, which makes it a candidate to regulate the Cap1-Crm1 interaction as this is specifically enhanced by cationic stress.

Rapid adaptive responses to H_2O_2 are necessary for *C. albicans* to avoid ROS-mediated killing (Patterson et al., 2013). Taken together, the generation of Cap1^{OX-1} and its enhanced interaction with the Crm1 nuclear export factor, both likely contribute to the delayed activation of oxidative stress-protective genes following combinatorial stress (Figure 3.23). The significant delay in Cap1-mediated new antioxidant enzyme synthesis following combinatorial stress is predicted to prevent adaptation resulting in sustained high ROS levels, leading to the pathogen's death. This model is supported by recently published work, which demonstrated that the ectopic expression of *CAT1* can rescue the sensitivity to combinatorial stress in *C. albicans* (Kalogriti et al., 2014). *CAT1* is a key antioxidant target of Cap1. Thus the ectopic expression of the catalase enzyme, likely allows cells to survive combinatorial stress-induced Cap1 inactivation, and the consequent increase in intracellular ROS levels. Moreover, such findings support the notion that it is the high intracellular ROS levels that is the primary mechanism underlying the potency of combinatorial stress in *C. albicans* killing. However, it is unknown whether exposure to high ROS levels would cause the same delay in Cap1 inactivation as that observed following combinatorial oxidative and cationic stress. This question is addressed in the next chapter.

The combinatorial stress-mediated stress pathway interference mechanisms, that has been dissected *in vitro*, is purposed to contribute to the potency of host defences in combating fungal infections *in vivo* (Kalogriti et al., 2014).

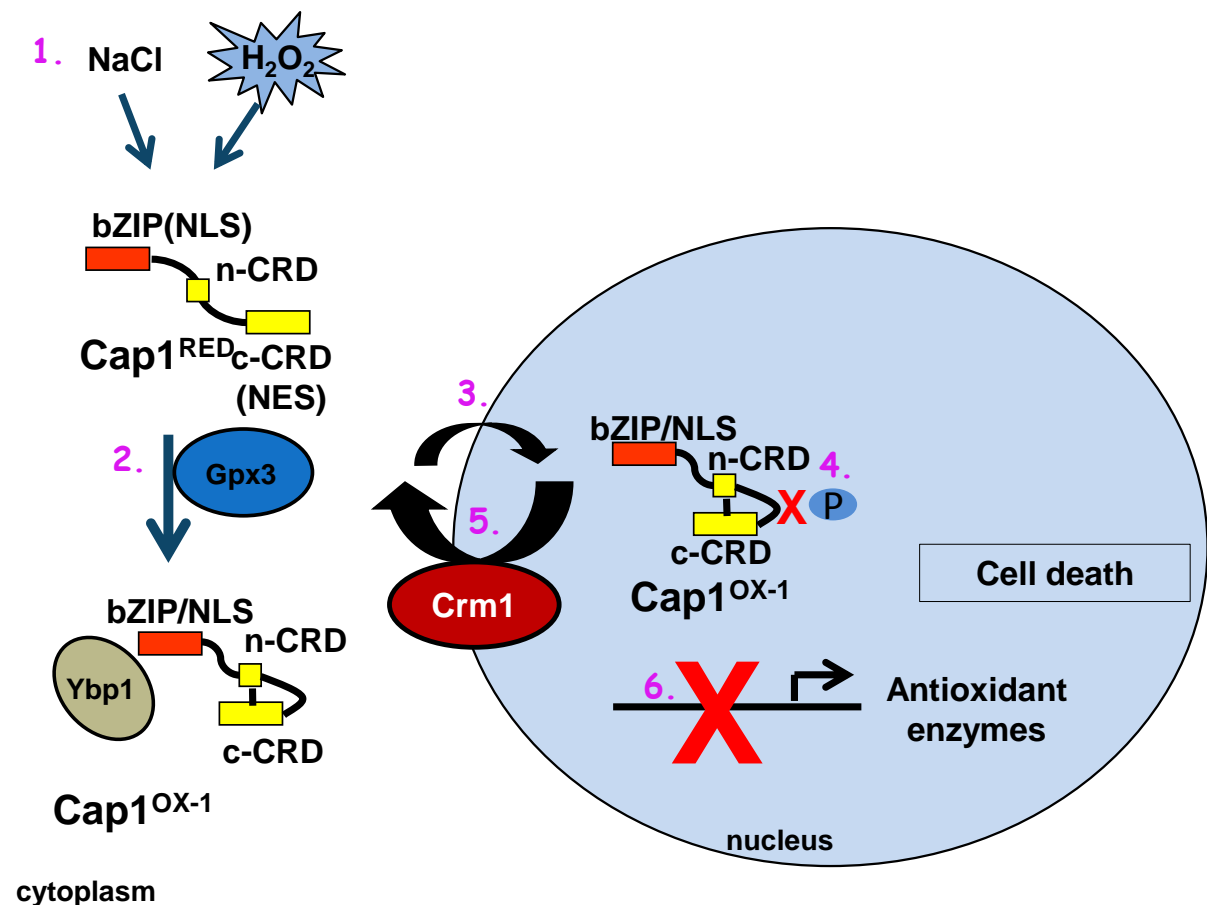


Figure 3.23 A model of combinatorial stress-mediated Cap1 inactivation.

Exposure of *C. albicans* to the combination of oxidative (5 mM H_2O_2) and cationic (1 M NaCl) stresses (1) results in the formation of the differentially oxidised $\text{Cap1}^{\text{OX-1}}$ form (2), mediated by Gpx3 and Ybp1. $\text{Cap1}^{\text{OX-1}}$ can enter the nucleus (3), but its phosphorylation (4) and nuclear accumulation is impaired due to cation-mediated enhanced interaction between $\text{Cap1}^{\text{OX-1}}$ and Crm1 exporter (5). Impaired Cap1 nuclear accumulation leads to the failure to activate the transcription of the antioxidant genes (6), thus resulting in the pathogen's death.

Pharmacological inhibition of both the respiratory burst and cationic fluxes in neutrophils, either separately or in combination, results in a similar, drastic impairment in their fungicidal function (Kalariti et al., 2014). In addition, antioxidant gene expression in *C. albicans* is observed one hour following phagocytosis (Fradin et al., 2005), and this could reflect a combinatorial stress-mediated delay in Cap1 activation. To explore this further, the time course of Cap1 activation following phagocytosis could be examined looking at markers of Cap1 activation – either Cap1-GFP to detect nuclear localisation, or Cap1-dependent gene expression. It would be also interesting to investigate whether the kinetics of Cap1 activation following phagocytosis is quicker upon pharmacologically blocking cation influx.

It is noteworthy that all fungi tested in this work and by other teams (Kalariti et al., 2012) are susceptible to combinatorial stress-mediated synergistic killing effects. In addition, all fungi have AP-1-like transcriptional factors that regulate antioxidant gene expression. Therefore, stress-responsive pathways in other fungi might also be inhibited by combinatorial stress, analogously to what is shown here for *C. albicans* Cap1. However, *C. glabrata* may also exhibit species-specific mechanisms to counteract combinatorial and oxidative stresses. This pathogen possesses four genes (*CRI1-4*), with unknown function(s) that are essential to withstand oxidative and combinatorial stresses. Orthologues are not found in any other species, which make these genes good candidates to explain the high degree of stress resistance exhibited by *C. glabrata*. In this work, data is presented illustrating that the stress-protective properties of the *CRI* genes do not involve modulation of intracellular ROS levels in *C. glabrata*. Furthermore, in contrast to *S. cerevisiae*, their ectopic expression in *C. albicans* does not promote stress resistance. This suggests that the mechanism behind *Cri1-4* stress protection is only operational in *C. glabrata* and closely related fungi such as *S. cerevisiae*, and not in more distant relatives such as *C. albicans*.

Chapter 4. Mechanisms underlying the delayed activation of Cap1 in response to high levels of ROS

4.1 Introduction

The results presented in Chapter 3 describe mechanisms underlying the delayed activation of the Cap1 transcription factor following exposure of *C. albicans* to combinatorial oxidative and cationic stress. Two main mechanisms appear to be evoked: Cap1 becomes trapped in a partially oxidised form, Cap1^{OX-1}, and the nuclear accumulation of Cap1^{OX-1} is delayed due to a cationic stress-enhanced interaction with the Crm1 nuclear export factor. Consistent with previous findings (Kalogriti et al., 2014), data is also presented showing that there is a dramatic increase in intracellular ROS levels following exposure of *C. albicans* cells to combinatorial oxidative plus cationic stress, compared to oxidative stress alone. There is evidence that it is the high level of intracellular ROS triggered by simultaneous exposure to oxidative and cationic stress, which is a key to the potency of this combinatorial stress in fungal killing. For example, ectopic expression of the Cap1 target gene *CAT1*, encoding catalase, suppresses the elevated intracellular ROS levels and synergistic killing caused by combinatorial cationic plus oxidative stress (Kalogriti et al., 2014). Thus, we hypothesised that the rise in intracellular ROS could contribute to the differential oxidation and inactivation of Cap1 observed following combinatorial stress. Hence, in this Chapter, the impact of high ROS levels on the activation of the Cap1 transcription factor in *C. albicans* was explored.

4.2 Results

4.2.1 *Cap1 activation, but not nuclear accumulation, is delayed in response to high doses of H₂O₂*

Quantification of the increase in intracellular ROS following treatment of cells with H₂O₂ or combinations of H₂O₂ and NaCl revealed that approximately 5-fold higher levels of intracellular ROS were observed following exposure of cells to 5 mM H₂O₂ in the presence of 1 M NaCl, compared to 5 mM H₂O₂ alone (Figure 3.18). To explore

Cap1 activation in response to a range of H_2O_2 concentrations, the standard concentration of 5 mM H_2O_2 was used as the medium dose, and a five-fold higher concentration of 25 mM H_2O_2 was used as the high dose (to mimic the 5-fold higher levels of intracellular ROS observed with the combinatorial stress). A low dose of 0.4 mM H_2O_2 was also used, as this is the lowest concentration of H_2O_2 that triggers Cap1 activation in *C. albicans* (J. Quinn, unpublished observations). *C. albicans* cells expressing Cap1-GFP were treated with this range of concentrations of H_2O_2 and the kinetics of Cap1 nuclear accumulation assessed. As illustrated in Figure 4.1, Cap1 rapidly localised to the nucleus irrespective of the H_2O_2 concentration applied. However, in response to low doses of H_2O_2 (0.4 mM), Cap1 nuclear accumulation was short-lived, in contrast to the sustained Cap1 nuclear localisation following exposure of cells to 5 and 25 mM H_2O_2 stress. These observations contrast to the delay in Cap1 nuclear accumulation that is observed following combinatorial stress (Figure 3.6).

Although Cap1 rapidly accumulates in the nucleus irrespective of the concentration of H_2O_2 , further experiments were necessary to check the functionality of this transcription factor. Subsequently, Cap1 phosphorylation was examined in response to increasing H_2O_2 concentrations. *C. albicans* cells expressing myc-tagged Cap1 were treated with different levels of H_2O_2 , and Cap1 phosphorylation assessed over time. Cap1 phosphorylation in response to 0.4 and 5 mM H_2O_2 was rapid (Figure 4.2) and mirrored the nuclear accumulation of the transcriptional factor. Specifically, Cap1 phosphorylation was evident at 10 minutes with both low and medium doses of stress, and whilst this was sustained for 60 minutes in response to 5 mM H_2O_2 , no Cap1 phosphorylation was evident 30 minutes post treatment with 0.4 mM H_2O_2 . Strikingly, however, there was a delay in Cap1 phosphorylation following treatment of cells with high ROS (25 mM H_2O_2). Significant phosphorylation of Cap1 was not observed until 30 minutes following the exposure to 25 mM H_2O_2 , despite the fact that this transcription factor rapidly accumulates in the nucleus following high dose H_2O_2 treatment. Nonetheless, this delay is similar to that previously described in Chapter 3 with the combinatorial cationic and oxidative stress.

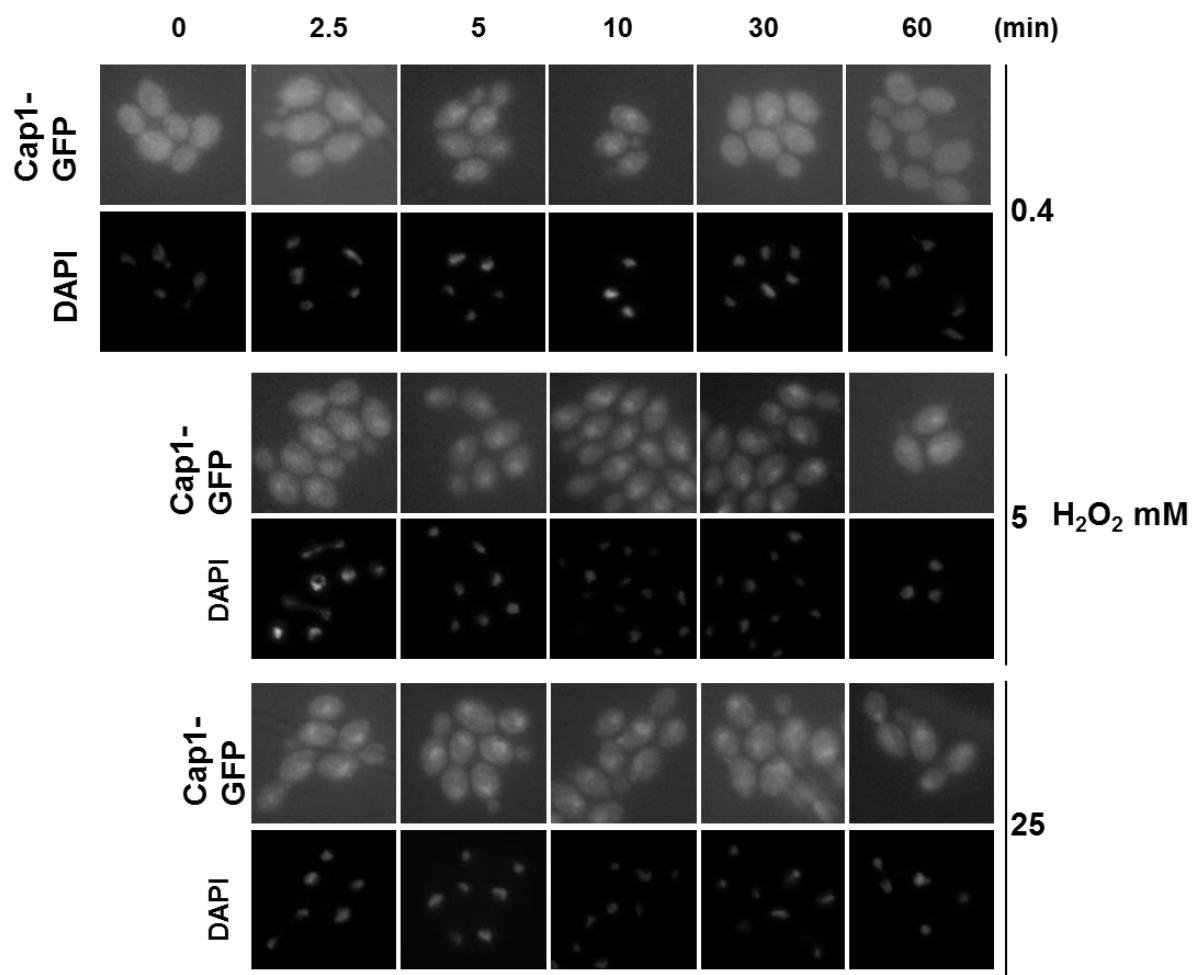


Figure 4.1 Cap1 nuclear accumulation in response to different doses of H₂O₂.

Cap1 localisation was detected by fluorescence microscopy of cells expressing Cap1-GFP (JC1060) following the exposure to 0.4, 5 or 25 mM H₂O₂ for the times indicated. DAPI staining was used to show the position of the nuclei.

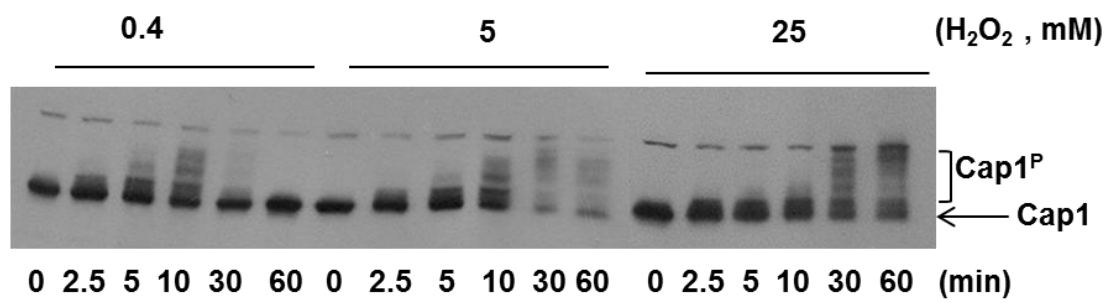


Figure 4.2 Cap1 phosphorylation in response to increasing H_2O_2 concentrations.

Lysates from cells expressing 2Myc- and 6His-tagged Cap1 (Cap1-MH-JC948), before and after the treatment with 0.4, 5 or 25 mM H₂O₂ for the indicated times were analysed by western blotting using an anti-Myc antibody. The positions of unphosphorylated (Cap1) and phosphorylated (Cap1^P) Cap1 are indicated. Data are shown as representative of five experiments.

The phosphorylation of AP-1 like transcriptional factors has been viewed as a marker of nuclear accumulation, as revealed by studies in *S. cerevisiae*, where nuclear accumulation of Yap1 was shown to be an essential prerequisite for Yap1 phosphorylation (Delaunay et al., 2000). However, as both the kinase and the target phosphorylation sites on Yap1 are unknown, it has not been possible to establish whether this posttranslational modification is important for the activation of this or other fungal AP-1-like transcription factors.

As Cap1 phosphorylation was delayed following high levels of H₂O₂ stress, this suggested that perhaps Cap1 function was perturbed. To test this, the kinetics of Cap1-dependent gene expression was examined. Two genes were chosen – *CTA1* and *TRR1* – as these are Cap1-dependent targets that show a delay in expression following combinatorial stress (Figure 3.8). Exponentially growing *C. albicans* wild-type cells were treated with 0.4, 5 and 25 mM H₂O₂ and subjected to northern blot analysis. Consistent with previous findings (da Silva Dantas et al., 2010), the kinetics of the induction of these Cap1-dependent genes largely correlated with the nuclear accumulation and phosphorylation of Cap1 following the treatment with low and medium doses of H₂O₂ (Figure 4.3A and 4.3B). Notably, while both genes were induced after 0.4 mM H₂O₂ treatment, the pattern and level of induction differed between the two Cap1 targets: while *CAT1* was induced as rapidly as 2-5 minutes post stress, its activation was diminished after 10 minutes, whereas *TRR1* induction was slower, but more profound, with a peak of induction at 30 minutes post stress treatment. However, importantly, exposure of *C. albicans* cells to high levels of H₂O₂ caused a significant delay of the induction of both *CTA1* and *TRR1*, and significant levels of expression were not seen until 30 minutes post 25 mM H₂O₂ treatment (Figure 4.3). This delay in Cap1-dependent gene expression mirrors the delay in Cap1 phosphorylation observed following high H₂O₂ stress (Figure 4.2).

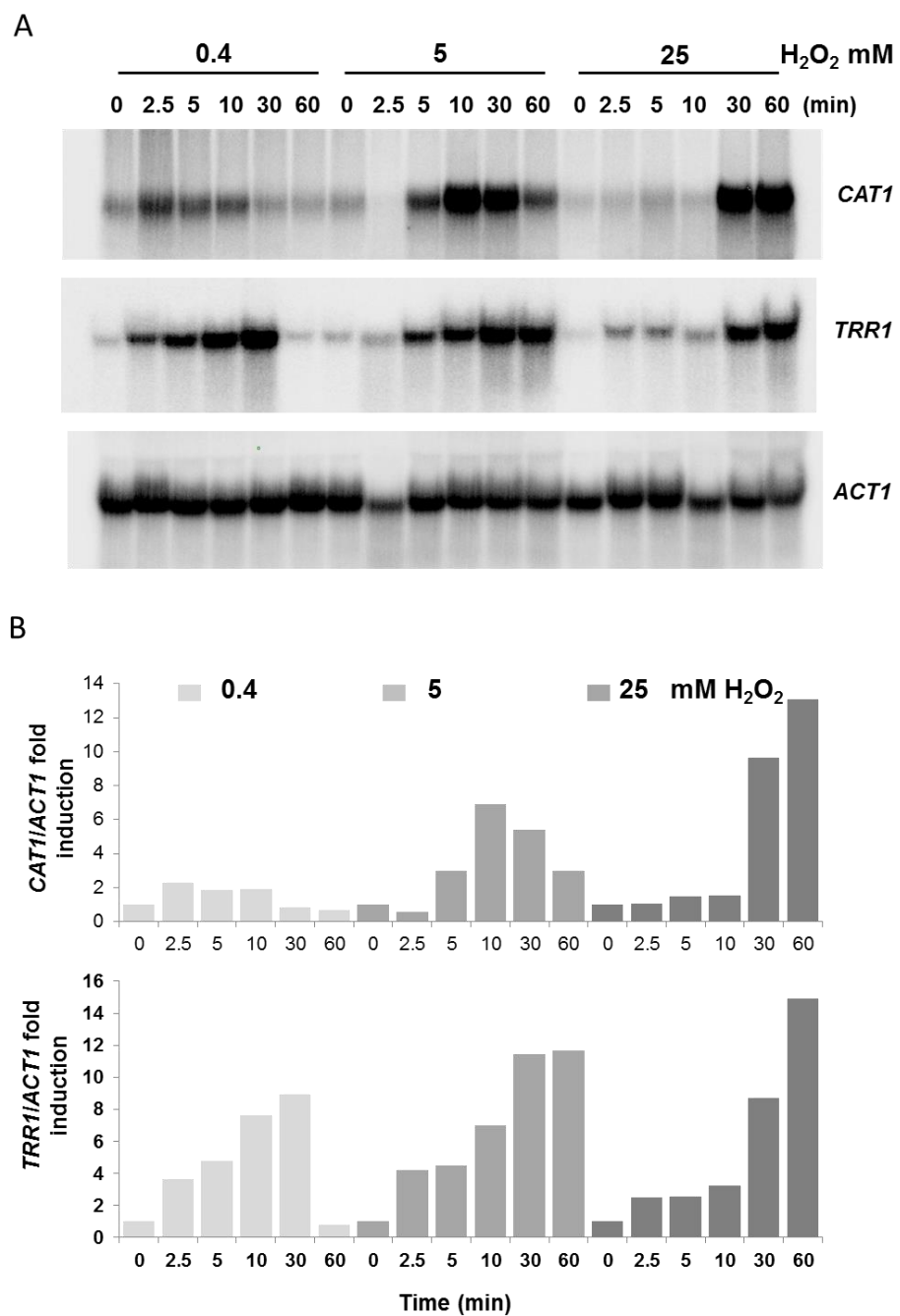


Figure 4.3 Cap1-dependent gene expression is delayed in response to high H_2O_2 concentrations.

(A) Northern blot analysis of RNA isolated from wild-type (JC747) cells before and following treatment with 0.4, 5, or 25 mM H_2O_2 for the indicated times. Blots were analysed with probes specific for the *CAT1* and *TRR1* genes. A probe against *ACT1* was used as a loading control. (B) The levels of *CAT1* and *TRR1* mRNA were quantified relative to the *ACT1* using Image quant software. Data are shown as representative of five experiments.

4.2.2 The oxidation profile of Cap1 is similar following exposure to high H₂O₂ and combinatorial H₂O₂ and cationic stresses

As Cap1 activation was delayed following high H₂O₂ treatment, it was possible that Cap1 may be differentially oxidised, as seen previously with the combinatorial stress treatment, which induces high intracellular ROS levels (Figure 3.2). To investigate this, *C. albicans* cells expressing myc-tagged Cap1 were treated with increasing H₂O₂ concentrations and Cap1 oxidation was monitored over a 60 minute period (Figure 4.4). Unexpectedly, at all levels of H₂O₂, the Cap1^{OX-1} form was observed. However, following exposure to low or medium levels of H₂O₂, the presence of Cap1^{OX-1} was short-lived being resolved to the Cap1^{OX} form by 10 minutes. In contrast, following exposure to high levels of H₂O₂ the Cap1^{OX-1} form persisted for up to 30 minutes. The observation that Cap1^{OX-1} form, generated following 0.4 and 5 mM H₂O₂ treatments, was rapidly resolved to the Cap1^{OX} form, likely explains why this form has not been detected previously. However, this differentially oxidised form of the protein was more sustained in cells treated with higher doses of H₂O₂, and its resolution to the Cap1^{OX} form appeared to coincide with the restoration of Cap1 phosphorylation and Cap1-dependent gene expression 30 minutes post stress (Figures 4.2 and 4.3). The observation that the Cap1^{OX-1} form is seen at all levels of H₂O₂, albeit with different kinetics, supports the hypothesis that Cap1^{OX-1} is an inactive intermediate in the formation of Cap1^{OX}. These observations are in line with previous findings in *S. cerevisiae*, where oxidation of all six redox-active cysteines of Yap1 is needed for the full activation of this transcription factor (Okazaki et al., 2007).

4.2.3 Comparison of the Cap1^{OX-1} form generated following high H₂O₂ and combinatorial stress.

Next experiments were performed to examine whether the differentially oxidised forms of Cap1 that are generated and sustained following high levels of H₂O₂, and those generated by combinatorial H₂O₂ and cationic stress, were similar. *C. albicans* cells expressing myc-tagged Cap1 were treated with high H₂O₂

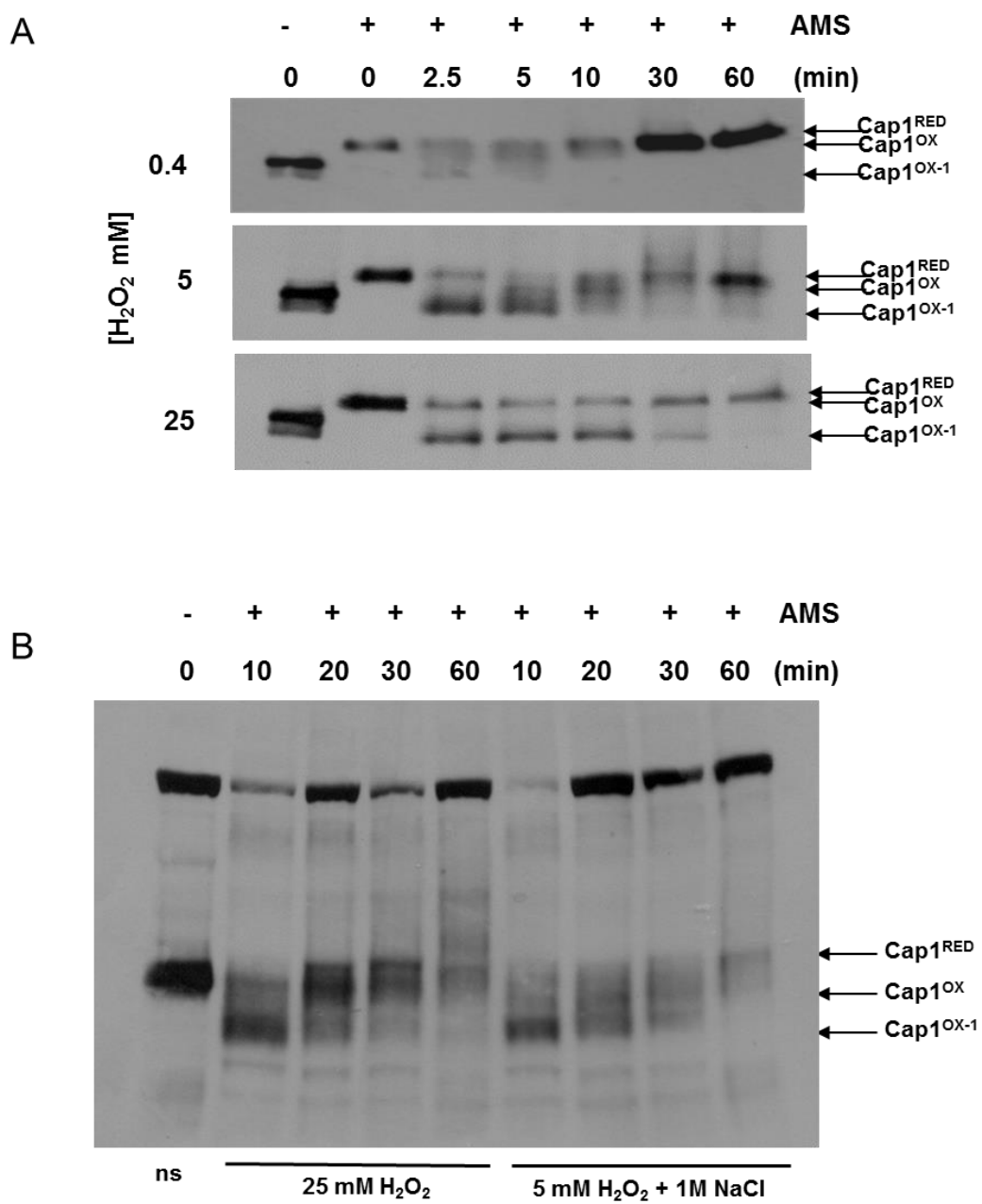


Figure 4.4 High levels of H₂O₂ result in sustained Cap1^{OX-1} formation.

(A) Cap1^{OX-1} is sustained following treatment with higher doses of H₂O₂. Cap1 oxidation was measured by western blotting of AMS-modified protein extracts following exposure of Cap1-MH cells to 0.4, 5 or 25 mM H₂O₂ for the times indicated. (B) Cap1^{OX-1} form generated in response to high ROS has the same AMS-dependent mobility as combinatorial stress-induced Cap^{OX-1}. Cap1 oxidation was assayed by western blotting of AMS-modified protein extracts following exposure of Cap1-MH cells to 25 mM H₂O₂ or 5 mM H₂O₂ plus 1 M NaCl for the times indicated. The data are representative of three biological replicates.

and combinatorial stress (5 mM H₂O₂+1 M NaCl), and AMS-treated protein extracts assessed by SDS-PAGE and western blotting to visualise the Cap1 oxidation profile (Figure 4.4A). This experiment confirmed that in response to both stresses Cap1 displays a similar oxidation profile with a Cap1^{OX-1} form generated post high ROS and combinatorial stress having a similar AMS-dependent electrophoretic mobility. However, the kinetics of the resolution of Cap1^{OX-1} to the Cap1^{OX} form differed. With both stress conditions the formation of Cap1^{OX-1} after 10 minutes was clear, however this resolved to the Cap1^{OX} more quickly following high H₂O₂ stress than following combinatorial stress (Figure 4.4B).

To explore whether the Cap1^{OX-1} form generated following high levels of H₂O₂ had less disulfides as seen with the Cap1^{OX-1} form observed after combinatorial stress, cell extracts were treated sequentially with NEM-DTT-AMS. The rationality for these treatments is described in section 3.2.1. Briefly, protein extracts obtained by acid lysis are treated with the small molecular weight thiol-binding agent NEM, thus blocking free thiols. Subsequent DTT treatment reduces all existing disulphide bonds, and the newly released thiols are then labelled with AMS. Thus, proteins with more disulfides have a slower mobility on SDS-PAGE, which can be detected by western blotting. Cells extracts were prepared from cells following a 10 minute exposure to 25 mM H₂O₂ and combinations of 5 mM H₂O₂ and 1 M NaCl, as under these conditions the Cap1^{OX-1} form is prevalent. In addition, extracts were prepared from cells following a 10 minute treatment with 5 mM H₂O₂, as under such conditions Cap1 is predominantly in the Cap1^{OX} form. The Cap1^{OX-1} forms generated post high H₂O₂ and combinatorial stress treatments, both demonstrated a slower mobility post NEM-DTT-AMS treatment, compared to the NEM-DTT treatment, indicating that both contain disulfides (Figure 4.5A). A fraction of the Cap1^{OX-1} generated following high H₂O₂ stress had a slower mobility than that generated following combinatorial stress, suggesting that this fraction had more disulfides (Figure 4.5A, right panel). However, the Cap1^{OX} form generated following 5 mM H₂O₂ treatment had an even slower mobility following NEM-DTT-AMS treatments (Figure 4.5A). This suggests that whilst the Cap1^{OX-1} forms generated following high H₂O₂ and combinatorial stress contain disulfides, the Cap1^{OX} form generated following 5 mM H₂O₂ treatment has more disulfides.

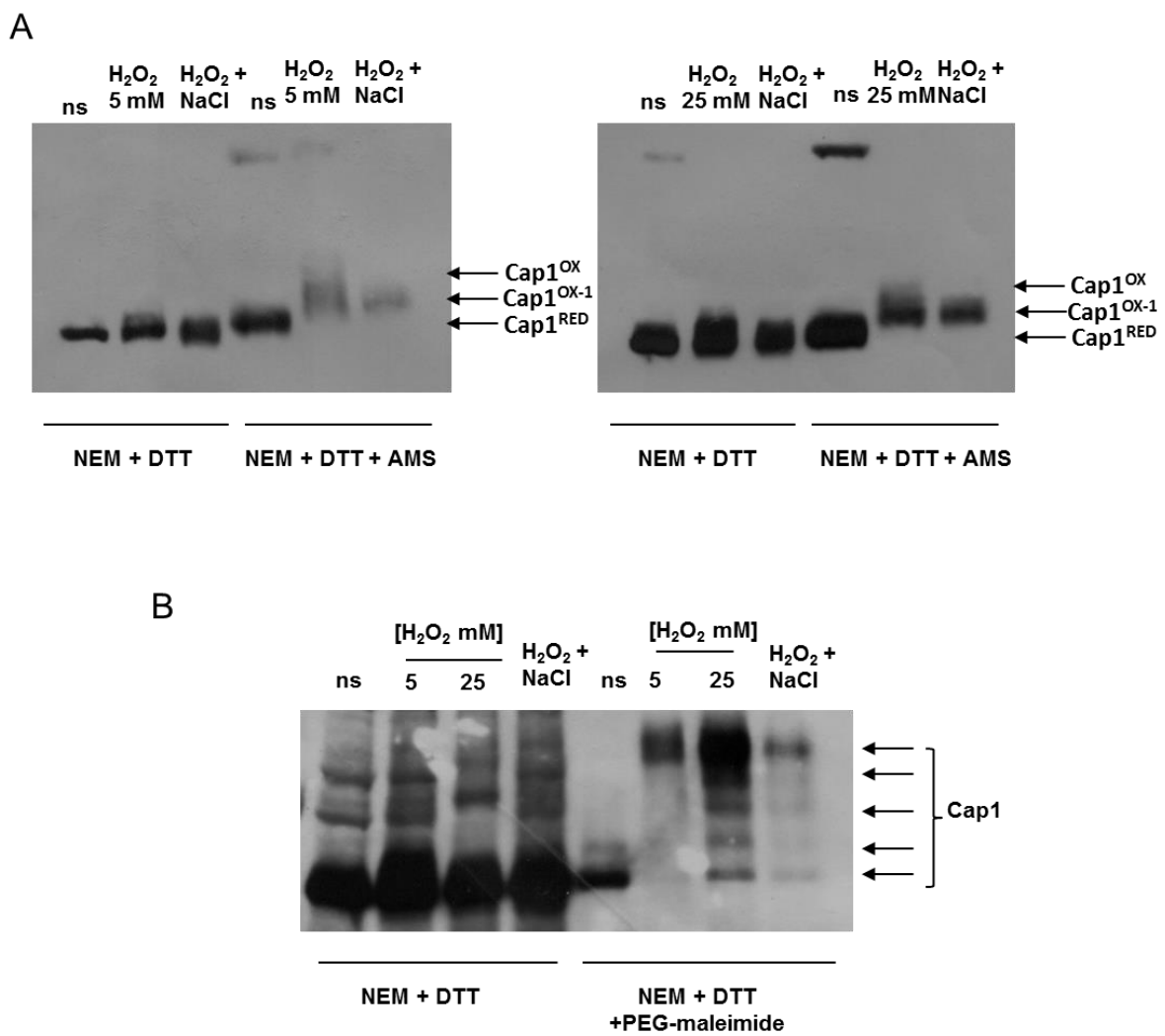


Figure 4.5 Differential Cap1 oxidation in response to high ROS.

(A) Cap1^{OX-1} generated post high ROS or combinatorial stress possess less disulfides than oxidative-stress induced Cap1^{OX}. The detection of disulfides in Cap1 was determined by western blotting of protein extracts following the exposure of Cap1-MH cells to 5 or 25 mM H₂O₂, and 5 mM H₂O₂ + 1 M NaCl for 10 minutes, with the subsequent treatment of extracts with NEM-DTT-AMS. (B) Comparison of Cap1 oxidation before (ns) and following the indicated stress treatments by PEG-maleimide binding to DTT-resolved disulfides. This shows that different oxidised forms of Cap1 are similarly triggered following high H₂O₂ and combinatorial stress, whereas a single form containing multiple disulfides is prevalent following medium H₂O₂ stress.

As described previously, to increase the resolution of these different oxidation states of Cap1, AMS was substituted with the higher molecular weight alkylating agent PEG-maleimide. Similar procedures were performed as described above, only now cells extracts were treated sequentially with NEM-DTT-PEG-maleimide. Consistent with that observed for the NEM-DTT-AMS treatments, similar partially oxidised forms of Cap1 are generated following high H_2O_2 and combinatorial stress (Figure 4.5B). Here, 5 distinct bands can be clearly observed. The faster mobility band runs at the same position as Cap1 before stress and thus likely represents a non-oxidised form of the transcription factor. The remaining slower mobility bands have different numbers of oxidised disulfides. In contrast, a single form of Cap1 containing multiple disulfides is prevalent following medium H_2O_2 stress. Notably, for unknown reasons, there is more Cap1 recovered post 25 mM H_2O_2 stress. Nonetheless, these experiments clearly demonstrate the appearance of the same $Cap1^{OX-1}$ form following both high H_2O_2 and combinatorial stress.

In summary, high levels of H_2O_2 trigger the sustained formation of $Cap1^{OX-1}$, which appears to be the same as the $Cap1^{OX-1}$ form generated following combinatorial stress. The kinetics of $Cap1^{OX-1}$ formation following high H_2O_2 stress mirrors the lack of Cap1-dependent gene expression and the delay in Cap1 phosphorylation. These observations suggest that the formation of $Cap1^{OX-1}$ following high H_2O_2 or combinatorial stress may be sufficient to prevent the activation of Cap1. A major difference, however, is that with combinatorial stress $Cap1^{OX-1}$ fails to accumulate in the nucleus, whereas following high H_2O_2 stress $Cap1^{OX-1}$ rapidly localises in the nucleus.

4.2.4 Investigation into whether the impaired oxidation of Cap1 following high ROS is due to the increased activity of the thioredoxin proteins Trx1 and Txl1

In *S. pombe* it is well documented that Pap1 activation is delayed in response to high H_2O_2 concentrations (Quinn et al., 2002). Pap1 oxidation is negatively regulated by the thioredoxin oxidoreductase proteins Trx1 and Txl1. In response to low levels

of H_2O_2 , the major substrate for Trx1 and Txl1, Tsa1 becomes oxidised. Thus, Trx1 and Txl1 function is directed towards reducing Tsa1, and not Pap1. However, in response to high levels of H_2O_2 , Tsa1 is hyperoxidised and no longer a substrate for Trx1 and Txl1. Thus these proteins are now free to reduce Pap1 and keep in its inactive reduced state (section 1.5.2.3.2). In *C. albicans*, the oxidoreductase Trx1 was previously shown to negatively regulate Cap1, as Cap1 oxidation is prolonged in *trx1* Δ cells (da Silva Dantas et al., 2010). Therefore, it was possible that similar to that seen in *S. pombe*, Trx1 and, possibly Txl1, remain reduced and are therefore more active following exposure to high H_2O_2 concentrations (25 mM) and combinatorial stress (5 mM H_2O_2 + 1 M NaCl). This in turn could explain why Cap1 is not fully oxidised under these conditions. If this hypothesis is correct, then two predictions can be made: (i) $\text{Cap1}^{\text{OX-1}}$ will not be sustained in cells lacking *TRX1* or *TXL1* and, (ii) Trx1 and Txl1 will be more reduced under conditions of high H_2O_2 and combinatorial stress compared to low/ medium doses of H_2O_2 . To test this hypothesis, *C. albicans* strains harbouring Myc-tagged Cap1 and lacking either *TRX1* or *TXL1* were subjected to high ROS or combinatorial stress treatment, and Cap1 oxidation was examined over time. As shown in Figure 4.6, similar to that seen in wild-type cells, both Cap1^{OX} and $\text{Cap1}^{\text{OX-1}}$ oxidised forms were seen in *trx1* Δ and *txl1* Δ cells with $\text{Cap1}^{\text{OX-1}}$ being resolved over time to the active Cap1^{OX} form. In *txl1* Δ cells, Cap1 showed identical oxidation kinetics as in wild-type cells. In *trx1* Δ cells, the oxidation kinetics largely followed that observed in wild-type cells, although the formation of $\text{Cap1}^{\text{OX-1}}$ was slightly inhibited following combinatorial stress. These results indicate that the formation of the partially oxidised $\text{Cap1}^{\text{OX-1}}$ form is not due to increased levels of the reduced active forms of the negative regulators, Trx1 and Txl1, following high H_2O_2 or combinatorial stress.

To confirm that the thioredoxins Trx1 and Txl1 are not more reduced following high H_2O_2 or combinatorial stress, the oxidation profile of Trx1 and Txl1 was determined under these conditions. *C. albicans* cells expressing Myc-tagged Trx1 were treated with 25 mM H_2O_2 or combinatorial (5 mM H_2O_2 + 1 M NaCl) stresses and AMS-binding assay was performed to detect the oxidation of Trx1 (Figure 4.6A).

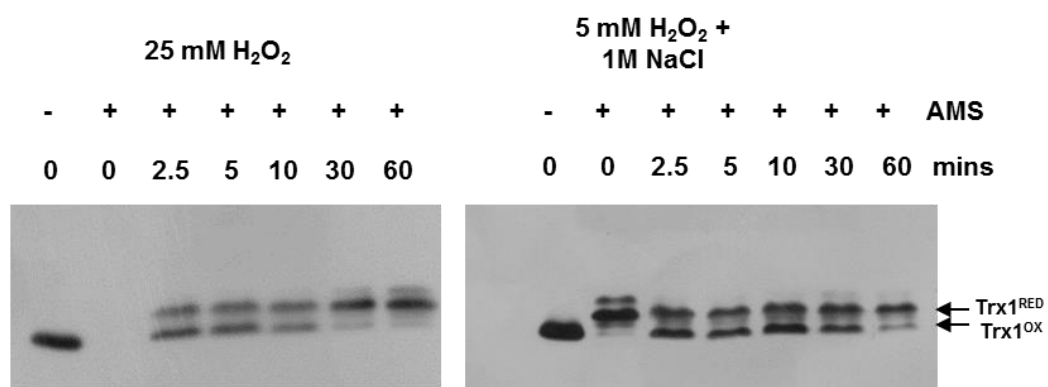
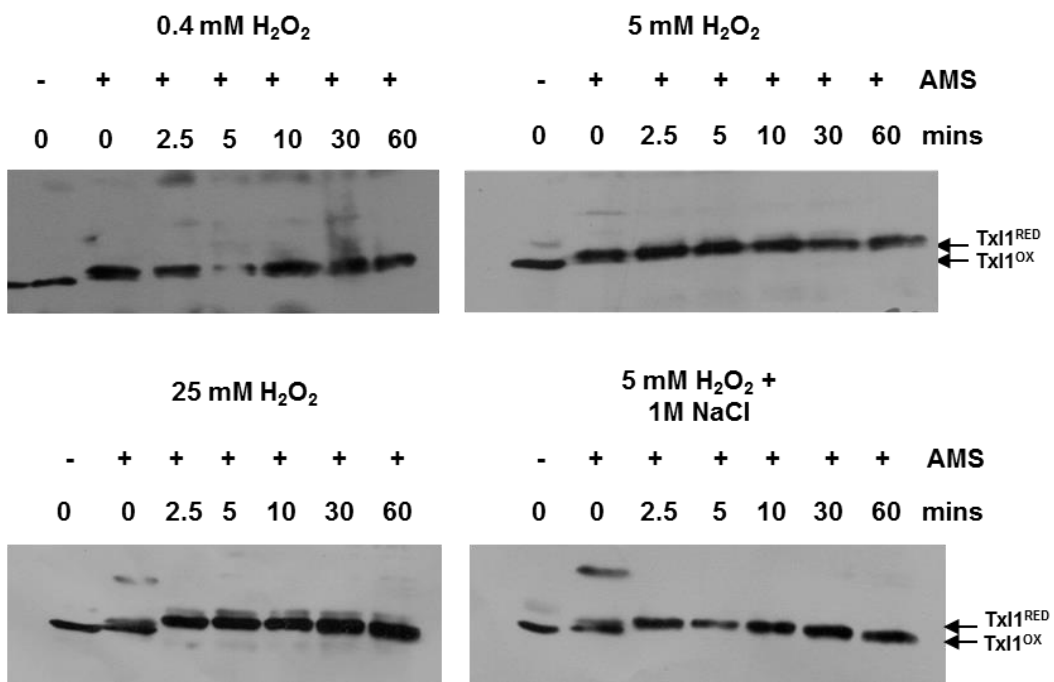
A**B**

Figure 4.6 The oxidation profile of *C. albicans* thioredoxins Trx1 and Txl1 in response to oxidative and combinatorial stress.

(A) *C. albicans* cells expressing Myc-tagged Trx1 (JC930) or (B) Txl1 (JC2101) were treated with the indicated stresses over time and processed by acid lysis protein extraction followed by AMS labelling. Protein extracts were then subjected to SDS-PAGE and western blotting using anti – myc antibodies.

Trx1 is rapidly oxidised following these stress treatments as observed by an AMS-dependent faster mobility form of the protein. Intriguingly, the resolution of Trx1 to the active reduced form appears to coincide with the same kinetics as that observed for Cap1 activation: Trx1 was resolved to the active reduced form 30 minutes post high H_2O_2 stress and 60 minutes post combinatorial stress. It is at these times when the induction of Cap1-dependent genes becomes evident. Whether active thioredoxin plays a role in the activation of Cap1 or whether the co-ordinated resolution of both Cap1 and Trx1 to their active forms is coincident with changes in intracellular ROS levels requires further investigation. However, the finding that this thioredoxin is not more reduced in response to high ROS or combinatorial stress is consistent with the observation that the generation of the $Cap1^{OX-1}$ form is largely Trx1-independent.

Next, the oxidation profile of Txl1 was examined. As this has not previously been studied, a *C. albicans* strain expressing Myc-tagged Txl1 was created and the oxidation of Txl1-Myc examined in response to low, medium and high H_2O_2 concentrations and combinatorial stress. Unexpectedly, there was no AMS-dependent increase in mobility of Txl1 following oxidative or combinatorial stress, indicating that this protein is not oxidised under these conditions (Figure 4.6B). In fact, Txl1 appears to run with a slower mobility following 25 mM H_2O_2 or combinatorial stress. However, whether this is due to a decreased oxidation of the protein is not known, as experiments were not performed (due to time constraints) to confirm that the increased mobility shift was AMS-dependent. Alternatively, it could be an alternative modification of Txl1 that causes the mobility shift. Nonetheless, as the formation of $Cap1^{OX-1}$ occurs independently of Txl1 (Figure 4.7), any such modification of Txl1 does not appear to impact on Cap1 oxidation.

To summarise, the high intracellular ROS levels generated either by high H_2O_2 concentrations or by combinatorial stress do not prevent the oxidation and inactivation of the thioredoxin proteins Trx1 and Txl1. Therefore, the delayed full oxidation of Cap1 under such conditions cannot be attributed to the increased activity of Trx1 and Txl1. Trx1 is possibly involved in Cap1 regulation following high ROS and combinatorial stress, as the appearance of active reduced Trx1 coincides with the

activation of Cap1. Further experiments are needed to explain the complex mechanism of oxidative stress-induced Cap1 regulation.

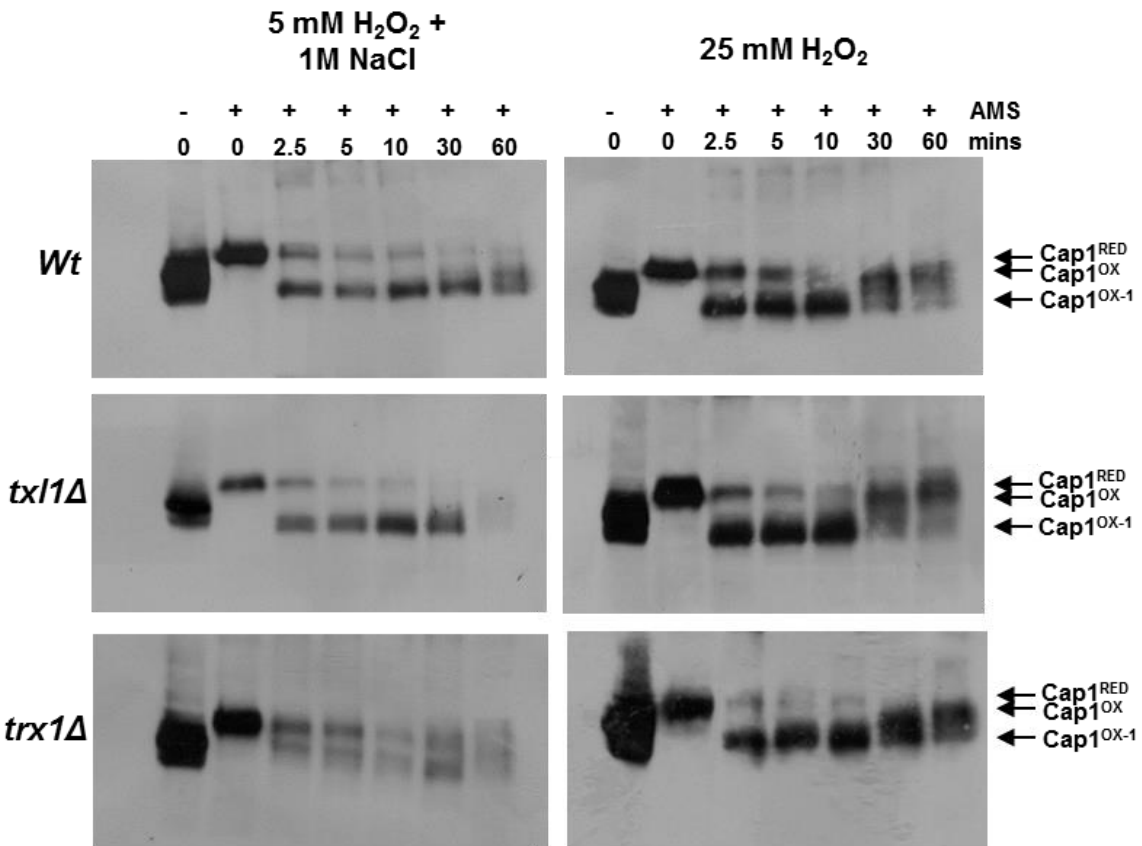


Figure 4.7 The formation of Cap1^{OX-1} following combinatorial stress and high H₂O₂ stress is independent of Trx1 and Txl1.

C. albicans JC747 (WT), JC983 (*trx1Δ*) and JC2092 (*txl1Δ*) were treated with 25 mM H₂O₂ or 5 mM H₂O₂ plus 1 M NaCl, and Cap1 oxidation was assessed at the indicated times by western blotting of AMS-modified protein extracts. Cap1 was detected using anti - myc antibodies.

4.2.5 Investigation into Cap1 promoter occupancy following exposure to high H₂O₂ concentrations

Cap1 rapidly localises to the nucleus of *C. albicans* cells in response to high concentrations of H₂O₂. However, Cap1-dependant gene expression is significantly delayed under such conditions. Thus, experiments were performed to examine whether Cap1^{OX-1} was able to bind to the promoters of target genes under such conditions. To examine where Cap1 preferentially binds to certain promoters, ChIP-sequencing datasets annotated by Znaidi et al. (Znaidi et al., 2009) were retrieved from Gene Expression Omnibus (GEO, <http://www.ncbi.nlm.nih.gov/geo/>) and analysed by IGV (Integrative Genomic Viewer) software (Robinson et al., 2011). The promoter sequences of the target genes were obtained using RSAT (Regulatory Sequence Analysis Tool) software (Medina-Rivera et al., 2015). The selection of the targets was based on a previous study confirming Cap1 enrichment on the promoters of these genes (Znaidi et al., 2009), and the existence of a Cap1 binding motif MTKASTMA at the promoter regions of these genes was confirmed by RSAT (Figure 4.8). A second criterion of the target selection was their Cap1-dependent induction in response to oxidative stress (5 mM H₂O₂) (Wang et al., 2006, Enjalbert et al., 2006, Urban et al., 2005). Lastly, the targets selected showed a clear inhibition of their induction following combinatorial stress (Kaloriti et al., 2014). Initially, five Cap1 targets were chosen: *GLR1*, *TSA1*, *CTA1*, *TRR1* and *TRX1* (Figure 4.8). However, *TRR1* and *TRX1* were not selected for further analysis as the specific primers failed to pass a quality test to produce a single amplicon. As a result, three Cap1 targets were chosen for further investigations: *CAT1*, *GLR1*, and *TSA1*. From previous microarray analysis (Kaloriti et al., 2014), the relative levels of induction of the selected targets in response to 5 mM H₂O₂ and 5 mM H₂O₂ + 1 M NaCl are listed in the Table 4.1.

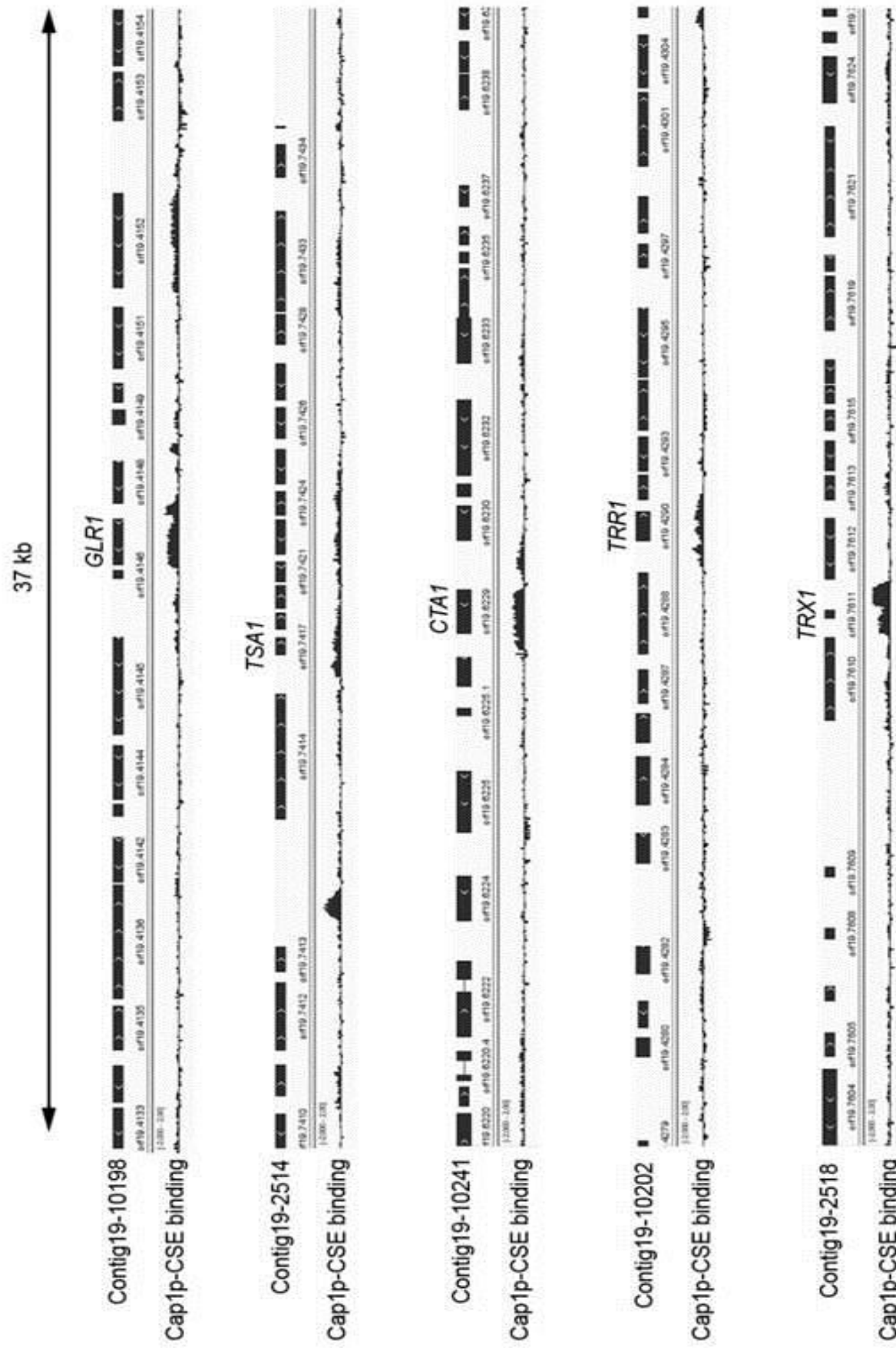


Figure 4.8 Analysis of Cap1-CSE binding to the selected gene promoters.

Plotted as normalized \log_2 -transformed signal intensities (lower graphs of each panel) of hyperactive (CSE) Cap1 binding (y-axis) versus the corresponding position of each signal (x-axis) in selected *C. albicans* genomic regions from assembly 19. ChIP-sequencing dataset from (Znaidi et al., 2009) was analysed for Cap1 enrichment on selected ORFs from assembly 19 using IGV software. The orientation of each ORF is depicted by the arrowed gray rectangle. To search for the MTKASTMA motif within Cap1-bound sequences, the sequences were analysed using the pattern-matching tool from Regulatory Sequence Analysis Tools ([RSAT] <http://rsat.ulb.ac.be/rsat/>).

Gene	5 mM H ₂ O ₂ , fold induction	5 mM H ₂ O ₂ + 1 M NaCl, fold induction
<i>CAT1</i> (orf 19.6229)	38.02	1.79
<i>GLR1</i> (orf 19.4147)	9.65	1.15
<i>TSA1</i> (orf 19.7417)	4.29	1.20

Table 4.1 Relative levels of induction of the selected Cap1 targets in response to oxidative and combinatorial stresses.

Adapted from (Kalariti et al., 2014).

C. albicans cells expressing myc-tagged Cap1 together with an untagged control strain were treated with the low, medium, and high levels of H₂O₂ detailed above, and Cap1 binding to the *CAT1*, *GLR1*, and *TSA1* promoters was determined by chromatin immunoprecipitation (ChIP) and quantitative PCR analysis. As illustrated in Figure 4.9, Cap1 was found to rapidly associate with *CAT1*, *GLR1*, and *TSA1* promoters irrespective of the level of H₂O₂ applied. Moreover, considerably higher levels of Cap1 were detected at these promoters following treatment with medium or high levels of H₂O₂, compared to low doses. Clearly therefore, the unphosphorylated Cap1^{OX-1} form generated following high levels of H₂O₂ was able to rapidly bind to the promoter regions of its target genes. However, in contrast to that seen at low and medium levels of H₂O₂, Cap1 promoter binding appeared to be insufficient to drive Cap1-dependent antioxidant gene expression, which was delayed until 30 minutes post high H₂O₂ treatment (Figure 4.3).

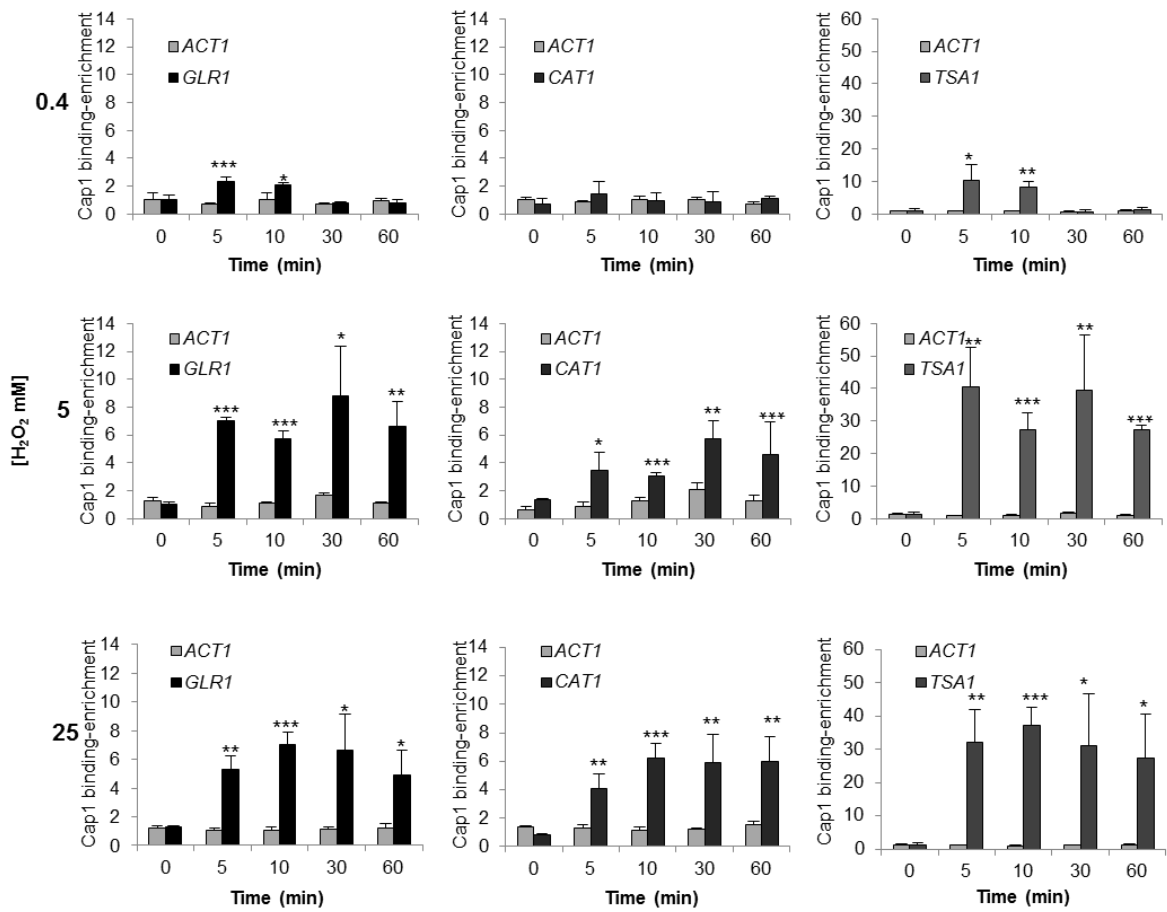


Figure 4.9 ChIP analysis of Cap1 binding to the promoters of its target genes in response to different H₂O₂ concentrations.

Cells expressing Cap1-MH (JC948) were treated with 0.4, 5 or 25 mM H₂O₂ for the indicated times and subjected to ChIP. The recovered DNA samples were analysed by qPCR using primers specific for promoter regions within *GLR1*, *CAT1* and *TSA1*. Relative Cap1-MH enrichment values (n-fold) are presented (mean \pm SD, n=3). The following P-values were considered: *, P \leq 0.05; **, P \leq 0.01; ***, P \leq 0.001.

4.2.6 High ROS levels and combinatorial stress cause the global inhibition of antioxidant gene expression

Previous microarray analysis of the gene expression profiles of *C. albicans* following combinatorial stress suggested that both Cap1-dependent and independent stress-responsive genes failed to be induced following a 10 minute stress treatment (Kalogeriti et al., 2014). As was shown in Chapter 3, combinatorial stress drives dramatic increases in intracellular ROS levels (Figure 3.18).

Thus, it was possible that treatment with high doses of H₂O₂ alone could also prevent the rapid activation of Cap1-independent H₂O₂ responsive genes. Therefore, it was important to confirm whether the high H₂O₂-induced transcriptional delay is specific to Cap1 targets. For this reason, it was decided to examine the induction of two genes – *NPR1* (orf19.6232) and *IPF9145* (orf19.6245), that are upregulated in response to H₂O₂, but their regulation is Cap1-independent (Enjalbert et al., 2006). *NPR1* encodes a serine/ threonine protein kinase, involved in the regulation of ammonium transport, and is induced in the core stress response (Enjalbert et al., 2006, Neuhäuser et al., 2011, Singh et al., 2011). *IPF9145* encodes a protein of unknown function, which is induced following oxidative and osmotic stresses, but its induction in response to oxidative stress is not regulated by Cap1 (Enjalbert et al., 2006, Bennett and Johnson, 2006, Nobile et al., 2012).

Northern blot analysis revealed that *NPR1* was not significantly induced following H₂O₂ stress and instead *NPR1* mRNA levels were reduced following H₂O₂ treatment; this was particularly evident with high doses of H₂O₂ stress (Figure 4.10). *IPF9145* was similarly unresponsive to low levels of H₂O₂. However, the induction was seen following treatment with both 5 and 25 mM H₂O₂, and this was significantly delayed with the high H₂O₂ dose (Figure 4.10). Thus at least with the Cap1-independent *IPF9145* gene it can be seen that there is a delay in induction following high H₂O₂ stress.

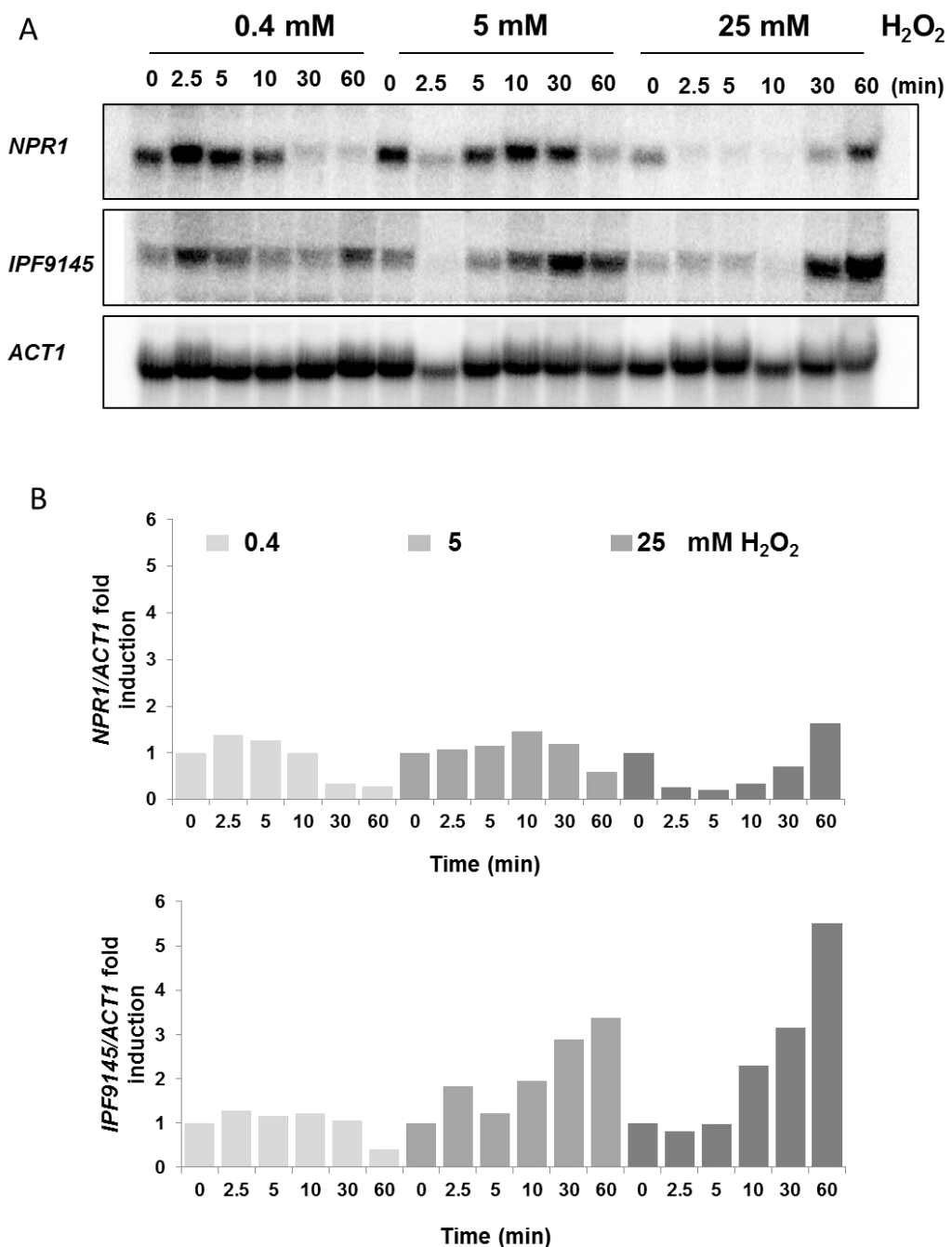


Figure 4.10 Cap1-independent antioxidant gene expression is inhibited in response to high H₂O₂ levels.

(A) Northern blot analysis of RNA isolated from wild-type (JC747) cells before and following treatment with 0.4, 5, or 25 mM H₂O₂. Blots were analysed with probes specific for the *NPR1* and *IPF9145* genes. A probe against *ACT1* was used as a loading control. (B) The levels of *NPR1* and *IPF9145* mRNA were quantified relative to the *ACT1* using Image quant software.

4.2.7 Impact of high ROS levels on global regulation of transcription

As both Cap1 and non-Cap1 targets show delayed induction in response to high H_2O_2 levels, this was indicative of perhaps a more global inhibition of gene transcription in response to high levels of ROS. In *S. cerevisiae* high levels of ROS trigger a global inhibition of translation (Shenton et al., 2006), and here we questioned whether high ROS treatment could globally impact on transcription in *C. albicans*. In mammalian cells it was found that high ROS levels globally inhibit gene transcription by decreasing the levels of total histone H3 acetylation (Berthiaume et al., 2006). Therefore, experiments were performed to explore whether high levels of ROS impact on chromatin remodelling in *C. albicans*, because certain histone modifications are linked to transcription activation. For instance, ADA2, part of the ADA/SAGA histone acetylation complex, is essential for transcriptional response to oxidative stress in *C. albicans* (Sellam et al., 2009), and therefore provides a link between chromatin remodelling and Cap1-dependant transcriptional responses. To determine whether high ROS levels specifically impacted on global histone acetylation profiles, *C. albicans* cells were treated with oxidative (5 and 25 mM H_2O_2), osmotic (1 M NaCl) and combinatorial (5 mM H_2O_2 + 1 M NaCl) stresses. Protein extracts were obtained by acid lysis, which facilitates extraction of the basic histones from chromatin, and analysed by SDS-PAGE and western blotting using antibodies against total H3 histone and specific H3 modifications – acetylation at H3K9 and H3K14. These modifications were chosen as H3 acetylation at position Lys9 and Lys14 is indicative of actively transcribed chromatin (Sellam et al., 2009, Johnsson et al., 2009). However, as seen in Figure 4.11, no global changes in the levels of H3K9 and H3K14 acetylation were observed following exposure to any of the stress treatments above. This indicates that the exposure of *C. albicans* cells to combinatorial stress, or high levels of H_2O_2 , has no detectable impact measured using this assay on specific histone modifications at a global level.

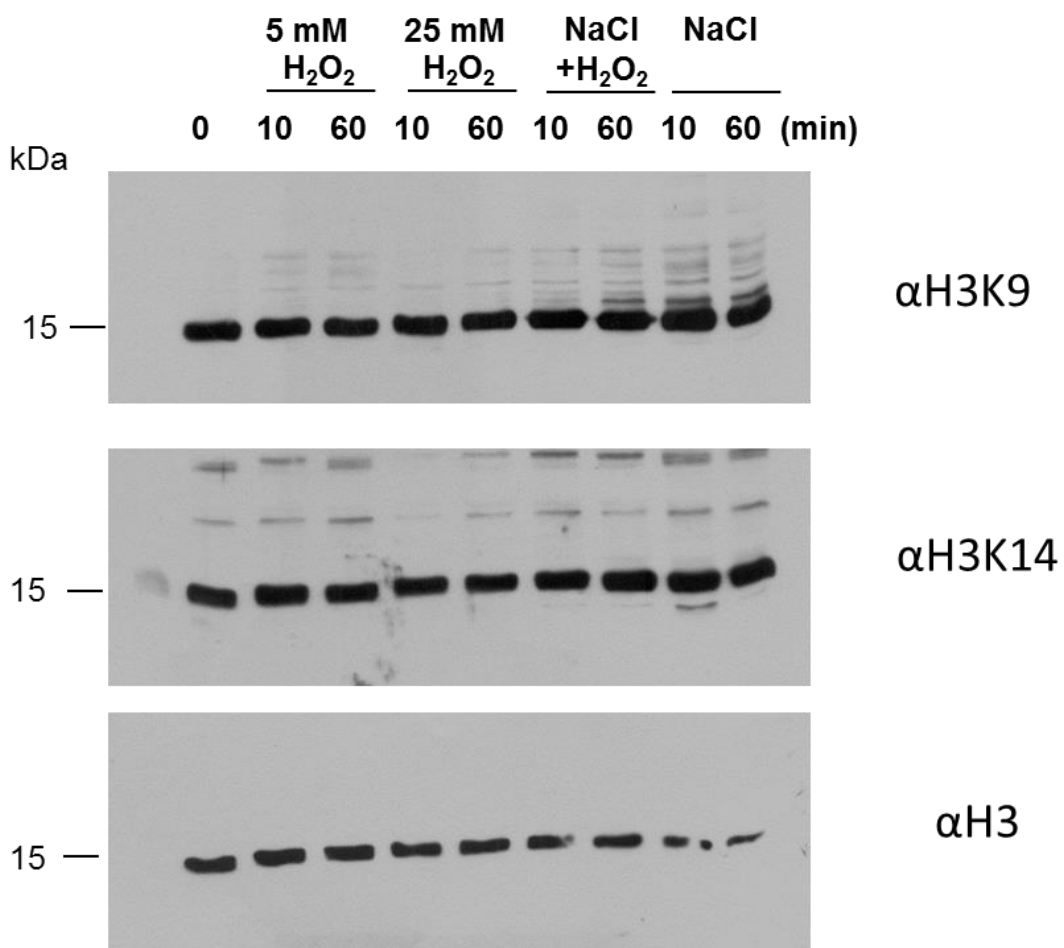


Figure 4.11 Impact of different stress conditions on histone acetylation.

C. albicans cells JC948 were treated with the indicated stresses and collected at 10 and 60 minutes. Pellets were subjected to acid lysis protein extraction and resolved by SDS-PAGE on 15% gels, following by the western blotting with antibodies raised against acetylated H3K9, acetylated H3K14 and total H3. The data are representative of three biological replicates

To further explore whether a global inhibition of transcription occurs following combinatorial and high H_2O_2 stress, we examined the phosphorylation status of RNA polymerase II (RNA Pol II). Transcription elongation is regulated by phosphorylation of the C-terminal domain (CTD) of the largest subunit of Pol II (RPB1). The major conserved phosphorylation sites are Ser2 and Ser5 within the repetitive YSPTSPS sequence in the CTD (Heidemann et al., 2013). *C. albicans* cells expressing 2myc-6His-tagged Cap1 were subjected to medium (5 mM) and high (25 mM) H_2O_2 levels in addition to combinatorial stress (5 mM H_2O_2 plus 1 M NaCl), and protein lysates were analysed by western blotting using antibodies that detect RNA Pol II CTD phosphorylation at serine 2 or serine 5 of the repeat sequence YSPTSPS. Total levels of RNA Pol II were determined using an antibody that recognises the CTD repeat sequence. As a control, a time “0” sample was treated with lambda phosphatase prior to loading. The RNA Pol II blot was stripped and reprobed with anti-Cap1 antibodies to reconfirm Cap1 phosphorylation kinetics in response to the stress treatments. This shows that although Cap1 phosphorylation (a marker of active Cap1) is significantly delayed following high H_2O_2 stress and combinatorial stress, RNA Pol II phosphorylation is not reduced following such treatments (Figure 4.12). This indicates that the defect in Cap1-mediated gene expression is not due to a global inhibition of RNA Pol II activity, as markers of active RNA Pol II remained unaffected by high levels of ROS or combinatorial stress. Further experiments are needed to address whether other components of the transcription machinery, such as those involved in the formation of the mediator complex, are not inhibited by high levels of the oxidative stress.

4.3 Discussion

Taken together, these results reveal novel mechanisms of Cap1 regulation in *C. albicans*. When *C. albicans* cells are exposed to high levels of H_2O_2 , Cap1 activation is delayed similar to that seen following combinatorial oxidative and cationic stress. Importantly, in both conditions there is an increase in intracellular ROS levels, resulting in partial Cap1 oxidation and the sustained formation of Cap1^{OX-1}.

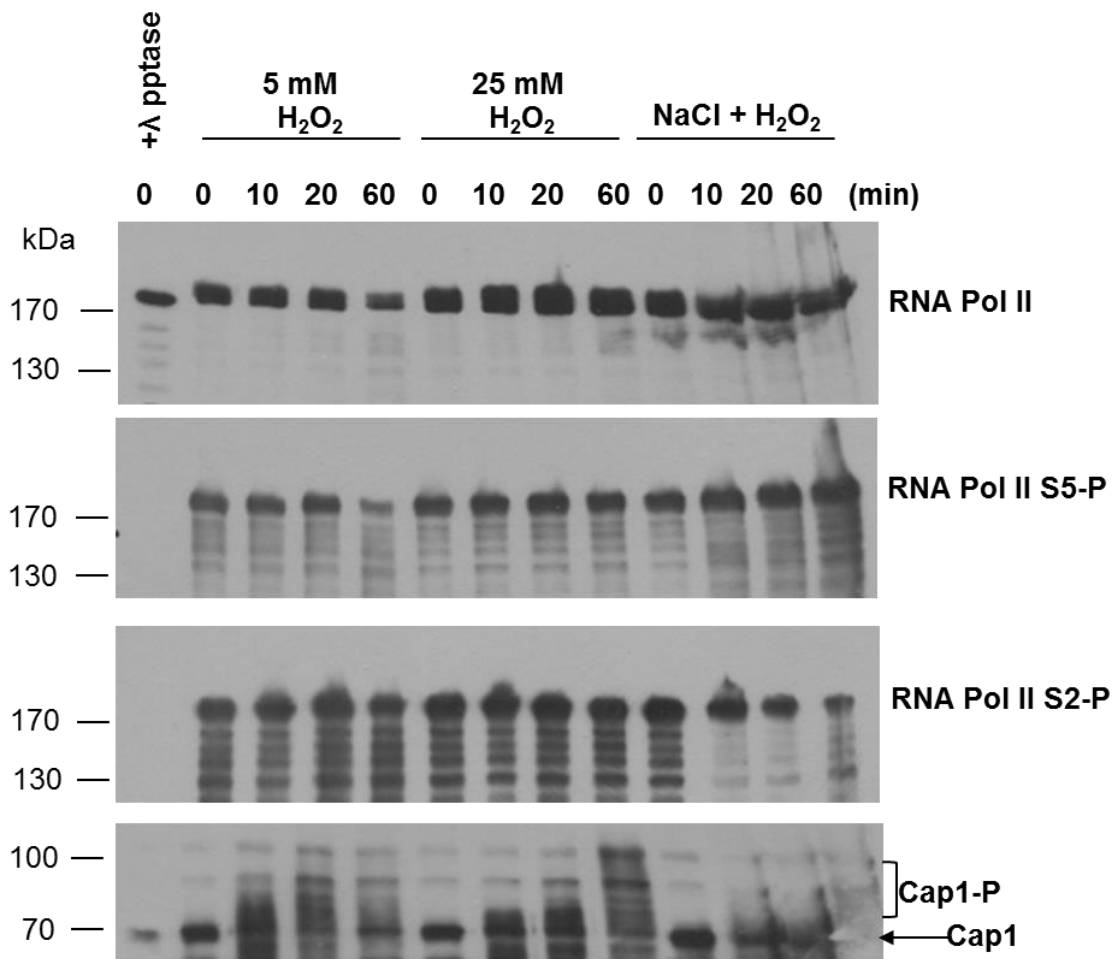


Figure 4.12 RNA Pol II phosphorylation is maintained following high H₂O₂ exposure and combinatorial stress.

Lysates from cells expressing 2myc-6His-tagged Cap1 (Cap1-MH, JC948), before (0) and after the indicated stress treatments for the indicated times, were analysed by western blotting using antibodies that detect RNA Pol II CTD phosphorylation at serine 2 or serine 5. Total levels of RNA Pol II were determined using an antibody that recognises the CTD repeat sequence. The RNA Pol II blot was stripped and reprobed with anti-Cap1 antibodies. The data are representative of three biological replicates.

Failure to generate an active oxidised form of the transcription factor correlates with the delayed phosphorylation pattern of Cap1^{OX-1}. Following combinatorial stress the lack of phosphorylation can be explained by the delay in Cap1 nuclear accumulation, whereas following high H₂O₂ stress Cap1^{OX-1} rapidly accumulates in the nucleus and yet is still not phosphorylated. Moreover, although the unphosphorylated Cap1^{OX-1} form generated following high H₂O₂ stress rapidly binds to the regulatory sequences within the promoter regions of its target genes, such genes are not expressed. A model comparing the deregulation of Cap1 activation following combinatorial and high H₂O₂ stress is shown in Figure 4.13. Whilst both combinatorial and high H₂O₂ stresses delay the activation of Cap1 – the inhibition of Cap1 activation is less sustained following high H₂O₂ compared to the combinatorial stress effect. This could be related to the cation-driven increased interaction of Cap1^{OX-1} with the Crm1 exporter, which is specific to the combinatorial stress. Thus, in contrast to high H₂O₂ stress, following combinatorial stress two mechanisms work in parallel to delay Cap1 activation, Cap1^{OX-1} formation and enhanced interaction with the Crm1 nuclear exporter (detailed in Chapter 3).

The finding presented in this Chapter support previous results that the Cap1^{OX-1} form may not be transcriptionally active and is most likely a partially oxidised intermediate in the formation of Cap1^{OX}. Moreover, the resolution of the Cap1^{OX-1} form to Cap1^{OX} is a necessary pre-requisite for the induction of the Cap1-mediated oxidative stress regulon. Intriguingly, activation of thioredoxin Trx1, which has previously been demonstrated to negatively regulate Cap1 by reducing active Cap1 (da Silva Dantas et al., 2010), coincides with the resolution of Cap1^{OX-1} to its active Cap1^{OX} form. This suggests a potential role for this redox sensitive regulator in the resolution of the Cap1^{OX-1} form to the active Cap1^{OX} form. However, this does not appear to be direct, as the kinetics of Cap1^{OX} formation is similar in wild-type and *trx1Δ* cells. A possible way to address the role of Trx1 and Txl1 thioredoxins on Cap1 alternative oxidation is to monitor Cap1 activation in *C. albicans* mutant strain lacking both *trx1* and *txl1*, because their action may be redundant. As discussed in Chapter 3, approaches to define the precise oxidation status of the Cap1^{OX-1} form are needed to further our understanding of why high ROS levels trigger the differentially oxidised form of Cap1.

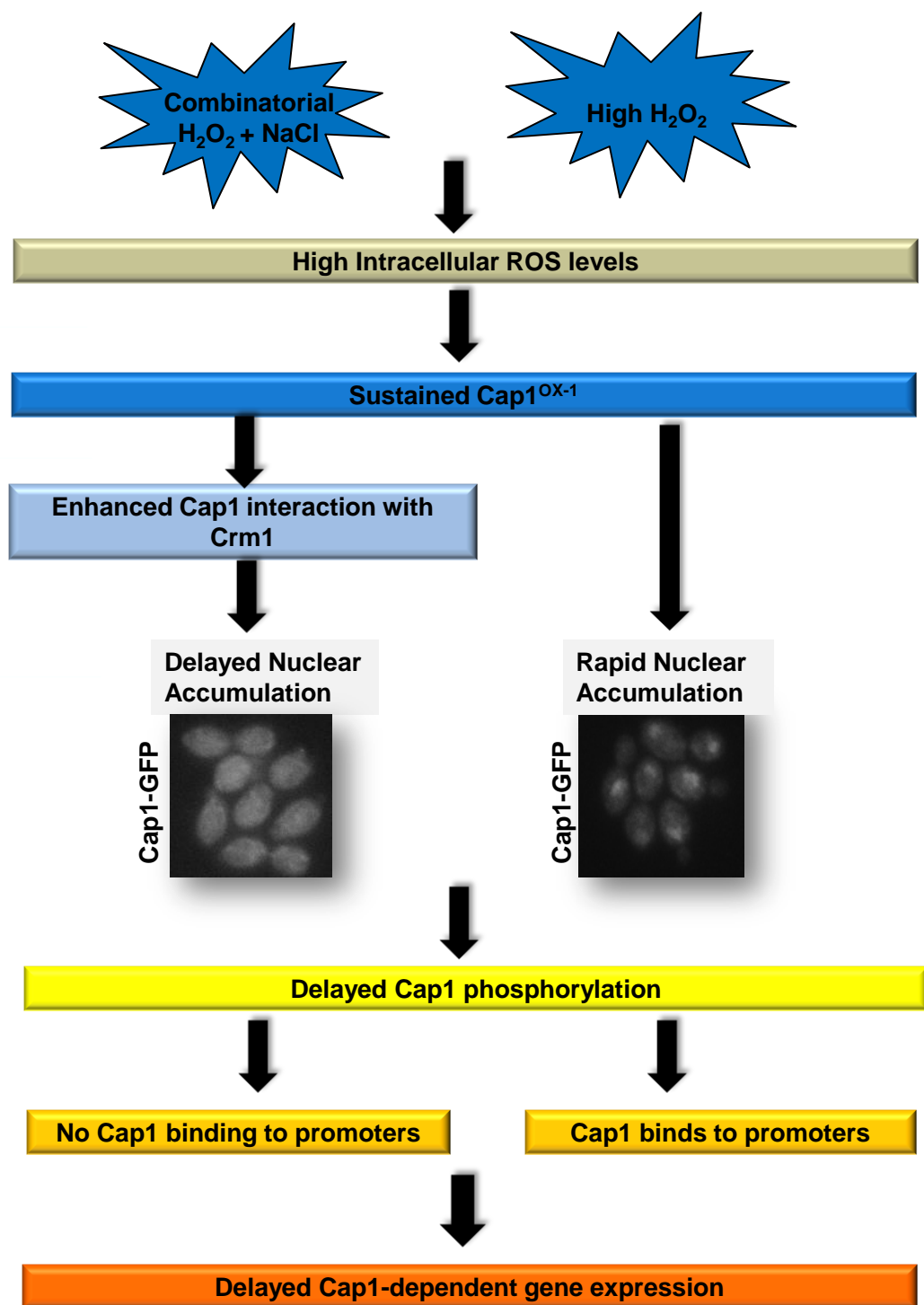


Figure 4.13 A model depicting the deregulation of Cap1 activation in response to high H₂O₂ levels and combinatorial oxidative plus cationic stress.

Following the treatment of *C. albicans* cells with high ROS (25 mM H₂O₂) or combinatorial stress (5 mM H₂O₂ + 1 M NaCl) there is an increase of intracellular ROS levels, and Cap1 is alternatively oxidised to Cap1^{OX-1}. The presence of cations promote the interaction between Cap1 and Crm1 exporter following combinatorial stress, leading to the delayed Cap1 nuclear accumulation. In contrast, following high H₂O₂ concentrations, Cap1 rapidly accumulates in the nucleus. In both conditions Cap1 phosphorylation is delayed. Following 25 mM H₂O₂ treatment Cap1 binds to the promoters of target genes, whereas the impairment of Cap1 nuclear accumulation post combinatorial stress prevents Cap1 binding to its targets. In response to both high ROS levels and combinatorial stress Cap1-dependant gene expression is delayed.

Many transcription factors are regulated by phosphorylation/ dephosphorylation. For instance, for the activation of *S. cerevisiae* Msn2/4 transcriptional factors, their nuclear localisation is necessary, but not sufficient for gene induction, and also requires other regulators, such as 2A-Cc55 protein phosphatase, to facilitate the chromatin recruitment in response to the hyperosmotic stress (Reiter et al., 2013). Similar intranuclear events could underlie the delayed activation of the Cap1 transcriptome in response to high doses of oxidative stress in *C. albicans*. Studies in *S. cerevisiae* revealed that the nuclear accumulation of Yap1 was necessary for this post-translational modification (Delaunay et al., 2000). However, as both the kinase and target phosphorylation sites on Yap1 are unknown, it has not been possible to establish whether this post-translational modification is important for the activation of this, or other fungal AP-1-like transcription factors. In this study we show that following high H₂O₂ stress, phosphorylation of Cap1 does not occur upon Cap1 entering the nucleus. Instead the delayed phosphorylation that is seen coincides with the generation of Cap1^{OX-1} and the induction of Cap1-dependent genes, suggesting that this posttranslational modification might be not only a marker of an active Cap1, but also important for its function. Possibly, high ROS may impact on the function of the hitherto unknown kinases/phosphatases that regulate the phosphorylation status of Cap1.

Studies in *S. cerevisiae* revealed that relatively high doses of oxidative stresses cause a decrease in the activation of stress responsive elements, directly interfering with transcriptional activation, and both Hog1- and Yap1-dependent gene promoters' activation correlates with the concentration of the oxidative stress stimuli, although the sensitivities of different promoters vary (Dolz-Edo et al., 2013). High ROS levels lead to the delay and decrease in regulatory sites activity in *S. cerevisiae* (Dolz-Edo et al., 2013), as well as the inhibition of transcription by the global changes in the levels of histone acetylation in human cells (Berthiaume et al., 2006). In addition to work presented in this Chapter, previous study (Kaloriti et al., 2014) suggests that the high ROS-driven inhibition of oxidative stress-responsive genes is not specific to Cap1 targets. To understand whether high ROS levels have global impacts on chromatin structure, the acetylation levels of certain histone H3 lysine residues – H3K9 and H3K14, were monitored, as these modifications are linked to actively transcribed chromatin in *C. albicans* (Sellam et al., 2009). However, this line of investigation has not uncovered any global impacts of high H₂O₂ stress on specific markers of transcriptional activation. Alternative approaches to investigate the impact of ROS on chromatin structure could include an examination for altered histone modifications over specific genes, exploring different histone modifications or investigating the nucleosome positioning over stress responsive genes.

Reports in *S. cerevisiae* suggest that for an effective oxidative stress response Yap1 needs to be specifically folded to recruit the Rox3 subunit of the RNA Pol II complex (Gulshan et al., 2005). Thus, as the oxidation and phosphorylation state of Cap1 is altered following high ROS, this may impact on the effectiveness of the bound transcription factor to recruit key components of the transcription machinery. In this work we show that high ROS does not seemingly impact on the activity of the core RNA polymerase II enzyme. RNA Pol II phosphorylation remained unaffected by combinatorial and high H₂O₂ stresses, suggesting that under such conditions the polymerase is active. However, further experiments could be directed at investigating the ability of Cap1^{OX-1} generated post high H₂O₂ stress to recruit RNA Pol II or RNA Pol II mediator subunits to the promoters of Cap1 target genes. In addition, as Cap1 has been shown to interact with the SAGA/ADA coactivator complex and recruits the ADA2 component to gene promoters (Sellam et al., 2009), such investigations could

be extended to test the ability of $\text{Cap1}^{\text{OX-1}}$ to recruit this chromatin remodelling complex to target promoters.

C. albicans possesses an additional oxidative stress-responsive transcription factor Skn7 which, based on studies in model yeasts, may co-regulate Cap1 -dependent genes. Hence, it is also possible that Skn7 might be deregulated in response to high ROS in *C. albicans*, which in turn could contribute to the delayed activation of Cap1 -target genes. Prr1, which is the Skn7 orthologue in *S. pombe*, was found to interact *in vivo* with Pap1, and affect the expression of important antioxidant genes, such as *CAT1* and *TRR1* (Calvo et al., 2012). Moreover, Pap1 oxidation is essential to form a nuclear heterodimer with Prr1 (Calvo et al., 2012), and Pap1 affinity to promoters was significantly enhanced upon association with Prr1. Taking into consideration the fact that following high ROS the Cap1 oxidation state is altered, this could impact on its putative interaction with Skn7 and the formation of Cap1 -Skn7 transcriptional complex. It is also noteworthy here that Prr1 is implicated in H_2O_2 -concentration dependent responses in *S. pombe*. Prr1 is important for cellular responses to both medium and high H_2O_2 concentrations, but the regulation differs: two-component regulation of Prr1 is specifically required for cellular response to high doses of the oxidative stress (Quinn et al., 2011, Chen et al., 2008). There are also several reports indicating the cooperation between Skn7 and Yap1 in *S. cerevisiae* in response to the oxidative stress (Morgan et al., 1997, Lee et al., 1999, He et al., 2009, Mulford and Fassler, 2011). Thus, based on these studies, which demonstrate co-operation between Skn7/Prr1 and AP-1 like transcription factors, and H_2O_2 -concentration dependent effects on Prr1 regulation, it would be interesting to explore the impact of high ROS on *C. albicans* Skn7/ Cap1 interactions and Skn7 functionality.

To conclude, in this Chapter we show that the exposure of *C. albicans* to high levels of H_2O_2 cause an alternative oxidation of the transcription factor and the generation of a transient $\text{Cap1}^{\text{OX-1}}$ form. Although $\text{Cap1}^{\text{OX-1}}$ generated post high ROS is nuclear and binds to the promoters of its target genes, the expression of Cap1 -dependant antioxidant genes is delayed. This results in the lack of a rapid oxidative stress response and ultimately results in the pathogen's death. A summary of Cap1

deregulation following high levels of H_2O_2 is depicted in Figure 4.14. Further work is needed to delineate how high ROS levels inhibit Cap1-dependent and independent targets. Nonetheless, it is likely that the high ROS levels directly produced by neutrophils, or indirectly through the production of combinations of ROS and cationic stresses, contribute to the potency of phagocytes in immunocompetent hosts by delaying *C. albicans* oxidative stress responses. In the next Chapter, the importance of the immune status of the host in both preventing lethal *C. albicans* infections and dictating *C. albicans* virulence traits is explored using a *Caenorhabditis elegans* model of infection.

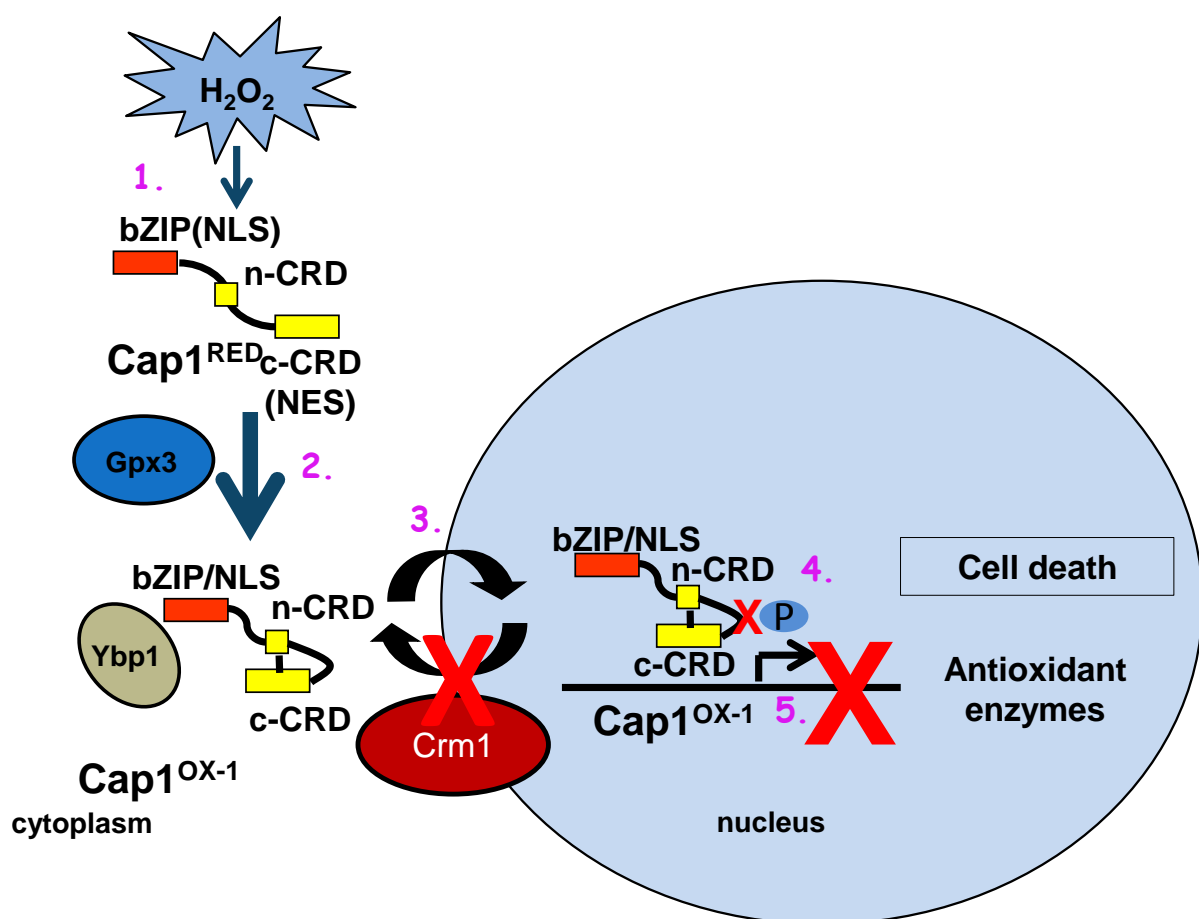


Figure 4.14 A model of Cap1 inactivation following high ROS.

When *C. albicans* cells are exposed to high (25 mM) levels of H_2O_2 (1), a $Cap1^{OX-1}$ form, containing less disulfides is prevalent (2), and although this rapidly accumulates in the nucleus (3) and binds to target genes, $Cap1$ is not phosphorylated (4) and the induction of $Cap1$ -dependent genes is significantly delayed (5), resulting in cell death.

Chapter 5. The Requirement for Stress Responses in Mediating *C. albicans* Virulence is Dependent on the Immune Status of the Host

5.1 Introduction

Numerous studies provide compelling evidence that stress responses are essential for the virulence of *C. albicans*. Transcript profiling studies *in vivo* have shown that stress protective or regulatory genes are induced in response to contact with the host, and that the inactivation of many stress functions attenuates virulence (Fiori et al., 2012, Wysong et al., 1998, Hwang et al., 2002, Martchenko et al., 2004, Lorenz et al., 2004, Fradin et al., 2005, Hromatka et al., 2005, Barelle et al., 2006, Enjalbert et al., 2006, Thewes et al., 2007, Ramírez and Lorenz, 2007, Zakikhany et al., 2007, Walker et al., 2009, da Silva Dantas et al., 2010, Patterson et al., 2013). Many of the stresses that these regulatory or protective proteins respond to are generated by the host innate immune system. Therefore, we reasoned that such stress responses may not be essential for *C. albicans* virulence if the immune system of the host is compromised. This could be highly significant as in general, it is immunocompromised patients that are susceptible to life-threatening systemic infections. As described in the introduction (section 1.2.2), immunosenescence that is associated with ageing, also increases the susceptibility of the human host to systemic *Candida* infections, similar to that seen in the immunocompromised host. *C. albicans* isolates, that showed decreased virulence in mammals, also exhibited attenuated virulence in *C. elegans* model (Pukkila-Worley et al., 2011, Pukkila-Worley et al., 2009). Various virulence factors that are required for fungal pathogens to colonise mammalian host are also indispensable for the establishing an infection in *C. elegans* model; using *C. elegans* model it is easy to monitor typical traits of *C. albicans* infection. For instance, fungal filamentation that is tightly associated with virulence of *C. albicans* is also observed in *C. elegans* model, where fungal filaments protrude and damage host tissues, whereas yeast form of fungi, that accumulate and proliferate within the animal, cause a distention of the worm's body with the subsequent killing of the animal (Pukkila-Worley et al., 2009). An early indication of lethal infection in *C. elegans* is DAR (Deformed anal region) phenotype (Jain et al., 2013). DAR phenotype is a distinctive tail swelling when *C. elegans* subjected to

ingest *C. albicans*, unlikely to what is seen by growth on *E. coli*. The formation of DAR was also seen during *C. elegans* infection with *S. cerevisiae* (Jain et al., 2009) or *Microbacterium nematophilum* (Hodgkin et al., 2000), and considered as a disease symptom of *C. elegans*. In this section I questioned whether the immune status of the host, or the age of the host, impact on the requirement of stress-protective virulence determinants following *C. albicans* infection.

To facilitate this study, the nematode worm *C. elegans* was chosen as a model of infection. *C. elegans* is a model organism that has been at the forefront of aging research (Gruber et al., 2015, Maglioni et al., 2016, Visscher et al., 2016, Shen et al., 2016, Ayyadevara et al., 2016, Komura et al., 2012, Tan et al., 1999), and that more recently has been exploited as an infection model to identify virulence traits in a range of pathogens, including *C. albicans* (Balla and Troemel, 2013, Cohen and Troemel, 2015, Simonsen et al., 2012, Marsh and May, 2012, Mylonakis et al., 2007, Means, 2010), innate immune responses (Shivers et al., 2008, Kim and Ausubel, 2005, Irazoqui et al., 2010b, Pukkila-Worley and Ausubel, 2012, Gravato-Nobre and Hodgkin, 2005), and the identification of anti-microbial compounds (Ewbank and Zugasti, 2011, Anastassopoulou et al., 2011, Squiban and Kurz, 2011, Arvanitis et al., 2013). The pathogen's genes that are required for the infection of human host are also indispensable for virulence in *C. elegans* model (Sifri et al., 2005). This model host has many advantages, such as ease of handling and maintenance in the laboratory and the ease in which large age-matched populations of animals can be generated. In addition, the *C. elegans* model of infection is useful for studying the relationship between innate immunity and pathogens, because the nematode lacks an adaptive immune system.

The epithelial cells lining the intestine of *C. elegans* mount the innate immune defences of the worm, as in nature pathogens are ingested, thus prompting the development and maintenance of a sophisticated innate immune system. Recent work showed that *C. albicans* can successfully colonise the nematode's intestine, and this is a useful model to monitor innate immune response upon *C. albicans* infection (Pukkila-Worley et al., 2011). Furthermore, *C. elegans* intestinal epithelial cells bear a striking resemblance to human intestinal cells (Troemel et al., 2008) and

ROS release as an important antimicrobial mechanism in the intestinal tissue of *C. elegans* (Chávez et al., 2007). In human host, the response to the fungal presence involves the activation of key signalling pathways – Mitogen Activated Protein Kinase (MAPK) pathways (JNK, p38 and ERK1/2), the Phosphatidylinositide-3-kinase (PI3K) pathway and the Nuclear Factor-kappa-enhancer of B cell function (NF- κ B) pathway (Moyes et al., 2015). The MAPK pathway is one of the major innate immune response pathways responsible for innate immune defence in mammals, and it is actively upregulated in response to *C. albicans*. MAPK activation is a biphasic process, which involves the first morphology-independent response, following by the second phase, which is specific to *C. albicans* in hyphal morphology (Moyes et al., 2010). This initial response is largely dependent on p38 MAPK (Moyes et al., 2010). MAPK signalling is also conserved in *C. elegans* (Kim et al., 2002). Nematode's PMK-1 MAPK is the homologue of mammalian p38 in *C. elegans*, and this plays a key role in the nematode's innate immune responses to both bacterial and fungal infections (Pukkila-Worley and Ausubel, 2012, Kurz and Tan, 2004). As with all MAPKs, PMK-1 is present in a three tier cascade which also comprises the NSY-1 MAPKKK and the SEK-1 MAPKK. *C. elegans* mutants lacking any functional component of this PMK-1 signalling cascade are highly susceptible to pathogen-mediated killing (Irazoqui et al., 2010a, Aballay et al., 2003, Pukkila-Worley and Ausubel, 2012). Such mutants provide an ideal system, in which responses on an 'immunocompromised' host to a pathogenic microbe can be explored. Thus, *C. elegans* "immunocompromised" mutants are useful model to study the impact of fungal stress-protective virulence determinants in establishing the infection.

Also there are striking similarities in downstream immune responses in mammalian cells and *C. elegans*: although nematode does not have phagocytes specialised for innate host defence, it produces a variety of humoral antimicrobial substances – lysozymes, caenopores, lipase, lectins, as well as C3-like thioester-containing proteins and defensin-like antibiotic peptides (Komura et al., 2012). While establishing infection, pathogens have to combat the humoral defence factors produced by the host, and consequently *C. elegans* may be most suitable to study anti-innate immune properties of pathogens.

The elderly population is more susceptible to *C. albicans* infection (section 1.2.2). *C. elegans* showed an increased susceptibility to bacterial infection with age, which is associated with immunosenescence and deterioration of PMK-1 MAPK signalling (Youngman et al., 2011). Hence, *C elegans* could be a suitable model to study the impact of aging of the virulence determinants needed by pathogenic microbes to cause infection. The major aim of this Chapter is to investigate age-associated increases in susceptibility to *C. albicans* using *C. elegans* as an infection model to determine whether stress response regulators of *C. albicans*, that are vital for the virulence of the pathogen, are still indispensable for causing an infection in aged population. Here, we will exploit the unique ability to generate synchronous populations of elderly worms, and immunosuppressed mutant worms, to determine: (i) the impact of the age of the worm on the ability to survive *C. albicans* infections, (ii) whether defects in fungal resistance are comparable between immunosuppressed and elderly worms and, (iii) whether *C. albicans* requires the same armoury of virulence determinants to cause lethal infections in immunosuppressed worms and worms of advanced age (using mutant libraries available in the J. Quinn lab).

5.2 Results

5.2.1 *C. elegans* is more susceptible to *C. albicans* infection with ageing

The first question we addressed in this section was whether old adult worms were more susceptible to *C. albicans* infection than young adult worms. In order to facilitate the generation of synchronised age-matched populations and to prevent germ-line proliferation, we used the temperature-sensitive sterile *C. elegans* mutants, *glp-4* (Table 2.7). Killing assays were performed as described previously (Pukkila-Worley et al., 2011). Briefly, age-matched animals were maintained at 25 °C and grown to the larval L4 stage on NGM agar plates containing a surface lawn of the standard non-pathogenic food source *Escherichia coli* OP 50. The day when animals have reached the L4 larval stage was counted as “Day 0”. An infection with *C. albicans* was initiated by moving the worms onto a plate seeded with *C. albicans* cells at the L4 larval stage (young adults), 3 days post L4 stage (L4+3, mature

adults), and 6 days post L4 stage (L4+6, aged adults). Approximately of 100-150 L4-stage larvae, 3 days after L4 stage and 6 days after L4 stage adults were placed on each of five Brain Heart Infusion (BHI) agar plates seeded in advance with *C. albicans*. Worm mortality was scored over time, with an animal being considered dead when it failed to respond to a touch and no pharyngeal pumping was detected.

Nematodes that were not recovered from the plates were censored from the study. Statistical analysis was performed using Student's t-test. At the same time, the survival of *C. elegans* maintained on *E. coli* was monitored in order to take into consideration any deaths occurring due to non-pathogenic factors, and to check the lifespan of the animals maintained in indicated conditions (Figure 5.1 A). *C. elegans* survival was expressed as a percentage of their viability at day zero. Results were analysed for statistical significance by Student's t-test. Values were considered to be statistically significant when the P value was <0.05 .

The results indicate that young (L4 stage) and mature (3 days old L4s) adults are able to combat the pathogen quite effectively with an average lifespan of 10 days in both groups (Figure 5.1 B, C). However, the third group, consisted of aged adults (6 days after L4 stage), demonstrated significant increase in susceptibility to *C. albicans* with the average lifespan of 4 days. These findings indicate that aged *C. elegans* are more susceptible to *C. albicans* infection. This is reminiscent with what has been shown for the bacterial pathogen *Pseudomonas aeruginosa*, where immunosenescence of *C. elegans* correlated with an increased susceptibility to bacterial infection (Youngman et al., 2011). The research on bacterial infection of *C. elegans* also highlighted that age-dependent increase in nematode's susceptibility to pathogens is linked to a decline in PMK-1 function (Youngman et al., 2011). Therefore, we next aimed to dissect whether this age-related decline in nematode's resistance to *C. albicans* killing was maintained in worms lacking a functional PMK-1 pathway.

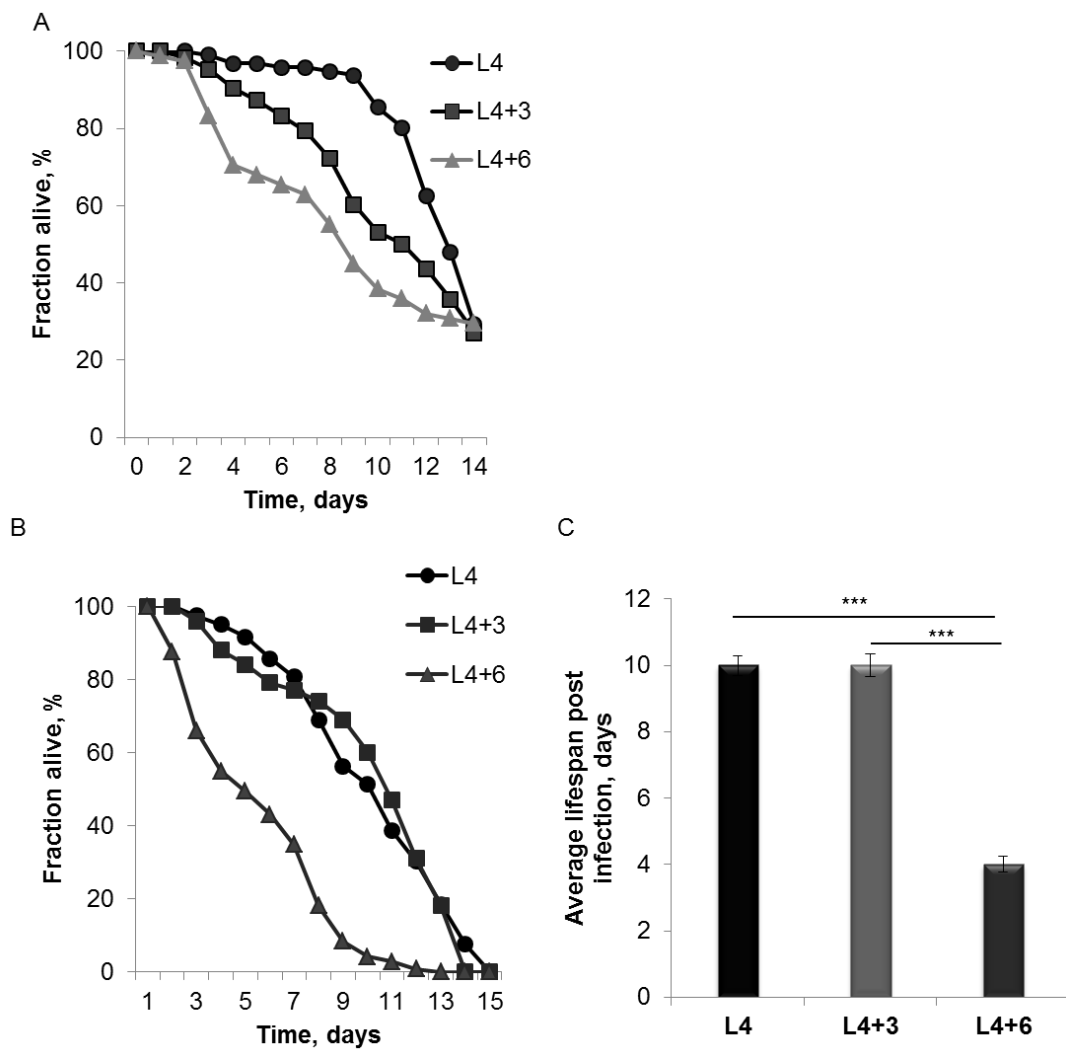


Figure 5.1 *C. elegans* are more susceptible to *C. albicans* infection with age

(A) Systematic analysis of the survival of immunocompetent *gfp-4* *C. elegans* maintained on *E. coli* OP50. L4 (circles), days 3 and 6 of adulthood (L4+3 and L4+6, squares and triangles respectively), plotted as a fraction of worms alive versus time. (B) Survival of immunocompetent *gfp-4* worms transferred from *E. coli* OP50 to *C. albicans* JC1732 at L4 (circles), and at days 3 and 6 of adulthood (L4+3 and L4+6, squares and triangles respectively), plotted as fraction of worms alive versus time. These data are from a single experiment representative of at least three independent biological replicates. (C) Average lifespan of the infected nematodes of different ages. Statistical analysis of *C. elegans* survival obtained from three independent biological replicates represents an average lifespan of different age groups of immunocompetent *gfp-4* worms upon *C. albicans* infection. Median values (\pm SD) are shown and t-test was used to determine statistically significant differences in *C. elegans* survival: **, $p<0.01$; ***, $p<0.001$.

5.2.2 Is the age-associated decline in resistance to *C. albicans* mediated due to a decline in PMK-1 function in *C. elegans*?

The PMK-1 pathway plays an important role in regulating innate immune responses in *C. elegans*, such as the infection-induced expression of secreted immune response genes, and thus is critical for the nematode to resist pathogen-mediated killing (Troemel et al., 2006). Previous studies have indicated that immunosenescence in *C. elegans* is due to a decline in the activity of the p38-related PMK-1 stress activated protein kinase pathway (Youngman et al., 2011).

To study the contribution of the PMK-1 MAPK pathway to the survival of the *C. elegans* host following infection with *C. albicans*, we conducted survival assays. These assays measured: (1) the survival of wild-type animals of different age groups compared to young worms when exposed to the pathogen and (2) the importance of functional PMK-1 pathway for the survival with age. As was mentioned previously, to examine the role of PMK-1 signalling in immunosenescence in *C. elegans* upon infection with *C. albicans*, the animals lacking functional PMK-1 signalling (*sek-1* mutant worms) were employed. SEK-1 encodes a mitogen-activated protein kinase kinase, which regulates the phosphorylation, and thus the activation, of PMK-1. For our study temperature-sensitive sterile *C. elegans* mutants lacking a functional PMK-1 pathway *glp-4 sek-1* (Table 2.7) were used to monitor an impact of the immune status of the host on *C. albicans* killing.

Firstly, we conducted the survival assay comparing the survival of the immunocompetent *glp-4* and immunocompromised *glp-4 sek-1* worms upon *C. albicans* infection. As predicted, *C. elegans* mutants lacking SEK-1 were shown to be much more sensitive to *C. albicans*-mediated killing with an average survival of 6 days post infection compare to 10 days in immunocompetent strain (Figure 5.2). These findings confirm the role of PMK-1 in resisting infection (Pukkila-Worley et al., 2011).

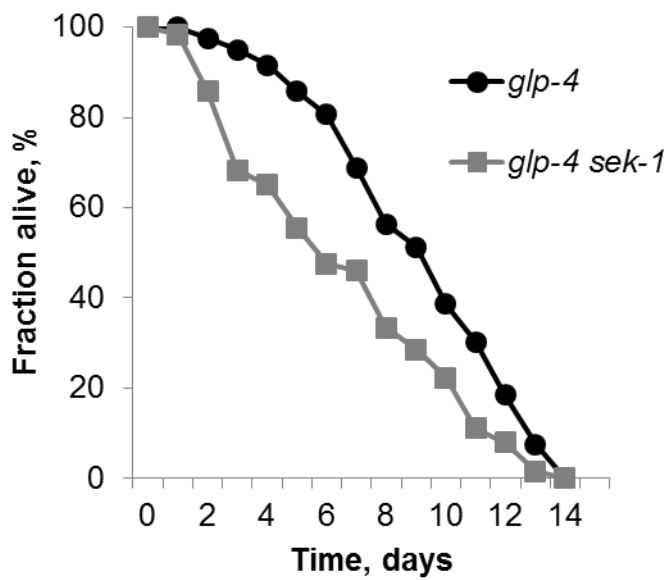


Figure 5.2 Immunocompromised *sek-1* mutants are more susceptible to *C. albicans* killing compare to the immunocompetent nematodes

Survival of immunocompetent *glp-4* (circles) or immunocompromised *glp-4 sek-1* (squares) worms transferred from *E. coli* OP50 to *C. albicans* JC1732 at L4 stage, plotted as fraction of worms alive versus time. 100-150 nematodes were infected with *C. albicans* JC1732 and survival was monitored daily. These data are from a single experiment representative of at least three independent biological replicates.

Secondly, we investigated whether *g/p-4 sek-1* immunocompromised *C. elegans* mutants exhibit age-related increases in susceptibility to *C. albicans*. Indeed, animals lacking SEK-1 showed more rapid killing by *C. albicans* with age, and decreased average lifespan to 3 and 2 days post infection in L4 + 3 and L4 + 6 age groups respectively. (Figure 5.3 A, B).

We compared the survival of immunocompetent and immunocompromised nematodes of different age groups (Figure 5.4). Young L4 animals lacking functional SEK-1 were more sensitive to *C. albicans*-mediated killing than wild-type immunocompetent worms (Figure 5.3 A). This trend was maintained during the infection of the L4+3 mature animals with *sek1* mutants being much less able to survive *C. albicans* infection (Figure 5.4 B). However, in L4+6 old animals the kinetics of *C. albicans*-mediated killing was very similar in both wild-type and *sek1* mutants (Figure 5.4 C). This is consistent with the hypothesis that the age-related reduction in survival seen in wild-type worms may be due to a decline in PMK-1 function. Reported that a pattern of PMK-1 activation display an age-dependant decline: in 5 days old animals (L4+3), PMK-1 signalling is only slightly attenuated, whereas in older animals (8 days, L4+6) the PMK-1 levels decrease tremendously (Youngman et al., 2011).

Taken together, these data show PMK1-dependent responses (as immunocompromised worms killed faster at all time points than wild-type worms) following *C. albicans* infection. In wild-type worms SEK-1 presence promotes resistance to *C. albicans* in young but not old animals. Interestingly, however in the *sek1* mutant animals an age-associated decline in resistance to *C. albicans* infection was observed, as mature immunocompromised adults (L4+3) were killed faster by *C. albicans* compare to young *sek1* mutant animals (L4) (Figure 5.3). This indicates that SEK-1 (PMK-1)-independent mechanisms could also contribute to the phenomenon of immunosenescence (Figure 5.3).

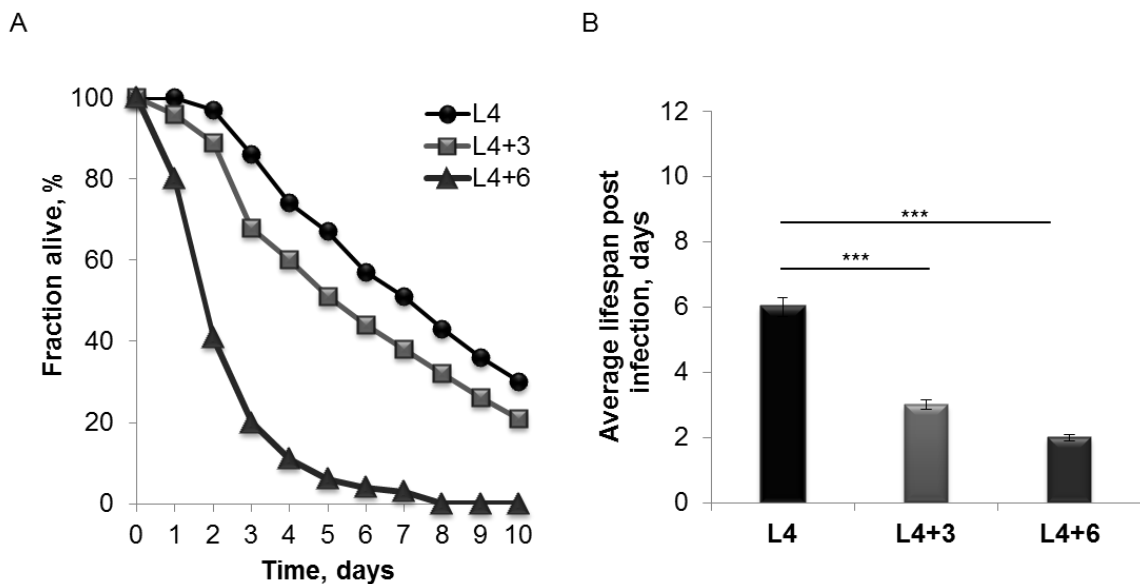


Figure 5.3 The increased susceptibility of *C. elegans sek1* mutants to *C. albicans* infection with age.

(A) Survival of immunocompromised *glp-4 sek-1* *C. elegans* transferred from *E. coli* OP50 to *C. albicans* JC1732 at L4 (circles), and at days 3 and 6 of adulthood (L4+3 and L4+6, squares and triangles respectively), plotted as fraction of worms alive versus time.

(B) Average lifespan of the infected nematodes of different ages. Statistical analysis of *C. elegans* survival obtained from three independent biological replicates represents an average lifespan of different age groups of immunocompromised *glp-4 sek-1* worms upon *C. albicans* infection. Mean values (\pm SD) are shown and t-test was used to determine statistically significant differences in *C. elegans* survival: **, $p<0.01$; ***, $p<0.001$.

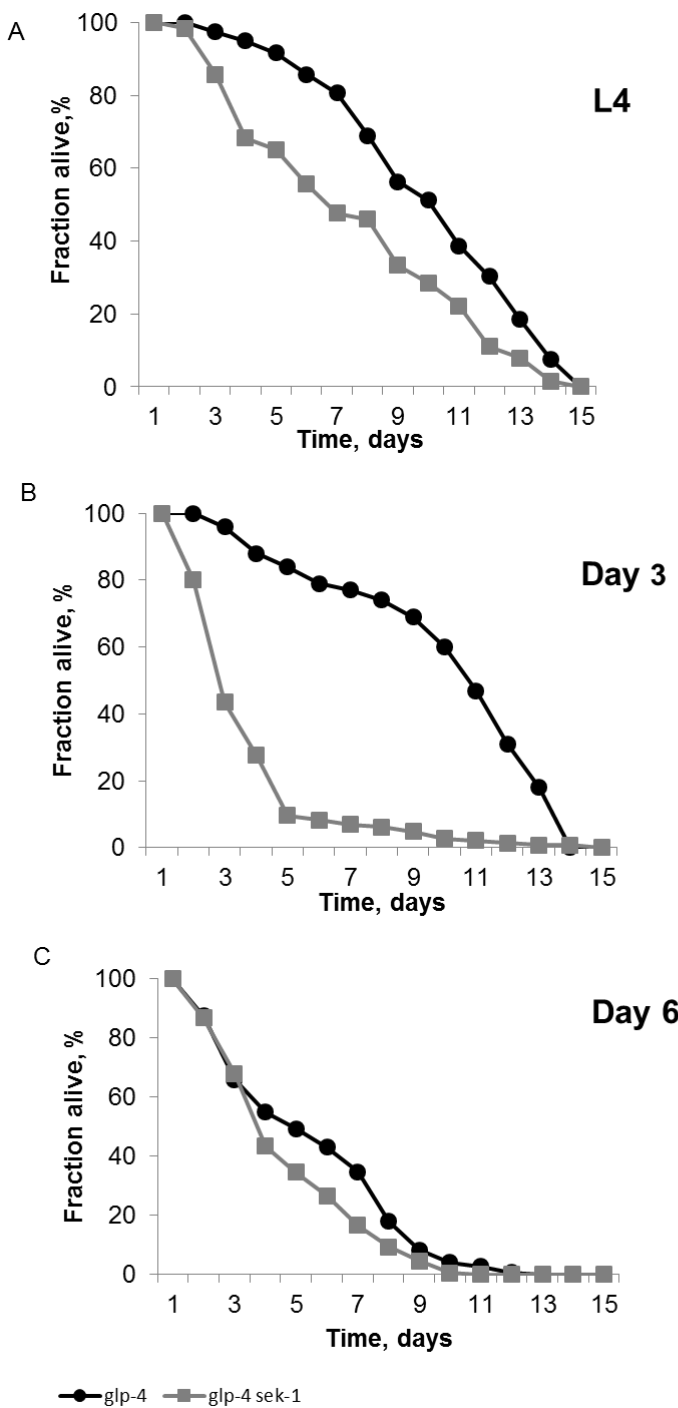


Figure 5.4 Age-associated decline in resistance may be related to impaired p38 (PMK-1) responses in *C. elegans*.

Survival of immunocompetent *glp-4* (circles) and immunocompromised *glp-4 sek-1* (squares) worms transferred from *E. coli* OP50 to *C. albicans* at L4 (A), and at days 3 and 6 of adulthood (B and C respectively), plotted as fraction of worms alive versus time. *C. elegans* infection with *C. albicans* was performed as described in Figure 5.2 legend.

5.2.3 *C. albicans* does not need to mount a *Hog1*-mediated stress response during infection of old nematodes

The above results are consistent with the decline in resistance in old-age animals to infection with *C. albicans* being, to some extent, related to a decline in PMK-1 function. Therefore, if PMK1-mediated innate immune defences are impaired in the elderly host, we hypothesised that *C. albicans* may not need to mount robust stress responses to survive in such hosts when PMK-1 signalling is impaired. To test this, we asked whether the *Hog1* stress-activated protein kinase was needed to promote *C. albicans* virulence in both young and elderly *C. elegans* hosts.

Initially, we examined the impact of *Hog1* loss on *C. albicans* virulence upon infecting young adult worms. The survival of age-synchronised L4 stage young adult (*glp-4*) worms following infection with *C. albicans* strains lacking *HOG1* (*hog1Δ*) as well as with the reconstituted strain (*hog1Δ + HOG1*) was followed. Young L4 worms infected with the *hog1Δ* mutant showed an increase in survival relative to animals infected with the *hog1Δ + HOG1* reconstituted strain (Figure 5.5 A). This showed that, as seen in many other infection models (Prieto et al., 2014, Alonso-Monge et al., 1999, Herrero-de-Dios et al., 2014), *Hog1* is essential for *C. albicans* virulence. These results demonstrate that the absence of *Hog1* has a detectable impact on the virulence potential of *C. albicans* in the worm infection model. Thus *Hog1*, similar to what seen in the murine infection models (Alonso-Monge et al., 1999), is important for *C. albicans* virulence in *C. elegans* model of infection.

Next, the role of *Hog1* in promoting *C. elegans* virulence in mature (L4+3) and elderly (L4+6) worms was examined. As shown in Figure 5.5 B, the role of *Hog1* in promoting *C. albicans* virulence was maintained upon infecting L4+3 stage worms, albeit that the kinetics of survival differed from that seen with L4 worms. Strikingly however, *Hog1* was dispensable for *C. albicans* virulence upon infecting elderly L4+6 adult worms. Similar survival kinetics was observed upon infection with either the *hog1Δ* mutant, or *hog1Δ + HOG1* reconstituted strain (Figure 5.5 C).

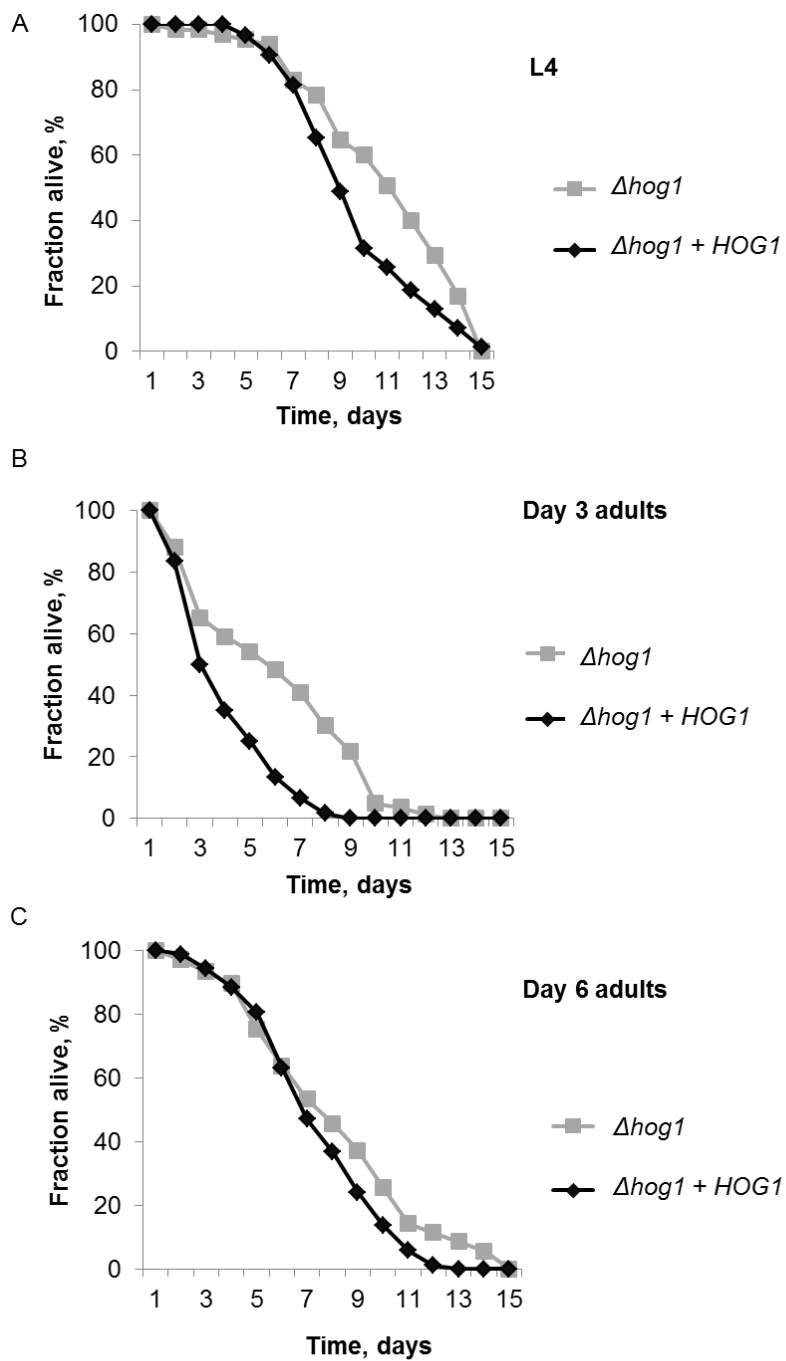


Figure 5.5 *C. albicans* SAPK Hog1 is required for virulence in young, but not old nematodes.

Survival of *glp-4* worms transferred from *E. coli* OP50 to *C. albicans* JC50 (Δhog1) and JC52 ($\Delta\text{hog1} + \text{HOG1}$) at L4 (A), and at Days 3 and 6 of adulthood (B–C, respectively), plotted as a fraction of worms alive versus time.

These findings, therefore, illustrate that whilst Hog1 is required for virulence in young worms, in elderly hosts *C. albicans* *hog1Δ* mutant cells are equally as virulent as wild-type cells. Therefore, Hog1 is required for *C. albicans* virulence in young, but not old nematodes.

Taken together, these preliminary investigations indicate that Hog1 plays an active role in mediating virulence in an invertebrate model of infection and moreover, that Hog1-mediated stress responses of *C. albicans* may only be required for virulence in young, but not elderly hosts.

5.2.4 *C. albicans* colonisation of *C. elegans*

The findings presented above, indicate that *C. elegans* susceptibility to *C. albicans* infection increases with age and that this may be due to a decline in innate immune defences in the host. To rationalise our data, and in order to understand whether aged animals are feeding as well as the young worms when maintained on *C. albicans*, we monitored the colonisation of the worm's intestine with *C. albicans* in worms of different age groups (L4, L4+3 and L4+6 old nematodes). In addition, we also compared the *C. albicans* colonisation of both immunocompetent and immunocompromised animals.

Age-synchronised immunocompetent (*glp-4*) and immunocompromised (*glp-4 sek-1*) animals of the three age groups were infected with *C. albicans* cells expressing GFP, to facilitate the visualisation of *C. albicans* colonisation and to monitor the progression of infection *in vivo*. The nematodes were picked from the experimental plate and mounted onto a 2% agar pad, following by the immobilisation with 0.25 mM levamisole. The colonisation of the worm intestine was captured by fluorescent microscopic imaging. The kinetics of infection was monitored with at least 10 animals scored per time point.

A time course of microscopic evaluation of infection using GFP-labelled *C. albicans* revealed that by 2-4 hours, yeast cells began to accumulate in the pharynx and the intestine of L4 young adult worms (Figure 5.6). At the initial stage of

infection, young adults showed rapid colonisation with *C. albicans*, and most examined animals were infected in pharynx and intestine by 4 hours.

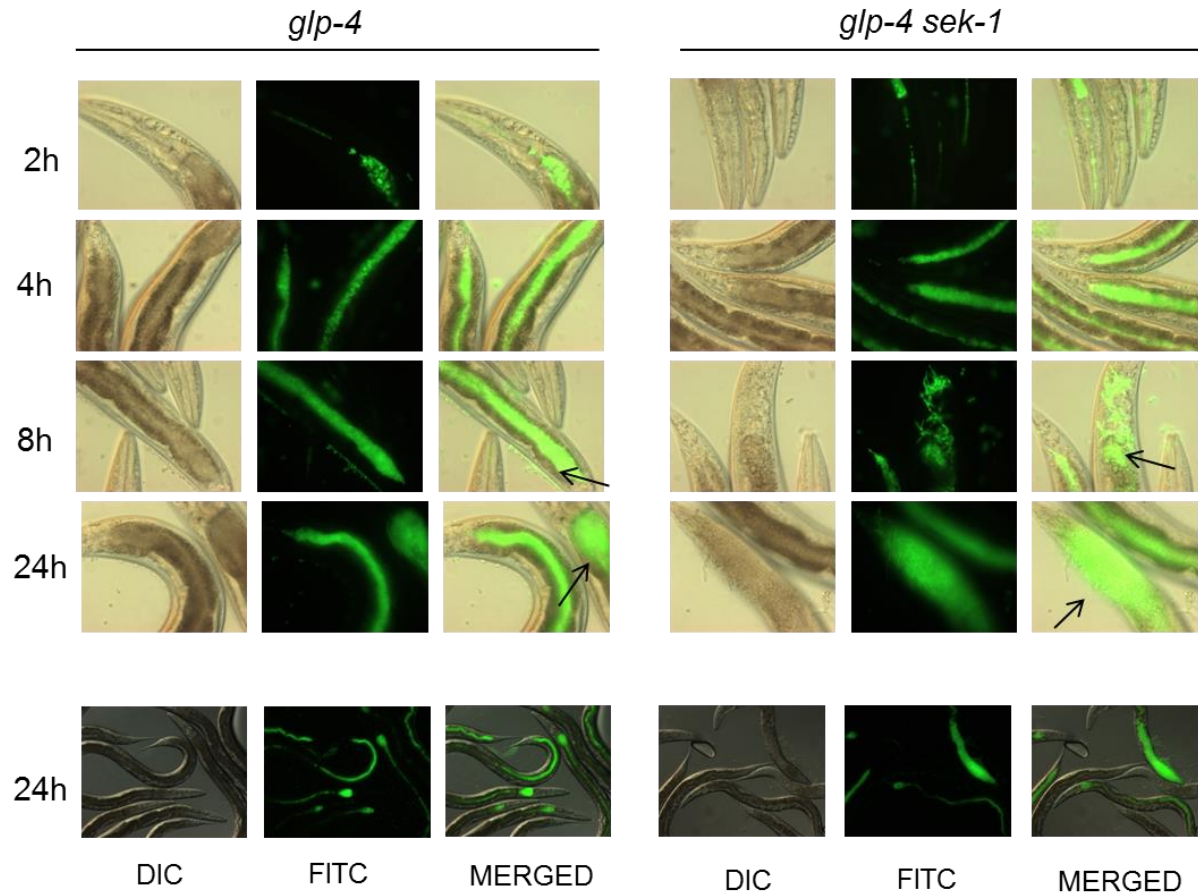


Figure 5.6 Kinetics of *C. albicans* intestinal colonisation of young *C. elegans*.

Glp-4 and *glp-4 sek-1* nematodes at L4 stage were infected with *C. albicans* carrying GFP marker (JC 1732) and the progression of infection was visualised by fluorescence over time. At least 10-15 animals per time point were subjected to fluorescent microscopy. Arrows indicate intestinal distension of the nematodes at 8 and 24 hours in immunocompetent animals (left panel) and *C. albicans* intraintestinal hyphal formation in immunocompromised animals (right panel).

At this stage, no difference was observed in terms of colonisation of young immunocompetent versus immunocompromised animals. By 8 hours, progressively more yeast cells accumulated in the pharynx and intestine, causing the lumen to be severely distended compare to uninfected worms, in which the intestinal lumen appeared as a narrow tube. Following 8 hours post infection *C. albicans* germ tubes were seen, and the DAR formation was observed in some animals. By 12 hours and later, *C. albicans* filamentation was observed in some animals, with protruding of the epithelial tissues by the pathogen and deep-seated invasion. *C. albicans* filamentation is commonly observed in liquid assays (Pukkila-Worley et al., 2009), and is considered as an important virulence determinant of the fungus. In contrast, in solid plate infection assays carried out in this study, only small numbers of animals were scored with *C. albicans* hyphae. Therefore, the main *C. albicans* virulence trait in solid plate assay is considered to be an intestinal distension (DAR phenotype). Interestingly however, most of the animals scored with *C. albicans* in hyphal form were *sek-1* mutants. Further investigations are needed to statistically prove the correlation between *C. albicans* hyphal formation and virulence dependency of the immune status of the host.

There was no or a very little difference between the colonisation of L4 and L4+3 animals: mature adults were as susceptible to *C. albicans* colonisation as L4 young adults, and there was very similar pattern of the progression of infection, with the formation of DAR phenotype and intestinal distention after 8 hours of co-incubation with pathogen in both immunocompetent and immunocompromised groups, as well as sporadic episodes of *C. albicans* hyphal growth in some *sek-1* immunocompromised nematodes (Figure 5.7).

The colonisation of aged adults (L4+6) progressed much slower compare to both L4 and L4+3 animals. These data support previously reported that *C. elegans* pharyngeal pumping declines with age. Nevertheless, *C. albicans* germ tubes were detected at earlier times by 8 hours post infection, with rapid subsequent filamentation in some animals (Figure 5.8).

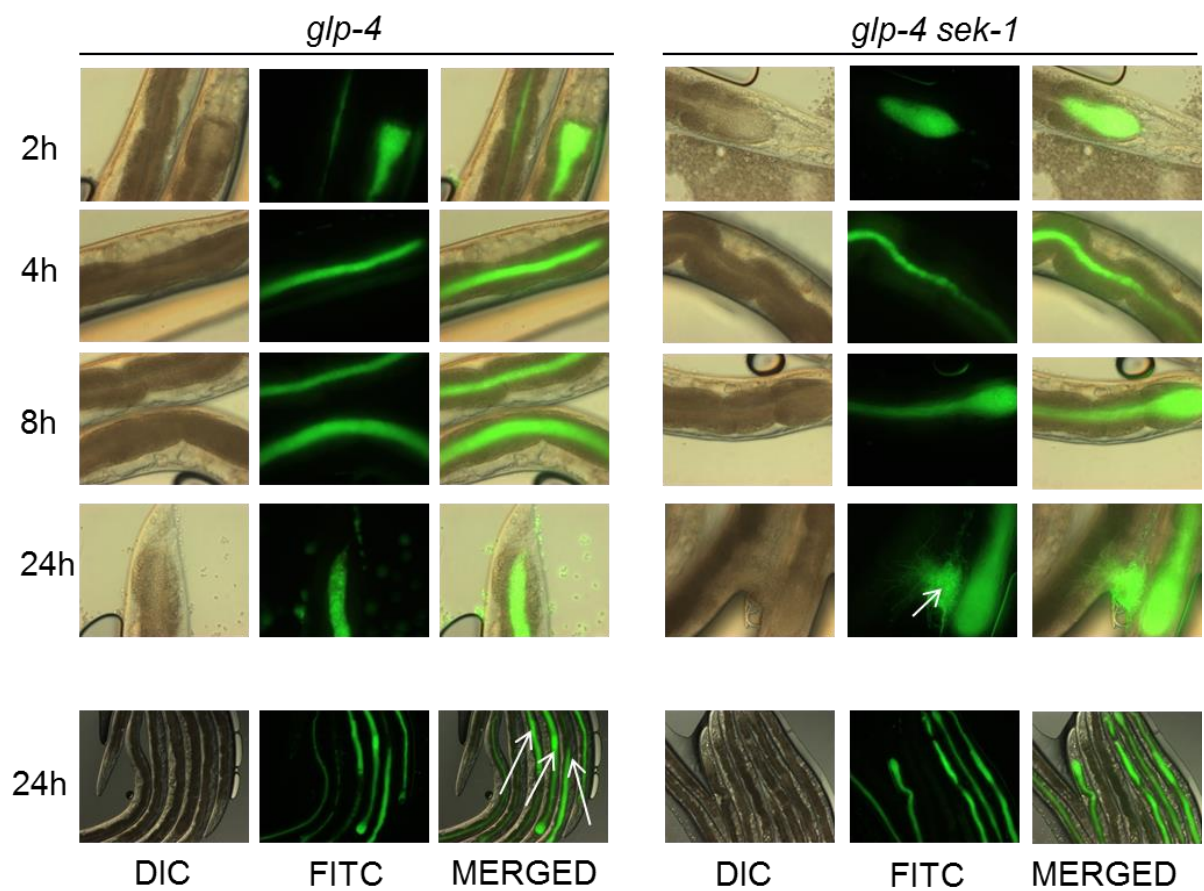


Figure 5.7 Kinetics of *C. albicans* intestinal colonisation of mature *C. elegans*.

L4 + 3 days old nematodes were infected with *C. albicans* carrying GFP marker (JC 1732) and the progression of infection was monitored over time. At least 10-15 animals per time point were subjected to fluorescent microscopy. Arrows indicate intestinal distension of the nematodes at 24 hours in immunocompetent animals (left panel) and *C. albicans* intraintestinal hyphal formation in immunocompromised animals (right panel).

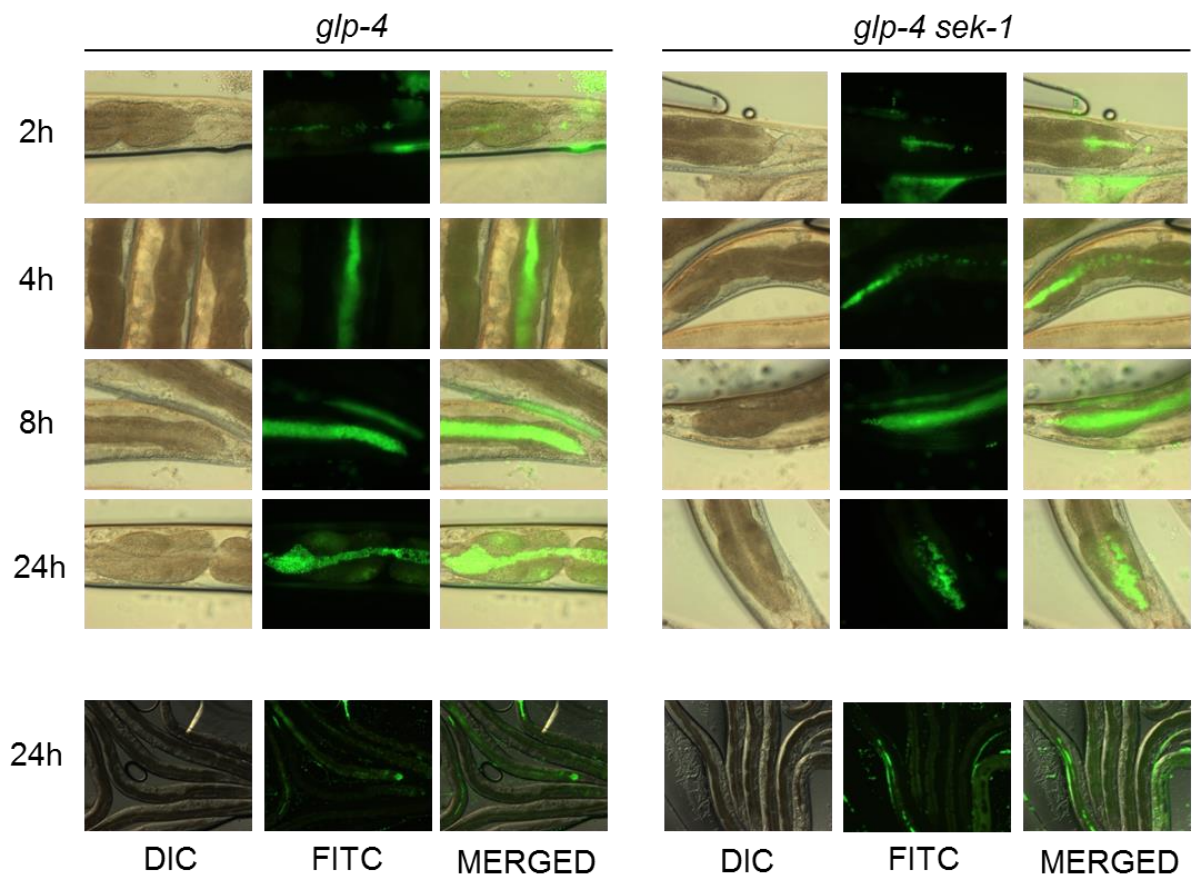


Figure 5.8 Kinetics of *C. albicans* intestinal colonisation of aged *C. elegans*.

L4+ 6 days old nematodes were infected with *C. albicans* carrying GFP marker (JC 1732) and the progression of infection was monitored over time. At least 10-15 animals per time point were subjected to fluorescent microscopy.

Following 24 hours post initiation of infection, some aged nematodes had intestinal distension, and most of them had filamenting fungus, allowing the pathogen to proliferate into deeper tissues. Surprisingly, some L4+6 animals were scored as dead at 24 hours post infection without clear signs of *C. albicans*-mediated intestinal distension.

Regarding the differences in colonisation of the immunocompetent and immunocompromised nematodes, it is worth noticing that although animals lacking SEK-1 did not exhibit more rapid colonisation by *C. albicans* at initial stages, but demonstrated more frequent and rapid worm killing of the infected *sek-1* mutants by *C. albicans* filaments at 24 h with pronounced intestinal distension (shown by arrows).

Taken together, these results indicate that in our model there are differences in susceptibility to colonisation of *C. elegans* by *C. albicans*; however, our findings suggest that there is no obvious correlation between the progression of the pathogenic colonisation and the immune status (age) of the host.

5.3 Discussion

Host innate immunity is a key factor in preventing life-threatening fungal infections. Therefore, immunosuppression of the host and age-related immunosenescence might result in increased susceptibility to pathogens. In this Chapter it was shown that aged *C. elegans* are more susceptible to *C. albicans*-mediated killing than young animals, and this effect is comparable to the increased susceptibility to fungal infections of immunocompromised nematodes compare to the immunocompetent animals (Figures 5.1 and 5.2). *C. elegans* *glp-4* *sek-1* mutants are hyper-susceptible to killing following infection with *C. albicans* yeast, supporting the observation that functional PMK-1 signalling is required for the basal and pathogen-induced expression of antifungal immune effectors (Pukkila-Worley et al., 2011). Similarly, we show that a decline in PMK-1 activity in elderly worms may underlie the increased susceptibility to *C. albicans* infection. Published data suggest that *C. elegans* mount a response to *C. albicans* infection at the level of transcription, and

this response vary for different bacterial and fungal species (Pukkila-Worley et al., 2011). Thus, fungal stress response regulators and ageing potentially can counteract the p38-mediated defences of the host.

Taking together all of the above statements, we hypothesised that the fungal stress regulators, such as Hog1, would be dispensable for virulence in the elderly worms due to a decline in PMK-1 activity in the host. In this study *C. albicans* *hog1Δ* mutant strain clearly demonstrated its reduced virulence in the *C. elegans* infection model. However, the stress regulator Hog1 is only required for the infection of young, but not elderly nematodes.

PMK-1 pathway is also sensitive to starvation, and there is a possibility that *C. albicans* as a food source is unable to provide enough nutrients for the nematode. However, it is very unlikely that *C. elegans* response to the pathogen is due to starvation. We and other teams (Jain et al., 2009) reported that the appearance of the DAR phenotype, that is an early marker of the nematode's infection, was detected when the ample food was present. In addition, heat-inactivated yeasts are avirulent and unable to evoke DAR phenotype, which strongly supports the hypothesis that the progression of infection is a response to the pathogenic species, rather than an outcome of starvation (Jain et al., 2009, Pukkila-Worley et al., 2011). Our data presented in this Chapter indicate the lower uptake of *C. albicans* in elderly worms, but it seemingly that malnutrition in aged animals does not contribute to the enhanced killing.

There is evidence that in liquid culture *C. albicans* filamentation is a virulence determinant in the *C. elegans* infection model (Pukkila-Worley et al., 2009). However, in our experiments we did not observe the correlation between fungal filamentation and nematode killing. Our observations support recent findings that *C. albicans* in its yeast morphology is pathogenic for *C. elegans*: the accumulation of fungal cells causes distention of the nematode intestine and premature death of the worms (Pukkila-Worley et al., 2011). Important observations regarding *C. albicans* colonisation of the nematode's intestine are also that the rate of fungal accumulation within the intestine seemingly does not increase with age, in contrast to what was reported for *P. aeruginosa* age-dependent increase in *C. elegans* intestinal

accumulation (Youngman et al., 2011). Previously other researchers were looking at colonisation of wild-type *C. elegans* intestine with *C. albicans* cells (Pukkila-Worley et al., 2011, Jain et al., 2013), and in our work we use for the first time *C. elegans* mutant strain lacking functional PMK-1 pathway and compare the colonisation rate to the wild-type strain in different age groups. Colonisation experiments allowed us to make an observation that the impairment of PMK-1 signalling (*sek-1* mutation) seemingly does not contribute to *C. albicans* ability to colonise nematode's intestine.

We carried out infection assays in order to understand the nature of the age-associated decline in fungal resistance. In this work we used *C. elegans* infection model, and confirmed the role of PMK-1 signalling for host potency of combatting fungal infection. It would be interesting also to determine whether such age-associated declines in p38 function are seen in other systems, such as epithelial cells or macrophages. If tissue-specific declination of the p38 pathways exists, it would be interesting to determine whether the inhibition of this signalling pathway would impact on the ability of innate immune cells to kill pathogenic *Candida* species, and impact of *C. albicans* virulence determinants in those systems.

This study supports the paradigm that fungal stress responses are less important for the infection of an elderly or immunocompromised host. Similar findings of the host's immune status dependency of fungal virulence determinants were reported for *A. fumigatus* in a murine model of systemic aspergillosis, where key stress-responsive transcriptional factor Afyap1, as well as AfSODs, were dispensable for fungal virulence in immunocompromised host (Qiao et al., 2008, Lambou et al., 2010). The current work only touches of the complexity of host-pathogen interactions and provides new insights into how the successful pathogen, such as *C. albicans*, can establish an infection in the susceptible host.

Chapter 6. Final Discussion

6.1 Summary

The overall aim of this PhD project was to investigate the potency of immune cells-derived stresses in fungal killing, and an assessment of whether robust stress responses are needed for fungal virulence if such immune defences are compromised.

Previous work from the Brown laboratory (Aberdeen) indicated that in order to combat *Candida* spp. infection, immune cells need to generate both ROS and cationic fluxes. The combination of oxidative and cationic stresses *in vitro* kills pathogenic fungi much more effectively than the corresponding single stresses (Kaloriti et al., 2012). Furthermore, both cationic fluxes and the NADPH oxidase-mediated generation of ROS are vital for effective neutrophil-mediated killing of *C. albicans* (Kaloriti et al., 2014). This is largely attributed to combinatorial stress-mediated inactivation of the major regulator of antioxidant gene expression in *C. albicans*, Cap1 (Kaloriti et al., 2014). However, *C. glabrata* can survive, and actually multiply within the phagosome (Kasper et al., 2015), and this may be due to the function of the *CRI* genes which confer resistance to combinatorial cationic and oxidative stress. A major aim of this thesis was to dissect the mechanism of Cap1 inactivation following combinatorial oxidative and cationic stress, and to investigate the mechanisms of *CRI*-mediated combinatorial stress resistance in *C. glabrata*.

As highlighted above, robust immune-based defence mechanisms operate to prevent systemic *Candida* infections. Consequently, *Candida* spp. in general cause fatal systemic infections only in susceptible hosts, when immune defences are diminished (section 1.2). These include immunocompromised hosts and also in the elderly due to the phenomenon of immunosenescence. Thus, as immune defences are weakened, we reasoned that robust fungal stress responses may be dispensable for virulence in such hosts. To investigate this, a *C. elegans* model of infection was employed to dissect the requirements of *C. albicans* stress regulators in promoting fungal virulence in both immunocompromised and elderly hosts.

6.2 Inhibition of Cap1-dependant oxidative stress response – a major antifungal defence mechanism?

The first aim addressed in this work was to delineate the mechanisms of Cap1 inactivation following combinatorial stress in *C. albicans*. This thesis highlights that combinatorial stress imposed *in vitro* drives the generation of extremely high levels of ROS inside fungal cells, as observed using ROS-sensitive fluorescent probes and FACS analysis (Figures 3.18 and 3.19). This is likely to underlie the extreme potency of the combinatorial oxidative and cationic stress in *C. albicans* killing.

Upon oxidative stress treatment with moderate H₂O₂ concentrations, the formation of multiple disulfides within Cap1 masks the nuclear export sequence in the protein, preventing its interaction with the nuclear export factor Crm1, and thus leading to the nuclear accumulation of the transcription factor (Zhang et al., 2000, da Silva Dantas et al., 2010). Nuclear Cap1^{OX} is phosphorylated and binds to Cap1-dependent gene targets. Consequently, the induction of the antioxidant-encoding genes aids the fungus to survive the oxidative burst generated by phagocytes (Figure 6.1 A).

In contrast, high ROS levels (25 mM H₂O₂) promote the generation of an inactive differentially oxidised Cap1^{OX-1} form, and this is also seen following the treatment of *C. albicans* cells with combinatorial oxidative and cationic stress (5 mM H₂O₂ + 1 M NaCl). Specifically, this differentially oxidised form comprises of multiple less oxidised intermediates, which contain less disulphides (Figure 4.5). Analysis of Cap1 oxidation kinetics revealed that this Cap1^{OX-1} form is most likely a transient inactive intermediate of active Cap1^{OX} (Figure 3.5). Although Cap1^{OX-1} generated post high H₂O₂ treatment is nuclear (Figure 4.1) and binds to the promoters of Cap1 targets (Figure 4.9), the phosphorylation of Cap1^{OX-1} is impaired (Figure 4.2). In addition, there is a significant delay in the induction of Cap1-dependent genes (Figure 4.3), ultimately leading to the cell death (Figure 6.1 B). In contrast to Cap1^{OX-1} generated post high ROS, combinatorial stress-induced Cap1^{OX-1} does not accumulate in the nucleus. This is due to cations promoting the interaction between Cap1 and the Crm1 nuclear export factor (Figure 3.8), thus preventing nuclear accumulation.

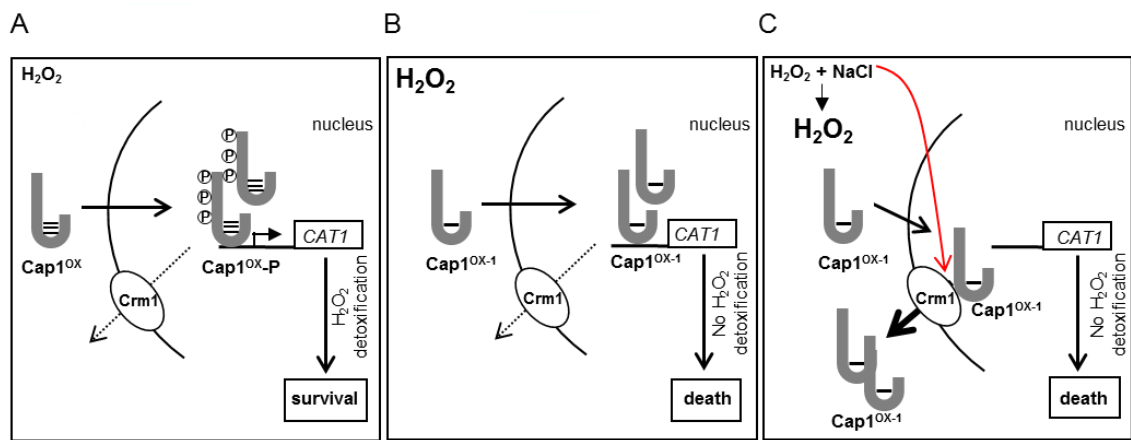


Figure 6.1 Impact of combinatorial stress and high H_2O_2 levels on *Cap1* activation.

(A) When *C. albicans* cells are exposed to medium (5 mM) levels of H_2O_2 , a *Cap1^{OX}* form containing multiple disulfides is swiftly generated, followed by the rapid accumulation of *Cap1* in the nucleus, where it is phosphorylated. The ensuing efficient induction of *Cap1*-dependent antioxidant genes follows, leading to stress adaptation and survival. (B) When *C. albicans* cells are exposed to high (25 mM) levels of H_2O_2 , a *Cap1^{OX-1}* form containing less disulfides is prevalent, and although this rapidly accumulates in the nucleus and binds to target genes, *Cap1* is not phosphorylated, and the induction of *Cap1*-dependent genes is significantly impaired, resulting in cell death. (C) Exposure of *C. albicans* to medium (5 mM) levels of H_2O_2 in the presence of NaCl triggers high intracellular ROS accumulation. This also results in the formation of *Cap1^{OX-1}*. However, an additional inhibitory mechanism is seen as *Cap1* fails to accumulate in the nucleus due to a cationic stress-mediated stabilization of the interaction between *Cap1* and the *Crm1* export factor. Consequently, the induction of *Cap1* target genes is prevented, leading to cell death.

Consequently, and as seen following high H_2O_2 concentrations, $\text{Cap1}^{\text{OX-1}}$ is unable to initiate antioxidant gene expression, leading to the pathogen's death (Figure 6.1C). The efficacy of combinatorial stress-mediated killing of *Candida* spp. may explain why these fungi only cause systemic infections in immunocompromised hosts. In healthy hosts, the failure of the pathogen to respond rapidly to high intracellular ROS levels likely results in the activation of cell death programs (Phillips et al., 2003), ultimately leading to *C. albicans* killing.

It is noteworthy that combination of oxidative and cationic stresses synergistically kills many fungal species (Kaloriti et al., 2012). In addition, AP-1 like transcription factors are conserved in fungi, such as Yap1 in *S. cerevisiae*, Cgap1 in *C. glabrata*, and Cap1 in *C. albicans*. Hence, similar mechanisms of combinatorial stress-mediated inhibition of fungal AP-1 like oxidative stress-responsive transcription factors might operate in a variety of pathogenic and non-pathogenic fungi. Moreover, the mechanism of stress pathway interference might be relevant to plant kingdom, as there are evidences that salt stress induces ROS accumulation in plant roots (Panda and Upadhyay, 2004, Tsai et al., 2004).

The outstanding question is why does combinatorial oxidative and cationic stress induce high intracellular ROS levels? This could be due to the cationic stress-mediated direct inhibition of catalase activity, preventing efficient H_2O_2 clearance (Kaloriti et al., 2014), and the impact of cationic stress on inhibiting the oxidative stress-mediated induction of the *CAT1* gene via Cap1 inactivation (Kos et al., 2016). Indeed, ectopic expression of *CAT1* from the Cap1-independent *ACT1* promoter reduced intracellular ROS levels and suppressed the synergistic killing of *C. albicans* cells by combinatorial oxidative and cationic stress. Another hypothesis is that cationic stress might impact on fungal cell wall permeability to ROS, resulting in elevated intracellular ROS levels. Evidence in support of this assumption is documented in fungal pathogen *C. neoformans*, where the redundant role of two cation transporters, Ena1 and Nha1, was shown to impact on pH homeostasis, membrane potential and drug resistance of this fungus; Ena1 was also shown to be essential for *C. neoformans* virulence (Jung et al., 2012). In addition, recent report indicate that high concentrations of cations suppress sensitivity of *S. pombe* to

various drugs (Alao et al., 2015). Similarly, cationic stress could impact on *C. albicans* membrane permeability to ROS following phagocytosis, resulting in the synergistic killing of the fungus.

A further question is why does cationic stress promote the Cap1-Crm1 interaction? This enhanced interaction with the Crm1 nuclear exporter in the presence of cations is seemingly specific to Cap1. For instance, the Hog1 SAPK, which is regulated by Crm1-dependent nuclear localisation, rapidly accumulates in the nucleus in response to combinatorial oxidative and cationic stress (Kalariti et al., 2014). Does perhaps cationic stress promote novel post-translational modifications on Crm1 and/or Cap1 that drives structural changes? Such possibilities could be addressed by mass-spectroscopy analysis of purified Crm1 and Cap1 proteins post-cationic stress to identify any such post-translational modifications. In addition, the structure of the Cap1-Crm1 complex would help decipher how such cation-induced modifications could promote interaction.

In conclusion, the data presented in this Chapter provide new insights into understanding the mechanisms behind combinatorial oxidative and cationic stress-mediated delay of Cap1 activation, which is due to (i) the generation of an intermediate Cap1^{OX-1} form, which fails to induce target antioxidant-encoding genes, and (ii) an increased interaction of Cap1 with the Crm1 exporter in the presence of cations, that leads to the impairment of the oxidative stress-induced nuclear accumulation of Cap1. We suggest that these findings on combinatorial stress-induced stress pathway interference contribute to the potency of phagocytic immune cells to combat fungal infections.

6.3 *C. glabrata* CRI genes as a novel mechanism of combinatorial stress resistance

To broad our knowledge of the mechanisms employed by pathogenic *Candida* spp. to withstand the stresses encountered following phagocytosis, we directed our attention to *C. glabrata*, a medically important fungus, which is highly stress resistant. *C. glabrata* possesses four unique uncharacterised ORFs within its genome (CRI1-

4), which are essential to counteract combinatorial oxidative and cationic stress *in vitro*, and thus may facilitate the proliferation of this fungus in immunocompetent macrophages. *C. glabrata* Δ *cri1* mutants are completely sensitive to combinatorial stress, whereas *CRI1* over-expression results in increased combinatorial stress tolerance (Figure 3.20). This data clearly demonstrates a role for *CRI1* in mediating *C. glabrata* combinatorial stress resistance. *CRI1* is not induced by combinatorial stress, and the *CRI* genes are, in general, not stress-responsive at the mRNA level (K. Haynes and J. Usher, unpublished). Thus, such genes are seemingly not susceptible to combinatorial stress-mediated stress pathway interference which would, as with Cap1-dependent targets, inhibit their induction. Hence, it is predicted that the basal level of *CRI1* expression provides initial protection against combinatorial stress, allowing the fungus to adapt its gene expression programme following phagocytosis by macrophages or neutrophils (Rai et al., 2012, Fukuda et al., 2013). In this thesis, data is presented which illustrates that *CRI1*, which tremendously impacts on *C. glabrata* survival upon combinatorial stress, does not function by preventing the combinatorial stress-induced increase in intracellular ROS levels in this fungus (Figure 3.21). Future research would aim to define the mechanism by which Cri1 promotes combinatorial stress tolerance, and to investigate the roles that the other CRIs play in combinatorial stress resistance. Answering these questions will facilitate further mechanistic understanding of host – *C. glabrata* interactions.

In this work we show that heterologous expression of *CgCRI1-4* in *C. albicans* failed to confer combinatorial stress resistance (Figure 3.22), and this contrasts with analogous experiments using *S. cerevisiae*, where the expression of the *CRI* genes led to considerably enhanced levels of resistance (J. Usher, unpublished). Although it remains to be validated that the *CRI* genes were successfully expressed *in C. albicans*, the data presented suggest that the mechanisms encompassing *CRI*-mediated stress protection is restricted to *C. glabrata* and closely related fungi, such as *S. cerevisiae*.

6.4 *C. elegans* age-dependant susceptibility to *C. albicans* infection

As highlighted throughout this thesis, *Candida* spp. are a serious threat only in susceptible hosts, when immune responses are compromised. In this work, a *C. elegans* infection model was employed to investigate links between age and the immune status of the host, and whether the immune status of the host dictated the importance of fungal stress responses in promoting virulence.

This work for the first time shows that there is an age-dependent increase in susceptibility to *C. albicans*-mediated killing, as aged nematodes were significantly more susceptible to *C. albicans*-mediated killing than young animals (Figure 5.1). In addition, using immunocompromised worms (which contain a mutation in the SEK-1 MAPKK, that regulates the PMK-1 SAPK necessary for innate immune defences), we could demonstrate that young immunocompetent worms are better to resist *C. albicans* infection than young immunocompromised (*sek-1* mutant) worms. However, aged immunocompetent and immunocompromised animals displayed similar levels of susceptibility to *C. albicans* infection. This suggests that the age-associated decline in *C. albicans* resistance in *C. elegans* may be due to a decline in immune function. Indeed, PMK-1-mediated innate defences are compromised in elderly worms (Youngman et al., 2011). However, the increased susceptibility with age in *sek-1* nematodes to *C. albicans* infection indicates that other, PMK-1-independent mechanisms of stress-protection, may exist. For instance, the G protein-coupled receptor FSHR-1 was shown to be essential for *C. elegans* innate immune response against bacterial pathogens, and is suggested to act in parallel with PMK-1-dependant mechanisms to regulate the transcriptional induction of antimicrobial effectors (Powell et al., 2009). Also the potential role of the insulin-like DAF-2 signalling pathway could be considered, as this pathway has been implicated in both ageing and susceptibility to pathogens (Evans et al., 2008b, Evans et al., 2008a).

The study on *C. elegans* highlights the role of innate immunity in response to the pathogens (Irazoqui and Ausubel, 2010). Further research into the generality of the mechanisms underlying the age-associated increases in susceptibility to pathogens to mammalian host would be an important area to be tackled. To date, little is known whether the signalling mechanisms underlying host-pathogen interactions are

impaired in human elderly hosts. It is suggested that numbers of phagocytes remain negligibly affected by age, although phagocytic capacity and some important phagocytic functions, such as ROS production, are compromised (Lord et al., 2001, Gomez et al., 2005). Investigations into the cellular responses of mammalian epithelial cells to *C. albicans* have implicated a critical role of the p38 SAPK (Moyes et al., 2010). It would be of high interest to model such experiments in mammalian aged cells to investigate whether the function of p38 MAPK and other important stress regulators is affected by ageing, and whether signalling regulators impact on the susceptibility to fungal infections. This could be modelled in different systems; for example, using neutrophils from elderly patients, or aged macrophages, or using pharmacological inhibitors of p38 signalling. Reported that elevated levels of pro-inflammatory cytokines in aged macrophages impact on their function and promote the increases of susceptibility to infections (Linton and Thoman, 2014). Consequently, pharmacological inhibitors that block p38 signalling might provide new insights into our understanding of the modulatory therapies necessary to restore immunocompetence in the immunodeficient (elderly) host.

Current research demonstrated that *C. albicans* might not need to mount a robust stress response to cause disease when colonising an elderly host (Figure 5.5). *C. albicans* strains lacking the Hog1 SAPK were avirulent in young immunocompetent animals, but were as virulent as wild-type cells in killing old and immunocompromised nematodes. These findings indicate that *C. albicans* does not require the same armoury of the virulence determinants to cause lethal infections in immunosuppressed and elderly worms. The data presented are in line with previously reported data for *Staphylococcus* spp. infection of *C. elegans*, where bacterial virulence determinants were shown to impact on infectiousness only in immunocompetent, but not immunocompromised nematodes (Begin et al., 2007). Future experiments might address the identification of the target pathogenic attributes that are the most important in infection of immunocompromised and aged animals.

One should note that despite all the benefits of invertebrate models of infection, such as *C. elegans*, we question how many features of *C. elegans* innate immunity

will apply to mammalian host, and what signalling pathways underlying the susceptibility to pathogens are conserved, and to what extent, between invertebrate models, such as nematode, and *Homo sapiens*.

6.5 Concluding remarks

Host niches are complex and dynamic. *Candida* species are highly successful pathogens in susceptible hosts due to their ability to adapt to rapidly changing microenvironments within the host. Synergistic killing by the combination of the oxidative and cationic stresses is a relatively new phenomenon in the stress-signalling field. This contrasts starkly with “stress cross protection”, where the exposure of fungal cells to one kind of stress results in higher tolerance to the subsequent exposure to a different stress (Gonzalez-Parraga et al., 2010).

In addition to ROS and cationic fluxes, there are many other stresses encountered by pathogenic fungi following phagocytosis, such as RNS, RCS, pH fluctuations, variations of temperature, nutrient deprivation and antimicrobial peptides (Miramon et al., 2013). Therefore, it is possible that different mechanisms of synergy between the phagocytic insults take place. For instance, *C. albicans* cells are more sensitive to ROS when simultaneously exposed to an acidic pH environment (Prof. J. Quinn, unpublished), and the combinatorial oxidative and nitrosative stress significantly extends the lag phase of growth in both *C. albicans* and *C. glabrata* *in vitro* (Kalogeriti et al., 2012), which is indicative that fungal pathogens require longer periods to adapt to the combination of stresses before the active growth can be resumed. Additionally, nutrient availability and carbon source drastically influence *C. albicans* stress resistance (Ene et al., 2013), and might also affect combinatorial stress outputs in this fungus. Further substantial research will be directed at understanding an impact of other combinations of physiologically relevant stresses and phagosomal microenvironmental cues on *C. albicans* killing, and the complex nature of fungal signaling in response to multiple stresses and conditions encountered within the host. This research area is relatively new, unexplored and

exciting, and furthering our knowledge of the mechanisms of combinatorial stress responses will facilitate our understanding of the battle between pathogen and host.

Chapter 7. References

ABAITUA, F., REMENTERÍA, A., SAN MILLAN, R., EGUZKIZA, A., RODRIGUEZ, J. A., PONTÓN, J. & SEVILLA, M. J. 1999. In vitro survival and germination of *Candida albicans* in the presence of nitrogen compounds. *Microbiology*, 145 (Pt 7), 1641-7.

ABALLAY, A., DRENKARD, E., HILBUN, L. R. & AUSUBEL, F. M. 2003. *Caenorhabditis elegans* innate immune response triggered by *Salmonella enterica* requires intact LPS and is mediated by a MAPK signaling pathway. *Curr Biol*, 13, 47-52.

ALAO, J. P., WEBER, A. M., SHABRO, A. & SUNNERHAGEN, P. 2015. Suppression of sensitivity to drugs and antibiotics by high external cation concentrations in fission yeast. *PLoS One*, 10, e0119297.

ALARCO, A. M., BALAN, I., TALIBI, D., MAINVILLE, N. & RAYMOND, M. 1997. AP1-mediated multidrug resistance in *Saccharomyces cerevisiae* requires FLR1 encoding a transporter of the major facilitator superfamily. *J Biol Chem*, 272, 19304-13.

ALARCO, A. M. & RAYMOND, M. 1999. The bZip transcription factor Cap1p is involved in multidrug resistance and oxidative stress response in *Candida albicans*. *J Bacteriol*, 181, 700-8.

ALONSO-MONGE, R., CARVAIHLLO, S., NOMBELA, C., RIAL, E. & PLA, J. 2009. The Hog1 MAP kinase controls respiratory metabolism in the fungal pathogen *Candida albicans*. *Microbiology*, 155, 413-23.

ALONSO-MONGE, R., NAVARRO-GARCIA, F., MOLERO, G., DIEZ-OREJAS, R., GUSTIN, M., PLA, J., SANCHEZ, M. & NOMBELA, C. 1999. Role of the mitogen-activated protein kinase Hog1p in morphogenesis and virulence of *Candida albicans*. *J Bacteriol*, 181, 3058-68.

ALONSO-MONGE, R., NAVARRO-GARCIA, F., ROMAN, E., NEGREDO, A. I., EISMAN, B., NOMBELA, C. & PLA, J. 2003. The Hog1 mitogen-activated protein kinase is essential in the oxidative stress response and chlamydospore formation in *Candida albicans*. *Eukaryot Cell*, 2, 351-61.

ALVAREZ-PERAL, F. J., ZARAGOZA, O., PEDRENO, Y. & ARGÜELLES, J. C. 2002. Protective role of trehalose during severe oxidative stress caused by hydrogen peroxide and the adaptive oxidative stress response in *Candida albicans*. *Microbiology*, 148, 2599-606.

AMOUTZIAS, G. D., BORNBERG-BAUER, E., OLIVER, S. G. & ROBERTSON, D. L. 2006. Reduction/oxidation-phosphorylation control of DNA binding in the bZIP dimerization network. *BMC Genomics*, 7, 107.

ANASTASSOPOULOU, C. G., FUCHS, B. B. & MYLONAKIS, E. 2011. *Caenorhabditis elegans*-based model systems for antifungal drug discovery. *Curr Pharm Des*, 17, 1225-33.

ANDREWS, T. & SULLIVAN, K. E. 2003. Infections in patients with inherited defects in phagocytic function. *Clin Microbiol Rev*, 16, 597-621.

ANDRÉS, M. T., VIEJO-DÍAZ, M. & FIERRO, J. F. 2008. Human lactoferrin induces apoptosis-like cell death in *Candida albicans*: critical role of K⁺-channel-mediated K⁺ efflux. *Antimicrob Agents Chemother*, 52, 4081-8.

AOKI, W., UEDA, T., TATSUKAMI, Y., KITAHARA, N., MORISAKA, H., KURODA, K. & UEDA, M. 2013. Time-course proteomic profile of *Candida albicans* during adaptation to a fetal serum. *Pathog Dis*, 67, 67-75.

ARANA, D. M., ALONSO-MONGE, R., DU, C., CALDERONE, R. & PLA, J. 2007. Differential susceptibility of mitogen-activated protein kinase pathway mutants to oxidative-mediated killing by phagocytes in the fungal pathogen *Candida albicans*. *Cell Microbiol*, 9, 1647-59.

ARANA, D. M., NOMBELA, C., ALONSO-MONGE, R. & PLA, J. 2005. The Pbs2 MAP kinase kinase is essential for the oxidative-stress response in the fungal pathogen *Candida albicans*. *Microbiology*, 151, 1033-49.

ARVANITIS, M., GLAVIS-BLOOM, J. & MYLONAKIS, E. 2013. *C. elegans* for anti-infective discovery. *Curr Opin Pharmacol*, 13, 769-74.

AYER, A., TAN, S. X., GRANT, C. M., MEYER, A. J., DAWES, I. W. & PERRONE, G. G. 2010. The critical role of glutathione in maintenance of the mitochondrial genome. *Free Radic Biol Med*, 49, 1956-68.

AYYADEVARA, S., BALASUBRAMANIAM, M., PARCON, P. A., BARGER, S. W., GRIFFIN, W. S., ALLA, R., TACKETT, A. J., MACKINTOSH, S. G., PETRICOIN, E., ZHOU, W. & SHMOOKLER REIS, R. J. 2016. Proteins that mediate protein aggregation and cytotoxicity distinguish Alzheimer's hippocampus from normal controls. *Aging Cell*, 15, 924-39.

BABIOR, B. M. 1999. NADPH oxidase: an update. *Blood*, 93, 1464-76.

BAIN, J. M., LEWIS, L. E., OKAI, B., QUINN, J., GOW, N. A. & ERWIG, L. P. 2012. Non-lytic expulsion/exocytosis of *Candida albicans* from macrophages. *Fungal Genet Biol*, 49, 677-8.

BAIN, J. M., LOUW, J., LEWIS, L. E., OKAI, B., WALLS, C. A., BALLOU, E. R., WALKER, L. A., REID, D., MUNRO, C. A., BROWN, A. J., BROWN, G. D., GOW, N. A. & ERWIG, L. P. 2014. *Candida albicans* hypha formation and mannan masking of β -glucan inhibit macrophage phagosome maturation. *MBio*, 5, e01874.

BAKER, S. P. & GRANT, P. A. 2007. The SAGA continues: expanding the cellular role of a transcriptional co-activator complex. *Oncogene*, 26, 5329-40.

BALLA, K. M. & TROEMEL, E. R. 2013. *Caenorhabditis elegans* as a model for intracellular pathogen infection. *Cell Microbiol*, 15, 1313-22.

BARELLE, C. J., MANSON, C. L., MACCALLUM, D. M., ODDS, F. C., GOW, N. A. & BROWN, A. J. 2004. GFP as a quantitative reporter of gene regulation in *Candida albicans*. *Yeast*, 21, 333-40.

BARELLE, C. J., PRIEST, C. L., MACCALLUM, D. M., GOW, N. A., ODDS, F. C. & BROWN, A. J. 2006. Niche-specific regulation of central metabolic pathways in a fungal pathogen. *Cell Microbiol*, 8, 961-71.

BEANAN, M. J. & STROME, S. 1992. Characterization of a germ-line proliferation mutation in *C. elegans*. *Development*, 116, 755-66.

BEDARD, K. & KRAUSE, K. H. 2007. The NOX family of ROS-generating NADPH oxidases: physiology and pathophysiology. *Physiol Rev*, 87, 245-313.

BEGUN, J., GAIANI, J. M., ROHDE, H., MACK, D., CALDERWOOD, S. B., AUSUBEL, F. M. & SIFRI, C. D. 2007. Staphylococcal biofilm exopolysaccharide protects against *Caenorhabditis elegans* immune defenses. *PLoS Pathog*, 3, e57.

BELLON, S., FITZGIBBON, M. J., FOX, T., HSIAO, H. M. & WILSON, K. P. 1999. The structure of phosphorylated p38gamma is monomeric and reveals a conserved activation-loop conformation. *Structure*, 7, 1057-65.

BENNETT, R. J. & JOHNSON, A. D. 2006. The role of nutrient regulation and the Gpa2 protein in the mating pheromone response of *C. albicans*. *Mol Microbiol*, 62, 100-19.

BERTHIAUME, M., BOUFAIED, N., MOISAN, A. & GAUDREAU, L. 2006. High levels of oxidative stress globally inhibit gene transcription and histone acetylation. *DNA Cell Biol*, 25, 124-34.

BOZONET, S. M., FINDLAY, V. J., DAY, A. M., CAMERON, J., VEAL, E. A. & MORGAN, B. A. 2005. Oxidation of a eukaryotic 2-Cys peroxiredoxin is a molecular switch controlling the transcriptional response to increasing levels of hydrogen peroxide. *J Biol Chem*, 280, 23319-27.

BRADFORD, M. M. 1976. A rapid and sensitive method for the quantitation of microgram quantities of protein utilizing the principle of protein-dye binding. *Anal Biochem*, 72, 248-54.

BRADLEY, S. F. & KAUFFMAN, C. A. 1990. Aging and the response to *Salmonella* infection. *Exp Gerontol*, 25, 75-80.

BRECHARD, S., PLANCON, S. & TSCHIRHART, E. J. 2013. New insights into the regulation of neutrophil NADPH oxidase activity in the phagosome: a focus on the role of lipid and Ca(2+) signaling. *Antioxid Redox Signal*, 18, 661-76.

BRENNER, S. 1974. The genetics of *Caenorhabditis elegans*. *Genetics*, 77, 71-94.

BREWSTER, J. L., DE VALOIR, T., DWYER, N. D., WINTER, E. & GUSTIN, M. C. 1993. An osmosensing signal transduction pathway in yeast. *Science*, 259, 1760-3.

BROTHERS, K. M., GRATACAP, R. L., BARKER, S. E., NEWMAN, Z. R., NORUM, A. & WHEELER, R. T. 2013. NADPH oxidase-driven phagocyte recruitment controls *Candida albicans* filamentous growth and prevents mortality. *PLoS Pathog*, 9, e1003634.

BROWN, A. J., BUDGE, S., KALORITI, D., TILLMANN, A., JACOBSEN, M. D., YIN, Z., ENE, I. V., BOHOVYCH, I., SANDAI, D., KASTORA, S., POTRYKUS, J., BALLOU, E. R., CHILDERS, D. S., SHAHANA, S. & LEACH, M. D. 2014. Stress adaptation in a pathogenic fungus. *J Exp Biol*, 217, 144-55.

BROWN, A. J., HAYNES, K. & QUINN, J. 2009. Nitrosative and oxidative stress responses in fungal pathogenicity. *Curr Opin Microbiol*, 12, 384-91.

BROWN, G. D., TAYLOR, P. R., REID, D. M., WILLMENT, J. A., WILLIAMS, D. L., MARTINEZ-POMARES, L., WONG, S. Y. & GORDON, S. 2002. Dectin-1 is a major beta-glucan receptor on macrophages. *J Exp Med*, 196, 407-12.

BROWN, J. D., DAY, A. M., TAYLOR, S. R., TOMALIN, L. E., MORGAN, B. A. & VEAL, E. A. 2013. A peroxiredoxin promotes H2O2 signaling and oxidative stress resistance by oxidizing a thioredoxin family protein. *Cell Rep*, 5, 1425-35.

BRUCE, C. R., SMITH, D. A., RODGERS, D., DA SILVA DANTAS, A., MACCALLUM, D. M., MORGAN, B. A. & QUINN, J. 2011. Identification of a novel response regulator, Crr1, that is required for hydrogen peroxide resistance in *Candida albicans*. *PLoS One*, 6, e27979.

BRUNKE, S. & HUBE, B. 2013. Two unlike cousins: *Candida albicans* and *C. glabrata* infection strategies. *Cell Microbiol*, 15, 701-8.

BRUNKE, S., SEIDER, K., FISCHER, D., JACOBSEN, I. D., KASPER, L., JABLONOWSKI, N., WARTENBERG, A., BADER, O., ENACHE-ANGOULVANT, A., SCHALLER, M., D'ENFERT, C. & HUBE, B. 2014. One small step for a yeast--microevolution within macrophages renders *Candida glabrata* hypervirulent due to a single point mutation. *PLoS Pathog*, 10, e1004478.

BURG, N. D. & PILLINGER, M. H. 2001. The neutrophil: function and regulation in innate and humoral immunity. *Clin Immunol*, 99, 7-17.

BUTLER, G., RASMUSSEN, M. D., LIN, M. F., SANTOS, M. A., SAKTHIKUMAR, S., MUNRO, C. A., RHEINBAY, E., GRABHERR, M., FORCHE, A., REEDY, J. L., AGRAFIOTI, I., ARNAUD, M. B., BATES, S., BROWN, A. J., BRUNKE, S., COSTANZO, M. C., FITZPATRICK, D. A., DE GROOT, P. W., HARRIS, D., HOYER, L. L., HUBE, B., KLIS, F. M., KODIRA, C., LENNARD, N., LOGUE, M. E., MARTIN, R., NEIMAN, A. M., NIKOLAOU, E., QUAIL, M. A., QUINN, J., SANTOS, M. C., SCHMITZBERGER, F. F., SHERLOCK, G., SHAH, P., SILVERSTEIN, K. A., SKRZYPEK, M. S., SOLL, D., STAGGS, R., STANSFIELD, I., STUMPF, M. P., SUDBERY, P. E., SRIKANTHA, T., ZENG, Q., BERMAN, J., BERRIMAN, M., HEITMAN, J., GOW, N. A., LORENZ, M. C., BIRREN, B. W., KELLIS, M. & CUOMO, C. A. 2009. Evolution of pathogenicity and sexual reproduction in eight *Candida* genomes. *Nature*, 459, 657-62.

CALERA, J. A., HERMAN, D. & CALDERONE, R. 2000. Identification of YPD1, a gene of *Candida albicans* which encodes a two-component phosphohistidine intermediate protein. *Yeast*, 16, 1053-9.

CALVO, I. A., AYTE, J. & HIDALGO, E. 2013. Reversible thiol oxidation in the H₂O₂-dependent activation of the transcription factor Pap1. *J Cell Sci*, 126, 2279-84.

CALVO, I. A., GARCÍA, P., AYTÉ, J. & HIDALGO, E. 2012. The transcription factors Pap1 and Prr1 collaborate to activate antioxidant, but not drug tolerance, genes in response to H₂O₂. *Nucleic Acids Res*, 40, 4816-24.

CASADEVALL, A. & PIROFSKI, L. 2001. Host-pathogen interactions: the attributes of virulence. *J Infect Dis*, 184, 337-44.

CHAI, L. Y., NETEA, M. G., VONK, A. G. & KULLBERG, B. J. 2009. Fungal strategies for overcoming host innate immune response. *Med Mycol*, 47, 227-36.

CHAUHAN, N., INGLIS, D., ROMAN, E., PLA, J., LI, D., CALERA, J. A. & CALDERONE, R. 2003. *Candida albicans* response regulator gene SSK1 regulates a subset of genes whose functions are associated with cell wall biosynthesis and adaptation to oxidative stress. *Eukaryot Cell*, 2, 1018-24.

CHAUHAN, N., LATGE, J. P. & CALDERONE, R. 2006. Signalling and oxidant adaptation in *Candida albicans* and *Aspergillus fumigatus*. *Nat Rev Microbiol*, 4, 435-44.

CHAVES, G. M., BATES, S., MACCALLUM, D. M. & ODDS, F. C. 2007. *Candida albicans* GRX2, encoding a putative glutaredoxin, is required for virulence in a murine model. *Genet Mol Res*, 6, 1051-63.

CHEETHAM, J., MACCALLUM, D. M., DORIS, K. S., DA SILVA DANTAS, A., SCORFIELD, S., ODDS, F., SMITH, D. A. & QUINN, J. 2011. MAPKKK-independent regulation of the Hog1 stress-activated protein kinase in *Candida albicans*. *J Biol Chem*, 286, 42002-16.

CHEETHAM, J., SMITH, D. A., DA SILVA DANTAS, A., DORIS, K. S., PATTERSON, M. J., BRUCE, C. R. & QUINN, J. 2007. A single MAPKKK regulates the Hog1 MAPK pathway in the pathogenic fungus *Candida albicans*. *Mol Biol Cell*, 18, 4603-14.

CHEN, D., TOONE, W. M., MATA, J., LYNE, R., BURNS, G., KIVINEN, K., BRAZMA, A., JONES, N. & BÄHLER, J. 2003. Global transcriptional responses of fission yeast to environmental stress. *Mol Biol Cell*, 14, 214-29.

CHEN, D., WILKINSON, C. R., WATT, S., PENKETT, C. J., TOONE, W. M., JONES, N. & BÄHLER, J. 2008. Multiple pathways differentially regulate global oxidative stress responses in fission yeast. *Mol Biol Cell*, 19, 308-17.

CHEN, K. H., MIYAZAKI, T., TSAI, H. F. & BENNETT, J. E. 2007. The bZip transcription factor Cgap1p is involved in multidrug resistance and required for activation of multidrug transporter gene CgFLR1 in *Candida glabrata*. *Gene*, 386, 63-72.

CHENG, S. C., JOOSTEN, L. A., KULLBERG, B. J. & NETEA, M. G. 2012. Interplay between *Candida albicans* and the mammalian innate host defense. *Infect Immun*, 80, 1304-13.

CHILDERS, D. S., RAZIUNAITE, I., MOL AVELAR, G., MACKIE, J., BUDGE, S., STEAD, D., GOW, N. A., LENARDON, M. D., BALLOU, E. R., MACCALLUM, D. M. & BROWN, A. J. 2016. The Rewiring of Ubiquitination Targets in a Pathogenic Yeast Promotes Metabolic Flexibility, Host Colonization and Virulence. *PLoS Pathog*, 12, e1005566.

CHIRANAND, W., MCLEOD, I., ZHOU, H., LYNN, J. J., VEGA, L. A., MYERS, H., YATES, J. R., 3RD, LORENZ, M. C. & GUSTIN, M. C. 2008. CTA4 transcription factor mediates induction of nitrosative stress response in *Candida albicans*. *Eukaryot Cell*, 7, 268-78.

CHÁVEZ, V., MOHRI-SHIOMI, A., MAADANI, A., VEGA, L. A. & GARSIN, D. A. 2007. Oxidative stress enzymes are required for DAF-16-mediated immunity due to generation of reactive oxygen species by *Caenorhabditis elegans*. *Genetics*, 176, 1567-77.

CITIULO, F., JACOBSEN, I. D., MIRAMON, P., SCHILD, L., BRUNKE, S., ZIPFEL, P., BROCK, M., HUBE, B. & WILSON, D. 2012. *Candida albicans* scavenges host zinc via Pra1 during endothelial invasion. *PLoS Pathog*, 8, e1002777.

COHEN, G., RAPATZ, W. & RUIS, H. 1988. Sequence of the *Saccharomyces cerevisiae* CTA1 gene and amino acid sequence of catalase A derived from it. *Eur J Biochem*, 176, 159-63.

COHEN, L. B. & TROEMEL, E. R. 2015. Microbial pathogenesis and host defense in the nematode *C. elegans*. *Curr Opin Microbiol*, 23, 94-101.

COHEN, M. S., ISTURIZ, R. E., MALECH, H. L., ROOT, R. K., WILFERT, C. M., GUTMAN, L. & BUCKLEY, R. H. 1981. Fungal infection in chronic granulomatous disease. The importance of the phagocyte in defense against fungi. *Am J Med*, 71, 59-66.

COLE, G. T., HALAWA, A. A. & ANAISSE, E. J. 1996. The role of the gastrointestinal tract in hematogenous candidiasis: from the laboratory to the bedside. *Clin Infect Dis*, 22 Suppl 2, S73-88.

COLEMAN, S. T., EPPING, E. A., STEGGERDA, S. M. & MOYE-ROWLEY, W. S. 1999. Yap1p activates gene transcription in an oxidant-specific fashion. *Mol Cell Biol*, 19, 8302-13.

CRUZ, M. R., GRAHAM, C. E., GAGLIANO, B. C., LORENZ, M. C. & GARSIN, D. A. 2013. Enterococcus faecalis inhibits hyphal morphogenesis and virulence of *Candida albicans*. *Infect Immun*, 81, 189-200.

CSANK, C., SCHRÖPPEL, K., LEBERER, E., HARCUS, D., MOHAMED, O., MELOCHE, S., THOMAS, D. Y. & WHITEWAY, M. 1998. Roles of the *Candida albicans* mitogen-activated protein kinase homolog, Cek1p, in hyphal development and systemic candidiasis. *Infect Immun*, 66, 2713-21.

CUÉLLAR-CRUZ, M., BRIONES-MARTIN-DEL-CAMPO, M., CAÑAS-VILLAMAR, I., MONTALVO-ARREDONDO, J., RIEGO-RUIZ, L., CASTAÑO, I. & DE LAS PEÑAS, A. 2008. High resistance to oxidative stress in the fungal pathogen *Candida glabrata* is mediated by a single catalase, Cta1p, and is controlled by the transcription factors Yap1p, Skn7p, Msn2p, and Msn4p. *Eukaryot Cell*, 7, 814-25.

CUÉLLAR-CRUZ, M., LÓPEZ-ROMERO, E., RUIZ-BACA, E. & ZAZUETA-SANDOVAL, R. 2014. Differential response of *Candida albicans* and *Candida glabrata* to oxidative and nitrosative stresses. *Curr Microbiol*, 69, 733-9.

D'OSTIANI, C. F., DEL SERO, G., BACCI, A., MONTAGNOLI, C., SPRECA, A., MENCACCI, A., RICCIARDI-CASTAGNOLI, P. & ROMANI, L. 2000. Dendritic cells discriminate between yeasts and hyphae of the fungus *Candida albicans*. Implications for initiation of T helper cell immunity in vitro and in vivo. *J Exp Med*, 191, 1661-74.

DA SILVA DANTAS, A., PATTERSON, M. J., SMITH, D. A., MACCALLUM, D. M., ERWIG, L. P., MORGAN, B. A. & QUINN, J. 2010. Thioredoxin regulates multiple hydrogen peroxide-induced signaling pathways in *Candida albicans*. *Mol Cell Biol*, 30, 4550-63.

DANTAS, A. A. S., DAY, A., IKEH, M., KOS, I., ACHAN, B. & QUINN, J. 2015. Oxidative stress responses in the human fungal pathogen, *Candida albicans*. *Biomolecules*, 5, 142-65.

DAVIES, A. N., BRAILSFORD, S. R. & BEIGHTON, D. 2006. Oral candidosis in patients with advanced cancer. *Oral Oncol*, 42, 698-702.

DAVIS, D., EDWARDS, J. E., JR., MITCHELL, A. P. & IBRAHIM, A. S. 2000a. *Candida albicans* RIM101 pH response pathway is required for host-pathogen interactions. *Infect Immun*, 68, 5953-9.

DAVIS, D., WILSON, R. B. & MITCHELL, A. P. 2000b. RIM101-dependent and-independent pathways govern pH responses in *Candida albicans*. *Mol Cell Biol*, 20, 971-8.

DE REPENTIGNY, L., LEWANDOWSKI, D. & JOLICOEUR, P. 2004. Immunopathogenesis of oropharyngeal candidiasis in human immunodeficiency virus infection. *Clin Microbiol Rev*, 17, 729-59, table of contents.

DELAUNAY, A., ISNARD, A. D. & TOLEDANO, M. B. 2000. H₂O₂ sensing through oxidation of the Yap1 transcription factor. *EMBO J*, 19, 5157-66.

DELAUNAY, A., PFLIEGER, D., BARRAULT, M. B., VINH, J. & TOLEDANO, M. B. 2002. A thiol peroxidase is an H₂O₂ receptor and redox-transducer in gene activation. *Cell*, 111, 471-81.

DEVEAU, A., PIIS PANEN, A. E., JACKSON, A. A. & HOGAN, D. A. 2010. Farnesol induces hydrogen peroxide resistance in *Candida albicans* yeast by inhibiting the Ras-cyclic AMP signaling pathway. *Eukaryot Cell*, 9, 569-77.

DIAMOND, R. D., CLARK, R. A. & HAUDENSCHILD, C. C. 1980. Damage to *Candida albicans* hyphae and pseudohyphae by the myeloperoxidase system and oxidative products of neutrophil metabolism in vitro. *J Clin Invest*, 66, 908-17.

DIAMOND, R. D., KRZESICKI, R. & JAO, W. 1978. Damage to pseudohyphal forms of *Candida albicans* by neutrophils in the absence of serum in vitro. *J Clin Invest*, 61, 349-59.

DIMOPOULOS, G., KOULENTI, D., BLOT, S., SAKR, Y., ANZUETO, A., SPIES, C., VIOLÁN, J. S., KETT, D., ARMAGANIDIS, A., MARTIN, C., VINCENT, J. L. & INVESTIGATORS, E. P. O. I. I. I. C. S. 2013. Critically ill elderly adults with infection: analysis of the extended prevalence of infection in intensive care study. *J Am Geriatr Soc*, 61, 2065-71.

DOLZ-EDO, L., RIENZO, A., POVEDA-HUERTES, D., PASCUAL-AHUIR, A. & PROFT, M. 2013. Deciphering dynamic dose responses of natural promoters and single cis elements upon osmotic and oxidative stress in yeast. *Mol Cell Biol*, 33, 2228-40.

DONGARI-BAGTZOGLOU, A., KASHLEVA, H., DWIVEDI, P., DIAZ, P. & VASILAKOS, J. 2009. Characterization of mucosal *Candida albicans* biofilms. *PLoS One*, 4, e7967.

DUJON, B., SHERMAN, D., FISCHER, G., DURRENS, P., CASAREGOLA, S., LAFONTAINE, I., DE MONTIGNY, J., MARCK, C., NEUVÉGLISE, C., TALLA, E., GOFFARD, N., FRANGEUL, L., AIGLE, M., ANTHOUARD, V., BABOUR, A., BARBE, V., BARNAY, S., BLANCHIN, S., BECKERICH, J. M., BEYNE, E., BLEYKASTEN, C., BOISRAMÉ, A., BOYER, J., CATTOLICO, L., CONFANIOLERİ, F., DE DARUVAR, A., DESPONS, L., FABRE, E., FAIRHEAD, C., FERRY-DUMAZET, H., GROPPY, A., HANTRAYE, F., HENNEQUIN, C., JAUNIAUX, N., JOYET, P., KACHOURI, R., KERREST, A., KOSZUL, R., LEMAIRE, M., LESUR, I., MA, L., MULLER, H., NICAUD, J. M., NIKOLSKI, M., OZTAS, S., OZIER-KALOGEROPOULOS, O., PELLENZ, S., POTIER, S., RICHARD, G. F., STRAUB, M. L., SULEAU, A., SWENNEN, D., TEKAIA, F., WÉSOLOWSKI-LOUVEL, M., WESTHOF, E., WIRTH, B., ZENIOU-MEYER, M., ZIVANOVIC, I., BOLOTIN-FUKUHARA, M., THIERRY, A., BOUCHIER, C., CAUDRON, B., SCARPELLI, C., GAILLARDIN, C., WEISSENBACH, J., WINCKER, P. & SOUCIET, J. L. 2004. Genome evolution in yeasts. *Nature*, 430, 35-44.

DÜHRING, S., GERMERODT, S., SKERKA, C., ZIPFEL, P. F., DANDEKAR, T. & SCHUSTER, S. 2015. Host-pathogen interactions between the human innate immune system and *Candida albicans*-understanding and modeling defense and evasion strategies. *Front Microbiol*, 6, 625.

EGGIMANN, P., GARBINO, J. & PITTEL, D. 2003. Epidemiology of *Candida* species infections in critically ill non-immunosuppressed patients. *Lancet Infect Dis*, 3, 685-702.

EL CHEMALY, A. & DEMAUREX, N. 2012. Do Hv1 proton channels regulate the ionic and redox homeostasis of phagosomes? *Mol Cell Endocrinol*, 353, 82-7.

ELIAS, A., MICHAEL, M. & MICHAEL, P. 2009. *Clinical mycology*, Edinburgh, Churchill Livingstone/Elsevier

ELLIS, M. E., AL-ABDELY, H., SANDRIDGE, A., GREER, W. & VENTURA, W. 2001. Fungal endocarditis: evidence in the world literature, 1965-1995. *Clin Infect Dis*, 32, 50-62.

ENE, I. V., CHENG, S. C., NETEA, M. G. & BROWN, A. J. 2013. Growth of *Candida albicans* cells on the physiologically relevant carbon source lactate affects their recognition and phagocytosis by immune cells. *Infect Immun*, 81, 238-48.

ENJALBERT, B., MACCALLUM, D. M., ODDS, F. C. & BROWN, A. J. 2007. Niche-specific activation of the oxidative stress response by the pathogenic fungus *Candida albicans*. *Infect Immun*, 75, 2143-51.

ENJALBERT, B., NANTEL, A. & WHITEWAY, M. 2003. Stress-induced gene expression in *Candida albicans*: absence of a general stress response. *Mol Biol Cell*, 14, 1460-7.

ENJALBERT, B., SMITH, D. A., CORNELL, M. J., ALAM, I., NICHOLLS, S., BROWN, A. J. & QUINN, J. 2006. Role of the Hog1 stress-activated protein kinase in the global transcriptional response to stress in the fungal pathogen *Candida albicans*. *Mol Biol Cell*, 17, 1018-32.

ERWIG, L. P. & GOW, N. A. 2016. Interactions of fungal pathogens with phagocytes. *Nat Rev Microbiol*, 14, 163-76.

EVANS, E. A., CHEN, W. C. & TAN, M. W. 2008a. The DAF-2 insulin-like signaling pathway independently regulates aging and immunity in *C. elegans*. *Aging Cell*, 7, 879-93.

EVANS, E. A., KAWLI, T. & TAN, M. W. 2008b. *Pseudomonas aeruginosa* suppresses host immunity by activating the DAF-2 insulin-like signaling pathway in *Caenorhabditis elegans*. *PLoS Pathog*, 4, e1000175.

EWBANK, J. J. & ZUGASTI, O. 2011. *C. elegans*: model host and tool for antimicrobial drug discovery. *Dis Model Mech*, 4, 300-4.

EYERICH, K., FOERSTER, S., ROMBOLD, S., SEIDL, H. P., BEHRENDT, H., HOFMANN, H., RING, J. & TRAIDL-HOFFMANN, C. 2008. Patients with chronic mucocutaneous candidiasis exhibit reduced production of Th17-associated cytokines IL-17 and IL-22. *J Invest Dermatol*, 128, 2640-5.

FABRY, W., SCHMID, E. N., SCHRAPS, M. & ANSORG, R. 2003. Isolation and purification of chlamydospores of *Candida albicans*. *Med Mycol*, 41, 53-8.

FANG, F. C. 2004. Antimicrobial reactive oxygen and nitrogen species: concepts and controversies. *Nat Rev Microbiol*, 2, 820-32.

FARAH, C. S., ELAHI, S., PANG, G., GOTJAMANOS, T., SEYMOUR, G. J., CLANCY, R. L. & ASHMAN, R. B. 2001. T cells augment monocyte and neutrophil function in host resistance against oropharyngeal candidiasis. *Infect Immun*, 69, 6110-8.

FASSLER, J. S. & WEST, A. H. 2013. Histidine phosphotransfer proteins in fungal two-component signal transduction pathways. *Eukaryot Cell*, 12, 1052-60.

FENG, Q., SUMMERS, E., GUO, B. & FINK, G. 1999. Ras signaling is required for serum-induced hyphal differentiation in *Candida albicans*. *J Bacteriol*, 181, 6339-46.

FERNANDES, L., RODRIGUES-POUSADA, C. & STRUHL, K. 1997. Yap, a novel family of eight bZIP proteins in *Saccharomyces cerevisiae* with distinct biological functions. *Mol Cell Biol*, 17, 6982-93.

FERNANDEZ-ARENAS, E., CABEZON, V., BERMEJO, C., ARROYO, J., NOMBELA, C., DIEZ-OREJAS, R. & GIL, C. 2007. Integrated proteomics and

genomics strategies bring new insight into *Candida albicans* response upon macrophage interaction. *Mol Cell Proteomics*, 6, 460-78.

FERNÁNDEZ-ARENAS, E., BLECK, C. K., NOMBELA, C., GIL, C., GRIFFITHS, G. & DIEZ-OREJAS, R. 2009. *Candida albicans* actively modulates intracellular membrane trafficking in mouse macrophage phagosomes. *Cell Microbiol*, 11, 560-89.

FERRIGNO, P., POSAS, F., KOEPP, D., SAITO, H. & SILVER, P. A. 1998. Regulated nucleo/cytoplasmic exchange of HOG1 MAPK requires the importin beta homologs NMD5 and XPO1. *EMBO J*, 17, 5606-14.

FIDEL, P. L., JR., VAZQUEZ, J. A. & SOBEL, J. D. 1999. *Candida glabrata*: review of epidemiology, pathogenesis, and clinical disease with comparison to *C. albicans*. *Clin Microbiol Rev*, 12, 80-96.

FINCH, C. E. & RUVKUN, G. 2001. The genetics of aging. *Annu Rev Genomics Hum Genet*, 2, 435-62.

FIORI, A., KUCHARÍKOVÁ, S., GOVAERT, G., CAMMUE, B. P., THEVISSEN, K. & VAN DIJCK, P. 2012. The heat-induced molecular disaggregase Hsp104 of *Candida albicans* plays a role in biofilm formation and pathogenicity in a worm infection model. *Eukaryot Cell*, 11, 1012-20.

FITZSIMMONS, N. & BERRY, D. R. 1994. Inhibition of *Candida albicans* by *Lactobacillus acidophilus*: evidence for the involvement of a peroxidase system. *Microbios*, 80, 125-33.

FLEVARI, A., THEODORAKOPOULOU, M., VELEGRAKI, A., ARMAGANIDIS, A. & DIMOPOULOS, G. 2013. Treatment of invasive candidiasis in the elderly: a review. *Clin Interv Aging*, 8, 1199-208.

FRADIN, C., DE GROOT, P., MACCALLUM, D., SCHALLER, M., KLIS, F., ODDS, F. C. & HUBE, B. 2005. Granulocytes govern the transcriptional response, morphology and proliferation of *Candida albicans* in human blood. *Mol Microbiol*, 56, 397-415.

FRADIN, C., KRETSCHMAR, M., NICHTERLEIN, T., GAILLARDIN, C., D'ENFERT, C. & HUBE, B. 2003. Stage-specific gene expression of *Candida albicans* in human blood. *Mol Microbiol*, 47, 1523-43.

FRANCESCHI, C., CAPRI, M., MONTI, D., GIUNTA, S., OLIVIERI, F., SEVINI, F., PANOURGIA, M. P., INVIDIA, L., CELANI, L., SCURTI, M., CEVENINI, E., CASTELLANI, G. C. & SALVIOLI, S. 2007. Inflammaging and anti-inflammaging: a systemic perspective on aging and longevity emerged from studies in humans. *Mech Ageing Dev*, 128, 92-105.

FROHNER, I. E., BOURGEOIS, C., YATSYK, K., MAJER, O. & KUCHLER, K. 2009. *Candida albicans* cell surface superoxide dismutases degrade host-derived reactive oxygen species to escape innate immune surveillance. *Mol Microbiol*, 71, 240-52.

FUKUDA, Y., TSAI, H. F., MYERS, T. G. & BENNETT, J. E. 2013. Transcriptional profiling of *Candida glabrata* during phagocytosis by neutrophils and in the infected mouse spleen. *Infect Immun*, 81, 1325-33.

GARCERÁ, A., CASAS, C. & HERRERO, E. 2010. Expression of *Candida albicans* glutathione transferases is induced inside phagocytes and upon diverse environmental stresses. *FEMS Yeast Res*, 10, 422-31.

GARCÍA-SANTAMARINA, S., BORONAT, S., ESPADAS, G., AYTÉ, J., MOLINA, H. & HIDALGO, E. 2011. The oxidized thiol proteome in fission yeast--

optimization of an ICAT-based method to identify H₂O₂-oxidized proteins. *J Proteomics*, 74, 2476-86.

GASCH, A. P., SPELLMAN, P. T., KAO, C. M., CARMEL-HAREL, O., EISEN, M. B., STORZ, G., BOTSTEIN, D. & BROWN, P. O. 2000. Genomic expression programs in the response of yeast cells to environmental changes. *Mol Biol Cell*, 11, 4241-57.

GIOULEKAS, E., GOUTZIOULIS, M., FARMAKIS, C., DROSSOU, V., KREMENOPPOULOS, G., TSIOURIS, J. & ROILIDES, E. 2001. Effects of macrophage colony-stimulating factor on antifungal activity of neonatal monocytes against *Candida albicans*. *Biol Neonate*, 80, 251-6.

GLEASON, J. E., GALALELDEEN, A., PETERSON, R. L., TAYLOR, A. B., HOLLOWAY, S. P., WANINGER-SARONI, J., CORMACK, B. P., CABELLI, D. E., HART, P. J. & CULOTTA, V. C. 2014. *Candida albicans* SOD5 represents the prototype of an unprecedented class of Cu-only superoxide dismutases required for pathogen defense. *Proc Natl Acad Sci U S A*, 111, 5866-71.

GLOVER, J. N. & HARRISON, S. C. 1995. Crystal structure of the heterodimeric bZIP transcription factor c-Fos-c-Jun bound to DNA. *Nature*, 373, 257-61.

GOMEZ, C. R., BOEHMER, E. D. & KOVACS, E. J. 2005. The aging innate immune system. *Curr Opin Immunol*, 17, 457-62.

GONZALEZ-PARRAGA, P., ALONSO-MONGE, R., PLA, J. & ARGUELLES, J. C. 2010. Adaptive tolerance to oxidative stress and the induction of antioxidant enzymatic activities in *Candida albicans* are independent of the Hog1 and Cap1-mediated pathways. *FEMS Yeast Res*, 10, 747-56.

GORDON, S. 2002. Pattern recognition receptors: doubling up for the innate immune response. *Cell*, 111, 927-30.

GOW, N. A., VAN DE VEERDONK, F. L., BROWN, A. J. & NETEA, M. G. 2011. *Candida albicans* morphogenesis and host defence: discriminating invasion from colonization. *Nat Rev Microbiol*, 10, 112-22.

GRANT, C. M., COLLINSON, L. P., ROE, J. H. & DAWES, I. W. 1996. Yeast glutathione reductase is required for protection against oxidative stress and is a target gene for yAP-1 transcriptional regulation. *Mol Microbiol*, 21, 171-9.

GRAVATO-NOBRE, M. J. & HODGKIN, J. 2005. *Caenorhabditis elegans* as a model for innate immunity to pathogens. *Cell Microbiol*, 7, 741-51.

GRUBER, J., CHEN, C. B., FONG, S., NG, L. F., TEO, E. & HALLIWELL, B. 2015. *Caenorhabditis elegans*: What We Can and Cannot Learn from Aging Worms. *Antioxid Redox Signal*, 23, 256-79.

GULSHAN, K., LEE, S. S. & MOYE-ROWLEY, W. S. 2011. Differential oxidant tolerance determined by the key transcription factor Yap1 is controlled by levels of the Yap1-binding protein, Ybp1. *J Biol Chem*, 286, 34071-81.

GULSHAN, K., ROVINSKY, S. A., COLEMAN, S. T. & MOYE-ROWLEY, W. S. 2005. Oxidant-specific folding of Yap1p regulates both transcriptional activation and nuclear localization. *J Biol Chem*, 280, 40524-33.

GULSHAN, K., ROVINSKY, S. A. & MOYE-ROWLEY, W. S. 2004. YBP1 and its homologue YBP2/YBH1 influence oxidative-stress tolerance by nonidentical mechanisms in *Saccharomyces cerevisiae*. *Eukaryot Cell*, 3, 318-30.

GULSHAN, K., THOMMANDRU, B. & MOYE-ROWLEY, W. S. 2012. Proteolytic degradation of the Yap1 transcription factor is regulated by subcellular localization and the E3 ubiquitin ligase Not4. *J Biol Chem*, 287, 26796-805.

GÖRNER, W., DURCHSCHLAG, E., MARTINEZ-PASTOR, M. T., ESTRUCH, F., AMMERER, G., HAMILTON, B., RUIS, H. & SCHÜLLER, C. 1998. Nuclear localization of the C2H2 zinc finger protein Msn2p is regulated by stress and protein kinase A activity. *Genes Dev*, 12, 586-97.

HAJJEH, R. A., SOFAIR, A. N., HARRISON, L. H., LYON, G. M., ARTHINGTON-SKAGGS, B. A., MIRZA, S. A., PHELAN, M., MORGAN, J., LEE-YANG, W., CIBLAK, M. A., BENJAMIN, L. E., SANZA, L. T., HUIE, S., YEO, S. F., BRANDT, M. E. & WARNOCK, D. W. 2004. Incidence of bloodstream infections due to *Candida* species and in vitro susceptibilities of isolates collected from 1998 to 2000 in a population-based active surveillance program. *J Clin Microbiol*, 42, 1519-27.

HALL, R. A. 2015. Dressed to impress: impact of environmental adaptation on the *Candida albicans* cell wall. *Mol Microbiol*, 97, 7-17.

HALLIWELL, B. 2006. Reactive species and antioxidants. Redox biology is a fundamental theme of aerobic life. *Plant Physiol*, 141, 312-22.

HAMPTON, M. B., KETTLE, A. J. & WINTERBOURN, C. C. 1998. Inside the neutrophil phagosome: oxidants, myeloperoxidase, and bacterial killing. *Blood*, 92, 3007-17.

HARRIOTT, M. M. & NOVERR, M. C. 2011. Importance of *Candida*-bacterial polymicrobial biofilms in disease. *Trends Microbiol*, 19, 557-63.

HE, X. J., MULFORD, K. E. & FASSLER, J. S. 2009. Oxidative stress function of the *Saccharomyces cerevisiae* Skn7 receiver domain. *Eukaryot Cell*, 8, 768-78.

HEALY, C. M., CAMPBELL, J. R., ZACCARIA, E. & BAKER, C. J. 2008. Fluconazole prophylaxis in extremely low birth weight neonates reduces invasive candidiasis mortality rates without emergence of fluconazole-resistant *Candida* species. *Pediatrics*, 121, 703-10.

HEIDEMANN, M., HINTERMAIR, C., VOß, K. & EICK, D. 2013. Dynamic phosphorylation patterns of RNA polymerase II CTD during transcription. *Biochim Biophys Acta*, 1829, 55-62.

HEILMANN, C. J., SORGO, A. G., SILIAKUS, A. R., DEKKER, H. L., BRUL, S., DE KOSTER, C. G., DE KONING, L. J. & KLIS, F. M. 2011. Hyphal induction in the human fungal pathogen *Candida albicans* reveals a characteristic wall protein profile. *Microbiology*, 157, 2297-307.

HERRERO-DE-DIOS, C., ALONSO-MONGE, R. & PLA, J. 2014. The lack of upstream elements of the Cek1 and Hog1 mediated pathways leads to a synthetic lethal phenotype upon osmotic stress in *Candida albicans*. *Fungal Genet Biol*, 69, 31-42.

HODGKIN, J., KUWABARA, P. E. & CORNELIUSSEN, B. 2000. A novel bacterial pathogen, *Microbacterium nematophilum*, induces morphological change in the nematode *C. elegans*. *Curr Biol*, 10, 1615-8.

HOLLAND, S. M. 2010. Chronic granulomatous disease. *Clin Rev Allergy Immunol*, 38, 3-10.

HOMANN, O. R., DEA, J., NOBLE, S. M. & JOHNSON, A. D. 2009. A phenotypic profile of the *Candida albicans* regulatory network. *PLoS Genet*, 5, e1000783.

HROMATKA, B. S., NOBLE, S. M. & JOHNSON, A. D. 2005. Transcriptional response of *Candida albicans* to nitric oxide and the role of the YHB1 gene in nitrosative stress and virulence. *Mol Biol Cell*, 16, 4814-26.

HUBE, B. & NAGLIK, J. 2001. *Candida albicans* proteinases: resolving the mystery of a gene family. *Microbiology*, 147, 1997-2005.

HUYCKE, M. M., ABRAMS, V. & MOORE, D. R. 2002. *Enterococcus faecalis* produces extracellular superoxide and hydrogen peroxide that damages colonic epithelial cell DNA. *Carcinogenesis*, 23, 529-36.

HWANG, C. S., RHIE, G. E., OH, J. H., HUH, W. K., YIM, H. S. & KANG, S. O. 2002. Copper- and zinc-containing superoxide dismutase (Cu/ZnSOD) is required for the protection of *Candida albicans* against oxidative stresses and the expression of its full virulence. *Microbiology*, 148, 3705-13.

IMLAY, J. A. 2003. Pathways of oxidative damage. *Annu Rev Microbiol*, 57, 395-418.

IRAZOQUI, J. E. & AUSUBEL, F. M. 2010. 99th Dahlem conference on infection, inflammation and chronic inflammatory disorders: *Caenorhabditis elegans* as a model to study tissues involved in host immunity and microbial pathogenesis. *Clin Exp Immunol*, 160, 48-57.

IRAZOQUI, J. E., TROEMEL, E. R., FEINBAUM, R. L., LUHACHACK, L. G., CEZAIRLIYAN, B. O. & AUSUBEL, F. M. 2010a. Distinct pathogenesis and host responses during infection of *C. elegans* by *P. aeruginosa* and *S. aureus*. *PLoS Pathog*, 1, 1000982.

IRAZOQUI, J. E., URBACH, J. M. & AUSUBEL, F. M. 2010b. Evolution of host innate defence: insights from *Caenorhabditis elegans* and primitive invertebrates. *Nat Rev Immunol*, 10, 47-58.

ISOYAMA, T., MURAYAMA, A., NOMOTO, A. & KUGE, S. 2001. Nuclear import of the yeast AP-1-like transcription factor Yap1p is mediated by transport receptor Pse1p, and this import step is not affected by oxidative stress. *J Biol Chem*, 276, 21863-9.

IZAWA, S., MAEDA, K., SUGIYAMA, K., MANO, J., INOUE, Y. & KIMURA, A. 1999. Thioredoxin deficiency causes the constitutive activation of Yap1, an AP-1-like transcription factor in *Saccharomyces cerevisiae*. *J Biol Chem*, 274, 28459-65.

JACOBSEN, I. D., BRUNKE, S., SEIDER, K., SCHWARZMÜLLER, T., FIRON, A., D'ENFÉRT, C., KUCHLER, K. & HUBE, B. 2010. *Candida glabrata* persistence in mice does not depend on host immunosuppression and is unaffected by fungal amino acid auxotrophy. *Infect Immun*, 78, 1066-77.

JACOBSEN, I. D., WILSON, D., WÄCHTLER, B., BRUNKE, S., NAGLIK, J. R. & HUBE, B. 2012. *Candida albicans* dimorphism as a therapeutic target. *Expert Rev Anti Infect Ther*, 10, 85-93.

JAIN, C., PASTOR, K., GONZALEZ, A. Y., LORENZ, M. C. & RAO, R. P. 2013. The role of *Candida albicans* AP-1 protein against host derived ROS in in vivo models of infection. *Virulence*, 4, 67-76.

JAIN, C., YUN, M., POLITZ, S. M. & RAO, R. P. 2009. A pathogenesis assay using *Saccharomyces cerevisiae* and *Caenorhabditis elegans* reveals novel roles for yeast AP-1, Yap1, and host dual oxidase BLI-3 in fungal pathogenesis. *Eukaryot Cell*, 8, 1218-27.

JAMIESON, D. J., STEPHEN, D. W. & TERRIÈRE, E. C. 1996. Analysis of the adaptive oxidative stress response of *Candida albicans*. *FEMS Microbiol Lett*, 138, 83-8.

JIMÉNEZ-LÓPEZ, C., COLLETTE, J. R., BROTHERS, K. M., SHEPARDSON, K. M., CRAMER, R. A., WHEELER, R. T. & LORENZ, M. C. 2013. *Candida albicans*

induces arginine biosynthetic genes in response to host-derived reactive oxygen species. *Eukaryot Cell*, 12, 91-100.

JOHNSON, A., DURAND-DUBIEF, M., XUE-FRANZÉN, Y., RÖNNERBLAD, M., EKWALL, K. & WRIGHT, A. 2009. HAT-HDAC interplay modulates global histone H3K14 acetylation in gene-coding regions during stress. *EMBO Rep*, 10, 1009-14.

JUNG, K. W., STRAIN, A. K., NIELSEN, K., JUNG, K. H. & BAHN, Y. S. 2012. Two cation transporters Ena1 and Nha1 cooperatively modulate ion homeostasis, antifungal drug resistance, and virulence of *Cryptococcus neoformans* via the HOG pathway. *Fungal Genet Biol*, 49, 332-45.

KALORITI, D., JACOBSEN, M., YIN, Z., PATTERSON, M., TILLMANN, A., SMITH, D. A., COOK, E., YOU, T., GRIMM, M. J., BOHOVYCH, I., GREBOGI, C., SEGAL, B. H., GOW, N. A., HAYNES, K., QUINN, J. & BROWN, A. J. 2014. Mechanisms underlying the exquisite sensitivity of *Candida albicans* to combinatorial cationic and oxidative stress that enhances the potent fungicidal activity of phagocytes. *MBio*, 5, e01334-14.

KALORITI, D., TILLMANN, A., COOK, E., JACOBSEN, M., YOU, T., LENARDON, M., AMES, L., BARAHONA, M., CHANDRASEKARAN, K., COGHILL, G., GOODMAN, D., GOW, N. A., GREBOGI, C., HO, H. L., INGRAM, P., MCDONAGH, A., DE MOURA, A. P., PANG, W., PUTTNAM, M., RADMANESHFAR, E., ROMANO, M. C., SILK, D., STARK, J., STUMPF, M., THIEL, M., THORNE, T., USHER, J., YIN, Z., HAYNES, K. & BROWN, A. J. 2012. Combinatorial stresses kill pathogenic *Candida* species. *Med Mycol*, 50, 699-709.

KAMTHAN, M., NALLA, V. K., RUHELA, D., KAMTHAN, A., MAITI, P. & DATTA, A. 2014. Characterization of a putative spindle assembly checkpoint kinase Mps1, suggests its involvement in cell division, morphogenesis and oxidative stress tolerance in *Candida albicans*. *PLoS One*, 9, e101517.

KASPER, L., SEIDER, K. & HUBE, B. 2015. Intracellular survival of *Candida glabrata* in macrophages: immune evasion and persistence. *FEMS Yeast Res*, 15, foy042.

KAUFFMAN, C. A. 2001. Fungal infections in older adults. *Clin Infect Dis*, 33, 550-5.

KAUR, R., DOMERGUE, R., ZUPANCIC, M. L. & CORMACK, B. P. 2005. A yeast by any other name: *Candida glabrata* and its interaction with the host. *Curr Opin Microbiol*, 8, 378-84.

KAUR, R., MA, B. & CORMACK, B. P. 2007. A family of glycosylphosphatidylinositol-linked aspartyl proteases is required for virulence of *Candida glabrata*. *Proc Natl Acad Sci U S A*, 104, 7628-33.

KAWASAKI, L., WYSONG, D., DIAMOND, R. & AGUIRRE, J. 1997. Two divergent catalase genes are differentially regulated during *Aspergillus nidulans* development and oxidative stress. *J Bacteriol*, 179, 3284-92.

KIM, D. H. & AUSUBEL, F. M. 2005. Evolutionary perspectives on innate immunity from the study of *Caenorhabditis elegans*. *Curr Opin Immunol*, 17, 4-10.

KIM, D. H., FEINBAUM, R., ALLOING, G., EMERSON, F. E., GARSIN, D. A., INOUE, H., TANAKA-HINO, M., HISAMOTO, N., MATSUMOTO, K., TAN, M. W. & AUSUBEL, F. M. 2002. A conserved p38 MAP kinase pathway in *Caenorhabditis elegans* innate immunity. *Science*, 297, 623-6.

KIRKPATRICK, C. H. 1994. Chronic mucocutaneous candidiasis. *J Am Acad Dermatol*, 31, S14-7.

KITADA, K., YAMAGUCHI, E. & ARISAWA, M. 1995. Cloning of the *Candida glabrata* TRP1 and HIS3 genes, and construction of their disruptant strains by sequential integrative transformation. *Gene*, 165, 203-6.

KITAMURA, K., TAKI, M., TANAKA, N. & YAMASHITA, I. 2011. Fission yeast Ubr1 ubiquitin ligase influences the oxidative stress response via degradation of active Pap1 bZIP transcription factor in the nucleus. *Mol Microbiol*, 80, 739-55.

KLAUNIG, J. E., KAMENDULIS, L. M. & HOCEVAR, B. A. 2010. Oxidative stress and oxidative damage in carcinogenesis. *Toxicol Pathol*, 38, 96-109.

KOH, A. Y., KÖHLER, J. R., COGGSSHALL, K. T., VAN ROOIJEN, N. & PIER, G. B. 2008. Mucosal damage and neutropenia are required for *Candida albicans* dissemination. *PLoS Pathog*, 4, e35.

KOMURA, T., IKEDA, T., HOSHINO, K., SHIBAMURA, A. & NISHIKAWA, Y. 2012. *Caenorhabditis elegans* as an alternative model to study senescence of host defense and the prevention by immunonutrition. *Adv Exp Med Biol*, 710, 19-27.

KOO, K. H., LEE, S., JEONG, S. Y., KIM, E. T., KIM, H. J., KIM, K., SONG, K. & CHAE, H. Z. 2002. Regulation of thioredoxin peroxidase activity by C-terminal truncation. *Arch Biochem Biophys*, 397, 312-8.

KOS, I., PATTERSON, M. J., ZNAIDI, S., KALORITI, D., DA SILVA DANTAS, A., HERRERO-DE-DIOS, C. M., D'ENFERT, C., BROWN, A. J. & QUINN, J. 2016. Mechanisms Underlying the Delayed Activation of the Cap1 Transcription Factor in *Candida albicans* following Combinatorial Oxidative and Cationic Stress Important for Phagocytic Potency. *MBio*, 7, e00331.

KRYSAN, D. J., SUTTERWALA, F. S. & WELLINGTON, M. 2014. Catching fire: *Candida albicans*, macrophages, and pyroptosis. *PLoS Pathog*, 10, e1004139.

KUGE, S., ARITA, M., MURAYAMA, A., MAETA, K., IZAWA, S., INOUE, Y. & NOMOTO, A. 2001. Regulation of the yeast Yap1p nuclear export signal is mediated by redox signal-induced reversible disulfide bond formation. *Mol Cell Biol*, 21, 6139-50.

KUGE, S. & JONES, N. 1994. YAP1 dependent activation of TRX2 is essential for the response of *Saccharomyces cerevisiae* to oxidative stress by hydroperoxides. *Embo j*, 13, 655-64.

KUGE, S., JONES, N. & NOMOTO, A. 1997. Regulation of yAP-1 nuclear localization in response to oxidative stress. *Embo j*, 16, 1710-20.

KUGE, S., TODA, T., IIZUKA, N. & NOMOTO, A. 1998. Crm1 (Xpol) dependent nuclear export of the budding yeast transcription factor yAP-1 is sensitive to oxidative stress. *Genes Cells*, 3, 521-32.

KURZ, C. L. & TAN, M. W. 2004. Regulation of aging and innate immunity in *C. elegans*. *Aging Cell*, 3, 185-93.

KUSCH, H., ENGELMANN, S., ALBRECHT, D., MORSCHHAUSER, J. & HECKER, M. 2007. Proteomic analysis of the oxidative stress response in *Candida albicans*. *Proteomics*, 7, 686-97.

LAEMMLI, U. K. 1970. Cleavage of structural proteins during the assembly of the head of bacteriophage T4. *Nature*, 227, 680-5.

LAMARRE, C., LEMAY, J. D., DESLAURIERS, N. & BOURBONNAIS, Y. 2001. *Candida albicans* expresses an unusual cytoplasmic manganese-containing

superoxide dismutase (SOD3 gene product) upon the entry and during the stationary phase. *J Biol Chem*, 276, 43784-91.

LAMBOU, K., LAMARRE, C., BEAU, R., DUFOUR, N. & LATGE, J. P. 2010. Functional analysis of the superoxide dismutase family in *Aspergillus fumigatus*. *Mol Microbiol*, 75, 910-23.

LEBERER, E., HARCUS, D., DIGNARD, D., JOHNSON, L., USHINSKY, S., THOMAS, D. Y. & SCHRÖPPEL, K. 2001. Ras links cellular morphogenesis to virulence by regulation of the MAP kinase and cAMP signalling pathways in the pathogenic fungus *Candida albicans*. *Mol Microbiol*, 42, 673-87.

LEE, J., GODON, C., LAGNIEL, G., SPECTOR, D., GARIN, J., LABARRE, J. & TOLEDANO, M. B. 1999. Yap1 and Skn7 control two specialized oxidative stress response regulons in yeast. *J Biol Chem*, 274, 16040-6.

LINTON, P. J. & THOMAN, M. L. 2014. Immunosenescence in monocytes, macrophages, and dendritic cells: lessons learned from the lung and heart. *Immunol Lett*, 162, 290-7.

LIU, T. T., ZNAIDI, S., BARKER, K. S., XU, L., HOMAYOUNI, R., SAIDANE, S., MORSCHHÄUSER, J., NANTEL, A., RAYMOND, M. & ROGERS, P. D. 2007. Genome-wide expression and location analyses of the *Candida albicans* Tac1p regulon. *Eukaryot Cell*, 6, 2122-38.

LIVAK, K. J. & SCHMITTGEN, T. D. 2001. Analysis of relative gene expression data using real-time quantitative PCR and the 2(-Delta Delta C(T)) Method. *Methods*, 25, 402-8.

LO, H. J., KÖHLER, J. R., DIDOMENICO, B., LOEBENBERG, D., CACCIAPUOTI, A. & FINK, G. R. 1997. Nonfilamentous *C. albicans* mutants are avirulent. *Cell*, 90, 939-49.

LOHSE, M. B. & JOHNSON, A. D. 2008. Differential phagocytosis of white versus opaque *Candida albicans* by *Drosophila* and mouse phagocytes. *PLoS One*, 3, e1473.

LOLL-KRIPPLEBER, R., D'ENFERT, C., FERI, A., DIOGO, D., PERIN, A., MARCET-HOUBEN, M., BOUGNOUX, M. E. & LEGRAND, M. 2014. A study of the DNA damage checkpoint in *Candida albicans*: uncoupling of the functions of Rad53 in DNA repair, cell cycle regulation and genotoxic stress-induced polarized growth. *Mol Microbiol*, 91, 452-71.

LORD, J. M., BUTCHER, S., KILLAMPALI, V., LASCELLES, D. & SALMON, M. 2001. Neutrophil ageing and immunosenescence. *Mech Ageing Dev*, 122, 1521-35.

LORENZ, M. C., BENDER, J. A. & FINK, G. R. 2004. Transcriptional response of *Candida albicans* upon internalization by macrophages. *Eukaryot Cell*, 3, 1076-87.

LORENZ, M. C. & FINK, G. R. 2001. The glyoxylate cycle is required for fungal virulence. *Nature*, 412, 83-6.

LOSSE, J., SVOBODOVA, E., HEYKEN, A., HUBE, B., ZIPFEL, P. F. & JOZSI, M. 2011. Role of pH-regulated antigen 1 of *Candida albicans* in the fungal recognition and antifungal response of human neutrophils. *Mol Immunol*, 48, 2135-43.

LU, H., ZHU, Z., DONG, L., JIA, X., SUN, X., YAN, L., CHAI, Y., JIANG, Y. & CAO, Y. 2011. Lack of trehalose accelerates H₂O₂-induced *Candida albicans*

apoptosis through regulating Ca²⁺ signaling pathway and caspase activity. *PLoS One*, 6, e15808.

LU, H. S., FAUSSET, P. R., NARHI, L. O., HORAN, T., SHINAGAWA, K., SHIMAMOTO, G. & BOONE, T. C. 1999. Chemical modification and site-directed mutagenesis of methionine residues in recombinant human granulocyte colony-stimulating factor: effect on stability and biological activity. *Arch Biochem Biophys*, 362, 1-11.

LUKACS, G. L., ROTSTEIN, O. D. & GRINSTEIN, S. 1990. Phagosomal acidification is mediated by a vacuolar-type H(+)-ATPase in murine macrophages. *J Biol Chem*, 265, 21099-107.

LUO, S., HOFFMANN, R., SKERKA, C. & ZIPFEL, P. F. 2013a. Glycerol-3-phosphate dehydrogenase 2 is a novel factor H-, factor H-like protein 1-, and plasminogen-binding surface protein of *Candida albicans*. *J Infect Dis*, 207, 594-603.

LUO, S., POLTERMANN, S., KUNERT, A., RUPP, S. & ZIPFEL, P. F. 2009. Immune evasion of the human pathogenic yeast *Candida albicans*: Pra1 is a Factor H, FHL-1 and plasminogen binding surface protein. *Mol Immunol*, 47, 541-50.

LUO, S., SKERKA, C., KURZAI, O. & ZIPFEL, P. F. 2013b. Complement and innate immune evasion strategies of the human pathogenic fungus *Candida albicans*. *Mol Immunol*, 56, 161-9.

MAGLIONI, S., ARSALAN, N. & VENTURA, N. 2016. *C. elegans* screening strategies to identify pro-longevity interventions. *Mech Ageing Dev*, 157, 60-9.

MAJOR, J., FLETCHER, J. E. & HAMILTON, T. A. 2002. IL-4 pretreatment selectively enhances cytokine and chemokine production in lipopolysaccharide-stimulated mouse peritoneal macrophages. *J Immunol*, 168, 2456-63.

MALLO, G. V., KURZ, C. L., COUILLAULT, C., PUJOL, N., GRANJEAUD, S., KOHARA, Y. & EWBANK, J. J. 2002. Inducible antibacterial defense system in *C. elegans*. *Curr Biol*, 12, 1209-14.

MANSOUR, M. K. & LEVITZ, S. M. 2002. Interactions of fungi with phagocytes. *Curr Opin Microbiol*, 5, 359-65.

MAROTTA, D. H., NANTEL, A., SUKALA, L., TEUBL, J. R. & RAUCEO, J. M. 2013. Genome-wide transcriptional profiling and enrichment mapping reveal divergent and conserved roles of Sko1 in the *Candida albicans* osmotic stress response. *Genomics*, 15, 00123-7.

MARSH, E. K. & MAY, R. C. 2012. *Caenorhabditis elegans*, a model organism for investigating immunity. *Appl Environ Microbiol*, 78, 2075-81.

MARSHALL, H. E., MERCHANT, K. & STAMLER, J. S. 2000. Nitrosation and oxidation in the regulation of gene expression. *FASEB J*, 14, 1889-900.

MARTCHENKO, M., ALARCO, A. M., HARCUS, D. & WHITEWAY, M. 2004. Superoxide dismutases in *Candida albicans*: transcriptional regulation and functional characterization of the hyphal-induced SOD5 gene. *Mol Biol Cell*, 15, 456-67.

MARTÍNEZ, P. & LJUNDAHL, P. O. 2005. Divergence of Stp1 and Stp2 transcription factors in *Candida albicans* places virulence factors required for proper nutrient acquisition under amino acid control. *Mol Cell Biol*, 25, 9435-46.

MARTÍNEZ-ESPARZA, M., AGUINAGA, A., GONZÁLEZ-PÁRRAGA, P., GARCÍA-PEÑARRUBIA, P., JOUAUT, T. & ARGÜELLES, J. C. 2007. Role of trehalose in resistance to macrophage killing: study with a *tps1/tps1* trehalose-deficient mutant of *Candida albicans*. *Clin Microbiol Infect*, 13, 384-94.

MASSEY, S. E., MOURA, G., BELTRÃO, P., ALMEIDA, R., GAREY, J. R., TUITE, M. F. & SANTOS, M. A. 2003. Comparative evolutionary genomics unveils the molecular mechanism of reassignment of the CTG codon in *Candida* spp. *Genome Res*, 13, 544-57.

MAYER, F. L., WILSON, D. & HUBE, B. 2013. *Candida albicans* pathogenicity mechanisms. *Virulence*, 4, 119-28.

MAYER, F. L., WILSON, D., JACOBSEN, I. D., MIRAMÓN, P., SLESIONA, S., BOHOVYCH, I. M., BROWN, A. J. & HUBE, B. 2012. Small but crucial: the novel small heat shock protein Hsp21 mediates stress adaptation and virulence in *Candida albicans*. *PLoS One*, 7, e38584.

MEANS, T. K. 2010. Fungal pathogen recognition by scavenger receptors in nematodes and mammals. *Virulence*, 1, 37-41.

MEDINA-RIVERA, A., DEFRENCE, M., SAND, O., HERRMANN, C., CASTRO-MONDAGON, J. A., DELERCE, J., JAEGER, S., BLANCHET, C., VINCENS, P., CARON, C., STAINES, D. M., CONTRERAS-MOREIRA, B., ARTUFEL, M., CHARBONNIER-KHAMVONGSA, L., HERNANDEZ, C., THIEFFRY, D., THOMAS-CHOLLIER, M. & VAN HELDEN, J. 2015. RSAT 2015: Regulatory Sequence Analysis Tools. *Nucleic Acids Res*, 43, W50-6.

MEDZHITOY, R. & JANEWAY, C. A. 1997. Innate immunity: the virtues of a nonclonal system of recognition. *Cell*, 91, 295-8.

MENON, V., LI, D., CHAUHAN, N., RAJNARAYANAN, R., DUBROVSKA, A., WEST, A. H. & CALDERONE, R. 2006. Functional studies of the Ssk1p response regulator protein of *Candida albicans* as determined by phenotypic analysis of receiver domain point mutants. *Mol Microbiol*, 62, 997-1013.

MILLER, E. & GAY, N. 1997. Effect of age on outcome and epidemiology of infectious diseases. *Biologicals*, 25, 137-42.

MIRAMON, P., DUNKER, C., WINDECKER, H., BOHOVYCH, I. M., BROWN, A. J., KURZAI, O. & HUBE, B. 2012. Cellular responses of *Candida albicans* to phagocytosis and the extracellular activities of neutrophils are critical to counteract carbohydrate starvation, oxidative and nitrosative stress. *PLoS One*, 7, 21.

MIRAMON, P., KASPER, L. & HUBE, B. 2013. Thriving within the host: *Candida* spp. interactions with phagocytic cells. *Med Microbiol Immunol*, 202, 183-95.

MITCHELL, A. P. 1998. Dimorphism and virulence in *Candida albicans*. *Curr Opin Microbiol*, 1, 687-92.

MORA-MONTES, H. M., MCKENZIE, C., BAIN, J. M., LEWIS, L. E., ERWIG, L. P. & GOW, N. A. 2012. Interactions between macrophages and cell wall oligosaccharides of *Candida albicans*. *Methods Mol Biol*, 845, 247-60.

MORGAN, B. A., BANKS, G. R., TOONE, W. M., RAITT, D., KUGE, S. & JOHNSTON, L. H. 1997. The Skn7 response regulator controls gene expression in the oxidative stress response of the budding yeast *Saccharomyces cerevisiae*. *EMBO J*, 16, 1035-44.

MORGAN, J. 2005. Global trends in candidemia: review of reports from 1995-2005. *Curr Infect Dis Rep*, 7, 429-39.

MOYE-ROWLEY, W. S. 2003. Regulation of the transcriptional response to oxidative stress in fungi: similarities and differences. *Eukaryot Cell*, 2, 381-9.

MOYE-ROWLEY, W. S., HARSHMAN, K. D. & PARKER, C. S. 1988. YAP1 encodes a yeast homolog of mammalian transcription factor AP-1. *Cold Spring Harb Symp Quant Biol*, 53 Pt 2, 711-7.

MOYE-ROWLEY, W. S., HARSHMAN, K. D. & PARKER, C. S. 1989. Yeast YAP1 encodes a novel form of the jun family of transcriptional activator proteins. *Genes Dev*, 3, 283-92.

MOYES, D. L., RICHARDSON, J. P. & NAGLIK, J. R. 2015. Candida albicans-epithelial interactions and pathogenicity mechanisms: scratching the surface. *Virulence*, 6, 338-46.

MOYES, D. L., RUNGLALL, M., MURCIANO, C., SHEN, C., NAYAR, D., THAVARAJ, S., KOHLI, A., ISLAM, A., MORA-MONTES, H., CHALLACOMBE, S. J. & NAGLIK, J. R. 2010. A biphasic innate immune MAPK response discriminates between the yeast and hyphal forms of Candida albicans in epithelial cells. *Cell Host Microbe*, 8, 225-35.

MULFORD, K. E. & FASSLER, J. S. 2011. Association of the Skn7 and Yap1 transcription factors in the *Saccharomyces cerevisiae* oxidative stress response. *Eukaryot Cell*, 10, 761-9.

MURAD, A. M., LEE, P. R., BROADBENT, I. D., BARELLE, C. J. & BROWN, A. J. 2000. Clp10, an efficient and convenient integrating vector for *Candida albicans*. *Yeast*, 16, 325-7.

MURPHY, J. W. 1991. Mechanisms of natural resistance to human pathogenic fungi. *Annu Rev Microbiol*, 45, 509-38.

MYLONAKIS, E., CASADEVALL, A. & AUSUBEL, F. M. 2007. Exploiting amoeboid and non-vertebrate animal model systems to study the virulence of human pathogenic fungi. *PLoS Pathog*, 3, e101.

NAGLIK, J. R., MOYES, D. L., WACHTLER, B. & HUBE, B. 2011. Candida albicans interactions with epithelial cells and mucosal immunity. *Microbes Infect*, 13, 963-76.

NAKAGAWA, Y., KANBE, T. & MIZUGUCHI, I. 2003. Disruption of the human pathogenic yeast *Candida albicans* catalase gene decreases survival in mouse-model infection and elevates susceptibility to higher temperature and to detergents. *Microbiol Immunol*, 47, 395-403.

NASUTION, O., SRINIVASA, K., KIM, M., KIM, Y. J., KIM, W., JEONG, W. & CHOI, W. 2008. Hydrogen peroxide induces hyphal differentiation in *Candida albicans*. *Eukaryot Cell*, 7, 2008-11.

NATHAN, C. & SHILOH, M. U. 2000. Reactive oxygen and nitrogen intermediates in the relationship between mammalian hosts and microbial pathogens. *Proc Natl Acad Sci U S A*, 97, 8841-8.

NETEA, M. G., BROWN, G. D., KULLBERG, B. J. & GOW, N. A. 2008. An integrated model of the recognition of *Candida albicans* by the innate immune system. *Nat Rev Microbiol*, 6, 67-78.

NETEA, M. G., FERWERDA, G., VAN DER GRAAF, C. A., VAN DER MEER, J. W. & KULLBERG, B. J. 2006. Recognition of fungal pathogens by toll-like receptors. *Curr Pharm Des*, 12, 4195-201.

NETEA, M. G., GIJZEN, K., COOLEN, N., VERSCHUEREN, I., FIGDOR, C., VAN DER MEER, J. W., TORENSMA, R. & KULLBERG, B. J. 2004. Human

dendritic cells are less potent at killing *Candida albicans* than both monocytes and macrophages. *Microbes Infect*, 6, 985-9.

NEUHÄUSER, B., DUNKEL, N., SATHEESH, S. V. & MORSCHHÄUSER, J. 2011. Role of the Npr1 kinase in ammonium transport and signaling by the ammonium permease Mep2 in *Candida albicans*. *Eukaryot Cell*, 10, 332-42.

NEWMAN, S. L. & HOLLY, A. 2001. *Candida albicans* is phagocytosed, killed, and processed for antigen presentation by human dendritic cells. *Infect Immun*, 69, 6813-22.

NG, W. F., VON DELWIG, A., CARMICHAEL, A. J., ARKWRIGHT, P. D., ABINUN, M., CANT, A. J., JOLLES, S. & LILIC, D. 2010. Impaired T(H)17 responses in patients with chronic mucocutaneous candidiasis with and without autoimmune polyendocrinopathy-candidiasis-ectodermal dystrophy. *J Allergy Clin Immunol*, 126, 1006-15.

NGUYEN, A. N. & SHIOZAKI, K. 1999. Heat-shock-induced activation of stress MAP kinase is regulated by threonine- and tyrosine-specific phosphatases. *Genes Dev*, 13, 1653-63.

NGUYEN, D. T., ALARCO, A. M. & RAYMOND, M. 2001. Multiple Yap1p-binding sites mediate induction of the yeast major facilitator FLR1 gene in response to drugs, oxidants, and alkylating agents. *J Biol Chem*, 276, 1138-45.

NIKOLAOU, E., AGRAFIOTI, I., STUMPF, M., QUINN, J., STANSFIELD, I. & BROWN, A. J. 2009. Phylogenetic diversity of stress signalling pathways in fungi. *BMC Evol Biol*, 9, 44.

NOBILE, C. J., FOX, E. P., NETT, J. E., SORRELLS, T. R., MITROVICH, Q. M., HERNDAY, A. D., TUCH, B. B., ANDES, D. R. & JOHNSON, A. D. 2012. A recently evolved transcriptional network controls biofilm development in *Candida albicans*. *Cell*, 148, 126-38.

NOBLE, S. M. & JOHNSON, A. D. 2005. Strains and strategies for large-scale gene deletion studies of the diploid human fungal pathogen *Candida albicans*. *Eukaryot Cell*, 4, 298-309.

NORDENFELT, P., WINBERG, M. E., LONNBRO, P., RASMUSSON, B. & TAPPER, H. 2009. Different requirements for early and late phases of azurophilic granule-phagosome fusion. *Traffic*, 10, 1881-93.

OBIN, M., SHANG, F., GONG, X., HANDELMAN, G., BLUMBERG, J. & TAYLOR, A. 1998. Redox regulation of ubiquitin-conjugating enzymes: mechanistic insights using the thiol-specific oxidant diamide. *FASEB J*, 12, 561-9.

ODDS, F. C. 1979. *Candida and candidosis*.

OEHLER, L., MAJDIC, O., PICKL, W. F., STÖCKL, J., RIEDL, E., DRACH, J., RAPPERSBERGER, K., GEISSLER, K. & KNAPP, W. 1998. Neutrophil granulocyte-committed cells can be driven to acquire dendritic cell characteristics. *J Exp Med*, 187, 1019-28.

OKADA, S., MARKLE, J. G., DEENICK, E. K., MELE, F., AVERBUCH, D., LAGOS, M., ALZAHARANI, M., AL-MUHSEN, S., HALWANI, R., MA, C. S., WONG, N., SOUDAIS, C., HENDERSON, L. A., MARZOUQA, H., SHAMMA, J., GONZALEZ, M., MARTINEZ-BARRICARTE, R., OKADA, C., AVERY, D. T., LATORRE, D., DESWARTE, C., JABOT-HANIN, F., TORRADO, E., FOUNTAIN, J., BELKADI, A., ITAN, Y., BOISSON, B., MIGAUD, M., ARLEHAMN, C. S., SETTE, A., BRETON, S., MCCLUSKEY, J., ROSSJOHN, J., DE VILLARTAY, J. P., MOSHOUS, D., HAMBLETON, S., LATOUR, S.,

ARKWRIGHT, P. D., PICARD, C., LANTZ, O., ENGELHARD, D., KOBAYASHI, M., ABEL, L., COOPER, A. M., NOTARANGELO, L. D., BOISSON-DUPUIS, S., PUEL, A., SALLUSTO, F., BUSTAMANTE, J., TANGYE, S. G. & CASANOVA, J. L. 2015. IMMUNODEFICIENCIES. Impairment of immunity to *Candida* and *Mycobacterium* in humans with bi-allelic RORC mutations. *Science*, 349, 606-13.

OKAZAKI, S., NAGANUMA, A. & KUGE, S. 2005. Peroxiredoxin-mediated redox regulation of the nuclear localization of Yap1, a transcription factor in budding yeast. *Antioxid Redox Signal*, 7, 327-34.

OKAZAKI, S., TACHIBANA, T., NAGANUMA, A., MANO, N. & KUGE, S. 2007. Multistep disulfide bond formation in Yap1 is required for sensing and transduction of H₂O₂ stress signal. *Mol Cell*, 27, 675-88.

OLINSKI, R., GACKOWSKI, D., FOKSINSKI, M., ROZALSKI, R., ROSZKOWSKI, K. & JARUGA, P. 2002. Oxidative DNA damage: assessment of the role in carcinogenesis, atherosclerosis, and acquired immunodeficiency syndrome. *Free Radic Biol Med*, 33, 192-200.

PALMER, G. E., KELLY, M. N. & STURTEVANT, J. E. 2007. Autophagy in the pathogen *Candida albicans*. *Microbiology*, 153, 51-8.

PANDA, A., ARJONA, A., SAPEY, E., BAI, F., FIKRIG, E., MONTGOMERY, R. R., LORD, J. M. & SHAW, A. C. 2009. Human innate immunosenescence: causes and consequences for immunity in old age. *Trends Immunol*, 30, 325-33.

PANDA, S. K. & UPADHYAY, R. K. 2004. Salt Stress Injury Induces Oxidative Alterations and Antioxidative Defence in the Roots of *Lemna minor*. *Biologia Plantarum*, 48, 249-253.

PAPPAS, P. G. 2006. Invasive candidiasis. *Infect Dis Clin North Am*, 20, 485-506.

PARIS, S., WYSONG, D., DEBEAUPUIS, J. P., SHIBUYA, K., PHILIPPE, B., DIAMOND, R. D. & LATGÉ, J. P. 2003. Catalases of *Aspergillus fumigatus*. *Infect Immun*, 71, 3551-62.

PASQUALOTTO, A. C., NEDEL, W. L., MACHADO, T. S. & SEVERO, L. C. 2006. Risk factors and outcome for nosocomial breakthrough candidaemia. *J Infect*, 52, 216-22.

PATTERSON, M. J., MCKENZIE, C. G., SMITH, D. A., DA SILVA DANTAS, A., SHERSTON, S., VEAL, E. A., MORGAN, B. A., MACCALLUM, D. M., ERWIG, L. P. & QUINN, J. 2013. Ybp1 and Gpx3 Signaling in *Candida albicans* Govern Hydrogen Peroxide-Induced Oxidation of the Cap1 Transcription Factor and Macrophage Escape. *Antioxid Redox Signal*.

PERLROTH, J., CHOI, B. & SPELLBERG, B. 2007. Nosocomial fungal infections: epidemiology, diagnosis, and treatment. *Med Mycol*, 45, 321-46.

PFALLER, M. A. & DIEKEMA, D. J. 2007. Epidemiology of invasive candidiasis: a persistent public health problem. *Clin Microbiol Rev*, 20, 133-63.

PFALLER, M. A., DIEKEMA, D. J., GIBBS, D. L., NEWELL, V. A., ELLIS, D., TULLIO, V., RODLOFF, A., FU, W., LING, T. A. & GROUP, G. A. S. 2010. Results from the ARTEMIS DISK Global Antifungal Surveillance Study, 1997 to 2007: a 10.5-year analysis of susceptibilities of *Candida* Species to fluconazole and voriconazole as determined by CLSI standardized disk diffusion. *J Clin Microbiol*, 48, 1366-77.

PFALLER, M. A., JONES, R. N., DOERN, G. V., SADER, H. S., HOLLIS, R. J. & MESSER, S. A. 1998. International surveillance of bloodstream infections due

to *Candida* species: frequency of occurrence and antifungal susceptibilities of isolates collected in 1997 in the United States, Canada, and South America for the SENTRY Program. The SENTRY Participant Group. *J Clin Microbiol*, 36, 1886-9.

PHILLIPS, A. J., SUDBERY, I. & RAMSDALE, M. 2003. Apoptosis induced by environmental stresses and amphotericin B in *Candida albicans*. *Proc Natl Acad Sci U S A*, 100, 14327-32.

POLTERMANN, S., KUNERT, A., VON DER HEIDE, M., ECK, R., HARTMANN, A. & ZIPFEL, P. F. 2007. Gpm1p is a factor H-, FHL-1-, and plasminogen-binding surface protein of *Candida albicans*. *J Biol Chem*, 282, 37537-44.

POSAS, F., CHAMBERS, J. R., HEYMAN, J. A., HOEFFLER, J. P., DE NADAL, E. & ARIÑO, J. 2000. The transcriptional response of yeast to saline stress. *J Biol Chem*, 275, 17249-55.

POSAS, F. & SAITO, H. 1998. Activation of the yeast SSK2 MAP kinase kinase kinase by the SSK1 two-component response regulator. *EMBO J*, 17, 1385-94.

POSAS, F., WURGLER-MURPHY, S. M., MAEDA, T., WITTEN, E. A., THAI, T. C. & SAITO, H. 1996. Yeast HOG1 MAP kinase cascade is regulated by a multistep phosphorelay mechanism in the SLN1-YPD1-SSK1 "two-component" osmosensor. *Cell*, 86, 865-75.

POWELL, J. R., KIM, D. H. & AUSUBEL, F. M. 2009. The G protein-coupled receptor FSHR-1 is required for the *Caenorhabditis elegans* innate immune response. *Proc Natl Acad Sci U S A*, 106, 2782-7.

PRIETO, D., ROMÁN, E., CORREIA, I. & PLA, J. 2014. The HOG pathway is critical for the colonization of the mouse gastrointestinal tract by *Candida albicans*. *PLoS One*, 9, e87128.

PUEL, A., CYPOWYJ, S., BUSTAMANTE, J., WRIGHT, J. F., LIU, L., LIM, H. K., MIGAUD, M., ISRAEL, L., CHRABIEH, M., AUDRY, M., GUMBLETON, M., TOULON, A., BODEMER, C., EL-BAGHDADI, J., WHITTERS, M., PARADIS, T., BROOKS, J., COLLINS, M., WOLFMAN, N. M., AL-MUHSEN, S., GALICCHIO, M., ABEL, L., PICARD, C. & CASANOVA, J. L. 2011. Chronic mucocutaneous candidiasis in humans with inborn errors of interleukin-17 immunity. *Science*, 332, 65-8.

PUKKILA-WORLEY, R. & AUSUBEL, F. M. 2012. Immune defense mechanisms in the *Caenorhabditis elegans* intestinal epithelium. *Curr Opin Immunol*, 24, 3-9.

PUKKILA-WORLEY, R., AUSUBEL, F. M. & MYLONAKIS, E. 2011. *Candida albicans* infection of *Caenorhabditis elegans* induces antifungal immune defenses. *PLoS Pathog*, 7, e1002074.

PUKKILA-WORLEY, R., PELEG, A. Y., TAMPAKAKIS, E. & MYLONAKIS, E. 2009. *Candida albicans* hyphal formation and virulence assessed using a *Caenorhabditis elegans* infection model. *Eukaryot Cell*, 8, 1750-8.

QIAO, J., KONTOYIANNIS, D. P., CALDERONE, R., LI, D., MA, Y., WAN, Z., LI, R. & LIU, W. 2008. Afyap1, encoding a bZip transcriptional factor of *Aspergillus fumigatus*, contributes to oxidative stress response but is not essential to the virulence of this pathogen in mice immunosuppressed by cyclophosphamide and triamcinolone. *Med Mycol*, 46, 773-82.

QUINN, J., FINDLAY, V. J., DAWSON, K., MILLAR, J. B., JONES, N., MORGAN, B. A. & TOONE, W. M. 2002. Distinct regulatory proteins control the graded

transcriptional response to increasing H₂O₂ levels in fission yeast *Schizosaccharomyces pombe*. *Mol Biol Cell*, 13, 805-16.

QUINN, J., MALAKASI, P., SMITH, D. A., CHEETHAM, J., BUCK, V., MILLAR, J. B. & MORGAN, B. A. 2011. Two-component mediated peroxide sensing and signal transduction in fission yeast. *Antioxid Redox Signal*, 15, 153-65.

QUINTIN, J., SAEED, S., MARTENS, J. H., GIAMARELLOS-BOURBOULIS, E. J., IFRIM, D. C., LOGIE, C., JACOBS, L., JANSEN, T., KULLBERG, B. J., WIJMENGA, C., JOOSTEN, L. A., XAVIER, R. J., VAN DER MEER, J. W., STUNNENBERG, H. G. & NETEA, M. G. 2012. *Candida albicans* infection affords protection against reinfection via functional reprogramming of monocytes. *Cell Host Microbe*, 12, 223-32.

QUINTIN, J., VOIGT, J., VAN DER VOORT, R., JACOBSEN, I. D., VERSCHUEREN, I., HUBE, B., GIAMARELLOS-BOURBOULIS, E. J., VAN DER MEER, J. W., JOOSTEN, L. A., KURZAI, O. & NETEA, M. G. 2014. Differential role of NK cells against *Candida albicans* infection in immunocompetent or immunocompromised mice. *Eur J Immunol*, 44, 2405-14.

RAI, M. N., BALUSU, S., GORITYALA, N., DANDU, L. & KAUR, R. 2012. Functional genomic analysis of *Candida glabrata*-macrophage interaction: role of chromatin remodeling in virulence. *PLoS Pathog*, 8, e1002863.

RAMÍREZ, M. A. & LORENZ, M. C. 2007. Mutations in alternative carbon utilization pathways in *Candida albicans* attenuate virulence and confer pleiotropic phenotypes. *Eukaryot Cell*, 6, 280-90.

RAMÍREZ-ZAVALA, B., MOGAVERO, S., SCHÖLLER, E., SASSE, C., ROGERS, P. D. & MORSCHHHÄUSER, J. 2014. SAGA/ADA complex subunit Ada2 is required for Cap1- but not Mrr1-mediated upregulation of the *Candida albicans* multidrug efflux pump MDR1. *Antimicrob Agents Chemother*, 58, 5102-10.

REEVES, E. P., LU, H., JACOBS, H. L., MESSINA, C. G., BOLSOVER, S., GABELLA, G., POTMA, E. O., WARLEY, A., ROES, J. & SEGAL, A. W. 2002. Killing activity of neutrophils is mediated through activation of proteases by K⁺ flux. *Nature*, 416, 291-7.

REITER, W., KLOPF, E., DE WEVER, V., ANRATHER, D., PETRYSHYN, A., ROETZER, A., NIEDERACHER, G., ROITINGER, E., DOHNAL, I., GÖRNER, W., MECHTLER, K., BROCARD, C., SCHÜLLER, C. & AMMERER, G. 2013. Yeast protein phosphatase 2A-Cdc55 regulates the transcriptional response to hyperosmolarity stress by regulating Msn2 and Msn4 chromatin recruitment. *Mol Cell Biol*, 33, 1057-72.

RICHARDSON, M. D. 2005. Changing patterns and trends in systemic fungal infections. *J Antimicrob Chemother*, 56 Suppl 1, i5-i11.

ROBINSON, J. T., THORVALDSDÓTTIR, H., WINCKLER, W., GUTTMAN, M., LANDER, E. S., GETZ, G. & MESIROV, J. P. 2011. Integrative genomics viewer. *Nat Biotechnol*, 29, 24-6.

ROCHA, C. R., SCHRÖPPEL, K., HARCUS, D., MARCIL, A., DIGNARD, D., TAYLOR, B. N., THOMAS, D. Y., WHITEWAY, M. & LEBERER, E. 2001. Signaling through adenylyl cyclase is essential for hyphal growth and virulence in the pathogenic fungus *Candida albicans*. *Mol Biol Cell*, 12, 3631-43.

ROETZER, A., GRATZ, N., KOVARIK, P. & SCHÜLLER, C. 2010. Autophagy supports *Candida glabrata* survival during phagocytosis. *Cell Microbiol*, 12, 199-216.

ROETZER, A., GREGORI, C., JENNINGS, A. M., QUINTIN, J., FERRANDON, D., BUTLER, G., KUCHLER, K., AMMERER, G. & SCHÜLLER, C. 2008. *Candida glabrata* environmental stress response involves *Saccharomyces cerevisiae* Msn2/4 orthologous transcription factors. *Mol Microbiol*, 69, 603-20.

ROETZER, A., KLOPF, E., GRATZ, N., MARCET-HOUBEN, M., HILLER, E., RUPP, S., GABALDÓN, T., KOVARIK, P. & SCHÜLLER, C. 2011. Regulation of *Candida glabrata* oxidative stress resistance is adapted to host environment. *FEBS Lett*, 585, 319-27.

ROMAGNOLI, G., NISINI, R., CHIANI, P., MARIOTTI, S., TELONI, R., CASSONE, A. & TOROSANTUCCI, A. 2004. The interaction of human dendritic cells with yeast and germ-tube forms of *Candida albicans* leads to efficient fungal processing, dendritic cell maturation, and acquisition of a Th1 response-promoting function. *J Leukoc Biol*, 75, 117-26.

ROMANI, L. 2004. Immunity to fungal infections. *Nat Rev Immunol*, 4, 1-23.

ROMANI, L. 2011. Immunity to fungal infections. *Nat Rev Immunol*, 11, 275-88.

ROMÁN, E., ARANA, D. M., NOMBELA, C., ALONSO-MONGE, R. & PLA, J. 2007. MAP kinase pathways as regulators of fungal virulence. *Trends Microbiol*, 15, 181-90.

ROMÁN, E., NOMBELA, C. & PLA, J. 2005. The Sho1 adaptor protein links oxidative stress to morphogenesis and cell wall biosynthesis in the fungal pathogen *Candida albicans*. *Mol Cell Biol*, 25, 10611-27.

RUBIN-BEJERANO, I., FRASER, I., GRISAFI, P. & FINK, G. R. 2003. Phagocytosis by neutrophils induces an amino acid deprivation response in *Saccharomyces cerevisiae* and *Candida albicans*. *Proc Natl Acad Sci U S A*, 100, 11007-12.

RUDKIN, F. M., BAIN, J. M., WALLS, C., LEWIS, L. E., GOW, N. A. & ERWIG, L. P. 2013. Altered dynamics of *Candida albicans* phagocytosis by macrophages and PMNs when both phagocyte subsets are present. *MBio*, 4, e00810-13.

SAIJO, T., MIYAZAKI, T., IZUMIKAWA, K., MIHARA, T., TAKAZONO, T., KOSAI, K., IMAMURA, Y., SEKI, M., KAKEYA, H., YAMAMOTO, Y., YANAGIHARA, K. & KOHNO, S. 2010. Skn7p is involved in oxidative stress response and virulence of *Candida glabrata*. *Mycopathologia*, 169, 81-90.

SASADA, M. & JOHNSTON, R. B. 1980. Macrophage microbicidal activity. Correlation between phagocytosis-associated oxidative metabolism and the killing of *Candida* by macrophages. *J Exp Med*, 152, 85-98.

SATO, K., YANG, X. L., YUDATE, T., CHUNG, J. S., WU, J., LUBY-PHELPS, K., KIMBERLY, R. P., UNDERHILL, D., CRUZ, P. D. & ARIIZUMI, K. 2006. Dectin-2 is a pattern recognition receptor for fungi that couples with the Fc receptor gamma chain to induce innate immune responses. *J Biol Chem*, 281, 38854-66.

SEGAL, A. W. 2005. How neutrophils kill microbes. *Annu Rev Immunol*, 23, 197-223.

SEGAL, A. W., GEISOW, M., GARCIA, R., HARPER, A. & MILLER, R. 1981. The respiratory burst of phagocytic cells is associated with a rise in vacuolar pH. *Nature*, 290, 406-9.

SEGAL, B. H., KWON-CHUNG, J., WALSH, T. J., KLEIN, B. S., BATTIWALLA, M., ALMYROUDIS, N. G., HOLLAND, S. M. & ROMANI, L. 2006. Immunotherapy for fungal infections. *Clin Infect Dis*, 42, 507-15.

SEIDER, K., BRUNKE, S., SCHILD, L., JABLONOWSKI, N., WILSON, D., MAJER, O., BARZ, D., HAAS, A., KUCHLER, K., SCHALLER, M. & HUBE, B. 2011.

The facultative intracellular pathogen *Candida glabrata* subverts macrophage cytokine production and phagolysosome maturation. *J Immunol*, 187, 3072-86.

SEIDER, K., GERWIEN, F., KASPER, L., ALLERT, S., BRUNKE, S., JABLONOWSKI, N., SCHWARZMÜLLER, T., BARZ, D., RUPP, S., KUCHLER, K. & HUBE, B. 2014. Immune evasion, stress resistance, and efficient nutrient acquisition are crucial for intracellular survival of *Candida glabrata* within macrophages. *Eukaryot Cell*, 13, 170-83.

SELLAM, A., ASKEW, C., EPP, E., LAVOIE, H., WHITEWAY, M. & NANTEL, A. 2009. Genome-wide mapping of the coactivator Ada2p yields insight into the functional roles of SAGA/ADA complex in *Candida albicans*. *Mol Biol Cell*, 20, 2389-400.

SELLAM, A., TEBBJI, F., WHITEWAY, M. & NANTEL, A. 2012. A novel role for the transcription factor Cwt1p as a negative regulator of nitrosative stress in *Candida albicans*. *PLoS One*, 7, 29.

SHANLEY, D. P., AW, D., MANLEY, N. R. & PALMER, D. B. 2009. An evolutionary perspective on the mechanisms of immunosenescence. *Trends Immunol*, 30, 374-81.

SHEN, P., YUE, Y. & PARK, Y. 2016. A Living Model for Obesity and Aging Research: *Caenorhabditis elegans*. *Crit Rev Food Sci Nutr*, 0.

SHENTON, D., SMIRNOVA, J. B., SELLEY, J. N., CARROLL, K., HUBBARD, S. J., PAVITT, G. D., ASHE, M. P. & GRANT, C. M. 2006. Global translational responses to oxidative stress impact upon multiple levels of protein synthesis. *J Biol Chem*, 281, 29011-21.

SHERMAN, F. 1991. Getting started with yeast. *Methods Enzymol*, 194, 3-21.

SHI, Q. M., WANG, Y. M., ZHENG, X. D., LEE, R. T. & WANG, Y. 2007. Critical role of DNA checkpoints in mediating genotoxic-stress-induced filamentous growth in *Candida albicans*. *Mol Biol Cell*, 18, 815-26.

SHIVERS, R. P., YOUNGMAN, M. J. & KIM, D. H. 2008. Transcriptional responses to pathogens in *Caenorhabditis elegans*. *Curr Opin Microbiol*, 11, 251-6.

SHOHAM, S. & LEVITZ, S. M. 2005. The immune response to fungal infections. *Br J Haematol*, 129, 569-82.

SIFRI, C. D., BEGUN, J. & AUSUBEL, F. M. 2005. The worm has turned--microbial virulence modeled in *Caenorhabditis elegans*. *Trends Microbiol*, 13, 119-27.

SIMONSEN, K. T., GALLEGOS, S. F., FÆRGEMAN, N. J. & KALLIPOLITIS, B. H. 2012. Strength in numbers: "Omics" studies of *C. elegans* innate immunity. *Virulence*, 3, 477-84.

SINGH, P., CHAUHAN, N., GHOSH, A., DIXON, F. & CALDERONE, R. 2004. SKN7 of *Candida albicans*: mutant construction and phenotype analysis. *Infect Immun*, 72, 2390-4.

SINGH, R. P., PRASAD, H. K., SINHA, I., AGARWAL, N. & NATARAJAN, K. 2011. Cap2-HAP complex is a critical transcriptional regulator that has dual but contrasting roles in regulation of iron homeostasis in *Candida albicans*. *J Biol Chem*, 286, 25154-70.

SMITH, D. A., MORGAN, B. A. & QUINN, J. 2010. Stress signalling to fungal stress-activated protein kinase pathways. *FEMS Microbiol Lett*, 306, 1-8.

SMITH, D. A., NICHOLLS, S., MORGAN, B. A., BROWN, A. J. & QUINN, J. 2004. A conserved stress-activated protein kinase regulates a core stress response in the human pathogen *Candida albicans*. *Mol Biol Cell*, 15, 4179-90.

SOBEL, J. D. 2007. Vulvovaginal candidosis. *Lancet*, 369, 1961-71.

SOLOVIEV, D. A., JAWHARA, S. & FONZI, W. A. 2011. Regulation of innate immune response to *Candida albicans* infections by alphaMbeta2-Pra1p interaction. *Infect Immun*, 79, 1546-58.

SQUIBAN, B. & KURZ, C. L. 2011. *C. elegans*: an all in one model for antimicrobial drug discovery. *Curr Drug Targets*, 12, 967-77.

SRINIVASA, K., KIM, N. R., KIM, J., KIM, M., BAE, J. Y., JEONG, W., KIM, W. & CHOI, W. 2012. Characterization of a putative thioredoxin peroxidase prx1 of *Candida albicans*. *Mol Cells*, 33, 301-7.

STEINBERG, B. E., HUYNH, K. K., BRODOVITCH, A., JABS, S., STAUBER, T., JENTSCH, T. J. & GRINSTEIN, S. 2010. A cation counterflux supports lysosomal acidification. *J Cell Biol*, 189, 1171-86.

STEINBERG, B. E., HUYNH, K. K. & GRINSTEIN, S. 2007. Phagosomal acidification: measurement, manipulation and functional consequences. *Biochem Soc Trans*, 35, 1083-7.

STEINMAN, R. M. 1991. The dendritic cell system and its role in immunogenicity. *Annu Rev Immunol*, 9, 271-96.

STOCK, A. M., ROBINSON, V. L. & GOUDREAU, P. N. 2000. Two-component signal transduction. *Annu Rev Biochem*, 69, 183-215.

SUDBERY, P., GOW, N. & BERMAN, J. 2004. The distinct morphogenic states of *Candida albicans*. *Trends Microbiol*, 12, 317-24.

SUDBERY, P. E. 2011. Growth of *Candida albicans* hyphae. *Nat Rev Microbiol*, 9, 737-48.

TACHIBANA, T., OKAZAKI, S., MURAYAMA, A., NAGANUMA, A., NOMOTO, A. & KUGE, S. 2009. A major peroxiredoxin-induced activation of Yap1 transcription factor is mediated by reduction-sensitive disulfide bonds and reveals a low level of transcriptional activation. *J Biol Chem*, 284, 4464-72.

TADA, H., NEMOTO, E., SHIMAUCHI, H., WATANABE, T., MIKAMI, T., MATSUMOTO, T., OHNO, N., TAMURA, H., SHIBATA, K., AKASHI, S., MIYAKE, K., SUGAWARA, S. & TAKADA, H. 2002. *Saccharomyces cerevisiae*- and *Candida albicans*-derived mannan induced production of tumor necrosis factor alpha by human monocytes in a CD14- and Toll-like receptor 4-dependent manner. *Microbiol Immunol*, 46, 503-12.

TAN, M. W., MAHAJAN-MIKLOS, S. & AUSUBEL, F. M. 1999. Killing of *Caenorhabditis elegans* by *Pseudomonas aeruginosa* used to model mammalian bacterial pathogenesis. *Proc Natl Acad Sci U S A*, 96, 715-20.

TAVANTI, A., CAMPA, D., BERTOZZI, A., PARDINI, G., NAGLIK, J. R., BARALE, R. & SENESI, S. 2006. *Candida albicans* isolates with different genomic backgrounds display a differential response to macrophage infection. *Microbes Infect*, 8, 791-800.

THEWES, S., KRETSCHMAR, M., PARK, H., SCHALLER, M., FILLER, S. G. & HUBE, B. 2007. In vivo and ex vivo comparative transcriptional profiling of invasive and non-invasive *Candida albicans* isolates identifies genes associated with tissue invasion. *Mol Microbiol*, 63, 1606-28.

THOMAS, E., ROMAN, E., CLAYPOOL, S., MANZOOR, N., PLA, J. & PANWAR, S. L. 2013. Mitochondria influence CDR1 efflux pump activity, Hog1-mediated oxidative stress pathway, iron homeostasis, and ergosterol levels in *Candida albicans*. *Antimicrob Agents Chemother*, 57, 5580-99.

THRASHER, A. J., KEEP, N. H., WIENTJES, F. & SEGAL, A. W. 1994. Chronic granulomatous disease. *Biochim Biophys Acta*, 1227, 1-24.

TILLMANN, A. T., STRIJBIS, K., CAMERON, G., RADMANESHFAR, E., THIEL, M., MUNRO, C. A., MACCALLUM, D. M., DISTEL, B., GOW, N. A. & BROWN, A. J. 2015. Contribution of Fdh3 and Glr1 to Glutathione Redox State, Stress Adaptation and Virulence in *Candida albicans*. *PLoS One*, 10, e0126940.

TODA, T., SHIMANUKI, M. & YANAGIDA, M. 1991. Fission yeast genes that confer resistance to staurosporine encode an AP-1-like transcription factor and a protein kinase related to the mammalian ERK1/MAP2 and budding yeast FUS3 and KSS1 kinases. *Genes Dev*, 5, 60-73.

TOONE, W. M., KUGE, S., SAMUELS, M., MORGAN, B. A., TODA, T. & JONES, N. 1998. Regulation of the fission yeast transcription factor Pap1 by oxidative stress: requirement for the nuclear export factor Crm1 (Exportin) and the stress-activated MAP kinase Sty1/Spc1. *Genes Dev*, 12, 1453-63.

TRICK, W. E., FRIDKIN, S. K., EDWARDS, J. R., HAJJEH, R. A., GAYNES, R. P. & HOSPITALS, N. N. I. S. S. 2002. Secular trend of hospital-acquired candidemia among intensive care unit patients in the United States during 1989-1999. *Clin Infect Dis*, 35, 627-30.

TRIPATHI, G., WILTSHERE, C., MACASKILL, S., TOURNU, H., BUDGE, S. & BROWN, A. J. 2002. Gcn4 co-ordinates morphogenetic and metabolic responses to amino acid starvation in *Candida albicans*. *EMBO J*, 21, 5448-56.

TROEMEL, E. R., CHU, S. W., REINKE, V., LEE, S. S., AUSUBEL, F. M. & KIM, D. H. 2006. p38 MAPK regulates expression of immune response genes and contributes to longevity in *C. elegans*. *PLoS Genet*, 2, e183.

TROEMEL, E. R., FÉLIX, M. A., WHITEMAN, N. K., BARRIÈRE, A. & AUSUBEL, F. M. 2008. Microsporidia are natural intracellular parasites of the nematode *Caenorhabditis elegans*. *PLoS Biol*, 6, 2736-52.

TSAI, Y.-C., HONG, C.-Y., LIU, L.-F. & KAO, C. H. 2004. Relative importance of Na⁺ and Cl⁻ in NaCl-induced antioxidant systems in roots of rice seedlings. *Physiologia Plantarum*, 122, 86-94.

UEDA, M., MOZAFFAR, S. & TANAKA, A. 1990. Catalase from *Candida boidinii* 2201. *Methods Enzymol*, 188, 463-7.

ULLMANN, B. D., MYERS, H., CHIRANAND, W., LAZZELL, A. L., ZHAO, Q., VEGA, L. A., LOPEZ-RIBOT, J. L., GARDNER, P. R. & GUSTIN, M. C. 2004. Inducible defense mechanism against nitric oxide in *Candida albicans*. *Eukaryot Cell*, 3, 715-23.

UNDERHILL, D. M. & OZINSKY, A. 2002. Phagocytosis of microbes: complexity in action. *Annu Rev Immunol*, 20, 825-52.

UNDERHILL, D. M. & PEARLMAN, E. 2015. Immune Interactions with Pathogenic and Commensal Fungi: A Two-Way Street. *Immunity*, 43, 845-58.

URBAN, C., XIONG, X., SOHN, K., SCHRÖPPEL, K., BRUNNER, H. & RUPP, S. 2005. The moonlighting protein Tsa1p is implicated in oxidative stress response and in cell wall biogenesis in *Candida albicans*. *Mol Microbiol*, 57, 1318-41.

URBAN, C. F., ERMERT, D., SCHMID, M., ABU-ABED, U., GOOSMANN, C., NACKEN, W., BRINKMANN, V., JUNGBLUT, P. R. & ZYCHLINSKY, A. 2009.

Neutrophil extracellular traps contain calprotectin, a cytosolic protein complex involved in host defense against *Candida albicans*. *PLoS Pathog*, 5, 30.

URBAN, C. F., REICHARD, U., BRINKMANN, V. & ZYCHLINSKY, A. 2006. Neutrophil extracellular traps capture and kill *Candida albicans* yeast and hyphal forms. *Cell Microbiol*, 8, 668-76.

VAZQUEZ-TORRES, A. & BALISH, E. 1997. Macrophages in resistance to candidiasis. *Microbiol Mol Biol Rev*, 61, 170-92.

VAZQUEZ-TORRES, A., JONES-CARSON, J. & BALISH, E. 1996. Peroxynitrite contributes to the candidacidal activity of nitric oxide-producing macrophages. *Infect Immun*, 64, 3127-33.

VEAL, E. A., FINDLAY, V. J., DAY, A. M., BOZONET, S. M., EVANS, J. M., QUINN, J. & MORGAN, B. A. 2004. A 2-Cys peroxiredoxin regulates peroxide-induced oxidation and activation of a stress-activated MAP kinase. *Mol Cell*, 15, 129-39.

VEAL, E. A., ROSS, S. J., MALAKASI, P., PEACOCK, E. & MORGAN, B. A. 2003. Ybp1 is required for the hydrogen peroxide-induced oxidation of the Yap1 transcription factor. *J Biol Chem*, 278, 30896-904.

VISSCHER, M., DE HENAU, S., WILDSCHUT, M. H., VAN ES, R. M., DHONDT, I., MICHELS, H., KEMMEREN, P., NOLLEN, E. A., BRAECKMAN, B. P., BURGERING, B. M., VOS, H. R. & DANSEN, T. B. 2016. Proteome-wide Changes in Protein Turnover Rates in *C. elegans* Models of Longevity and Age-Related Disease. *Cell Rep*, 16, 3041-51.

VIVANCOS, A. P., CASTILLO, E. A., JONES, N., AYTÉ, J. & HIDALGO, E. 2004. Activation of the redox sensor Pap1 by hydrogen peroxide requires modulation of the intracellular oxidant concentration. *Mol Microbiol*, 52, 1427-35.

YVLKOVA, S., CARMAN, A. J., DANHOF, H. A., COLLETTE, J. R., ZHOU, H. & LORENZ, M. C. 2011. The fungal pathogen *Candida albicans* autoinduces hyphal morphogenesis by raising extracellular pH. *MBio*, 2, 00055-11.

YVLKOVA, S. & LORENZ, M. C. 2014. Modulation of phagosomal pH by *Candida albicans* promotes hyphal morphogenesis and requires Stp2p, a regulator of amino acid transport. *PLoS Pathog*, 10, e1003995.

WALKER, L. A., MACCALLUM, D. M., BERTRAM, G., GOW, N. A., ODDS, F. C. & BROWN, A. J. 2009. Genome-wide analysis of *Candida albicans* gene expression patterns during infection of the mammalian kidney. *Fungal Genet Biol*, 46, 210-9.

WALTHER, A. & WENDLAND, J. 2003. An improved transformation protocol for the human fungal pathogen *Candida albicans*. *Curr Genet*, 42, 339-43.

WANG, Y., CAO, Y. Y., CAO, Y. B., WANG, D. J., JIA, X. M., FU, X. P., ZHANG, J. D., XU, Z., YING, K., CHEN, W. S. & JIANG, Y. Y. 2007. Cap1p plays regulation roles in redox, energy metabolism and substance transport: an investigation on *Candida albicans* under normal culture condition. *Front Biosci*, 12, 145-53.

WANG, Y., CAO, Y. Y., JIA, X. M., CAO, Y. B., GAO, P. H., FU, X. P., YING, K., CHEN, W. S. & JIANG, Y. Y. 2006. Cap1p is involved in multiple pathways of oxidative stress response in *Candida albicans*. *Free Radic Biol Med*, 40, 1201-9.

WEMMIE, J. A., STEGGERDA, S. M. & MOYE-ROWLEY, W. S. 1997. The *Saccharomyces cerevisiae* AP-1 protein discriminates between oxidative stress elicited by the oxidants H₂O₂ and diamide. *J Biol Chem*, 272, 7908-14.

WHITEWAY, M. & BACHEWICH, C. 2007. Morphogenesis in *Candida albicans*. *Annu Rev Microbiol*, 61, 529-53.

WILSON, D., THEWES, S., ZAKIKHANY, K., FRADIN, C., ALBRECHT, A., ALMEIDA, R., BRUNKE, S., GROSSE, K., MARTIN, R., MAYER, F., LEONHARDT, I., SCHILD, L., SEIDER, K., SKIBBE, M., SLESIONA, S., WAECHTLER, B., JACOBSEN, I. & HUBE, B. 2009. Identifying infection-associated genes of *Candida albicans* in the postgenomic era. *FEMS Yeast Res*, 9, 688-700.

WINTERBOURN, C. C., HAMPTON, M. B., LIVESEY, J. H. & KETTLE, A. J. 2006. Modeling the reactions of superoxide and myeloperoxidase in the neutrophil phagosome: implications for microbial killing. *J Biol Chem*, 281, 39860-9.

WISPLINGHOFF, H., BISCHOFF, T., TALLENT, S. M., SEIFERT, H., WENZEL, R. P. & EDMOND, M. B. 2004. Nosocomial bloodstream infections in US hospitals: analysis of 24,179 cases from a prospective nationwide surveillance study. *Clin Infect Dis*, 39, 309-17.

WOOD, M. J., ANDRADE, E. C. & STORZ, G. 2003. The redox domain of the Yap1p transcription factor contains two disulfide bonds. *Biochemistry*, 42, 11982-91.

WOOD, M. J., STORZ, G. & TJANDRA, N. 2004. Structural basis for redox regulation of Yap1 transcription factor localization. *Nature*, 430, 917-21.

WOZNIOK, I., HORNBACH, A., SCHMITT, C., FROSCH, M., EINSELE, H., HUBE, B., LÖFFLER, J. & KURZAI, O. 2008. Induction of ERK-kinase signalling triggers morphotype-specific killing of *Candida albicans* filaments by human neutrophils. *Cell Microbiol*, 10, 807-20.

WU, C. J., LEE, H. C., YANG, Y. L., CHANG, C. M., CHEN, H. T., LIN, C. C., LEE, N. Y., CHU, W. L., HSIEH, L. Y., WANG, Y. L., LAUDERALE, T. L., TSENG, F. C., KO, N. Y., KO, W. C. & LO, H. J. 2012. Oropharyngeal yeast colonization in HIV-infected outpatients in southern Taiwan: CD4 count, efavirenz therapy and intravenous drug use matter. *Clin Microbiol Infect*, 18, 485-90.

WYSONG, D. R., CHRISTIN, L., SUGAR, A. M., ROBBINS, P. W. & DIAMOND, R. D. 1998. Cloning and sequencing of a *Candida albicans* catalase gene and effects of disruption of this gene. *Infect Immun*, 66, 1953-61.

YADAV, A. K., DESAI, P. R., RAI, M. N., KAUR, R., GANESAN, K. & BACHHAWAT, A. K. 2011. Glutathione biosynthesis in the yeast pathogens *Candida glabrata* and *Candida albicans*: essential in *C. glabrata*, and essential for virulence in *C. albicans*. *Microbiology*, 157, 484-95.

YAMADA-OKABE, T., MIO, T., ONO, N., KASHIMA, Y., MATSUI, M., ARISAWA, M. & YAMADA-OKABE, H. 1999. Roles of three histidine kinase genes in hyphal development and virulence of the pathogenic fungus *Candida albicans*. *J Bacteriol*, 181, 7243-7.

YAN, C., LEE, L. H. & DAVIS, L. I. 1998. Crm1p mediates regulated nuclear export of a yeast AP-1-like transcription factor. *EMBO J*, 17, 7416-29.

YIN, Z., STEAD, D., WALKER, J., SELWAY, L., SMITH, D. A., BROWN, A. J. & QUINN, J. 2009. A proteomic analysis of the salt, cadmium and peroxide stress responses in *Candida albicans* and the role of the Hog1 stress-

activated MAPK in regulating the stress-induced proteome. *Proteomics*, 9, 4686-703.

YOUNGMAN, M. J., ROGERS, Z. N. & KIM, D. H. 2011. A decline in p38 MAPK signaling underlies immunosenescence in *Caenorhabditis elegans*. *PLoS Genet*, 7, e1002082.

ZAKIKHANY, K., NAGLIK, J. R., SCHMIDT-WESTHAUSEN, A., HOLLAND, G., SCHALLER, M. & HUBE, B. 2007. In vivo transcript profiling of *Candida albicans* identifies a gene essential for interepithelial dissemination. *Cell Microbiol*, 9, 2938-54.

ZARAGOZA, O., BLAZQUEZ, M. A. & GANCEDO, C. 1998. Disruption of the *Candida albicans* TPS1 gene encoding trehalose-6-phosphate synthase impairs formation of hyphae and decreases infectivity. *J Bacteriol*, 180, 3809-15.

ZHANG, X., DE MICHELI, M., COLEMAN, S. T., SANGLARD, D. & MOYE-ROWLEY, W. S. 2000. Analysis of the oxidative stress regulation of the *Candida albicans* transcription factor, Cap1p. *Mol Microbiol*, 36, 618-29.

ZNAIDI, S., BARKER, K. S., WEBER, S., ALARCO, A. M., LIU, T. T., BOUCHER, G., ROGERS, P. D. & RAYMOND, M. 2009. Identification of the *Candida albicans* Cap1p regulon. *Eukaryot Cell*, 8, 806-20.

Review

Oxidative Stress Responses in the Human Fungal Pathogen, *Candida albicans*

Alessandra da Silva Dantas ^{1,†}, Alison Day ^{2,†}, Mélanie Ikeh ^{2,†}, Iaroslava Kos ^{2,†}, Beatrice Achan ^{2,†} and Janet Quinn ^{2,*}

¹ Departamento de Biologia Celular e Genética, Instituto de Biologia Roberto Alcantara Gomes, Universidade do Estado do Rio de Janeiro (UERJ), Rio de Janeiro 20550-013, Brazil; E-Mail: alesdantas@gmail.com

² Institute for Cell and Molecular Biosciences, Faculty of Medical Sciences, Newcastle University, Newcastle upon Tyne NE2 4HH, UK; E-Mails: a.m.day@ncl.ac.uk (A.D.); m.ikeh@ncl.ac.uk (M.I.); i.kos@ncl.ac.uk (I.K.); b.achan@ncl.ac.uk (B.A.)

† These authors contributed equally to this work.

* Author to whom correspondence should be addressed; E-Mail: janet.quinn@ncl.ac.uk; Tel.: +44-191-208-7434; Fax: +44-191-208-7424.

Academic Editors: Michael Breitenbach and Peter Eckl

Received: 12 January 2015 / Accepted: 12 February 2015 / Published: 25 February 2015

Abstract: *Candida albicans* is a major fungal pathogen of humans, causing approximately 400,000 life-threatening systemic infections world-wide each year in severely immunocompromised patients. An important fungicidal mechanism employed by innate immune cells involves the generation of toxic reactive oxygen species (ROS), such as superoxide and hydrogen peroxide. Consequently, there is much interest in the strategies employed by *C. albicans* to evade the oxidative killing by macrophages and neutrophils. Our understanding of how *C. albicans* senses and responds to ROS has significantly increased in recent years. Key findings include the observations that hydrogen peroxide triggers the filamentation of this polymorphic fungus and that a superoxide dismutase enzyme with a novel mode of action is expressed at the cell surface of *C. albicans*. Furthermore, recent studies have indicated that combinations of the chemical stresses generated by phagocytes can actively prevent *C. albicans* oxidative stress responses through a mechanism termed the stress pathway interference. In this review, we present an up-date of our current understanding of the role and regulation of oxidative stress responses in this important human fungal pathogen.

Keywords: fungal pathogenesis; *Candida albicans*; oxidative stress; stress signaling

1. *Candida albicans* Is a Major Fungal Pathogen of Humans

The polymorphic fungus, *Candida albicans*, is a constituent of the normal human microbiome. This fungus, together with other *Candida* family members, is present on the skin and in the oral cavity and gastrointestinal and urogenital tracts of most healthy individuals [1,2]. In the healthy host, *C. albicans* normally exists as a benign commensal organism. However, as an opportunistic pathogen, this fungus can also cause superficial infections, such as oral or vaginal candidiasis, or life-threatening systemic infections [2]. Perturbation of the microbiome through antibiotic usage or mild to severe defects in immune defences, such as in patients with HIV, can result in superficial oral and vaginal infections (thrush), termed oral (OC) and vulvovaginal (VVC) candidiasis, respectively. OC occurs in about 90% of HIV-infected persons as an AIDS-defining illness [3]. Defective immunity in premature infants and the elderly can also result in OC [4,5]. Significantly, 75% of women of childbearing age suffer from VVC, 45% of whom go on to have at least one recurrent infection [6]. Superficial candidiasis can also manifest as chronic infections of the skin and nails, resulting in mucocutaneous candidiasis (CMC) [7]. Although superficial infections are remarkably commonplace, they are non-life threatening and can be easily treated.

In contrast, systemic candidiasis is associated with unacceptably high crude and attributable mortality rates of 42 and 27%, respectively, despite the availability of antifungal drugs, such as the polyenes, azoles and echinocandins. These mortality rates exceed those attributed to sepsis caused by the most aggressive bacterial and viral pathogens [8] and are attributed to difficulties in diagnosing fungal systemic infections and the consequential delays in treatment [9]. Patients who are severely immunocompromised, such as those on immunosuppressive treatments for cancer or transplant surgery, are at risk of systemic candidiasis [10]. In such patients, the innate defence mechanisms, which are vital to prevent invasive disease, are significantly compromised [11]. Consequently, the fungus can survive in the bloodstream and subsequently colonise a number of internal organs [2]. Other risk factors include invasive clinical procedures or trauma, which disrupt the protective anatomical barrier of the mucosa, and the use of venous catheters, which can allow access of the fungus to the bloodstream [10]. Indeed, overall, *Candida* spp. are the fourth most common nosocomial (hospital acquired) systemic infection in the United States [8]. Clearly, *C. albicans* poses a significant medical problem, and thus, it is important that we understand what makes this fungus such a successful pathogen.

2. Reactive Oxygen Species Are a Core Component of the Immune Cell Armoury

In healthy hosts, the first line of defence against *C. albicans* is through phagocytosis by innate immune cells, including macrophages and neutrophils. A major antimicrobial defence mechanism mounted by these phagocytes is the production of reactive oxygen species (ROS) through a process known as the respiratory burst. Following stimulation by cytokines, phagocytic cells activate the assembly of the NADPH oxidase complex, which results in the generation of superoxide ($O_2^{-\bullet}$). Given the potency of the ROS produced by NADPH oxidase [12], activation of this multi-subunit enzyme is tightly regulated. The NADPH oxidase complex consists of the Nox2 (gp91^{phox}) catalytic subunit,

the p22^{phox} transmembrane protein and three cytosolic subunits, p47^{phox}, p67^{phox} and p40^{phox}. Nox2 and p22^{phox} make up the membrane-associated cytochrome *b*₅₅₈ heterodimer. Activation of Nox2 is dependent on the interaction with the cytosolic components, in particular p67^{phox}, which translocate to the membrane following phagocytosis [13]. This interaction is dependent on the binding of the small GTPase Rac to p67^{phox}, which induces a conformation change in this subunit, thus promoting its interaction with Nox2 [14]. Activation of Nox2 drives the production of superoxide via the NADPH-driven reduction of molecular oxygen. This is generated at an extremely high rate of 5 to 10 nmol per s within the neutrophil phagosome [15], and it has been estimated that approximately 4 mol L⁻¹ of O₂^{−•} is produced per bacterium engulfed in the phagocytic vacuole [16]. The superoxide is then dismutated to hydrogen peroxide (H₂O₂) by superoxide dismutase or to hydroxyl anions (OH[−]) and hydroxyl radicals (OH) via the Haber-Weiss reaction. The importance of the NADPH oxidase-mediated respiratory burst as an antimicrobial mechanism is manifested in patients with chronic granulomatous disease (CGD). CGD is a human genetic disorder characterized by a deficiency in the NAPDH oxidase complex and is associated with recurrent and life-threatening bacterial and fungal infections [17]. Significantly, patients with CGD have an increased susceptibility to *Candida* infections [18]. Interestingly, in addition to the fungicidal roles of ROS, recent work has revealed that the ROS produced by NADPH oxidase also functions to recruit phagocytes to *C. albicans* infection foci. This NADPH oxidase-regulated recruitment of phagocytes is important for efficient phagocytosis, containment of the fungus within the phagocyte and survival of the host [19].

Other toxic chemicals are subsequently derived from the ROS in the phagosome [20]. For example, H₂O₂ can react with chloride ions (Cl[−]) to form hypochlorous acid (HOCl) in a reaction catalysed by myeloperoxidase (MPO). In addition, the nitric oxide radical generated by the action of the inducible nitric oxide synthase (iNOS) interacts with superoxide to produce the highly toxic peroxynitrite (ONOO) [21]. Recently, work has also revealed that the combination of reactive oxygen species together with the cationic stress generated during phagocyte maturation underlies the potency of phagocytes in *C. albicans* killing [22]. Thus, phagocytic cells synthesize an array of toxic chemicals that work in combination to promote fungal killing. It is also noteworthy that, in addition to ROS production within the phagosome, phagocytes secrete ROS into the external milieu [23]. Consistent with this, *C. albicans* cells have been shown to mount an oxidative stress response prior to phagocytosis [24]. Furthermore, *C. albicans* will also come in contact with ROS produced by H₂O₂-producing bacteria in the mouth and gut. Several commensal bacteria, for example *Enterococcus faecalis* [25] and *Lactobacillus* species [26], secrete ROS into their surroundings, and this may have an inhibitory effect on the growth of *C. albicans* in host niches, other than the phagosomal environment. Consistent with this, using a *Caenorhabditis elegans* model of polymicrobial infection, *E. faecalis* was shown to reduce the virulence of *C. albicans* [27].

The ROS generated within the phagosome creates a toxic environment that induces oxidative stress in *C. albicans*. Indeed, exogenous ROS can induce programmed cell death in this fungal pathogen [28]. ROS interact with proteins, lipids and nucleic acids [29], causing irreversible damage to the pathogen. DNA damage caused by ROS can result in chemical base changes, structural alterations, single- and double-strand breaks and cross-linkage. Lipid peroxidation occurs by a free radical chain reaction, which culminates in peroxidation events at many fatty acid side chains, leading to the damage of the cell membrane. ROS reactions with proteins can lead to the formation of protein-protein cross-links, oxidation of the peptide backbone and reversible or irreversible oxidation of amino acid side chains. Although this

can be deleterious to protein function, as discussed below, several oxidative stress-sensing proteins are activated by the reversible oxidation of cysteine residues.

3. Response of *Candida albicans* to ROS

3.1. Transcriptional Responses to ROS

A well-characterized response of eukaryotic microbes to ROS is the rapid induction of mRNAs that encode oxidative stress detoxification and repair proteins. Interestingly, *C. albicans* is considerably more resistant to oxidative stress than the benign model yeasts, *Schizosaccharomyces pombe* and *Saccharomyces cerevisiae* [30,31]. However, the basis for this resistance does not appear to be due to differences in transcriptional responses to oxidative stress, as all three fungi appear to induce a similar set of core antioxidant genes following exposure to H_2O_2 [32,33]. These include catalase (*CAT1*), glutathione peroxidase (*GPX*) and superoxide dismutase (*SOD*) antioxidant-encoding genes, in addition to genes encoding components of the glutathione/glutaredoxin (*GSH1*, *TTR1*) and thioredoxin (*TSA1*, *TRX1*, *TRR1*) systems, which play critical roles in repairing oxidatively-damaged proteins, protein folding and sulphur metabolism. Such oxidative stress-responsive genes are also induced in *C. albicans* following exposure to macrophages or neutrophils [34–38], illustrating that this pathogen induces the respiratory burst in these phagocytes. The analyses of GFP-reporter fusions, under the control of oxidative stress-responsive promoters, have also revealed that *C. albicans* is exposed to significant levels of ROS prior to phagocytosis [24]. In contrast, however, oxidative stress responses do not appear to be induced once *C. albicans* cells have established systemic kidney infections [34,39,40]. Thus, inducible oxidative stress responses appear vital for *C. albicans* to survive phagocytosis by innate immune cells, but are seemingly less important for the fungus to develop systemic infections. Indeed, whilst a number of genes encoding key antioxidants (such as *CAT1*, *TRX1*, *GRX2*, *SOD1*, *SOD5*) are important for virulence in systemic models of infection [41–45], others (including *TSA1*, *GPXs*) are dispensable [46,47].

3.2. Transcriptional Responses to ROS Are Inhibited in the Presence of Cationic Stress

In healthy individuals, *C. albicans* cannot evade the oxidative-killing mechanisms mounted by innate immune cells. Such cells prevent infection by employing a battery of toxic chemicals in addition to ROS. For example, phagocytes expose *C. albicans* to cationic fluxes (K^+) and acidification, as well as to superoxide anions [16,21,48]. However, as *C. albicans* is resistant to each of these individual stresses *in vitro* [30,31], a key question, therefore, is: what accounts for the potency of innate immune defences? Although host microenvironments are complex and dynamic, our understanding of *C. albicans* stress responses is based on studies of individual stresses. Significantly, however, recent work has revealed that *C. albicans* is exquisitely sensitive to combinations of oxidative and cationic stresses [49], which are encountered following phagocytosis. Cationic stress can be imposed *in vitro* by exposure of the fungus to either NaCl or KCl and in the phagocyte is caused by increased flux of K^+ into the phagosome [16]. Strikingly, exposure to cationic stress results in the inhibition of *C. albicans* oxidative stress responses. This phenomenon has been termed “stress pathway interference” [22]. The combinatorial stress-mediated synergistic killing of *C. albicans* contrasts starkly with the stress cross-protection described in model yeasts, whereby exposure to one stress protects against subsequent exposure to a

different stresses [50]. The existence of stress pathway interference was revealed through gene expression analysis in *C. albicans*. Transcript profiling showed that H₂O₂-induced gene expression is severely attenuated, and intracellular ROS levels increase dramatically, following combinatorial oxidative and cationic stress. For example, key antioxidant genes, such as *CAT1* encoding catalase and *TRR1* encoding thioredoxin reductase, which are significantly induced following H₂O₂ stress, fail to be induced following exposure of cells to H₂O₂ in the presence of cationic stress [22]. This cationic stress-mediated inhibition of oxidative stress responses appears to be of physiological relevance, as the high fungicidal activity of human neutrophils is dependent on the combinatorial effects of the oxidative burst and cationic fluxes [22]. However, as discussed above, oxidative stress-responsive genes are induced following co-culture of *C. albicans* with phagocytes [34,35], so how is this reconciled with the combinatorial stress-mediated inactivation of such genes? It has been suggested [22] that the activation of *C. albicans* antioxidant genes during interaction with phagocytes may be due to exposure to extracellular ROS prior to engulfment [24]. Furthermore, as exposure of cells to combinatorial oxidative and cationic stresses prevents the normal activation of oxidative stress-responsive genes, this may explain why *C. albicans* oxidative stress genes are not expressed in certain host niches, such as during systemic infections of the kidney, despite the presence of neutrophil infiltrates [34].

3.3. Extracellular Antioxidant Enzymes as a Pathogen-Specific Adaptation Mechanism

As *C. albicans* appears to mount standard transcription responses to oxidative stress, the high level of resistance of this pathogen to ROS could, instead, be related to the evolutionary expansion of the SOD family and the fact that this pathogen expresses SODs and other antioxidant enzymes on the cell surface. *C. albicans* contains six SOD enzymes distributed between different cellular compartments. Sod1–3 are intracellular enzymes, while Sod4–6 are glycosylphosphatidylinositol (GPI)-anchored cell wall-associated enzymes. The Cu-/Zn-containing Sod1 is induced following phagocytosis and is required for *C. albicans* to resist macrophage-mediated killing [43]. The extracellular Sods also have vital roles in the detoxification of superoxide radicals generated by phagocytes; co-culture of macrophages with *C. albicans* cells lacking Sod4 and Sod5 leads to massive extracellular ROS accumulation *in vitro* [23]. Consequently, inactivation of Sod4 and Sod5 results in *C. albicans* cells that are exquisitely more susceptible to phagocyte-mediated killing [23,35]. Interestingly, the expression of Sod4 and Sod5 is dependent on the morphology of *C. albicans*, as Sod4 is expressed in yeast cells, whereas Sod5 is a hyphal-induced gene [44,51]. Sod5 is also induced following phagocytosis by neutrophils independently of hyphae formation [35]. Recently, structural analysis of Sod5 revealed that it represents a novel class of superoxide dismutases that only depends on Cu for activity. Furthermore, it is secreted in its apo-form and can readily capture extracellular copper without the aid of a Cu chaperone, which rapidly induces activity [52]. It is suggested that this novel mode of activation is uniquely adapted to the host environment, as macrophages release copper in an attempt to kill invading microbes through copper toxicity [53]. In addition to specific Sods, two key peroxidase enzymes have also been found at the cell surface of *C. albicans*; the thiol-specific peroxidase Tsa1 [47,54] and the peroxide detoxifying enzyme catalase [54]. Tsa1 and Cat1 were identified as major plasminogen-binding proteins in isolated cell wall protein preparations [54], and the cell wall localization of Tsa1 has also been illustrated using fluorescence microscopy [47]. These extracellular mechanisms for protection against ROS likely reflect an adaptation of this pathogenic fungus to prevent the intracellular accumulation of toxic levels of ROS.

3.4. Morphogenesis as an Oxidative Stress Response

Following phagocytosis, *C. albicans* can evade oxidative-killing by macrophages and neutrophils by switching from budding to filamentous cells, which can pierce the phagosomal membrane [37]. Not only does this allow the pathogen to escape, but this also results in the *C. albicans*-mediated killing of the phagocyte [55]. It has recently been demonstrated that the ability of *C. albicans* to mount robust oxidative stress responses is vital for this polymorphic pathogen to filament in the phagosome [46,56]. *C. albicans* mutants that are sensitive to ROS *in vitro* fail to filament once phagocytosed and, thus, are trapped within the macrophage and unable to evade phagocyte-mediated killing. Consistent with the requirement of fungal oxidative stress defences to allow filamentation and macrophage escape, the phagocyte NADPH oxidase is important in inhibiting filamentation *in vivo* [57]. The ROS produced by the NADPH oxidase also function to recruit phagocytes, thereby increasing phagocytosis and inhibiting filamentation [19]. Thus, the outcome of the battle between *C. albicans* and innate immune cells appears dependent on the NADPH oxidase-regulated functions of the phagocyte and the robustness of the fungal oxidative stress responses.

The mechanisms underlying *C. albicans* filamentation following phagocytosis remain to be fully explored. A recent study reported that the ROS-induced induction of arginine biosynthesis genes is important for hyphal formation following phagocytosis of *C. albicans* [58]. Moreover, exposure of *C. albicans* to the ROS H₂O₂ triggers the filamentation of this polymorphic fungus *in vitro* [42,59]. A close examination of the morphology of these cells revealed that H₂O₂-induced filaments are hyperpolarized buds, which are morphologically distinct from hyphae and pseudohyphae filamentous forms [42]. The hyperpolarised bud is a relatively recently characterized filamentous form of *C. albicans* and is normally associated with either mutations or chemicals that perturb cell cycle progression [60,61]. The observation that H₂O₂ stimulates hyperpolarised bud formation provided the first example of a physiologically relevant condition that induces this filamentous form of growth in *C. albicans*. Does exposure of ROS following phagocytosis trigger the formation of hyperpolarised buds allowing this pathogen to pierce the phagocyte membrane and escape? Evidence so far indicates that ROS-stimulated hyperpolarized bud formation may not contribute to *C. albicans* filamentation within the macrophage. For example, ROS-sensitive *C. albicans* mutants that cannot filament within the macrophage [56] can form H₂O₂-induced hyperpolarized buds *in vitro* [42]. Nonetheless, ROS-stimulated filamentation of *C. albicans* may be beneficial for survival in other host niches, such as the gut, where *C. albicans* co-exists with ROS-producing bacteria.

4. Signalling Pathways that Mediate *C. albicans* Responses to ROS

To date, three signalling pathways have been demonstrated to be directly activated in response to ROS in *C. albicans*. These include the Cap1 transcription factor, the Hog1 stress-activated protein kinase and the Rad53 DNA damage checkpoint kinase. Here, we discuss the role and regulation of these pathways in oxidative stress responses in *C. albicans*. Other signalling pathways not known to be activated by ROS, but which contribute to oxidative stress tolerance in *C. albicans* are also briefly summarized.

4.1. The Cap1 ROS-Responsive Transcription Factor

In *C. albicans*, the Cap1 transcription factor is the major regulator of the oxidative stress-induced transcriptome and proteome, both *in vitro* [62,63] and *ex vivo*, following exposure to neutrophils [35]. Cap1 is a bZip transcription factor of the AP-1 family and is closely related to the *S. cerevisiae* Yap1 and *S. pombe* Pap1 proteins, which have well-characterized roles in oxidative stress and multi-drug resistance [64,65]. Similarly, *C. albicans* *cap1Δ* cells are sensitive to several reactive oxygen species and drugs [33,66,67]. Chromatin immunoprecipitation (ChIP) analysis to determine direct targets of Cap1 identified many key antioxidant genes, including *CTA1* and *TRX1*, and those involved in the response to drugs, such as *MDR1* [68]. Cap1 plays a role in recruiting the Ada2 component of the SAGA/ADA histone acetylase co-activator complex to the promoters of oxidative stress and drug-responsive target genes [69,70]. Cells lacking Ada2 are highly sensitive to ROS, and the oxidative stress-induced transcription of key Cap1 target genes is significantly impaired; therefore, Cap1 recruitment of the SAGA complex appears to be a vital component of the oxidative stress response in *C. albicans*.

4.1.1. Regulation of Cap1

Similar to that reported for *S. cerevisiae* Yap1, *C. albicans* Cap1 rapidly accumulates in the nucleus in response to H₂O₂ [56,67]. Under non-stressed conditions, Yap1 shuttles between the cytoplasm and the nucleus due to the interaction of a nuclear export sequence (NES), located at the C-terminus of these transcription factors, with the Crm1 nuclear export factor [71]. However, following exposure to H₂O₂, Yap1 is activated by oxidation of specific cysteine residues, resulting in disulphide bond formation between two cysteine-rich domains (n-CRD and c-CRD). This triggers a conformational change within Yap1 that masks the NES, thereby preventing its interaction with Crm1. The inability to be recognized by Crm1 leads to the nuclear accumulation of Yap1, the nuclear-dependent phosphorylation of this transcription factor and the induction of Yap1-dependent genes [72]. Conversely, activation of Yap1 is counteracted by the thioredoxins Trx1 and Trx2, which function to reduce oxidised Yap1 [72]. This basic mechanism of regulation is conserved in *C. albicans* (Figure 1). Mutation of the c-CRD affects Cap1 regulation [67], and Cap1 is rapidly oxidised following exposure to H₂O₂ [42]. In addition, following the nuclear accumulation of Cap1, this transcription factor becomes phosphorylated, and the induction of Cap1-dependent genes is observed. Furthermore, as seen in *S. cerevisiae*, thioredoxin functions to reverse the H₂O₂-induced oxidation and activation of Cap1 [42].

Fungal AP-1-like transcription factors are not directly oxidised by H₂O₂, but instead, specific peroxidase enzymes sense and transduce the H₂O₂ signal to these transcription factors (Figure 1). Similar to that observed in *S. cerevisiae* [72], Cap1 oxidation requires Gpx3, a glutathione peroxidase (Gpx)-like enzyme [56]. Studies with Yap1 showed that this transcription factor undergoes multiple oxidation events, with Gpx3 initiating Yap1 oxidation [73–75]. Similarly, multiple oxidized forms of Cap1 are also observed [56]. Gpx3-mediated oxidation of Yap1 and Cap1 also requires a second protein, Ybp1, which binds to and forms a complex with the AP-1-like factors [56,76]. A recent study has provided insight into an additional function of Ybp1 in both *C. albicans* and *S. cerevisiae*, as Cap1 and Yap1 are highly unstable in *ybp1Δ* cells [56]. Ubiquitin-mediated degradation of oxidised AP-1-like factors has recently been shown to be an important regulatory mechanism [77,78]; therefore, Ybp1 binding to the

reduced cytoplasmic pools of Yap1 or Cap1 possibly functions to prevent this proteasome-mediated degradation [56].

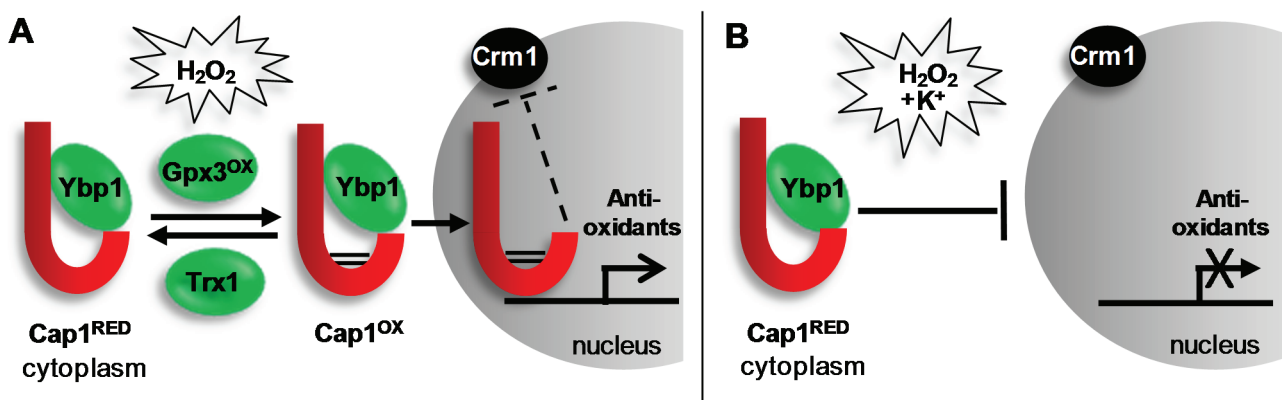


Figure 1. H_2O_2 -induced activation of Cap1 is inhibited in the presence of cations. (A) Exposure of *C. albicans* to H_2O_2 promotes the Gpx3/Ybp1-mediated oxidation and activation the Cap1 transcription factor (Cap1^{ox}). Cap1^{ox} can no longer interact with the Crm1 nuclear export factor resulting in its nuclear accumulation, and the subsequent Cap1-dependent induction of genes with antioxidant functions necessary for cell survival. Following cellular adaptation, Cap1^{ox} is returned to the inactive reduced form (Cap1^{RED}) by thioredoxin (Trx1); (B) Remarkably, when *C. albicans* cells are exposed to H_2O_2 in the presence of cations, Cap1 fails to accumulate in the nucleus and therefore antioxidant gene expression is not induced leading to cell death. This is important as, following phagocytosis, *C. albicans* is exposed simultaneously to ROS and cationic fluxes. See text for details.

In *S. cerevisiae*, Yap1 functions alongside the Skn7 response regulator transcription factor, to regulate antioxidant gene expression [79]. An orthologue of Skn7 has been identified in *C. albicans* [80]. The overall domain architecture is conserved and comprised of a DNA-binding domain, a coiled-coil domain and a receiver domain (analogous to those in response regulator proteins of two-component signal transduction pathways). It is not known whether Skn7 acts alongside Cap1 in *C. albicans*. However, *C. albicans* cells lacking Skn7 display increased sensitivity to ROS, including H_2O_2 , consistent with this transcription factor regulating oxidative stress-induced gene expression [80].

Interestingly, Cap1 fails to be activated following exposure to combinatorial oxidative and cationic stress (Figure 1), which underlies the lack of antioxidant gene expression following this combinatorial stress treatment (Section 3.2). In contrast with that seen following oxidative stress, following combinatorial cationic plus oxidative stress treatments, Cap1 fails to accumulate in the nucleus [22]. Consequently, Cap1 is not phosphorylated, and Cap1-dependent oxidative stress genes are not induced [22]. The impact of stress pathway interference upon Cap1 signalling underlies the potency of combinatorial cationic plus oxidative stress, as ectopic expression of the Cap1-dependent catalase gene, *CAT1*, rescues the hypersensitivity to the combinatorial stress [22]. However, the mechanism underlying combinatorial stress-mediated inactivation of Cap1 is not known. Cations inhibit catalase function, which results in high levels of intracellular ROS [22]. Whether high levels of ROS result in Cap1 inactivation or whether cations inhibit Cap1 activation in other ways remains to be determined.

4.1.2. Role of Cap1 in Virulence

Loss of Cap1 or its regulators Gpx3 and Ybp1 attenuates virulence in some, but not all infection models. For example, cells lacking Cap1, Gpx3 or Ybp1 are unable to kill macrophages, due to the inability of these mutant strains to filament following phagocytosis [56]. Consequently, cells lacking Cap1 or its regulators are sensitive to macrophage- and neutrophil-mediated killing [35,56,81]. Cap1, Gpx3 and Ybp1 are also vital for *C. albicans* virulence in a *Galleria mellonella* model of infection [56], and Cap1 is important for virulence in a *Caenorhabditis elegans* infection model in nematode hosts that have a functional NADPH oxidase [81]. In contrast, Cap1, Gpx3 and Ybp1 are dispensable for *C. albicans* virulence in murine systemic infection models [56,81]. Similar findings were reported for Skn7 [80]. The observation that Cap1 is dispensable for virulence in murine systemic models of infection was unexpected, as certain genes that are induced by Cap1 in response to H₂O₂, such as *CTA1* and *TRX1*, are important for *C. albicans* survival in such models [42,45]. This indicates that Cap1-independent basal levels of such genes may be important for virulence in such models and that Cap1-mediated gene expression is not vital for the establishment of systemic infections.

4.2. The Hog1 SAPK

Stress-activated MAPKs are conserved signalling molecules that promote the ability of cells to adapt to environmental change [82]. They are components of a three-tiered core signalling module that comprises the SAPK itself, a MAP kinase kinase (MAPKK) and a MAPKK kinase (MAPKKK). Activation of the MAPKKK results in the phosphorylation and activation of the MAPKK, which, in turn, culminates in the phosphorylation of the SAPK on conserved threonine and tyrosine residues located within the TGY motif in the phosphorylation lip of the catalytic domain. This induces the activation and nuclear accumulation of the kinase [83] and the proline-directed phosphorylation of Ser/Thr residues on diverse substrates, including transcription factors, kinases, cell cycle regulators and membrane proteins, thus eliciting appropriate cellular responses. In *C. albicans*, Hog1 is robustly phosphorylated and rapidly accumulates in the nucleus following exposure of cells to H₂O₂ [33]. In addition, cells lacking Hog1 display increased sensitivity to a range of ROS, indicating that Hog1 activation is a critical component of the oxidative stress response in *C. albicans* [84,85]. Interestingly, Hog1 is only activated following exposure of *C. albicans* cells to relatively high levels of H₂O₂ compared to the analogous Sty1 SAPK in the model yeast, *S. pombe*. This may reflect an adaption of this pathogenic fungus to restrict Hog1 activation to ROS-rich environments during infection [85]. Despite the increased H₂O₂ sensitivity exhibited by *hog1Δ* cells and significant phosphorylation of Hog1 in response to H₂O₂, transcript profiling experiments revealed that Hog1 is largely dispensable for H₂O₂-induced gene expression [33]. Although a small subset of H₂O₂-responsive genes were identified that showed Hog1-dependent induction, subsequent analysis failed to identify any genes coding for proteins with known antioxidant functions [33]. This is in contrast with *S. pombe*, where Sty1 is required for the activation of the core stress genes in response to H₂O₂, including genes encoding important antioxidants, such as catalase and glutathione peroxidase [86]. What, therefore, is the role of Hog1 in the *C. albicans* oxidative stress response if it is not required for the induction of antioxidant gene expression? One possibility is that Hog1 contributes to the oxidative stress response at a post-transcriptional level in *C. albicans*. Indeed,

the *S. pombe* Sty1 SAPK has been shown to interact with translation factors [87]. However, Hog1 does not play a major role in regulating the oxidative stress-induced proteome, although proteomic experiments did indicate that Hog1 might be required to ensure the prolonged expression of some proteins during recovery from H₂O₂ stress [88]. Loss of Hog1 has been shown to affect respiratory function [89], although it is unclear whether this underlies the sensitivity of *hog1Δ* cells to ROS. One downstream target of Hog1 regulated by H₂O₂ stress is the Mkc1 cell integrity MAPK. Mkc1 is rapidly phosphorylated in response to H₂O₂ stress in a Hog1-dependent mechanism, although Mkc1 is not required for cell survival in response to H₂O₂ stress [90]. In addition, the Sko1 transcription factor is a target of the Hog1 SAPK in *C. albicans*, as this becomes phosphorylated following stress in a Hog1-dependent manner [91]. However, consistent with Hog1 not playing a major role in regulating oxidative stress-induced gene expression, the H₂O₂-induced transcriptome is not dependent on Sko1 [92]. Thus, in *C. albicans*, Hog1 regulation of the oxidative stress response must involve targets in addition to Mkc1 and Sko1 (Figure 2).

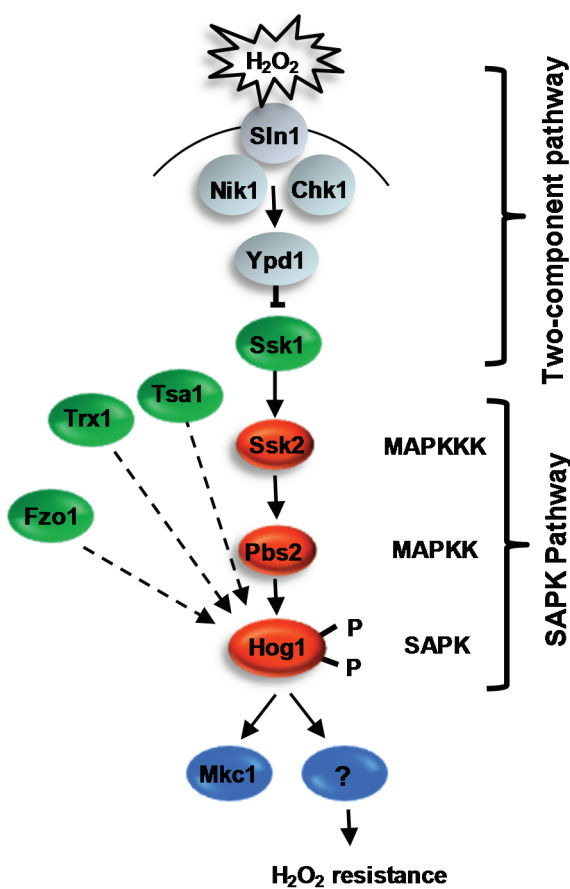


Figure 2. H₂O₂-induced activation of the Hog1 SAPK. In response to H₂O₂, Hog1 becomes rapidly phosphorylated and accumulates in the nucleus, and *C. albicans* cells lacking Hog1 are sensitive to oxidative stress. Proteins required for H₂O₂-induced activation of Hog1 are shown in green. These include the response regulator Ssk1 (but no other two-component protein), the redox sensitive antioxidants Tsa1 and Trx1, and the mitochondria biogenesis factor Fzo1. Following H₂O₂-induced activation, Hog1 phosphorylates the Mkc1 MAPK. However, cells lacking Mkc1 are not sensitive to oxidative stress, suggesting that an, as yet, unknown Hog1 substrate(s), mediates oxidative stress resistance.

4.2.1. Regulation of Hog1 in Response to ROS

Whilst little is known regarding the cellular targets of Hog and the cellular role(s) of this kinase in promoting oxidative stress tolerance, more progress has been made in delineating how H_2O_2 signals are relayed to Hog1 (Figure 2). Oxidative stress-induced activation of Hog1 is entirely dependent on the Pbs2 MAPKK [93], which, in turn, is regulated by a single MAPKKK Ssk2 [94]. Furthermore, a recent study reported that deletion of a mitochondrial biogenesis factor, Fzo1, significantly impairs the H_2O_2 -induced activation of Hog1 [95]. Thus, intriguingly, functional mitochondria may play an important role in the regulation of the Hog1 pathway in response to oxidative stress. In addition, both two-component related proteins and redox-sensitive antioxidants are necessary for the activation of the Hog1 SAPK in response to oxidative stress, and these will be described in turn.

4.2.1.1. Two-Component Mediated Regulation of Hog1

In the model yeasts, two-component signalling pathways have been shown to play an important role in the sensing and transmission of stress signals to their respective SAPK pathways. Such pathways are comprised of a histidine kinase, an intermediary phosphorelay protein and a response regulator protein. In *S. cerevisiae*, the Sln1 histidine kinase is inactivated in response to osmotic stress. This halts phosphorelay through the Ypd1 phosphorelay protein, leading to the rapid dephosphorylation of the Ssk1 response regulator. Dephosphorylated Ssk1 is a potent activator of the Ssk2/Ssk22 MAPKKs in *S. cerevisiae*, which regulate Hog1 activation [96,97]. In *C. albicans*, deletion of the analogous *SSK1* gene prevents Hog1 activation in response to oxidative stress, and consistent with this, *ssk1Δ* cells are sensitive to oxidative stress [98]. Although Ssk1 is involved in the transmission of oxidative stress signals to Hog1, the identity of the histidine kinase(s) responsible for sensing and signalling oxidative stress signals to Ssk1 in *C. albicans* remains elusive [99,100]. Of the three histidine kinases present in *C. albicans*, Chk1 would appear to be the most likely candidate for a potential peroxide-sensing histidine kinase, as this shows significant similarity to the *S. pombe* peroxide-sensing histidine kinases, Mak2 and Mak3 [101,102]. However, deletion of *CHK1* alone or in combination with either of the genes encoding the two remaining histidine kinases, *SLN1* or *NIK1*, does not impair H_2O_2 -induced activation of Hog1 [100,103]. Hence, it is currently unclear as to which histidine kinase(s) senses oxidative stress and regulates phosphorelay to Ssk1. Moreover, observations that Hog1 activation is seen in cells expressing a non-phosphorylatable Ssk1 mutant [103] or in cells lacking the Ypd1 phosphorelay protein in which Ssk1 is predicted to be unphosphorylated [104] indicate that Ssk1 may relay H_2O_2 signals to Hog1 in a mechanism independent of two-component signalling. It is also noteworthy that a novel response regulator, named Crr1/Srr1, has been recently identified that is only present in fungi belonging to the *Candida* clade [105,106]. Cells lacking Crr1 or expressing a mutant lacking the predicted aspartate phosphorylation site are sensitive to H_2O_2 [105]. However, in contrast with Ssk1, Crr1 is not required for the H_2O_2 -induced activation of Hog1 [105]. Thus, whilst this novel response regulator mediates the response of *C. albicans* to H_2O_2 , it does so in a Hog1-independent manner. Finally, in *S. cerevisiae*, the transmembrane protein, Sho1, relays osmotic stress signals to the Hog1 SAPK in parallel with the Sln1-mediated two-component signalling pathway [107]. In *C. albicans*, the analogous Sho1 protein appears to have been reassigned to oxidative stress signalling [100]. However, it is not clear how this is mediated, as Sho1 is not required for ROS-stimulated activation of the Hog1 pathway [100].

4.2.1.2. Redox-Sensitive Antioxidant Proteins as Regulators of Hog1

It is now well recognized that redox-sensitive antioxidant proteins have important sensing and signalling roles in the cellular response to oxidative stress [108]. In *C. albicans*, the redox-sensitive thioredoxin peroxidase enzyme, Tsa1, is specifically required for H₂O₂-induced activation of Hog1 [42]. This is similar to that previously reported in *S. pombe*, as H₂O₂-induced activation of the Sty1 SAPK also requires the analogous thioredoxin peroxidase enzyme, Tpx1 [109]. In *S. pombe*, intermolecular disulphide bonds are formed between conserved cysteine residues in Sty1 and Tpx1 following H₂O₂ stress, which suggests that Tpx1 regulates Sty1 function directly. However, the mechanism of Tsa1 regulation of Hog1 in *C. albicans* may be different, as the conserved peroxidatic cysteine residue of Tsa1, which is essential for Tpx1 regulation of Sty1, is dispensable for Tsa1 regulation of Hog1 [42]. Furthermore, the thioredoxin enzyme, Trx1, which regulates the redox status of Tsa1, is also essential for the relay of oxidative stress signals to the Hog1 SAPK module [42]. Deletion of *TRX1* or mutation of the catalytic cysteine residues of Trx1 drastically impairs Hog1 phosphorylation in response to H₂O₂. However, it would appear that Trx1 regulates Hog1 independently of Tsa1, as the catalytic cysteine residues of Tsa1, which are reduced by Trx1, are dispensable for Hog1 activation [42]. In mammalian systems, thioredoxin functions as a repressor of the Hog1-related JNK and p38 SAPK signalling cascades [110]. The upstream Ask1 MAPKKK in the mammalian SAPK pathways is activated via cysteine oxidation, and Trx1 negatively regulates this pathway by reducing the oxidized cysteines of Ask1 [111,112]. As Trx1 is a positive regulator of the Hog1 SAPK in *C. albicans*, it seems unlikely that a similar mechanism is in place. It is also interesting to note that protein tyrosine phosphatases, which are negative regulators of SAPKs, are susceptible to inactivation by oxidation of their catalytic cysteine residue [113]. Whether thioredoxin regulates such phosphatases that dephosphorylate Hog1 in *C. albicans*, however, remains to be established.

4.2.2. Role of the Hog1 SAPK in Virulence

The stress-activated MAPK Hog1 in *C. albicans* is phosphorylated and accumulates in the nucleus, in response to a range of stresses likely to be encountered in the host, including ROS, osmotic stress and anti-microbial peptides [114]. Cells lacking Hog1 display impaired virulence in a wide range of infection models, including murine systemic and commensal models [114–116], and are more susceptible to killing by macrophages or neutrophils [117]. As Hog1 regulates a number of distinct stress responses, it is difficult to dissect whether it is the role of Hog1 in oxidative stress responses or a different aspect of Hog1 signalling that is important for virulence in these models. Importantly, however, although Hog1 signalling has also been implicated in morphogenetic regulation, mutational analysis has inferred that the importance of Hog1 in virulence is due to its role in stress protection, rather than its role in repressing the yeast to hyphal transition [115].

4.3. The Rad53 DNA Damage Checkpoint Kinase

Following exposure to H₂O₂, *C. albicans* forms hyperpolarised buds, which are morphologically distinct from hyphae and pseudohyphae filamentous forms (Section 3.4). Consistent with this, H₂O₂-induced hyperpolarized bud formation occurs independently of the key hyphal regulators, Efg1 and Cph1, and, instead, depends on the activation of the Rad53 DNA damage checkpoint pathway [42,61] (Figure 3). A wide range of genotoxic stresses, including UV, methyl methanesulfonate (MMS) and the ribonucleotide reductase inhibitor hydroxyurea have been shown to activate the Rad53 kinase in *C. albicans* [61], and loss of Rad53 or upstream regulators of Rad53, prevents hyperpolarised bud formation [61,118]. ROS are also genotoxic agents due to the induction of DNA damage [119], which, in turn, triggers the activation of the Rad53 DNA checkpoint pathway [120]. Indeed, treatment of *C. albicans* cells with H₂O₂ elicits the phosphorylation of Rad53, and cells lacking *RAD53* fail to form hyperpolarised buds in response to H₂O₂ [42].

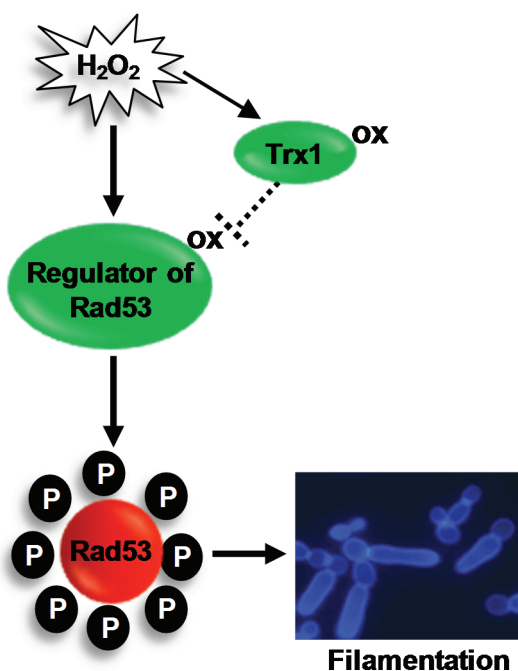


Figure 3. H₂O₂-induced activation of Rad53 triggers filamentation in *C. albicans*. The redox sensitive oxidoreductase Trx1 inhibits H₂O₂-induced activation of the DNA damage checkpoint kinase Rad53. This suggests that a regulator of Rad53 is activated by oxidation, and this active oxidised form is reduced by Trx1. Activation of the DNA damage checkpoint triggers the formation of hyperpolarised buds. See text for details.

Regulation of Rad53

Regarding the H₂O₂-mediated activation of Rad53, a recent study illustrated that H₂O₂-induced oxidation, and inactivation, of the thioredoxin protein Trx1 is important for the activation of Rad53 and polarized cell growth [42]. Rad53 is constitutively phosphorylated in cells lacking Trx1, which display a hyperpolarized bud morphology. Conversely, ectopic expression of the thioredoxin reductase gene, *TRR1*, which reduces oxidized Trx1, inhibited H₂O₂-induced filamentation [42]. Taken together, these

results illustrate that oxidation of Trx1 following H_2O_2 exposure is key in the activation of Rad53 that drives hyperpolarised bud formation. The finding that Trx1 inhibits Rad53 activation under non-stressed conditions may be conserved in higher eukaryotes, as ectopic expression of thioredoxin inhibits the phosphorylation of the analogous DNA damage checkpoint kinase, Chk2, in mammalian cells [121]. However, the mechanism of Trx1 regulation of Rad53 is unclear. As Trx1 functions to reduce oxidised proteins, an attractive hypothesis is that Rad53, or a regulator of this kinase, is activated by oxidation (Figure 3). In this regard, it is interesting that the human homologue (ATM) of the fungal Tel1 DNA-damage sensing kinase, which regulates Rad53, has recently been shown to be activated by oxidation [122]. Further studies are needed to determine if Tel1 is similarly regulated to mediate H_2O_2 -induced filamentation in *C. albicans*.

4.4. Other Signaling Pathways that Contribute to Oxidative Stress Resistance

The cAMP/PKA signalling pathway has a negative impact on oxidative stress responses in *C. albicans*. For example, induction of the pathway by inactivation of the phosphodiesterase, Pde2, which degrades cAMP, results in increased sensitivity to H_2O_2 [123]. Related to this, farnesol treatment of *C. albicans* cells results in increased resistance to H_2O_2 , due to the inhibition of the cAMP/PKA signalling pathway [124]. Such changes in resistance are possibly due to changes in the levels of anti-oxidant gene expression [124]; however, the mechanism linking cAMP/PKA to their regulation is unknown.

There is also evidence that the spindle assembly checkpoint is required for *C. albicans* oxidative stress resistance. Cells lacking the spindle checkpoint protein kinase, Mps1, are sensitive to H_2O_2 [125] and, similar to other oxidative stress sensitive mutants [56], fail to filament following phagocytosis. Related to this, the spindle assembly checkpoint protein, Mad2, is essential for *C. albicans* survival in macrophages [126].

5. Conclusions and Future Perspectives

In this review, we have summarized the current literature of oxidative stress responses and how they are regulated in the human fungal pathogen *C. albicans*. This is an important area of research, as oxidative stress adaptation is emerging as an important virulence trait in this, and other, fungal pathogens. Table 1 summarizes studies that have documented the impact of the loss of oxidative stress regulatory proteins or antioxidant enzymes on *C. albicans* virulence in either a murine systemic infection model or a macrophage/neutrophil phagocyte-survival infection model. From this summary, a number of observations can be made. First of all, when examined, mutants that display an impaired tolerance to oxidative stress show an impaired ability to survive phagocyte killing. This is consistent with previous observations that *C. albicans* mounts a robust transcriptional response to oxidative stress following phagocytosis [34–38]. Secondly, not all oxidative stress-sensitive *C. albicans* mutants display attenuated virulence in a murine systemic infection model. Perhaps most striking is the observation that the major regulator of anti-oxidant gene expression, Cap1, is dispensable for virulence in such an infection model. This is particularly intriguing, as certain genes, which are dependent on Cap1 for induction following oxidative stress, are important for virulence in systemic models. Thirdly, the role of many other oxidative stress-responsive proteins in mediating *C. albicans* virulence, such as the Rad53-mediated DNA damage checkpoint pathway, have yet to be explored.

Table 1. Summary of the role of oxidative stress-responsive signalling proteins and antioxidant enzymes in *C. albicans* virulence. The importance of proteins needed for resistance to oxidative stress in mediating *C. albicans* virulence in either a systemic infection model (SIM) or phagocyte infection model (PIM) is indicated; +, important for virulence; –, dispensable for virulence; nd, not determined. For further explanation, see the text.

Protein	Function	SIM	PIM	References
<i>Signalling Proteins</i>				
Hog1	Stress-activated protein kinase	+	+	[114,115,117]
Ssk1	Response regulator	+	+	[127,128]
Cap1	Transcription factor	–	+	[56,81]
Ybp1	Cap1 regulator	–	+	[56]
Gpx3	Cap1 regulator	–	+	[56]
Skn7	Transcription factor	–	nd	[80]
<i>Signalling Proteins</i>				
Pde2	Phosphodiesterase	+	nd	[123]
Mps1	Spindle checkpoint	nd	+	[125]
Mad2	Spindle checkpoint	+	+	[126]
<i>Antioxidant Enzymes</i>				
Cat1	Catalase	+	+	[45]
Trx1	Thioredoxin	+	nd	[42]
Tsa1	Thioredoxin peroxidase	–	nd	[47]
Sod1	Superoxide dismutase	+	+	[43]
Sod5	Superoxide dismutase	+	+	[23,44]
Grx2	Glutaredoxin	+	nd	[41]
Gpx31-33	Glutathione peroxidases	nd	+	[46]

In addition to gaps in our knowledge regarding the relative importance of specific oxidative stress responses in mediating *C. albicans* virulence, there are also additional key questions that remain to be addressed. For example, what is the role of the Hog1 SAPK in mediating oxidative stress resistance in *C. albicans*, and how is this regulated? This is important, as, although Hog1 is an essential virulence determinant in *C. albicans*, the conservation with highly related SAPKs in human cells suggests that Hog1 itself may be unsuitable as a specific antifungal target. Thus, there is much interest in identifying fungal-specific SAPK regulators or substrates, as such proteins hold greater promise for future therapeutic strategies. In addition, the recent findings that *C. albicans* is exquisitely sensitive to combinations of stress that are encountered following phagocytosis represent a new unchartered area in the field of stress signalling. A key question for the future is how do combinations of stress imposed by the phagosome inhibit oxidative stress adaptation and survival of *C. albicans*? Addressing this question is critical to further our understanding of *Candida*-host interactions during disease progression.

Acknowledgments

We thank our friends and colleagues, in particular Al Brown, Lars Erwig, Ken Haynes, Brian Morgan and Elizabeth Veal, for stimulating discussions on oxidative stress signalling mechanisms and fungal pathogenesis. Research in the Janet Quinn lab is funded by the BBSRC BB/K016393/1, an MRC-DTP

studentship, the NIHR Newcastle Biomedical Research Centre and the Wellcome Trust Strategic Award for Medical Mycology and Fungal Immunology 097377/Z/11/Z.

Author Contributions

All authors contributed to the initial draft of this review, which was edited by Janet Quinn.

Conflicts of Interest

The authors declare no conflict of interest.

References and Notes

1. Odds, F.C. *Candida and Candidosis*, 2nd ed.; Bailliere-Tindall: London, UK, 1988.
2. Calderone, R.A.; Clancy, C.J. *Candida and Candidiasis*; ASM Press: Washington, DC, USA, 2012.
3. Anaissie, E.J.; McGinnis, M.R.; Pfaller, M.A. *Clinical Mycology*; Churchill Livingstone: London, UK, 2009.
4. Flevari, A.; Theodorakopoulou, M.; Velegraki, A.; Armaganidis, A.; Dimopoulos, G. Treatment of invasive candidiasis in the elderly: A review. *Clin. Interv. Aging* **2013**, *8*, 1199–1208.
5. Healy, C.M.; Campbell, J.R.; Zaccaria, E.; Baker, C.J. Fluconazole prophylaxis in extremely low birth weight neonates reduces invasive candidiasis mortality rates without emergence of fluconazole-resistant candida species. *Pediatrics* **2008**, *121*, 703–710.
6. Sobel, J.D. Vulvovaginal candidosis. *Lancet* **2007**, *369*, 1961–1971.
7. Lilic, D. Unravelling fungal immunity through primary immune deficiencies. *Curr. Opin. Microbiol.* **2012**, *15*, 420–426.
8. Morgan, J. Global trends in candidemia: Review of reports from 1995–2005. *Curr. Infect. Dis. Rep.* **2005**, *7*, 429–439.
9. Brown, G.D.; Denning, D.W.; Gow, N.A.; Levitz, S.M.; Netea, M.G.; White, T.C. Hidden killers: Human fungal infections. *Sci. Transl. Med.* **2012**, doi:10.1126/scitranslmed.3004404.
10. Koh, A.Y.; Kohler, J.R.; Coggshall, K.T.; van Rooijen, N.; Pier, G.B. Mucosal damage and neutropenia are required for *Candida albicans* dissemination. *PLOS Pathog.* **2008**, *4*, e35.
11. Seider, K.; Heyken, A.; Luttich, A.; Miramon, P.; Hube, B. Interaction of pathogenic yeasts with phagocytes: Survival, persistence and escape. *Curr. Opin. Microbiol.* **2010**, *13*, 392–400.
12. Babior, B.M. NADPH oxidase. *Curr. Opin. Immunol.* **2004**, *16*, 42–47.
13. Bedard, K.; Krause, K.H. The NOX family of ROS-generating NADPH oxidases: Physiology and pathophysiology. *Physiol. Rev.* **2007**, *87*, 245–313.
14. Pick, E. Role of the Rho GTPase Rac in the activation of the phagocyte NADPH oxidase: Outsourcing a key task. *Small GTPases* **2014**, *5*, e27952.
15. Hampton, M.B.; Kettle, A.J.; Winterbourn, C.C. Involvement of superoxide and myeloperoxidase in oxygen-dependent killing of *Staphylococcus aureus* by neutrophils. *Infect. Immun.* **1996**, *64*, 3512–3517.

16. Reeves, E.P.; Lu, H.; Jacobs, H.L.; Messina, C.G.; Bolsover, S.; Gabella, G.; Potma, E.O.; Warley, A.; Roes, J.; Segal, A.W. Killing activity of neutrophils is mediated through activation of proteases by K^+ flux. *Nature* **2002**, *416*, 291–297.
17. Holland, S.M. Chronic granulomatous disease. *Clin. Rev. Allerg. Immunol.* **2010**, *38*, 3–10.
18. Cohen, M.S.; Isturiz, R.E.; Malech, H.L.; Root, R.K.; Wilfert, C.M.; Gutman, L.; Buckley, R.H. Fungal infection in chronic granulomatous disease. The importance of the phagocyte in defense against fungi. *Am. J. Med.* **1981**, *71*, 59–66.
19. Brothers, K.M.; Gratacap, R.L.; Barker, S.E.; Newman, Z.R.; Norum, A.; Wheeler, R.T. NADPH oxidase-driven phagocyte recruitment controls *Candida albicans* filamentous growth and prevents mortality. *PLOS Pathog.* **2013**, *9*, e1003634.
20. Brown, A.J.; Haynes, K.; Quinn, J. Nitrosative and oxidative stress responses in fungal pathogenicity. *Curr. Opin. Microbiol.* **2009**, *12*, 384–391.
21. Fang, F.C. Antimicrobial reactive oxygen and nitrogen species: Concepts and controversies. *Nat. Rev. Microbiol.* **2004**, *2*, 820–832.
22. Kaloriti, D.; Jacobsen, M.; Yin, Z.; Patterson, M.; Tillmann, A.; Smith, D.A.; Cook, E.; You, T.; Grimm, M.J.; Bohovych, I.; et al. Mechanisms underlying the exquisite sensitivity of *Candida albicans* to combinatorial cationic and oxidative stress that enhances the potent fungicidal activity of phagocytes. *MBio* **2014**, *5*, e01334–e01314.
23. Frohner, I.E.; Bourgeois, C.; Yatsyk, K.; Majer, O.; Kuchler, K. *Candida albicans* cell surface superoxide dismutases degrade host-derived reactive oxygen species to escape innate immune surveillance. *Mol. Microbiol.* **2009**, *71*, 240–252.
24. Miramon, P.; Dunker, C.; Windecker, H.; Bohovych, I.M.; Brown, A.J.; Kurzai, O.; Hube, B. Cellular responses of *Candida albicans* to phagocytosis and the extracellular activities of neutrophils are critical to counteract carbohydrate starvation, oxidative and nitrosative stress. *PLOS ONE* **2012**, *7*, e52850.
25. Huycke, M.M.; Abrams, V.; Moore, D.R. *Enterococcus faecalis* produces extracellular superoxide and hydrogen peroxide that damages colonic epithelial cell DNA. *Carcinogenesis* **2002**, *23*, 529–536.
26. Fitzsimmons, N.; Berry, D.R. Inhibition of *Candida albicans* by *Lactobacillus acidophilus*: Evidence for the involvement of a peroxidase system. *Microbios* **1994**, *80*, 125–133.
27. Cruz, M.R.; Graham, C.E.; Gagliano, B.C.; Lorenz, M.C.; Garsin, D.A. *Enterococcus faecalis* inhibits hyphal morphogenesis and virulence of *Candida albicans*. *Infect. Immun.* **2013**, *81*, 189–200.
28. Phillips, A.J.; Sudbery, I.; Ramsdale, M. Apoptosis induced by environmental stresses and amphotericin B in *Candida albicans*. *Proc. Natl. Acad. Sci. USA* **2003**, *100*, 14327–14332.
29. Halliwell, B. Oxidative stress and cancer: Have we moved forward? *Biochem. J.* **2007**, *401*, 1–11.
30. Jamieson, D.J.; Stephen, D.W.; Terriere, E.C. Analysis of the adaptive oxidative stress response of *Candida albicans*. *FEMS Microbiol. Lett.* **1996**, *138*, 83–88.
31. Nikolaou, E.; Agrafioti, I.; Stumpf, M.; Quinn, J.; Stansfield, I.; Brown, A.J. Phylogenetic diversity of stress signalling pathways in fungi. *BMC Evol. Biol.* **2009**, doi:10.1186/1471-2148-9-44.
32. Enjalbert, B.; Nantel, A.; Whiteway, M. Stress-induced gene expression in *Candida albicans*: Absence of a general stress response. *Mol. Biol. Cell* **2003**, *14*, 1460–1467.

33. Enjalbert, B.; Smith, D.A.; Cornell, M.J.; Alam, I.; Nicholls, S.; Brown, A.J.; Quinn, J. Role of the Hog1 stress-activated protein kinase in the global transcriptional response to stress in the fungal pathogen *Candida albicans*. *Mol. Biol. Cell* **2006**, *17*, 1018–1032.

34. Enjalbert, B.; MacCallum, D.M.; Odds, F.C.; Brown, A.J. Niche-specific activation of the oxidative stress response by the pathogenic fungus *Candida albicans*. *Infect. Immun.* **2007**, *75*, 2143–2151.

35. Fradin, C.; de Groot, P.; MacCallum, D.; Schaller, M.; Klis, F.; Odds, F.C.; Hube, B. Granulocytes govern the transcriptional response, morphology and proliferation of *Candida albicans* in human blood. *Mol. Microbiol.* **2005**, *56*, 397–415.

36. Fradin, C.; Kretschmar, M.; Nichterlein, T.; Gaillardin, C.; d'Enfert, C.; Hube, B. Stage-specific gene expression of *Candida albicans* in human blood. *Mol. Microbiol.* **2003**, *47*, 1523–1543.

37. Lorenz, M.C.; Bender, J.A.; Fink, G.R. Transcriptional response of *Candida albicans* upon internalization by macrophages. *Eukaryot. Cell* **2004**, *3*, 1076–1087.

38. Rubin-Bejerano, I.; Fraser, I.; Grisafi, P.; Fink, G.R. Phagocytosis by neutrophils induces an amino acid deprivation response in *Saccharomyces cerevisiae* and *Candida albicans*. *Proc. Natl. Acad. Sci. USA* **2003**, *100*, 11007–11012.

39. Thewes, S.; Kretschmar, M.; Park, H.; Schaller, M.; Filler, S.G.; Hube, B. *In vivo* and *ex vivo* comparative transcriptional profiling of invasive and non-invasive *Candida albicans* isolates identifies genes associated with tissue invasion. *Mol. Microbiol.* **2007**, *63*, 1606–1628.

40. Walker, L.A.; MacCallum, D.M.; Bertram, G.; Gow, N.A.; Odds, F.C.; Brown, A.J. Genome-wide analysis of *Candida albicans* gene expression patterns during infection of the mammalian kidney. *Fungal Genet. Biol.* **2009**, *46*, 210–219.

41. Chaves, G.M.; Bates, S.; MacCallum, D.M.; Odds, F.C. *Candida albicans* GRX2, encoding a putative glutaredoxin, is required for virulence in a murine model. *Genet. Mol. Res.* **2007**, *6*, 1051–1063.

42. Da Silva Dantas, A.; Patterson, M.J.; Smith, D.A.; MacCallum, D.M.; Erwig, L.P.; Morgan, B.A.; Quinn, J. Thioredoxin regulates multiple hydrogen peroxide-induced signaling pathways in *Candida albicans*. *Mol. Cell. Biol.* **2010**, *30*, 4550–4563.

43. Hwang, C.S.; Rhie, G.E.; Oh, J.H.; Huh, W.K.; Yim, H.S.; Kang, S.O. Copper- and zinc-containing superoxide dismutase (Cu/ZnSOD) is required for the protection of *Candida albicans* against oxidative stresses and the expression of its full virulence. *Microbiology* **2002**, *148*, 3705–3713.

44. Martchenko, M.; Alarco, A.M.; Harcus, D.; Whiteway, M. Superoxide dismutases in *Candida albicans*: Transcriptional regulation and functional characterization of the hyphal-induced *SOD5* gene. *Mol. Biol. Cell* **2004**, *15*, 456–467.

45. Wysong, D.R.; Christin, L.; Sugar, A.M.; Robbins, P.W.; Diamond, R.D. Cloning and sequencing of a *Candida albicans* catalase gene and effects of disruption of this gene. *Infect. Immun.* **1998**, *66*, 1953–1961.

46. Miramon, P.; Dunker, C.; Kasper, L.; Jacobsen, I.D.; Barz, D.; Kurzai, O.; Hube, B. A family of glutathione peroxidases contributes to oxidative stress resistance in *Candida albicans*. *Med. Mycol.* **2014**, *52*, 223–239.

47. Urban, C.; Xiong, X.; Sohn, K.; Schroppel, K.; Brunner, H.; Rupp, S. The moonlighting protein tsa1p is implicated in oxidative stress response and in cell wall biogenesis in *Candida albicans*. *Mol. Microbiol.* **2005**, *57*, 1318–1341.

48. Steinberg, B.E.; Huynh, K.K.; Grinstein, S. Phagosomal acidification: Measurement, manipulation and functional consequences. *Biochem. Soc. Trans.* **2007**, *35*, 1083–1087.

49. Kaloriti, D.; Tillmann, A.; Cook, E.; Jacobsen, M.; You, T.; Lenardon, M.; Ames, L.; Barahona, M.; Chandrasekaran, K.; Coghill, G.; *et al.* Combinatorial stresses kill pathogenic *Candida* species. *Med. Mycol.* **2012**, *50*, 699–709.

50. Schuller, C.; Brewster, J.L.; Alexander, M.R.; Gustin, M.C.; Ruis, H. The hog pathway controls osmotic regulation of transcription via the stress response element (STRE) of the *Saccharomyces cerevisiae* CTT1 gene. *EMBO J.* **1994**, *13*, 4382–4389.

51. Heilmann, C.J.; Sorgo, A.G.; Siliakus, A.R.; Dekker, H.L.; Brul, S.; de Koster, C.G.; de Koning, L.J.; Klis, F.M. Hyphal induction in the human fungal pathogen *Candida albicans* reveals a characteristic wall protein profile. *Microbiology* **2011**, *157*, 2297–2307.

52. Gleason, J.E.; Galaleldeen, A.; Peterson, R.L.; Taylor, A.B.; Holloway, S.P.; Waninger-Saroni, J.; Cormack, B.P.; Cabelli, D.E.; Hart, P.J.; Culotta, V.C. *Candida albicans* SOD5 represents the prototype of an unprecedented class of Cu-only superoxide dismutases required for pathogen defense. *Proc. Natl. Acad. Sci. USA* **2014**, *111*, 5866–5871.

53. Festa, R.A.; Thiele, D.J. Copper at the front line of the host-pathogen battle. *PLOS Pathog.* **2012**, *8*, e1002887.

54. Crowe, J.D.; Sievwright, I.K.; Auld, G.C.; Moore, N.R.; Gow, N.A.; Booth, N.A. *Candida albicans* binds human plasminogen: Identification of eight plasminogen-binding proteins. *Mol. Microbiol.* **2003**, *47*, 1637–1651.

55. Lewis, L.E.; Bain, J.M.; Okai, B.; Gow, N.A.; Erwig, L.P. Live-cell video microscopy of fungal pathogen phagocytosis. *J. Vis. Exp.* **2013**, doi:10.3791/50196.

56. Patterson, M.J.; McKenzie, C.G.; Smith, D.A.; da Silva Dantas, A.; Sherston, S.; Veal, E.A.; Morgan, B.A.; MacCallum, D.M.; Erwig, L.P.; Quinn, J. Ybp1 and Gpx3 signaling in *Candida albicans* govern hydrogen peroxide-induced oxidation of the Cap1 transcription factor and macrophage escape. *Antioxid. Redox Signal.* **2013**, *19*, 2244–2260.

57. Brothers, K.M.; Newman, Z.R.; Wheeler, R.T. Live imaging of disseminated candidiasis in zebrafish reveals role of phagocyte oxidase in limiting filamentous growth. *Eukaryot. Cell* **2011**, *10*, 932–944.

58. Jimenez-Lopez, C.; Collette, J.R.; Brothers, K.M.; Shepardson, K.M.; Cramer, R.A.; Wheeler, R.T.; Lorenz, M.C. *Candida albicans* induces arginine biosynthetic genes in response to host-derived reactive oxygen species. *Eukaryot. Cell* **2013**, *12*, 91–100.

59. Nasution, O.; Srinivasa, K.; Kim, M.; Kim, Y.J.; Kim, W.; Jeong, W.; Choi, W. Hydrogen peroxide induces hyphal differentiation in *Candida albicans*. *Eukaryot. Cell* **2008**, *7*, 2008–2011.

60. Bachewich, C.; Nantel, A.; Whiteway, M. Cell cycle arrest during S or M phase generates polarized growth via distinct signals in *Candida albicans*. *Mol. Microbiol.* **2005**, *57*, 942–959.

61. Shi, Q.M.; Wang, Y.M.; Zheng, X.D.; Lee, R.T.; Wang, Y. Critical role of DNA checkpoints in mediating genotoxic-stress-induced filamentous growth in *Candida albicans*. *Mol. Biol. Cell* **2007**, *18*, 815–826.

62. Kusch, H.; Engelmann, S.; Albrecht, D.; Morschhauser, J.; Hecker, M. Proteomic analysis of the oxidative stress response in *Candida albicans*. *Proteomics* **2007**, *7*, 686–697.

63. Wang, Y.; Cao, Y.Y.; Jia, X.M.; Cao, Y.B.; Gao, P.H.; Fu, X.P.; Ying, K.; Chen, W.S.; Jiang, Y.Y. Cap1p is involved in multiple pathways of oxidative stress response in *Candida albicans*. *Free Radic. Biol. Med.* **2006**, *40*, 1201–1209.

64. Moye-Rowley, W.S. Regulation of the transcriptional response to oxidative stress in fungi: Similarities and differences. *Eukaryot. Cell* **2003**, *2*, 381–389.

65. Toone, W.M.; Morgan, B.A.; Jones, N. Redox control of AP-1-like factors in yeast and beyond. *Oncogene* **2001**, *20*, 2336–2346.

66. Alarco, A.M.; Raymond, M. The bzip transcription factor Cap1p is involved in multidrug resistance and oxidative stress response in *Candida albicans*. *J. Bacteriol.* **1999**, *181*, 700–708.

67. Zhang, X.; de Micheli, M.; Coleman, S.T.; Sanglard, D.; Moye-Rowley, W.S. Analysis of the oxidative stress regulation of the *Candida albicans* transcription factor, Cap1p. *Mol. Microbiol.* **2000**, *36*, 618–629.

68. Znaidi, S.; Barker, K.S.; Weber, S.; Alarco, A.M.; Liu, T.T.; Boucher, G.; Rogers, P.D.; Raymond, M. Identification of the *Candida albicans* Cap1p regulon. *Eukaryot. Cell* **2009**, *8*, 806–820.

69. Ramirez-Zavala, B.; Mogavero, S.; Scholler, E.; Sasse, C.; Rogers, P.D.; Morschhauser, J. SAGA/ADA complex subunit Ada2 is required for Cap1- but not Mrr1-mediated upregulation of the *Candida albicans* multidrug efflux pump Mdr1. *Antimicrob. Agents Chemother.* **2014**, *58*, 5102–5110.

70. Sellam, A.; Askew, C.; Epp, E.; Lavoie, H.; Whiteway, M.; Nantel, A. Genome-wide mapping of the coactivator Ada2p yields insight into the functional roles of SAGA/ADA complex in *Candida albicans*. *Mol. Biol. Cell* **2009**, *20*, 2389–2400.

71. Delaunay, A.; Isnard, A.D.; Toledano, M.B. H₂O₂ sensing through oxidation of the Yap1 transcription factor. *EMBO J.* **2000**, *19*, 5157–5166.

72. Delaunay, A.; Pfleiger, D.; Barrault, M.B.; Vinh, J.; Toledano, M.B. A thiol peroxidase is an H₂O₂ receptor and redox-transducer in gene activation. *Cell* **2002**, *111*, 471–481.

73. Okazaki, S.; Tachibana, T.; Naganuma, A.; Mano, N.; Kuge, S. Multistep disulfide bond formation in Yap1 is required for sensing and transduction of H₂O₂ stress signal. *Mol. Cell.* **2007**, *27*, 675–688.

74. Okazaki, S.; Naganuma, A.; Kuge, S. Peroxiredoxin-mediated redox regulation of the nuclear localization of Yap1, a transcription factor in budding yeast. *Antioxid. Redox Signal.* **2005**, *7*, 327–334.

75. Tachibana, T.; Okazaki, S.; Murayama, A.; Naganuma, A.; Nomoto, A.; Kuge, S. A major peroxiredoxin-induced activation of Yap1 transcription factor is mediated by reduction-sensitive disulfide bonds and reveals a low level of transcriptional activation. *J. Biol. Chem.* **2009**, *284*, 4464–4472.

76. Veal, E.A.; Ross, S.J.; Malakasi, P.; Peacock, E.; Morgan, B.A. Ybp1 is required for the hydrogen peroxide-induced oxidation of the Yap1 transcription factor. *J. Biol. Chem.* **2003**, *278*, 30896–30904.

77. Gulshan, K.; Thommandru, B.; Moye-Rowley, W.S. Proteolytic degradation of the Yap1 transcription factor is regulated by subcellular localization and the E3 ubiquitin ligase Not4. *J. Biol. Chem.* **2012**, *287*, 36796–36805.

78. Kitamura, K.; Taki, M.; Tanaka, N.; Yamashita, I. Fission yeast Ubr1 ubiquitin ligase influences the oxidative stress response via degradation of active Pap1 bZIP transcription factor in the nucleus. *Mol. Microbiol.* **2011**, *80*, 739–755.

79. Morgan, B.A.; Banks, G.R.; Toone, W.M.; Raitt, D.; Kuge, S.; Johnston, L.H. The Skn7 response regulator controls gene expression in the oxidative stress response of the budding yeast *Saccharomyces cerevisiae*. *EMBO J.* **1997**, *16*, 1035–1044.

80. Singh, P.; Chauhan, N.; Ghosh, A.; Dixon, F.; Calderone, R. Skn7 of *Candida albicans*: Mutant construction and phenotype analysis. *Infect. Immun.* **2004**, *72*, 2390–2394.

81. Jain, C.; Pastor, K.; Gonzalez, A.Y.; Lorenz, M.C.; Rao, R.P. The role of *Candida albicans* AP-1 protein against host derived ROS in *in vivo* models of infection. *Virulence* **2013**, *4*, 67–76.

82. Smith, D.A.; Morgan, B.A.; Quinn, J. Stress signalling to fungal stress-activated protein kinase pathways. *FEMS Microbiol. Lett.* **2010**, *306*, 1–8.

83. Bellon, S.; Fitzgibbon, M.J.; Fox, T.; Hsiao, H.M.; Wilson, K.P. The structure of phosphorylated p38gamma is monomeric and reveals a conserved activation-loop conformation. *Structure* **1999**, *7*, 1057–1065.

84. Alonso-Monge, R.; Navarro-Garcia, F.; Roman, E.; Negredo, A.I.; Eisman, B.; Nombela, C.; Pla, J. The Hog1 mitogen-activated protein kinase is essential in the oxidative stress response and chlamydospore formation in *Candida albicans*. *Eukaryot. Cell* **2003**, *2*, 351–361.

85. Smith, D.A.; Nicholls, S.; Morgan, B.A.; Brown, A.J.; Quinn, J. A conserved stress-activated protein kinase regulates a core stress response in the human pathogen *Candida albicans*. *Mol. Biol. Cell* **2004**, *15*, 4179–4190.

86. Chen, D.; Toone, W.M.; Mata, J.; Lyne, R.; Burns, G.; Kivinen, K.; Brazma, A.; Jones, N.; Bahler, J. Global transcriptional responses of fission yeast to environmental stress. *Mol. Biol. Cell* **2003**, *14*, 214–229.

87. Asp, E.; Nilsson, D.; Sunnerhagen, P. Fission yeast mitogen-activated protein kinase Sty1 interacts with translation factors. *Eukaryot. Cell* **2008**, *7*, 328–338.

88. Yin, Z.; Stead, D.; Walker, J.; Selway, L.; Smith, D.; Brown, A.J.P.; Quinn, J. A proteomic analysis of the salt, cadmium and peroxide stress responses in *Candida albicans* and the role of the Hog1 Sapk in regulating the stress-induced proteome. *Proteomics* **2009**, *9*, 4680–4703.

89. Alonso-Monge, R.; Carvaihlo, S.; Nombela, C.; Rial, E.; Pla, J. The Hog1 MAP kinase controls respiratory metabolism in the fungal pathogen *Candida albicans*. *Microbiology* **2009**, *155*, 413–423.

90. Navarro-Garcia, F.; Eisman, B.; Fiuza, S.M.; Nombela, C.; Pla, J. The MAP kinase Mkc1p is activated under different stress conditions in *Candida albicans*. *Microbiology* **2005**, *151*, 2737–2749.

91. Rauceo, J.M.; Blankenship, J.R.; Fanning, S.; Hamaker, J.J.; Deneault, J.S.; Smith, F.J.; Nantel, A.; Mitchell, A.P. Regulation of the *Candida albicans* cell wall damage response by transcription factor Sko1 and PAS kinase Psk1. *Mol. Biol. Cell* **2008**, *19*, 2741–2751.

92. Alonso-Monge, R.; Roman, E.; Arana, D.M.; Prieto, D.; Urrialde, V.; Nombela, C.; Pla, J. The sko1 protein represses the yeast-to-hypha transition and regulates the oxidative stress response in *Candida albicans*. *Fungal Genet. Biol.* **2010**, *47*, 587–601.

93. Arana, D.M.; Nombela, C.; Alonso-Monge, R.; Pla, J. The Pbs2 MAP kinase kinase is essential for the oxidative-stress response in the fungal pathogen *Candida albicans*. *Microbiology* **2005**, *151*, 1033–1049.

94. Cheetham, J.; Smith, D.A.; da Silva Dantas, A.; Doris, K.S.; Patterson, M.J.; Bruce, C.R.; Quinn, J. A single MAPKKK regulates the Hog1 MAPK pathway in the pathogenic fungus *Candida albicans*. *Mol. Biol. Cell* **2007**, *18*, 4603–4614.

95. Thomas, E.; Roman, E.; Claypool, S.; Manzoor, N.; Pla, J.; Panwar, S.L. Mitochondria influence Cdr1 efflux pump activity, Hog1-mediated oxidative stress pathway, iron homeostasis, and ergosterol levels in *Candida albicans*. *Antimicrob. Agents Chemother.* **2013**, *57*, 5580–5599.

96. Horie, T.; Tatebayashi, K.; Yamada, R.; Saito, H. Phosphorylated Ssk1 prevents unphosphorylated Ssk1 from activating the Ssk2 mitogen-activated protein kinase kinase kinase in the yeast high-osmolarity glycerol osmoregulatory pathway. *Mol. Cell. Biol.* **2008**, *28*, 5172–5183.

97. Posas, F.; Saito, H. Activation of the yeast Ssk2 map kinase kinase kinase by the Ssk1 two-component response regulator. *EMBO J.* **1998**, *17*, 1385–1394.

98. Chauhan, N.; Inglis, D.; Roman, E.; Pla, J.; Li, D.; Calera, J.A.; Calderone, R. *Candida albicans* response regulator gene Ssk1 regulates a subset of genes whose functions are associated with cell wall biosynthesis and adaptation to oxidative stress. *Eukaryot. Cell* **2003**, *2*, 1018–1024.

99. Li, D.; Gurkowska, V.; Sheridan, M.; Calderone, R.; Chauhan, N. Studies on the regulation of the two-component histidine kinase gene *CHK1* in *Candida albicans* using the heterologous lacZ reporter gene. *Microbiology* **2004**, *150*, 3305–3313.

100. Roman, E.; Nombela, C.; Pla, J. The *SHO1* adaptor protein links oxidative stress to morphogenesis and cell wall biosynthesis in the fungal pathogen *Candida albicans*. *Mol. Cell. Biol.* **2005**, *25*, 10611–10627.

101. Buck, V.; Quinn, J.; Soto Pino, T.; Martin, H.; Saldanha, J.; Makino, K.; Morgan, B.A.; Millar, J.B. Peroxide sensors for the fission yeast stress-activated mitogen-activated protein kinase pathway. *Mol. Biol. Cell* **2001**, *12*, 407–419.

102. Quinn, J.; Malakasi, P.; Smith, D.A.; Cheetham, J.; Buck, V.; Millar, J.B.; Morgan, B.A. Two-component mediated peroxide sensing and signal transduction in fission yeast. *Antioxid. Redox Signal.* **2011**, *15*, 153–165.

103. Menon, V.; Li, D.; Chauhan, N.; Rajnarayanan, R.; Dubrovska, A.; West, A.H.; Calderone, R. Functional studies of the Ssk1p response regulator protein of *Candida albicans* as determined by phenotypic analysis of receiver domain point mutants. *Mol. Microbiol.* **2006**, *62*, 997–1013.

104. Mavrianos, J.; Desai, C.; Chauhan, N. Two-component histidine phosphotransfer protein Ypd1 is not essential for viability in *Candida albicans*. *Eukaryot. Cell* **2014**, *13*, 452–460.

105. Bruce, C.R.; Smith, D.A.; Rodgers, D.; da Silva Dantas, A.; MacCallum, D.M.; Morgan, B.A.; Quinn, J. Identification of a novel response regulator, Crr1, that is required for hydrogen peroxide resistance in *Candida albicans*. *PLOS ONE* **2011**, *6*, e27979.

106. Desai, C.; Mavrianos, J.; Chauhan, N. *Candida albicans* Srr1, a putative two-component response regulator gene, is required for stress adaptation, morphogenesis, and virulence. *Eukaryot. Cell* **2011**, *10*, 1370–1374.

107. O'Rourke, S.M.; Herskowitz, I. A third osmosensing branch in *Saccharomyces cerevisiae* requires the Msb2 protein and functions in parallel with the Sho1 branch. *Mol. Cell. Biol.* **2002**, *22*, 4739–4749.

108. Veal, E.A.; Day, A.M.; Morgan, B.A. Hydrogen peroxide sensing and signaling. *Mol. Cell* **2007**, *26*, 1–14.

109. Veal, E.A.; Findlay, V.J.; Day, A.M.; Bozonet, S.M.; Evans, J.M.; Quinn, J.; Morgan, B.A. A 2-cys peroxiredoxin regulates peroxide-induced oxidation and activation of a stress-activated MAP kinase. *Mol. Cell* **2004**, *15*, 129–139.

110. Saitoh, M.; Nishitoh, H.; Fujii, M.; Takeda, K.; Tobiume, K.; Sawada, Y.; Kawabata, M.; Miyazono, K.; Ichijo, H. Mammalian thioredoxin is a direct inhibitor of apoptosis signal-regulating kinase (ASK) 1. *EMBO J.* **1998**, *17*, 2596–2606.

111. Nadeau, P.J.; Charette, S.J.; Landry, J. Redox reaction at ASK1-Cys250 is essential for activation of jnk and induction of apoptosis. *Mol. Biol. Cell* **2009**, *20*, 3628–3637.

112. Nadeau, P.J.; Charette, S.J.; Toledano, M.B.; Landry, J. Disulfide bond-mediated multimerization of ASK1 and its reduction by thioredoxin-1 regulate H₂O₂-induced c-Jun NH₂-terminal kinase activation and apoptosis. *Mol. Biol. Cell* **2007**, *18*, 3903–3913.

113. Brandes, N.; Schmitt, S.; Jakob, U. Thiol-based redox switches in eukaryotic proteins. *Antioxid. Redox Signal.* **2009**, *11*, 997–1014.

114. Alonso-Monge, R.; Navarro-Garcia, F.; Molero, G.; Diez-Orejas, R.; Gustin, M.; Pla, J.; Sanchez, M.; Nombela, C. Role of the mitogen-activated protein kinase Hog1p in morphogenesis and virulence of *Candida albicans*. *J. Bacteriol.* **1999**, *181*, 3058–3068.

115. Cheetham, J.; MacCallum, D.M.; Doris, K.S.; da Silva Dantas, A.; Scorfield, S.; Odds, F.; Smith, D.A.; Quinn, J. MAPKKK-independent regulation of the Hog1 stress-activated protein kinase in *Candida albicans*. *J. Biol. Chem.* **2011**, *286*, 42002–42016.

116. Prieto, D.; Roman, E.; Correia, I.; Pla, J. The Hog pathway is critical for the colonization of the mouse gastrointestinal tract by *Candida albicans*. *PLOS ONE* **2014**, *9*, e87128.

117. Arana, D.M.; Alonso-Monge, R.; Du, C.; Calderone, R.; Pla, J. Differential susceptibility of mitogen-activated protein kinase pathway mutants to oxidative-mediated killing by phagocytes in the fungal pathogen *Candida albicans*. *Cell. Microbiol.* **2007**, *9*, 1647–1659.

118. Loll-Krippleber, R.; d’Enfert, C.; Feri, A.; Diogo, D.; Perin, A.; Marcet-Houben, M.; Bougnoux, M.E.; Legrand, M. A study of the DNA damage checkpoint in *Candida albicans*: Uncoupling of the functions of Rad53 in DNA repair, cell cycle regulation and genotoxic stress-induced polarized growth. *Mol. Microbiol.* **2014**, *91*, 452–471.

119. Shockley, A.H.; Doo, D.W.; Rodriguez, G.P.; Crouse, G.F. Oxidative damage and mutagenesis in *Saccharomyces cerevisiae*: Genetic studies of pathways affecting replication fidelity of 8-oxoguanine. *Genetics* **2013**, *195*, 359–367.

120. Leroy, C.; Mann, C.; Marsolier, M.C. Silent repair accounts for cell cycle specificity in the signaling of oxidative DNA lesions. *EMBO J.* **2001**, *20*, 2896–2906.

121. Muniyappa, H.; Song, S.; Mathews, C.K.; Das, K.C. Reactive oxygen species-independent oxidation of thioredoxin in hypoxia: Inactivation of ribonucleotide reductase and redox-mediated checkpoint control. *J. Biol. Chem.* **2009**, *284*, 17069–17081.

122. Guo, Z.; Kozlov, S.; Lavin, M.F.; Person, M.D.; Paull, T.T. ATM activation by oxidative stress. *Science* **2010**, *330*, 517–521.

123. Wilson, D.; Tutulan-Cunita, A.; Jung, W.; Hauser, N.C.; Hernandez, R.; Williamson, T.; Piekarska, K.; Rupp, S.; Young, T.; Stateva, L. Deletion of the high-affinity camp phosphodiesterase encoded by Pde2 affects stress responses and virulence in *Candida albicans*. *Mol. Microbiol.* **2007**, *65*, 841–856.

124. Deveau, A.; Piispanen, A.E.; Jackson, A.A.; Hogan, D.A. Farnesol induces hydrogen peroxide resistance in *Candida albicans* yeast by inhibiting the Ras-cyclic AMP signaling pathway. *Eukaryot. Cell* **2010**, *9*, 569–577.

125. Kamthan, M.; Nalla, V.K.; Ruhela, D.; Kamthan, A.; Maiti, P.; Datta, A. Characterization of a putative spindle assembly checkpoint kinase Mps1, suggests its involvement in cell division, morphogenesis and oxidative stress tolerance in *Candida albicans*. *PLOS ONE* **2014**, *9*, e101517.
126. Bai, C.; Ramanan, N.; Wang, Y.M.; Wang, Y. Spindle assembly checkpoint component CaMad2p is indispensable for *Candida albicans* survival and virulence in mice. *Mol. Microbiol.* **2002**, *45*, 31–44.
127. Du, C.; Calderone, R.; Richert, J.; Li, D. Deletion of the SSK1 response regulator gene in *Candida albicans* contributes to enhanced killing by human polymorphonuclear neutrophils. *Infect. Immun.* **2005**, *73*, 865–871.
128. Calera, J.A.; Zhao, X.J.; Calderone, R. Defective hyphal development and avirulence caused by a deletion of the SSK1 response regulator gene in *Candida albicans*. *Infect. Immun.* **2000**, *68*, 518–525.

© 2015 by the authors; licensee MDPI, Basel, Switzerland. This article is an open access article distributed under the terms and conditions of the Creative Commons Attribution license (<http://creativecommons.org/licenses/by/4.0/>).

Mechanisms Underlying the Delayed Activation of the Cap1 Transcription Factor in *Candida albicans* following Combinatorial Oxidative and Cationic Stress Important for Phagocytic Potency

Iaroslava Kos,^a Miranda J. Patterson,^a Sadri Znaidi,^{b,c} Despoina Kaloriti,^d Alessandra da Silva Dantas,^a Carmen M. Herrero-de-Dios,^d Christophe d'Enfert,^{b,c} Alistair J. P. Brown,^d Janet Quinn^a

Institute for Cell and Molecular Biosciences, Faculty of Medicine, Newcastle University, Newcastle upon Tyne, United Kingdom^a; Institut Pasteur, Unité Biologie et Pathogénicité Fongiques, Département Mycologie, Paris, France^b; INRA, USC2019, Paris, France^c; School of Medical Sciences, University of Aberdeen, Aberdeen, United Kingdom^d

ABSTRACT Following phagocytosis, microbes are exposed to an array of antimicrobial weapons that include reactive oxygen species (ROS) and cationic fluxes. This is significant as combinations of oxidative and cationic stresses are much more potent than the corresponding single stresses, triggering the synergistic killing of the fungal pathogen *Candida albicans* by “stress pathway interference.” Previously we demonstrated that combinatorial oxidative plus cationic stress triggers a dramatic increase in intracellular ROS levels compared to oxidative stress alone. Here we show that activation of Cap1, the major regulator of antioxidant gene expression in *C. albicans*, is significantly delayed in response to combinatorial stress treatments and to high levels of H₂O₂. Cap1 is normally oxidized in response to H₂O₂; this masks the nuclear export sequence, resulting in the rapid nuclear accumulation of Cap1 and the induction of Cap1-dependent genes. Here we demonstrate that following exposure of cells to combinatorial stress or to high levels of H₂O₂, Cap1 becomes trapped in a partially oxidized form, Cap1^{OX-1}. Notably, Cap1-dependent gene expression is not induced when Cap1 is in this partially oxidized form. However, while Cap1^{OX-1} readily accumulates in the nucleus and binds to target genes following high-H₂O₂ stress, the nuclear accumulation of Cap1^{OX-1} following combinatorial H₂O₂ and NaCl stress is delayed due to a cationic stress-enhanced interaction with the Crm1 nuclear export factor. These findings define novel mechanisms that delay activation of the Cap1 transcription factor, thus preventing the rapid activation of the stress responses vital for the survival of *C. albicans* within the host.

IMPORTANCE Combinatorial stress-mediated synergistic killing represents a new unchartered area in the field of stress signaling. This phenomenon contrasts starkly with “stress cross-protection,” where exposure to one stress protects against subsequent exposure to a different stress. Previously we demonstrated that the pathogen *Candida albicans* is acutely sensitive to combinations of cationic and oxidative stresses, because the induction of H₂O₂-responsive genes is blocked in the presence of cationic stress. We reveal that this is due to novel mechanisms that delay activation of the Cap1 AP-1-like transcription factor, the major regulator of the H₂O₂-induced regulon. Cap1 becomes trapped in a partially oxidized form following simultaneous exposure to oxidative and cationic stresses. In addition, cationic stress promotes the interaction of Cap1 with the Crm1 nuclear export factor, thus inhibiting its nuclear accumulation. These mechanisms probably explain the potency of neutrophils, which employ multiple stresses to kill fungal pathogens.

Received 24 February 2016 Accepted 1 March 2016 Published 29 March 2016

Citation Kos I, Patterson MJ, Znaidi S, Kaloriti D, da Silva Dantas A, Herrero-de-Dios CM, d'Enfert C, Brown AJP, Quinn J. 2016. Mechanisms underlying the delayed activation of the Cap1 transcription factor in *Candida albicans* following combinatorial oxidative and cationic stress important for phagocytic potency. *mBio* 7(2):e00331-16. doi:10.1128/mBio.00331-16.

Invited Editor Ana Traven, Monash University **Editor** Bernhard Hube, Friedrich Schiller University, Jena

Copyright © 2016 Kos et al. This is an open-access article distributed under the terms of the [Creative Commons Attribution 4.0 International license](http://creativecommons.org/licenses/by/4.0/).

Address correspondence to Janet Quinn, janet.quinn@ncl.ac.uk.

Candida albicans is a major fungal pathogen of humans. Recent estimates indicate that invasive *C. albicans* infections are associated with disturbingly high mortality rates of between 46 and 75% and are responsible for over 400,000 life-threatening systemic infections each year (1). Immunocompromised patients are most at risk of systemic candidiasis, such as those receiving immunosuppressive treatments for cancer or transplant surgery. In contrast, in healthy hosts, robust immune protection mechanisms prevent such systemic infections, with innate immune cells such as macrophages and neutrophils providing the first line of defense.

A major antimicrobial defense mechanism mounted by innate

immune cells is the production of superoxide anions (O₂⁻) by the NADPH oxidase complex (2). The importance of this oxidative burst in fungal killing is exemplified by patients with chronic granulomatous disease (CGD). CGD is a genetic disorder in which patients have a defective phagocytic NADPH oxidase complex. These patients are significantly more susceptible to systemic *Candida* infections (3). The levels of O₂⁻ generated by neutrophils in the phagocytic vacuole are estimated to range between 1 (4) and 4 mol liter⁻¹ (5). The steady-state levels of O₂⁻ are, however, likely to be much lower (4) due to its rapid dismutation to the more reactive hydrogen peroxide, H₂O₂ (6). Moreover, the resul-

tant H_2O_2 can also generate hypochlorous acid (HOCl) by the action of myeloperoxidase. O_2^- can also react with the nitric oxide radical, generated by nitric oxide synthase, to form peroxynitrite (ONOO^-). Thus, the production of superoxide leads to the generation of a range of reactive oxygen, nitrogen, and chloride species (reviewed in references 4 and 6).

The prevailing view that reactive oxygen species (ROS) are a major factor underlying the fungicidal action of phagocytes does, however, conflict with previous studies which have demonstrated that *C. albicans* is more resistant to multiple oxidative stress-inducing agents than other fungi (7, 8). Following exposure to ROS, the activation of several pathways allows *C. albicans* to detoxify the stress and repair the oxidative damage to cellular components (9). One major mechanism involves the rapid induction of genes with antioxidant properties (10–14), and this is largely regulated by the AP-1-like transcription factor Cap1 (15, 16). Similar to the homologous *Saccharomyces cerevisiae* Yap1 and *Schizosaccharomyces pombe* Pap1 transcription factors (17, 18), H_2O_2 -mediated-Cap1 activation is triggered by the oxidation of redox-active cysteine residues located within two cysteine-rich domains (n-CRD and c-CRD). Based on studies in *S. cerevisiae* (19, 20), this is predicted to trigger a conformational change within Cap1 that masks the nuclear export sequence (NES) from the Crm1 nuclear export factor, thereby allowing the nuclear accumulation of this transcription factor. Once in the nucleus, Cap1 is phosphorylated, and the induction of Cap1-dependent genes ensues (21). As many key antioxidant genes, including *CAT1* encoding catalase and *TRX1* encoding thioredoxin, are direct Cap1 targets (22), *C. albicans* cells lacking Cap1 are exquisitely sensitive to ROS (11, 23, 24) and to phagocyte-mediated killing (25, 26).

As *C. albicans* mounts a robust response to oxidative stress *in vitro* and is more resistant to ROS than many other fungi, why is this pathogen unable to survive phagocytosis in the immunocompetent host? Recently, we demonstrated that the sensitivity of *C. albicans* to oxidative stress increases dramatically if cells are simultaneously exposed to cationic stress (27). This is relevant in the context of innate immune defenses, as following phagocytosis, there is an increased flux of the K^+ cation into the phagosome to compensate for the anionic charge that accumulates due to the high levels of O_2^- generated (5). Thus, the potency of innate immune defenses against *C. albicans* can be attributed to exposure to both oxidative and cationic stresses within the phagosome. At the molecular level, this combinatorial oxidative and cationic stress-mediated synergistic killing of *C. albicans* is due to stress pathway interference (28). Specifically, Cap1 fails to accumulate in the nucleus following exposure of *C. albicans* to combinatorial oxidative and cationic stress, and thus Cap1-dependent antioxidant genes are not induced (28). Importantly, the cationic stress-mediated inhibition of oxidative stress responses appears to be of physiological relevance, as the high fungicidal activity of human neutrophils is impaired to similar extents when either the oxidative burst or the cationic flux is inhibited (28).

Here, we dissect the mechanisms underlying the combinatorial stress-mediated inhibition of Cap1 activation. We show that Cap1 becomes trapped in a partially oxidized form for sustained periods following combinatorial oxidative and cationic stress and also in response to high levels of oxidative stress. Significantly, Cap1-dependent gene expression does not occur when Cap1 is in this partially oxidized state. However, the failure of Cap1 to accumulate in the nucleus is specific to the combinatorial cationic and

oxidative stress, due to the cation-mediated stabilization of the interaction between Cap1 and the Crm1 nuclear export factor. We propose that these previously uncharacterized mechanisms, which prevent the rapid activation of Cap1, underlie the exquisite sensitivity of *C. albicans* to combinatorial cationic and oxidative stress and hence the potency of innate immune defenses.

RESULTS

Differential oxidation of Cap1 following combinatorial stress. Previously we demonstrated that the normal transcriptional response to oxidative stress is not induced following the simultaneous exposure of *C. albicans* cells to cationic (1 M NaCl) and oxidative (5 mM H_2O_2) stress and that the major regulator of oxidative stress response gene expression, Cap1, fails to accumulate in the nucleus following such combinatorial stress treatments (28). However, the mechanisms underlying this inhibition of Cap1 function are unknown. As described above, the oxidative stress-induced nuclear accumulation of fungal AP-1-like transcription factors, such as Cap1, is triggered by the oxidation of redox-active cysteine residues. Therefore, we examined Cap1 oxidation alongside other readouts of Cap1 activation following combinatorial oxidative plus cationic stress treatments. Cells expressing Cap1 tagged with 2 copies of the Myc epitope were collected following a 10-min treatment with H_2O_2 or combinatorial H_2O_2 plus NaCl, and samples were simultaneously processed to examine Cap1 oxidation, phosphorylation, and Cap1-dependent gene expression. In addition, cells expressing Cap1-green fluorescent protein (GFP) were exposed to the same stress treatments. As expected, Cap1 failed to accumulate in the nucleus following a 10-min combinatorial H_2O_2 plus NaCl treatment but rapidly accumulated in the nucleus following H_2O_2 treatment alone (Fig. 1A). Furthermore, consistent with the effects of these stress conditions on nuclear accumulation, Cap1 was not phosphorylated following combinatorial stress treatment but was robustly phosphorylated following exposure to H_2O_2 alone (Fig. 1B). Analysis of the Cap1-dependent transcripts *CAT1* and *TRR1* reaffirmed our previous microarray data (28) that exposure of *C. albicans* to oxidative stress in the presence of cationic stress prevents the rapid induction of Cap1-regulated genes (Fig. 1C). As Cap1 oxidation is essential to drive the nuclear accumulation of Cap1 and Cap1-dependent gene expression, it was possible that cationic stress interferes with the H_2O_2 -induced oxidation of Cap1. To examine this hypothesis, the redox status of Cap1 was determined using the alkylating agent 4-aceto-4'-maleimidylstilbene-2,2'-disulfonic acid (AMS) (Fig. 1D), which reacts specifically with the thiol groups of reduced cysteine residues, thereby increasing the molecular mass of thiol-modified proteins by 0.64 kDa/cysteine (21). The oxidation of cysteine residues prevents AMS binding, and consequently oxidized proteins have a lower molecular mass and faster mobility on nonreducing PAGE compared to the corresponding reduced proteins. We detected this mobility shift by Western blotting. Cells were subjected to acid lysis and reduced cysteine residues labeled with AMS. Strikingly, AMS-treated Cap1 exhibited a faster mobility following the combinatorial oxidative and cationic stress, compared to oxidative stress alone (Fig. 1E). Importantly the increased mobility of Cap1 following combinatorial stress was AMS dependent (Fig. 1E), indicating this was due to a greater number of cysteine residues being oxidized in Cap1 under these conditions, thus preventing AMS binding. We designated this differentially oxidized form “Cap1^{OX-1}” and the form

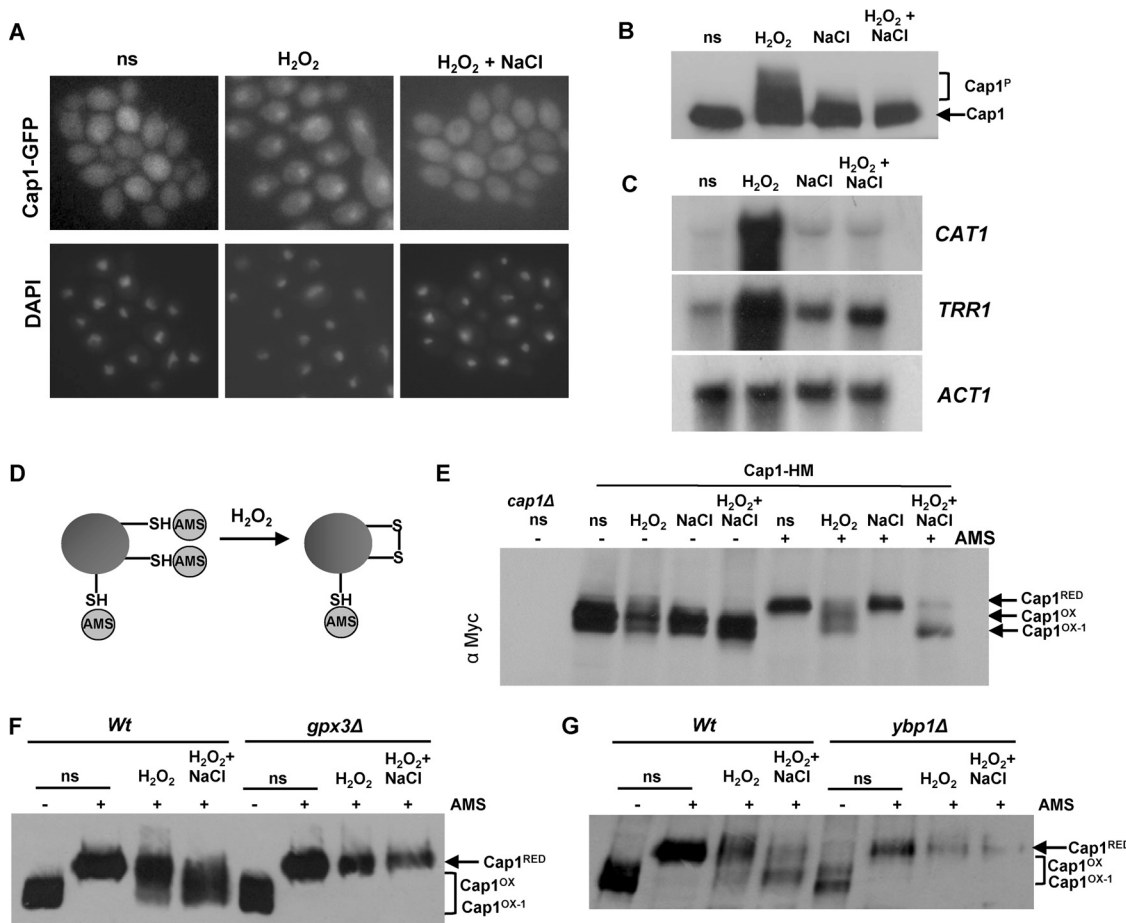


FIG 1 The lack of antioxidant gene expression following combinatorial stress is accompanied by a differentially oxidized form of the Cap1 transcription factor. (A) Cap1 does not accumulate in the nucleus following combinatorial stress. Localization of Cap1 was detected by fluorescence microscopy of cells expressing Cap1-GFP (JC1060) under non-stress conditions (ns) and after exposure to 5 mM H₂O₂ or 5 mM H₂O₂ plus 1 M NaCl for 10 min. The position of the nuclei is shown by DAPI staining. (B) Cap1 is phosphorylated following H₂O₂ exposure but not combinatorial stress. Lysates from cells expressing 2Myc- and 6His-tagged Cap1 (Cap1-HM [JC948]), before (ns) and after the indicated stress treatments, were analyzed by Western blotting using an anti-Myc antibody. The positions of nonphosphorylated (Cap1) and phosphorylated (Cap1^P) Cap1 are indicated. (C) Combinatorial stress inhibits H₂O₂-induced antioxidant gene expression. Northern blot analysis of RNA isolated from wild-type (Wt [JC747]) cells before (ns) and following a 10-min treatment with 5 mM H₂O₂, 1 M NaCl, or 5 mM H₂O₂ plus 1 M NaCl. Blots were analyzed with probes specific for the catalase (CAT1) and thioredoxin reductase (TRR1) genes. A probe against ACT1 was used as the loading control. (D) Diagram illustrating the detection of protein oxidation by AMS binding to reduced thiols. (E) Cap1 is differentially oxidized following combinatorial stress. Cap1 oxidation was analyzed by nonreducing SDS-PAGE and Western blotting of AMS-modified or untreated proteins prepared from cells expressing Cap1-HM before (ns) and following the stress treatments described above. Extracts from cap1Δ cells were included as a control. The positions of reduced (Cap1^{RED}), oxidized (Cap1^{OX}), and differentially oxidized (Cap1^{OX-1}) Cap1 are indicated. (F) Differential oxidation of Cap1 is dependent on Gpx3. Cap1 oxidation was determined as described above in wild-type (Wt [JC948]) and gpx3Δ (JC1311) cells expressing Cap1-MH before (ns) and following the stress treatments described above. (G) Differential oxidation of Cap1 is dependent on Ypb1. Cap1 oxidation was determined as described above in wild-type (Wt [JC948]) and ybp1Δ (JC954) cells.

generated following H₂O₂ treatment alone “Cap1^{OX}” (Fig. 1E). We also confirmed that the faster-mobility forms seen following oxidative and combinatorial stresses were not due to proteolysis. These forms were not seen in the absence of AMS following acid lysis (Fig. 1E) or following analysis of native extracts (see Fig. S1A in the supplemental material), and the cellular levels of Cap1 were not affected by any of the stress treatments employed above (see Fig. S1A and S1B).

The oxidation of *C. albicans* Cap1 in response to H₂O₂ requires the thiol peroxidase Gpx3 (26). Hence, we next investigated whether the formation of Cap1^{OX-1} following combinatorial cationic and oxidative stress is also dependent on Gpx3. Wild-type cells and cells lacking GPX3 were exposed to both oxidative and

combinatorial oxidative and cationic stresses, and Cap1 oxidation was examined. Interestingly, the formation of Cap1^{OX-1} following combinatorial stress, as well as Cap1^{OX} following oxidative stress, was abolished in gpx3Δ cells (Fig. 1F). Gpx3-mediated Cap1 oxidation also requires an orthologue of the *S. cerevisiae* Yap1 binding protein, Ypb1, which additionally functions to prevent the degradation of these AP-1-like transcription factors (26). Similar to what was observed in gpx3Δ cells, no Cap1 oxidation was evident in cells lacking YPB1 following exposure to either oxidative or combinatorial stress (Fig. 1G). Furthermore, consistent with previous findings, Cap1 levels were significantly reduced in ybp1Δ cells (Fig. 1G). Based on these results, we conclude that differentially oxidized forms of Cap1 are generated following a 10-min

exposure to oxidative and combinatorial stresses and that Gpx3 and Ybp1 are crucial for this differential Cap1 oxidation.

Cap1^{OX} contains more disulfides than Cap1^{OX-1}. In *S. cerevisiae*, the stepwise oxidation of all six redox-active cysteines within Yap1, leading to three interdomain disulfides between the n-CRD and c-CRD cysteine-rich domains, is necessary for maximal activation (29). Hence, to investigate the nature of the Cap1^{OX-1} form, labeling experiments were performed to allow for the detection of H₂O₂-induced disulfide bond formation. Cells were subjected to acid lysis, and free reduced cysteines were blocked with the low-molecular-mass thiol-binding reagent *N*-ethylmaleimide (NEM). Any disulfides present were then reduced with dithiothreitol (DTT), and subsequent free thiols were labeled with AMS (Fig. 2A). Thus, in this experiment, the presence of oxidized intramolecular disulfides is indicated by the reduced mobility of Cap1 upon SDS-PAGE. Cap1 exhibited reduced mobility after the sequential NEM-DTT-AMS treatment in cells treated with either oxidative stress or combinatorial oxidative plus cationic stress (Fig. 2B; see Fig. S2A in the supplemental material). Thus, both Cap1^{OX} and Cap1^{OX-1} forms contain oxidized intramolecular disulfides. Based on our previous experiment, in which Cap^{OX-1} displayed a faster mobility than Cap1^{OX} following AMS treatment alone (Fig. 1E), we predicted that this form of Cap1 may have more disulfides than Cap1^{OX}. If this was the case, then following sequential NEM-DTT-AMS treatment, Cap1^{OX-1} would have a slower mobility than Cap1^{OX} due to more AMS binding. However, this was not observed: Cap1 displayed a slightly slower mobility following oxidative stress than following combinatorial stress (Fig. 2B). This suggested that Cap1^{OX-1} has fewer disulfides than Cap1^{OX}. It was possible, however, that this slower mobility of Cap1 following oxidative stress was due to residual phosphorylation of this transcription factor, even after phosphatase treatment, as phosphorylation occurs following H₂O₂, but not combinatorial, stress treatments (Fig. 1C). To avoid this complication, we repeated the experiment by monitoring mobility retardation mediated by another thiol-alkylation probe, polyethylene glycol (PEG)-linked maleimide, which has a higher molecular mass (2 kDa) than AMS (Fig. 2C). Using PEG-maleimide, clear differences were observed in the oxidized forms of Cap1 generated following oxidative and combinatorial stress treatment (Fig. 2D). Following H₂O₂ stress, Cap1 was present predominantly as a single species with significantly retarded mobility following the sequential NEM-DTT-PEG maleimide treatment. In contrast, following combinatorial stress, multiple differentially oxidized forms of Cap1 were observed, with only a fraction displaying the same retarded mobility as that seen for Cap1^{OX} following oxidative stress alone (Fig. 2D). Thus, although the previous AMS binding experiment indicated that Cap1^{OX-1} was more oxidized than Cap1^{OX} (Fig. 1E), these experiments indicate that Cap1^{OX} has more H₂O₂-induced disulfides than Cap1^{OX-1}, generated following combinatorial stress. This seemingly contradictory observation could be explained by the hyperoxidation of cysteine thiols to sulfenic or sulfonic acid derivatives in the Cap1^{OX-1} form.

Differential oxidation and inactivation of Cap1 following combinatorial stress is transient. Next, we determined whether the differential oxidation and inactivation of Cap1 following combinatorial stress was short-lived or irreversible. Cells expressing either Myc-tagged Cap1 or Cap1-GFP were treated with H₂O₂ or H₂O₂ plus NaCl, and samples were collected over a 2-h period. First of all, we determined the redox status of Cap1 using the AMS

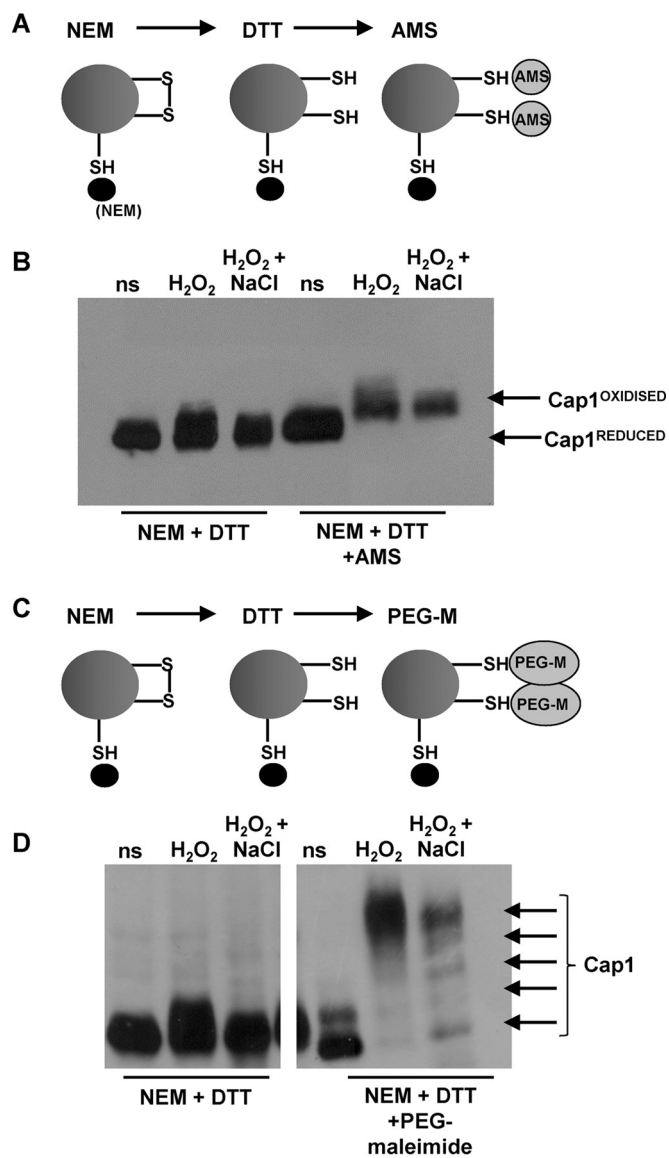


FIG 2 Cap1 oxidation following oxidative and combinatorial stresses. (A) Diagram showing the sequential NEM-DTT-AMS treatments employed to allow for the detection of disulfide bonds. (B) The oxidized forms generated following both oxidative and combinatorial stresses contain disulfide bonds. Cap1 mobility was monitored by nonreducing SDS-PAGE and Western blotting of proteins prepared from cells expressing Cap1-HM, under non-stress conditions (ns [Cap1^{REDUCED}]) or following treatment with the indicated compounds. Samples were phosphatase treated prior to loading. The presence of disulfide bonds is indicated by the retarded mobility of Cap1 due to AMS binding to DTT-resolved disulfides (Cap1^{OXIDISED}). (C) Diagram showing the sequential NEM-DTT-PEG-maleimide (PEG-M) treatments that allow for the detection of disulfide bonds. (D) Comparison of Cap1 oxidation before (ns) and following oxidative and combinatorial stresses by PEG-maleimide binding to DTT-resolved thiols. As in panel B, samples were phosphatase treated prior to loading. This shows that different oxidized forms of Cap1 are present following combinatorial stress, whereas a single form containing multiple disulfides is prevalent following oxidative stress.

alkylating agent as described in the legend to Fig. 1D. The double band of Cap1 seen in the non-AMS-treated time zero sample is likely due to oxidation during protein extraction as this is prevented by the addition of the low-molecular-mass thiol binding

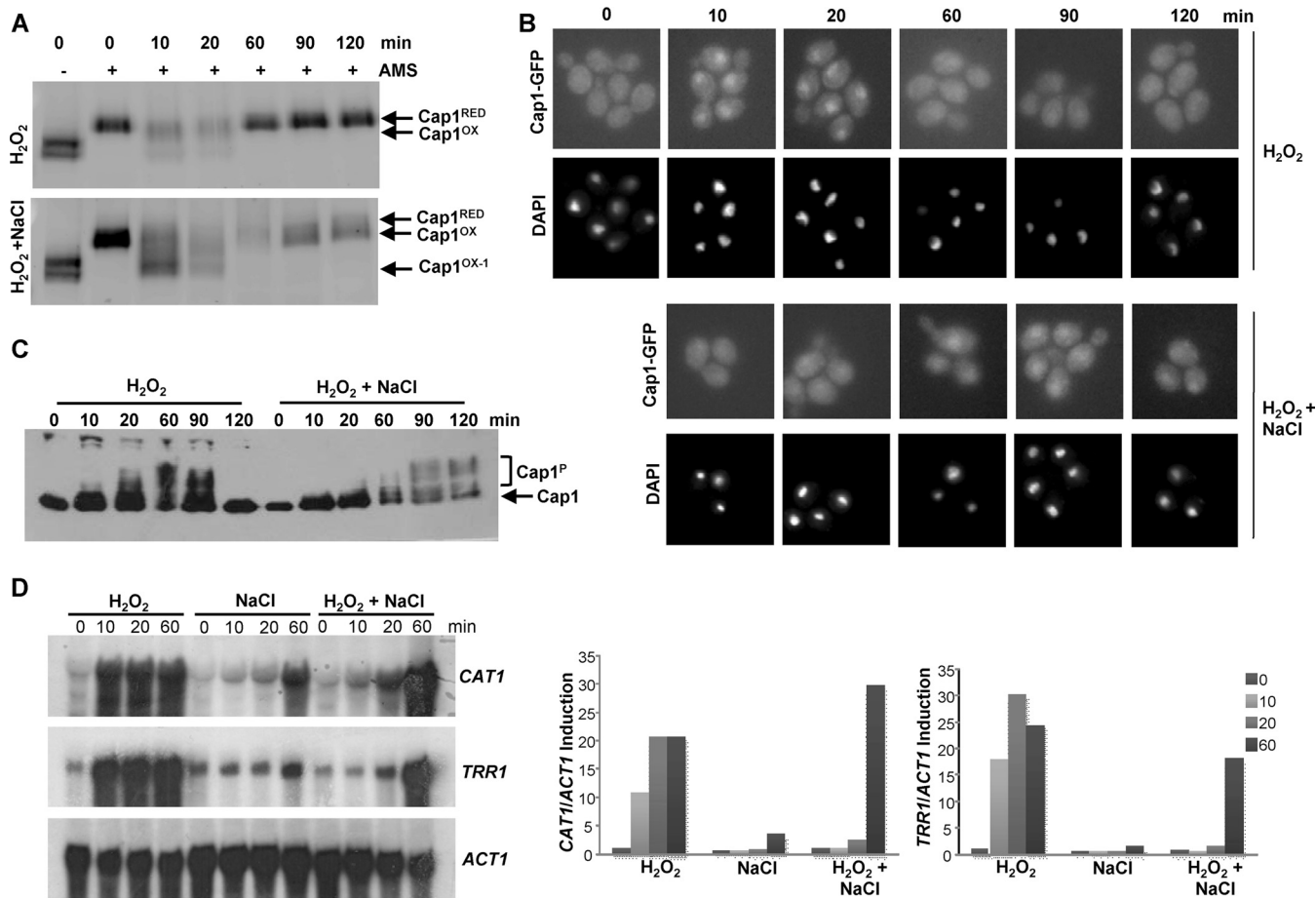


FIG 3 Combinatorial stress-mediated inhibition of Cap1 activation is transient. (A) Differential oxidation of Cap1 following combinatorial stress is not sustained. Cap1 oxidation was measured as described in the legend to Fig. 1E following exposure of Cap1-MH cells to 5 mM H_2O_2 or 5 mM H_2O_2 plus 1 M NaCl for the indicated times. (B) Cap1 nuclear accumulation is delayed following combinatorial stress. Cap1 localization was detected as described in the legend to Fig. 1B following treatment of Cap1-GFP cells for the indicated times with the stress treatments described above. (C) Cap1 phosphorylation is delayed following combinatorial stress treatment. Cap1 phosphorylation was detected as described in the legend to Fig. 1C, following treatment of Cap1-MH cells with the stress treatments described above for the indicated times. (D) The inhibition of Cap1-dependent gene expression following combinatorial stress is transient. Northern blots were performed as described in the legend to Fig. 1A, after wild-type cells were treated with the stress treatments described above for the indicated times (left panel). The levels of *CAT1* and *TRR1* mRNA were quantified relative to the *ACT1* loading control (right panel).

agent NEM during extraction (see Fig. S2B in the supplemental material). Consistent with previous findings, the Cap1^{OX} form was quickly generated following H_2O_2 stress and then resolved back to the reduced form within 60 min. Similarly, the $\text{Cap1}^{\text{OX-1}}$ form appeared rapidly after H_2O_2 plus NaCl stress (Fig. 3A). However, by 60 min, the combinatorial stress-induced $\text{Cap1}^{\text{OX-1}}$ form was resolved to a form with mobility similar to that of Cap1^{OX} (Fig. 3A). This indicates that the $\text{Cap1}^{\text{OX-1}}$ form generated following combinatorial stress is transient.

To examine whether the inactivation of Cap1 following combinatorial stress was coincident with the presence of the $\text{Cap1}^{\text{OX-1}}$ form, the kinetics of Cap1 nuclear accumulation, phosphorylation, and Cap1-dependent gene expression were determined. As illustrated in Fig. 3B, Cap1 did accumulate in the nucleus following combinatorial H_2O_2 plus NaCl stress, but with significantly delayed kinetics compared to H_2O_2 stress. Cap1 located to the nucleus 10 min following H_2O_2 stress, whereas nuclear accumulation of Cap1 post-combinatorial H_2O_2 and NaCl stress was not evident until 60 min. Notably the appearance of Cap1 in the nu-

cleus coincided with Cap1 being resolved to the Cap1^{OX} form (Fig. 3A and B). We next examined Cap1 phosphorylation, as this posttranslational modification is associated with the nuclear accumulation of fungal AP-1-like transcription factors (30). Cap1 phosphorylation was only seen 60 min after the combinatorial H_2O_2 plus NaCl stress, coincident with the point at which Cap1 accumulated in the nucleus (Fig. 3C). Significantly, the delayed nuclear accumulation and phosphorylation of Cap1 observed following combinatorial stress was mirrored by a delay in Cap1-dependent gene induction (Fig. 3D). Northern analysis revealed that the Cap1-dependent genes *CAT1* and *TRR1* are significantly induced following the combinatorial H_2O_2 plus NaCl stress, but not until 60 min after the combinatorial stress treatment. In contrast, these key antioxidant-encoding genes were induced within 10 min of H_2O_2 stress exposure (Fig. 3D). This is entirely consistent with our previous microarray data which failed to detect Cap1-dependent gene expression following a 10-min exposure to the combinatorial oxidative plus cationic stress (28). The significant delay in Cap1-dependent gene expression following simulta-

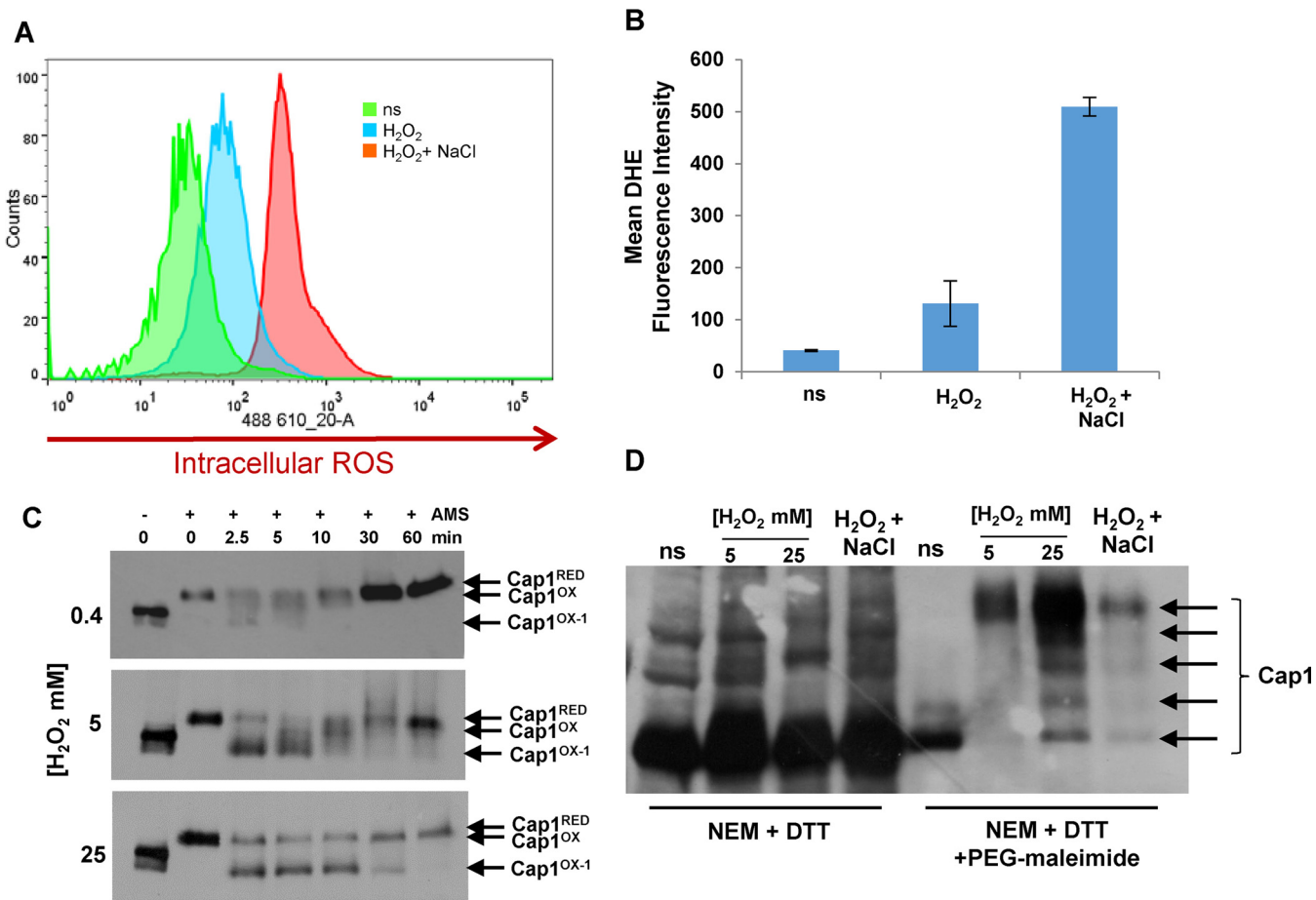


FIG 4 Combinatorial stress induces high levels of intracellular ROS, and high levels of H_2O_2 also result in sustained differential Cap1 oxidation. (A) Fluorescence-activated cell sorter (FACS) analysis of intracellular ROS levels in DHE-treated *C. albicans* cells before stress (ns) or following the treatment with 5 mM H_2O_2 or 5 mM H_2O_2 plus 1 M NaCl for 60 min. (B) Quantification of intracellular ROS production before (ns) and following treatment with the indicated stresses by calculating the mean DHE fluorescence intensity of the area under the curve. The mean \pm standard deviation (SD) from three independent experiments is shown. (C) Cap1^{OX-1} is sustained following treatment with higher doses of H_2O_2 . Cap1 oxidation was measured as described in the legend to Fig. 1D following exposure of Cap1-MH cells to 0.4, 5, or 25 mM H_2O_2 for the times indicated. (D) Comparison of Cap1 oxidation before (ns) and following the indicated stress treatments by PEG-maleimide binding to DTT-resolved thiols. This shows that different oxidized forms of Cap1 are similarly triggered following high- H_2O_2 and combinatorial stresses, whereas a single form containing multiple disulfides is prevalent following medium- H_2O_2 stress.

neous exposure to H_2O_2 plus NaCl likely underlies the inability of *C. albicans* to survive this combination of stresses.

Differential Cap1 oxidation triggered by high levels of H_2O_2 . Why does Cap1 become differentially oxidized following combinatorial H_2O_2 and NaCl stress? We previously reported that there is a dramatic increase in intracellular ROS levels following exposure to combinatorial oxidative plus cationic stress, compared to oxidative stress alone (28). This rise in intracellular ROS could drive the differential oxidation and inactivation of Cap1. To explore this, we first quantified the increase in intracellular ROS following treatment of cells with H_2O_2 or combinations of H_2O_2 and NaCl. Approximately 5-fold-higher levels of intracellular ROS were observed following exposure of cells to 5 mM H_2O_2 in the presence of 1 M NaCl, compared to 5 mM H_2O_2 alone (Fig. 4A and B). Based on this observation, we hypothesized that Cap1 may also become differentially oxidized to the Cap1^{OX-1} form following exposure of cells to high levels of ROS. To investigate this, cells expressing Myc-tagged Cap1 were treated with low (0.4 mM), medium (5 mM), and high (25 mM) levels of H_2O_2 , and Cap1

oxidation was monitored over a 60-min period. Strikingly, this kinetic analysis revealed that, at all levels of H_2O_2 tested, a faster-mobility Cap1^{OX-1} form is rapidly observed after stress treatment. However, following exposure to low or medium levels of H_2O_2 , the presence of Cap1^{OX-1} is short-lived, whereas following exposure to high levels of H_2O_2 , Cap1^{OX-1} persists for up to 30 min (Fig. 4C). Significantly, as a Cap1^{OX-1} form is seen at all H_2O_2 concentrations, albeit with different kinetics, this indicates that such a form may in fact be a normal intermediate in the formation of the Cap1^{OX} form following H_2O_2 stress.

We explored whether the Cap1^{OX-1} form, generated for a sustained period following high levels of H_2O_2 , was similar to the Cap1^{OX-1} form observed after combinatorial cationic and oxidative stress, using the sequential NEM-DTT-PEG maleimide treatments described above. As observed previously (Fig. 2D), exposure of cells to medium (5 mM) doses of H_2O_2 results in a single species of Cap1 predicted to contain multiple disulfide bonds, as evidenced by the slow, PEG-maleimide-dependent mobility on SDS-PAGE (Fig. 4D). In contrast, treatment of cells with either

high (25 mM) doses of H_2O_2 or combinatorial stress results in the formation of multiple different oxidized forms of Cap1. For unknown reasons, we consistently recovered more Cap1 following high- H_2O_2 stress than other treatments (Fig. 4D). However, it is clear that the same differentially oxidized forms of Cap1 are observed following either high- H_2O_2 or combinatorial stress (Fig. 4D).

As Cap1-dependent gene expression is delayed following combinatorial oxidative and osmotic stress when the Cap1^{OX-1} form is prevalent (Fig. 3D), we hypothesized that the delayed conversion of Cap1^{OX-1} to Cap1^{OX} following higher levels of H_2O_2 (Fig. 4C) may also result in an H_2O_2 concentration-dependent lag in Cap1-dependent gene expression. To investigate this, we examined the kinetics of Cap1 nuclear accumulation, phosphorylation, and Cap1-dependent gene expression following the exposure of cells to low (0.4 mM), medium (5 mM), and high (25 mM) doses of H_2O_2 . The first observation made was that, in contrast to combinatorial H_2O_2 and NaCl stress, Cap1 rapidly accumulated in the nucleus irrespective of the level of H_2O_2 stress (Fig. 5A). Following exposure of cells to 0.4 mM H_2O_2 , this nuclear accumulation is short-lived, consistent with the transient oxidation of Cap1 (Fig. 4C). However, Cap1 nuclear accumulation persists for 60 min following treatment with either 5 or 25 mM H_2O_2 (Fig. 5A). Thus, while the Cap1^{OX-1} form generated following combinatorial stress fails to accumulate in the nucleus, Cap1^{OX-1} formed in response to high levels of H_2O_2 rapidly accumulates in the nucleus (compare Fig. 5A with Fig. 3B).

Strikingly, however, despite the fast nuclear accumulation following high levels of H_2O_2 , Cap1 phosphorylation (Fig. 5B) and Cap1-dependent gene expression (Fig. 5C) were not observed until 30 min post-stress treatment. The delayed phosphorylation of Cap1 appeared to coincide with the resolution of the Cap1^{OX-1} form to the Cap1^{OX} form (Fig. 4C), which in turn correlated with the timing of Cap1-dependent gene expression. Such observations are indicative of a connection between these Cap1 modifications and the activity of this transcription factor. In contrast, consistent with previous findings (31), following low and medium doses of H_2O_2 , the kinetics of induction of Cap1-dependent genes (Fig. 5C) largely correlated with the oxidation, phosphorylation, and nuclear accumulation profiles of Cap1 (Fig. 4C and Fig. 5A and B).

Cap1-dependent gene expression is delayed following high levels of H_2O_2 , despite the clear nuclear accumulation of Cap1. Therefore, we explored whether Cap1 was bound to its target genes under such conditions. To examine Cap1 promoter binding, three targets were selected—*CAT1*, *GLR1*, and *TSA1*—based upon previous studies showing Cap1 enrichment at their promoters (22) and the Cap1-dependent induction of such genes in response to 5 mM H_2O_2 (11, 16, 32). *C. albicans* cells expressing Myc-tagged Cap1 together with an untagged control strain were treated with the low, medium, and high levels of H_2O_2 employed above, and Cap1 binding to the *CAT1*, *GLR1*, and *TSA1* promoters was determined by chromatin immunoprecipitation (ChIP) and quantitative PCR analysis. As illustrated in Fig. 6, Cap1 was found to rapidly associate with *CAT1*, *GLR1*, and *TSA1* promoters irrespective of the level of H_2O_2 (Fig. 6). Moreover, considerably higher levels of Cap1 were detected at these promoters following treatment with medium or high levels H_2O_2 compared to low doses (Fig. 6). Clearly therefore, the unphosphorylated Cap1^{OX-1} form generated following high levels of H_2O_2 is able to bind to the

promoter region of its target genes. However, in contrast to the effect seen at low and medium levels of H_2O_2 , this is not sufficient to drive Cap1-dependent antioxidant gene expression (Fig. 5C).

Taken together, these results highlight a number of significant findings regarding Cap1 regulation in *C. albicans*. First, it is apparent that Cap1-dependent gene expression is delayed following exposure of cells to high levels of H_2O_2 . Importantly, this may underlie the delayed Cap1-dependent gene expression seen following the combinatorial H_2O_2 and NaCl stress, as this combination of stresses triggers high levels of intracellular ROS. Second, the nuclear Cap1^{OX-1} form, generated following high levels of oxidative stress, although bound to the promoters of Cap1-regulated genes, is not phosphorylated and fails to activate its target genes. These findings suggest that the resolution of the Cap1^{OX-1} form to Cap1^{OX} and Cap1 phosphorylation are necessary prerequisites for the induction of the Cap1-mediated oxidative stress regulon.

Cationic stress promotes the interaction of Cap1 with the Crm1 nuclear export factor. The results presented above illustrate that exposure of cells to either high levels of H_2O_2 (25 mM) or medium doses of H_2O_2 (5 mM) in the presence of NaCl results in the sustained formation of Cap1^{OX-1} and a delay in the activation of Cap1-dependent gene expression. However, while Cap1^{OX-1} rapidly accumulates in the nucleus in response to high levels of H_2O_2 (Fig. 5A), Cap1^{OX-1} does not accumulate in the nucleus until 1 h following combinatorial H_2O_2 and NaCl treatment (Fig. 3B). The H_2O_2 -induced nuclear accumulation of fungal AP-1-like transcription factors is triggered by the oxidation of key cysteine residues, which results in a conformational change that masks the NES from the nuclear export factor Crm1 (20). Thus, the Cap1^{OX-1} forms generated following high-level H_2O_2 stress and combinatorial stress could conceivably be different, with the combinatorial stress Cap1^{OX-1} form adopting a structural conformation that still permits interaction with the Crm1 nuclear export factor. However, our data indicate that the oxidation profiles of Cap1^{OX-1} observed following high- H_2O_2 and combinatorial stresses are similar (Fig. 4D). Alternatively, it was possible that cationic stress modulates the interaction between Cap1 with the Crm1 nuclear export factor and thus affects the nuclear accumulation of Cap1^{OX-1}. To test the latter hypothesis, we first created strains in which Crm1 tagged with 6His residues and 2Myc epitopes (Crm1-MH) was expressed from its native chromosomal locus. Crm1-MH was immunoprecipitated from extracts prepared from cells before and after exposure to H_2O_2 , NaCl, and H_2O_2 plus NaCl. The interaction between Cap1 and Crm1 was then examined by Western blot analysis of these coimmunoprecipitates (Fig. 7A; see Fig. S3A in the supplemental material). Similar to previous studies of Yap1 in *S. cerevisiae* (33), Cap1 was found to interact with Crm1 *in vivo*, and moreover, this interaction was reduced in the presence of medium (5 mM) levels of H_2O_2 after 10 min (Fig. 7B; see Fig. S3A). Strikingly, the interaction of Cap1 with Crm1 was dramatically enhanced following the cationic stress (NaCl) and the combinatorial H_2O_2 and NaCl stress treatments (Fig. 7B; see Fig. S3A). Input controls confirmed that the cationic stress-induced interaction with Crm1 was not due to differences in Cap1 levels (Fig. 7B). The input controls, in contrast to the immunoprecipitated samples, were not phosphatase treated, which explains the slower mobility of Cap1 following oxidative stress seen in the input panel (Fig. 7B). The enhanced interaction between Cap1 and Crm1 following the combinatorial H_2O_2 and NaCl stress was transient, declining 1 h post-stress.

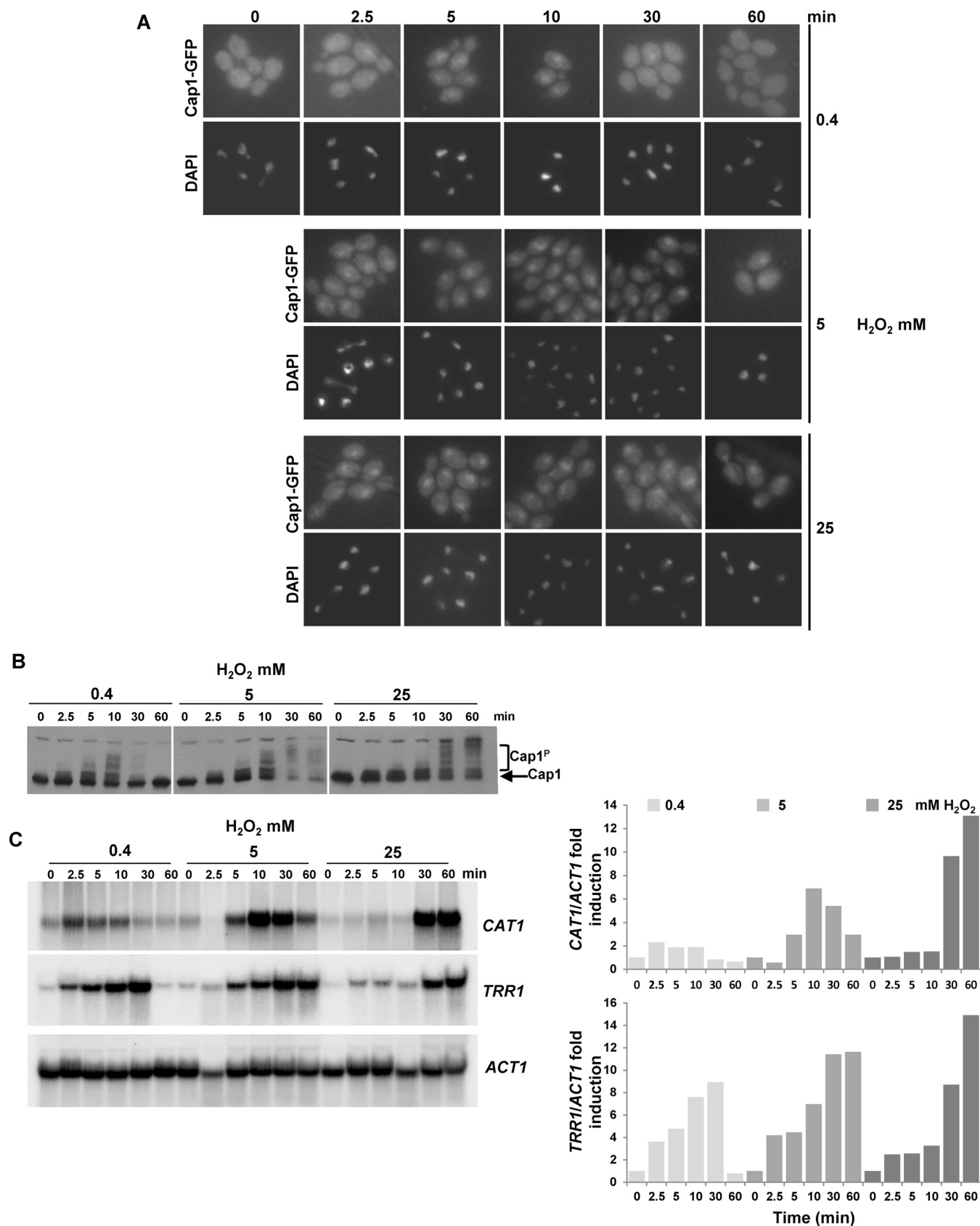


FIG 5 Cap1 rapidly accumulates in the nucleus in response to high levels of H_2O_2 , but Cap1 phosphorylation and Cap1-dependent gene expression are delayed. (A) Cap1 localization was detected as described in the legend to Fig. 1B following treatment of Cap1-GFP cells with 0.4, 5, or 25 mM H_2O_2 for the times indicated.

(Continued)

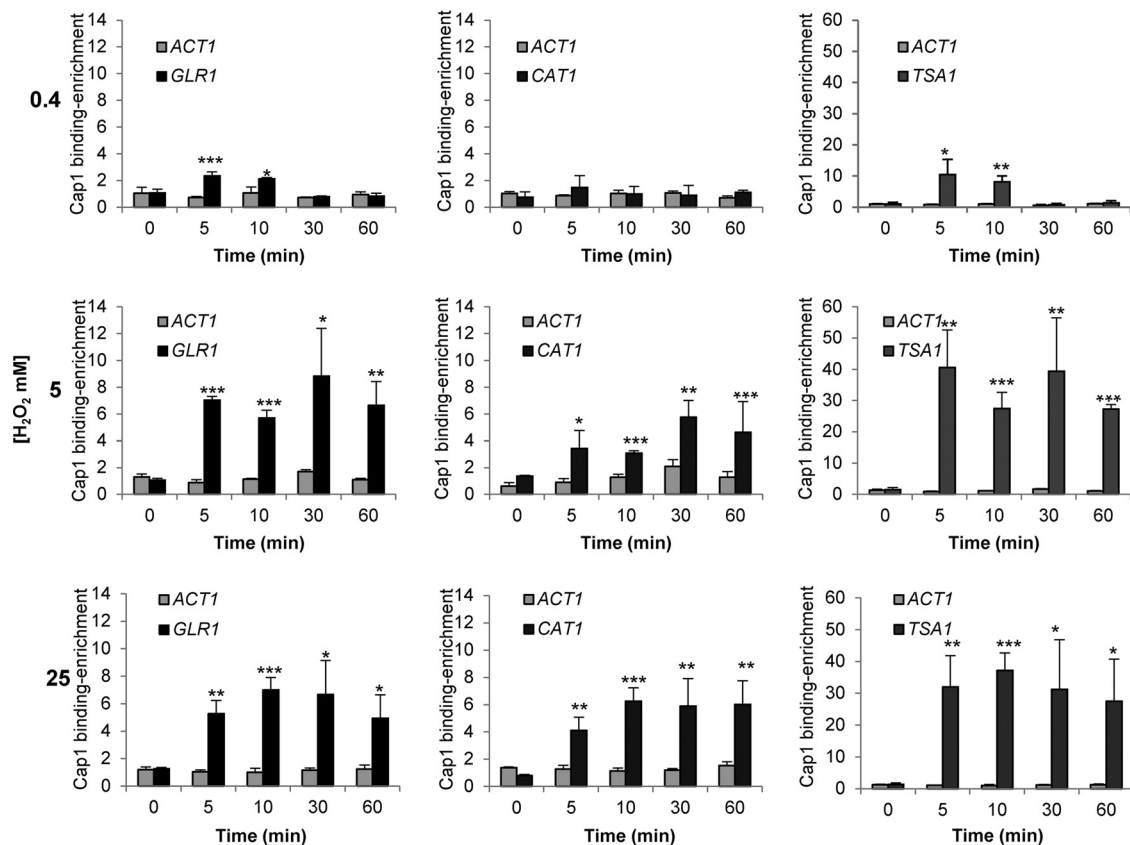


FIG 6 Quantification of Cap1 enrichment at the *GLR1*, *CAT1*, and *TSA1* promoter targets. Cells expressing Cap1-MH (JC948) were treated with 0.4, 5, or 25 mM H₂O₂ for the indicated times and subjected to ChIP. The recovered DNA samples were analyzed by qPCR using primers specific for promoter regions within *GLR1*, *CAT1*, and *TSA1*. Relative Cap1-MH enrichment values (*n*-fold) are presented (mean \pm SD; *n* = 3). The following *P* values were considered: *, *P* \leq 0.05; **, *P* \leq 0.01; and ***, *P* \leq 0.001.

treatment (Fig. 7C). Quantification of the interaction of Cap1 with Crm1 from four biological replicates indicated a significant increase in Cap1 binding 10 and 20 min after combinatorial stress, but not after 60 min (Fig. 7D). This is consistent with the timing of Cap1 nuclear accumulation, which is observed 1 h following combinatorial H₂O₂ and NaCl stress (Fig. 3B). However, it is noteworthy that multiple species of Cap1 were often detected during the immunoprecipitation experiment (Fig. 7C; see Fig. S3A). These may reflect degradation products generated during the immunoprecipitation procedure. Taken together, these results support a model in which Cap1^{OX-1} fails to accumulate in the nucleus following exposure of cells to H₂O₂ in the presence of NaCl, due to the cation-enhanced interaction between Cap1 and the Crm1 nuclear export factor.

DISCUSSION

In this study, we have demonstrated that exposure of *C. albicans* cells to combinatorial H₂O₂ plus NaCl stress, which triggers high levels of intracellular ROS, results in the sustained formation of a differentially oxidized form of Cap1, Cap1^{OX-1}. Furthermore, we

show that Cap1^{OX-1} contains less oxidized disulfide bonds compared to those seen in the active Cap1^{OX} form. This differentially oxidized Cap1^{OX-1} form is also observed following treatment of *C. albicans* cells with a range of H₂O₂ doses but is only sustained following high doses of H₂O₂ (Fig. 4). Notably, Cap1-dependent gene expression is not induced when Cap1 is in the Cap1^{OX-1} form. However, while Cap1^{OX-1} readily accumulates in the nucleus following high-H₂O₂ stress, the nuclear accumulation of Cap1^{OX-1} following combinatorial H₂O₂ and NaCl stress is delayed due to an enhanced interaction with the Crm1 nuclear export factor. Thus, at least two distinct mechanisms exist to inhibit Cap1 activation following combinatorial stress. This may explain why Cap1 inhibition is more sustained following combinatorial stress than high-H₂O₂ stress. A model comparing the mechanisms underlying the delayed activation of Cap1 following combinatorial H₂O₂ plus NaCl stress and high-H₂O₂ stress is shown in Fig. 8. We predict that the significant delay in Cap1-dependent gene expression following exposure of cells to H₂O₂ in the presence of NaCl underlies the exquisite sensitivity of *C. albicans* to this combinatorial stress. This is supported by the observation that ectopic

Figure Legend Continued

(B) Cap1 phosphorylation was detected as described in the legend to Fig. 1C following treatment of wild-type cells with 0.4, 5, or 25 mM H₂O₂ for the times indicated. (C) Northern blots were performed as described in the legend to Fig. 1A, using the same cells that were processed for Cap1 phosphorylation analysis in panel B (left panel). The levels of *CAT1* and *TRR1* mRNA were quantified relative to the *ACT1* loading control (right panel).

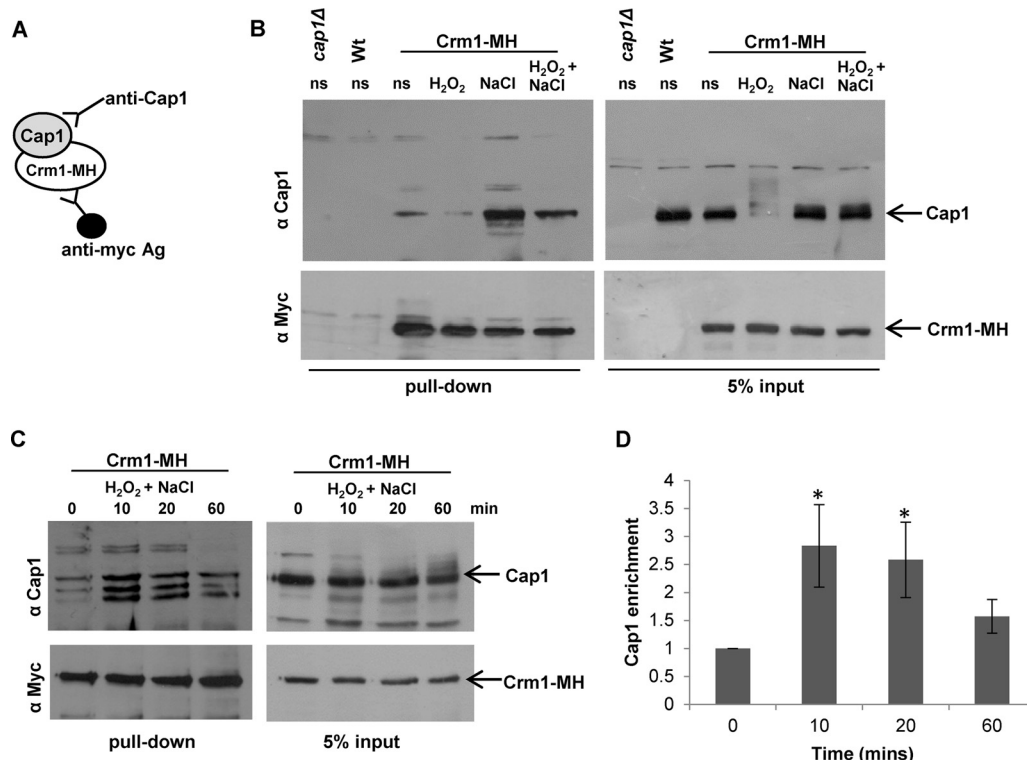


FIG 7 Cationic stress promotes Cap1 interaction with the Crm1 nuclear export factor. (A) Strategy used to examine Cap1 association with Crm1. (B) Stress effects on Cap1 interaction with Crm1. Extracts were prepared from wild-type cells (Wt [JC747]), *cap1Δ* cells (JC842), and wild-type cells expressing 2Myc- and 6His-tagged Crm1 (Crm1-MH [JC1925]) before (ns) and following exposure to 5 mM H₂O₂, 1 M NaCl, or combinations of the stresses for 10 min. Crm1-MH was immunoprecipitated using anti-Myc agarose, and precipitated proteins and 5% input were subjected to SDS-PAGE. Coprecipitation of Cap1 was assayed by Western blotting using an anti-Cap1 antibody (top panel), and precipitation of Crm1-MH was assayed using anti-Myc antibodies (bottom panel). (C) The increased interaction of Cap1 with Crm1 following combinatorial stress is transient. Cap1 interaction with Crm1 was analyzed as described for panel B before (ns) and following treatment of Crm1-MH cells with 5 mM H₂O₂ plus 1 M NaCl for the times indicated. (D) Quantification of the increased interaction of Cap1 with Crm1 following combinatorial stress. Quantitative densitometric analysis of Western blots from four biological replicates was conducted to determine the fold enrichment of Cap1 interaction with Crm1 relative to time zero. Mean values (±standard errors of the mean [SEM]) are shown, and ANOVA was used to determine statistically significant differences in Cap1 enrichment levels (*, *P* < 0.01).

expression of the Cap1-target gene, *CAT1*, can restore *C. albicans* resistance to combinatorial H₂O₂ and NaCl stress (28). In addition, our findings reported here that Cap1-dependent gene expression is also delayed following high-level H₂O₂ stress, albeit not to the same extent as following combinatorial stress, likely contributes to the increased sensitivity of *C. albicans* to high doses of oxidative stress. Moreover, the failure to respond rapidly to high intracellular ROS likely results in the activation of cell death programs (34).

How is Cap1 activated in *C. albicans*? Genetic and biochemical studies in *S. cerevisiae* support the stepwise oxidation of multiple redox-active cysteine residues in Yap1 following H₂O₂ exposure. This is initiated by the H₂O₂-induced oxidation of the catalytic cysteine (Cys36) of the thiol-peroxidase Gpx3, which subsequently reacts with Cys598 located within the c-CRD of Yap1 to form a mixed Yap1-Gpx3 disulfide intermediate. This is followed by thiol-disulfide exchange with Cys303 of Yap1 to generate the first interdomain disulfide bond between Cys303 and Cys598 (21). This disulfide is sufficient to mask the NES within the c-CRD of Yap1, prevent interaction with the Crm1 nuclear export factor, and thus stimulate nuclear accumulation (30). However, it is clear that disulfides in addition to Cys303 and Cys598 are required for optimal Yap1 function. Mass spectrometry analysis of oxidized

Yap1 identified Cys303-Cys598 and Cys310-Cys629 disulfides (35), both of which are required to recruit the mediator component Rox3 to the *TRX2* promoter (36). Furthermore, an *in vitro* analysis of Yap1 oxidation identified a third disulfide, Cys315-Cys620, which appears to sustain Yap1 activation following H₂O₂ exposure (29). Thus, the stepwise oxidation of all six redox-active cysteines is necessary for maximal Yap1 activation in *S. cerevisiae*. In this study, we present evidence for a similar stepwise formation of multiple disulfides in *C. albicans* Cap1. The Cap1^{OX-1} form would appear to be a normal intermediate in the formation of active Cap1^{OX}, and our experiments, in which we examine the binding of PEG-maleimide to DTT-resolved disulfides (Fig. 4D), show that Cap1^{OX} has more disulfides than Cap1^{OX-1}. This result, however, seemingly conflicts with the oxidation profiles of Cap1 observed when we use the thiol binding agent AMS to detect differentially oxidized forms of this transcription factor. In such experiments, oxidation of cysteine residues precludes the binding of AMS, and thus oxidized proteins run with a faster mobility. Employing such an approach, we observe a faster-mobility form generated immediately following H₂O₂ stress (Cap1^{OX-1}), which is then resolved into the Cap1^{OX} slower-mobility state (Fig. 4C). How can these findings be reconciled with our observations that Cap1^{OX} has more H₂O₂-induced disulfides than Cap1^{OX-1}? Oxi-

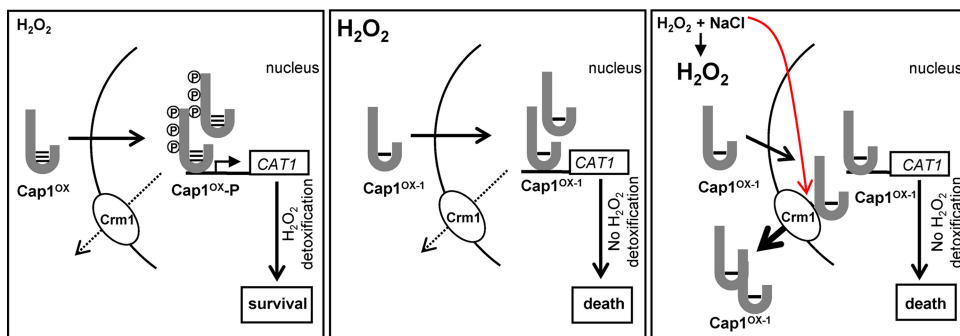


FIG 8 Impact of combinatorial stress and high H_2O_2 on Cap1 activation. When *C. albicans* cells are exposed to medium (5 mM) levels of H_2O_2 , a Cap1^{OX} form containing multiple disulfides is swiftly generated, followed by the rapid accumulation of Cap1 in the nucleus, where it is phosphorylated. The ensuing efficient induction of Cap1-dependent antioxidant genes follows, leading to stress adaptation and survival (left panel). However, when *C. albicans* cells are exposed to high (25 mM) levels of H_2O_2 , a Cap1^{OX-1} form containing less disulfides is prevalent, and although this rapidly accumulates in the nucleus and binds to target genes, Cap1 is not phosphorylated, and the induction of Cap1-dependent genes is significantly impaired, resulting in cell death (middle panel). Exposure of *C. albicans* to medium (5 mM) levels of H_2O_2 in the presence of NaCl triggers high intracellular ROS accumulation. This also results in the formation of Cap1^{OX-1}, which is seemingly unable to induce Cap1-dependent genes. However, following combinatorial stress, an additional inhibitory mechanism is seen as Cap1 fails to accumulate in the nucleus due to a cationic stress-mediated stabilization of the interaction between Cap1 and the Crm1 export factor. Consequently, the induction of Cap1 target genes is prevented, leading to cell death (right panel).

dation events, in addition to disulfide bond formation, such as the hyperoxidation of cysteine thiols to sulfenic or sulfonic acid derivatives, would preclude AMS binding. Alternatively, AMS binding to the Cap^{OX-1} form may induce a conformation change that results in the observed faster mobility. Further investigations are required to distinguish between these hypotheses and identify the precise oxidation states of the Cap1^{OX} and Cap1^{OX-1} forms in *C. albicans*.

The sustained formation of Cap1^{OX-1} following high- H_2O_2 and combinatorial stresses in *C. albicans* correlates with a lack of Cap1-dependent gene expression. Why is Cap1-dependent gene expression inhibited when Cap1 is in the Cap1^{OX-1} form? Following combinatorial oxidative plus cationic stress, Cap1^{OX-1} fails to accumulate in the nucleus, which would explain the lack of induction of Cap1-dependent genes. However, following high levels of H_2O_2 , Cap1^{OX-1} rapidly accumulates in the nucleus, where it binds to the promoters of its target genes (Fig. 6), and yet still, Cap1-dependent gene induction is not observed (Fig. 5C). Here it is interesting to note that although Cap1^{OX-1} accumulates in the nucleus, it is not phosphorylated. Studies of *S. cerevisiae* revealed that the nuclear accumulation of Yap1 was necessary for this post-translational modification (30). However, as both the kinase and target phosphorylation sites on Yap1 are unknown, it has not been possible to establish whether this posttranslational modification is important for the activation of this or other fungal AP-1-like transcription factors. Results from this study which show that there is a coordinated delay in Cap1 phosphorylation and Cap1-dependent gene expression following high- H_2O_2 stress, despite the nuclear accumulation of Cap1, are consistent with a model in which Cap1 phosphorylation is important for function. In this scenario, either the kinase responsible is inactivated following high- H_2O_2 stress, or it fails to recognize the Cap1^{OX-1} form. Indeed, Cap1 phosphorylation coincides with the appearance of the active Cap1^{OX} form. However, other, phosphorylation-independent, mechanisms may also contribute to the delay in Cap1-induced gene expression. For example, in *S. cerevisiae*, the correct oxidation of Yap1 is necessary to recruit the polymerase II (Pol II) mediator subunit Rox3 (36). Thus, the

Cap1^{OX-1} form may not be competent to recruit the general transcriptional machinery. Alternatively, high levels of intracellular ROS, generated following combinatorial and high- H_2O_2 stresses, may have a global inhibitory effect on transcription. Indeed, high levels of ROS have been previously demonstrated to result in a global inhibition of protein translation in *S. cerevisiae* (37). To explore whether a global inhibition of transcription occurs following combinatorial and high- H_2O_2 stresses, we examined the phosphorylation status of RNA Pol II. Phosphorylation of serine 2 and 5 within the repetitive YSPTSPS sequence, located in the carboxyl-terminal domain (CTD), is associated with transcriptionally active RNA Pol II (38). No obvious change in RNA Pol II phosphorylation status was seen following combinatorial and high- H_2O_2 stresses, suggesting that under such conditions, the polymerase is active (see Fig. S4 in the supplemental material). However, additional experiments are needed to further explore the potential global impacts of these stress treatments on gene expression.

The inhibition of Cap1 nuclear accumulation following combinatorial stress represents a clear difference in Cap1 regulation following high- H_2O_2 stress and combinatorial cationic and oxidative stress. Strikingly, in this study we find that cationic stress appears to enhance the interaction between Cap1 and Crm1 in *C. albicans*, and this interaction is maintained following combinatorial cationic and oxidative stress treatments (Fig. 7B; see Fig. S3A in the supplemental material). Structural analysis of Yap1 revealed that in the active oxidized form, the nuclear export signal (NES) in the c-CRD is masked by disulfide-bond-mediated interactions with a conserved amino-terminal α -helix. Upon reduction of the disulfide bonds, Yap1 undergoes a change to an unstructured conformation that exposes the NES and allows redistribution to the cytoplasm (20). As cationic stress alone can promote the interaction of Cap1 with Crm1, this indicates that this phenomenon occurs independently of changes in the oxidation status of Cap1. We reasoned that the production of osmolytes, triggered by cationic stress, may be responsible for the enhanced interaction between Cap1 and Crm1. However, the cation-induced interaction between Cap1 and Crm1 is maintained in cells lacking the Hog1 stress-activated protein kinase (SAPK) (see Fig. S3B), which fail to

produce glycerol following osmotic stress (39). Furthermore, the enhanced interaction appears to be cation specific, as treatment of cells with the osmotic stress agent sorbitol fails to stimulate Cap1 interaction with Crm1 (see Fig. S3C). Although the molecular basis underlying the cation-stimulated Cap1-Crm1 association is unknown, this observation can account for the significant delay in Cap1 nuclear accumulation following combinatorial oxidative and osmotic stress. Interestingly, it is possible that the cationic stress-stimulated interaction with Crm1 may be Cap1 specific, rather than a global phenomenon. For example, we have previously shown that the Hog1 SAPK, whose cellular localization is predicted to be regulated by Crm1 (40), rapidly accumulates in the nucleus following combinatorial stress (28). Further investigation into the mechanisms underlying the cationic-stress mediated association between Cap1 and Crm1 is clearly warranted. Although seemingly Hog1 dependent, the Rim101 pathway is worthy of consideration as this pathway is implicated in cationic but not osmotic stress. *C. albicans* cells lacking the Rim101 transcription factor are sensitive to cationic stress (41), and a role of Rim101 in regulating the Ena1 Na⁺-ATPase in the model yeast *S. cerevisiae* is well documented (42).

In conclusion, our results provide significant new insight into why combinatorial cationic plus oxidative stress treatments delay the activation of the Cap1 transcription factor, leading to stress pathway interference. Indeed, cationic stress appears to inhibit oxidative stress responses in two ways. First, cations inhibit catalase activity in *C. albicans*, thereby leading to significant increases in intracellular ROS levels observed following combinations of cationic and oxidative stresses (28). Here we show that such high levels of intracellular ROS trap Cap1 in an intermediate Cap1^{OX-1} form that fails to induce target antioxidant-encoding genes. Second, we find that cations stimulate the interaction of Cap1 with the nuclear export factor Crm1, thus delaying the oxidative stress-induced nuclear accumulation of this transcription factor. This combinatorial stress-mediated stress pathway interference that we have dissected *in vitro* is thought to contribute to the potency of host defenses in combating fungal infections *in vivo*. Indeed, pharmacological inhibition of ROS production and cationic fluxes, either separately or in combination, results in a similar, drastic, impaired ability of neutrophils to kill *C. albicans* (28). Thus, the efficacy of combinatorial stress-mediated killing of *C. albicans* may explain why this fungus only causes systemic infections in immunocompromised hosts. How does the exquisite sensitivity to combinatorial stress benefit *C. albicans*? It could be speculated that it is nonbeneficial for this pathogen to cause systemic infections as the likely outcome is killing of the host. It seems more likely that *Candida albicans* has evolved as a commensal organism in the human gut and urogenital tracts. In these environments, such combinations of oxidative and cationic stresses may not be encountered. Finally, it is important to note that *C. albicans* is exposed to many other combinations of stresses, in addition to oxidative and cationic stresses, following phagocytosis, such as reactive nitrogen and chloride species, antimicrobial peptides, pH fluctuations, and nutrient limitation (reviewed in reference 43). Therefore, future work will be directed at investigating the impact of other combinations of physiologically relevant stress conditions on killing *C. albicans* and other important fungal pathogens.

MATERIALS AND METHODS

Strains and media. The strains used in this study are listed in Table S1 in the supplemental material. *C. albicans* cells were grown in Tris-buffered yeast extract-peptone-dextrose medium (YPDT [pH 7.4]) (27, 44). Oxidative stress was imposed by treating cells with a range of H₂O₂ (Sigma) concentrations as indicated, and cationic stress was imposed with 1 M NaCl. To stress cells with a combination of oxidative and cationic stresses, medium was supplemented with 5 mM H₂O₂ plus 1 M NaCl, as detailed previously (27, 28).

Tagging of Crm1. To C-terminally tag Crm1, expressed from its native chromosomal locus, with 2 copies of the Myc epitope and 6 His residues, the 3' region of *CRM1* was amplified by PCR using the oligonucleotide primers Crm1MHPstF (AATGTCTGCAGCAATTATCTGGAG AAGC) and CrmMHPstR (AATGTCTGCAGTCGTATCCATTTCAG AAGG) and genomic DNA template. The resulting PCR product was digested with PstI and ligated into the PstI site of CIP-MH-PstI plasmid (31) to generate pCRM1-MH. pCRM1-MH was linearized by digestion with EcoRV to target integration at the *CRM1* locus in SN148 wild-type cells (45) or *hog1*^Δ cells (JC45) to generate strains JC1925 and JC1940, respectively. Correct insertion and tagging of Crm1 were verified by PCR and DNA sequencing.

Cap1 localization. *C. albicans* cells expressing GFP-tagged Cap1 (JC1060) were prepared as described previously (11, 46). 4',6-Diamidino-2-phenylindole (DAPI) and GFP fluorescence was captured using a Zeiss Axioscope with a 63× oil immersion objective and the AxioVision imaging system.

Cap1 phosphorylation and oxidation assays. To monitor Cap1 phosphorylation, protein extracts were prepared as described previously (47) from exponentially growing *C. albicans* cells expressing 2Myc- and 6His-tagged Cap1 (JC948) before and after treatments with 5 mM H₂O₂, 1 M NaCl, or 5 mM H₂O₂ plus 1 M NaCl for the indicated times. Twenty-five micrograms of protein was subjected to SDS-PAGE, and Cap1-MH was detected using anti-Myc antibodies (9E10 [Sigma]) (31).

To monitor Cap1 oxidation, protein extracts were prepared under acid lysis conditions and treated with the thiol alkylating agent AMS, as described previously (31). To determine the nature of Cap1 oxidation following combinatorial stress and high ROS levels, protein extracts were obtained under acid lysis conditions and incubated with *N*-ethylmaleimide (NEM [Thermo Scientific, Paisley, United Kingdom]) at a final concentration of 10 mM at 30°C for 30 min in order to block free thiols, precipitated with 1 vol of 20% trichloroacetic acid (TCA) on ice for 30 min, and washed extensively three times with acetone. NEM-labeled samples were resuspended in sample buffer (200 mM Tris-HCl [pH 8], 1% SDS, 1 mM EDTA) supplemented with 20 mM DTT and incubated at 37°C for 60 min in order to reduce the existing disulfides. Acid precipitation and acetone washes were repeated, and protein pellets were resuspended in sample buffer containing methoxy PEG-maleimide (mPEG-Mal) (PEG-maleimide with a molecular weight of 2,000 [Nanocs, Inc., Boston, MA]) at a final concentration of 10 mM at 30°C for 30 min (29) in order to label free thiols that were involved in the formation of disulfides. Acid precipitation and acetone washes were repeated, and samples were treated with 5 U of alkaline phosphatase (New England Biolabs) at 37°C for 1 h to prevent phosphorylation from having an impact on AMS/PEG-maleimide-dependent mobility shifts (26). Samples were subjected to SDS-PAGE on 8% gels under nonreducing conditions, and Cap1-MH was detected as described above.

Northern blotting. Northern blotting was performed as described previously (11). Gene-specific probes were amplified by PCR from genomic DNA using oligonucleotide primers specific for *ACT1*, *CAT1*, and *TRR1* (11). RNA levels were quantified using the Typhoon phosphorimaging system (Amersham Biosciences) and Image Quant software (GE Healthcare Life Sciences).

Detection of intracellular ROS levels. For intracellular ROS detection, exponentially growing *C. albicans* cells were treated with 20 μM of the fluorescent probe dihydroethidium (DHE [Sigma]) and incubated at

30°C for 45 min in the dark. Cells were washed with phosphate-buffered saline (PBS), sonicated for 15 s, and subjected to fluorescence-activated cell sorting using a FACS Aria Fusion (BD Biosciences, Sydney, Australia) with an argon 488-nm laser emitting at 595 nm. Data were analyzed from three independent biological replicates using FlowJo software (TreeStar, Inc., Ashland, OR).

ChIP-qPCR. Chromatin immunoprecipitation (ChIP) assays were performed as described by Liu et al. (48), with slight modifications. Briefly, three independent cultures of exponentially growing *C. albicans* JC465 (untagged control strain) and JC948 (Cap1-MH-tagged strain) cells were collected and chromatin fixed by the addition of formaldehyde (1% vol/vol) for 30 min at room temperature with agitation at 20 rpm. Formaldehyde was quenched by the addition of 125 mM glycine at room temperature at 20 rpm for 10 min. Samples were centrifuged, washed twice with ice-cold Tris-buffered saline (TBS) buffer (20 mM Tris-HCl [pH 7.5], 150 mM NaCl), and snap-frozen in liquid nitrogen. The preparation of the total cell extracts and sonication was performed as described previously (48), followed by the overnight immunoprecipitation of the soluble chromatin extracts from both tagged and untagged strains with monoclonal mouse c-Myc antibody (9E10) (Santa Cruz Biotech) coupled to magnetic beads (Dynabeads [Invitrogen Life Technologies]) at 4°C. Beads were washed and reverse cross-linked, and DNA was recovered as described previously (48). The DNA concentrations were quantified using Quant-iT Picogreen double-stranded DNA assay kit (Molecular Probes/Invitrogen) as described previously (48). The DNA concentrations ranged from 0.03 ng/μl to 0.69 ng/μl for the tagged strains and 0.49 ng/μl to 0.72 ng/μl for the untagged strains. Quantitative PCRs (qPCRs) were performed on the Mastercycler ep realplex (Eppendorf) qPCR system using the Takyon ROX Probe MasterMix (Eurogentec) and the conditions described previously (49). Oligonucleotides for the *CAT1*, *TSA1*, and *GLR1* promoter regions (targets) (see Table S2 in the supplemental material) were optimized using Primer3Web software (version 4.0.0.). *ACT1* was used as a control for statistical analyses by *t* test, with *TEF1* (orf19.1435) as a reference for normalization (50). All PCR products had melting curves indicating the presence of a single amplicon. qPCR data were analyzed using the threshold cycle ($2^{-\Delta\Delta CT}$) method (51), and statistical significance was determined using Welsh's two-sample *t* test.

Crm1-Cap1 coimmunoprecipitation assay. Exponentially growing wild-type (JC1925) or *hog1Δ* (JC1940) cells expressing 2Myc- and 6His-tagged Crm1 were harvested before and after stress treatments. Total protein extracts were prepared as described previously (47), and Crm1-MH was immunoprecipitated using anti-Myc (9E10) antibody-coupled agarose (Santa Cruz Biotechnologies), followed by incubation with 200 U of Lambda protein phosphatase (New England Biolabs) for 30 min at 30°C. Precipitated proteins and 5% of protein input were subjected to SDS-PAGE. Coprecipitation of Cap1 was monitored by Western blotting using anti-Cap1 polyclonal antibodies (kindly provided by Scott Moye-Rowley, University of Iowa). Membranes were subsequently probed with anti-Myc antibodies (9E10 [Sigma]) to determine the levels of precipitated Crm1 levels. Quantitative densitometric analysis of Western blots was conducted using ImageJ 1.44 to determine the fold enrichment of Cap1 interaction with Crm1 relative to time zero. Analysis of variance (ANOVA) was used to determine statistically significant differences in Cap1 enrichment levels.

Detection of RNA Pol II phosphorylation. To monitor RNA Pol II phosphorylation, protein extracts were prepared as described previously (47) from exponentially growing *C. albicans* cells expressing 2Myc- and 6His-tagged Cap1 (JC948) before and after treatments with 5 mM H₂O₂, 25 mM H₂O₂, or 5 mM H₂O₂ plus 1 M NaCl for the indicated times. Fifteen micrograms of protein was subjected to SDS-PAGE, and Pol II phosphorylation was detected using anti-RNA Pol II phospho S2 (ab5095 [Abcam]) and anti-RNA Pol II phospho S5 (ab5408 [Abcam]) antibodies. Total levels of RNA Pol II were detected using an anti-RNA Pol II CTD repeat antibody (ab817 [Abcam]). Blots were stripped, and Cap1-MH was detected using anti-Myc antibodies (9E10 [Sigma]) (31).

SUPPLEMENTAL MATERIAL

Supplemental material for this article may be found at <http://mbio.asm.org/lookup/suppl/doi:10.1128/mBio.00331-16/-/DCSupplemental>.

Figure S1, TIF file, 1.2 MB.

Figure S2, TIF file, 1.2 MB.

Figure S3, TIF file, 1.9 MB.

Figure S4, TIF file, 1.7 MB.

Table S1, DOCX file, 0.02 MB.

Table S2, DOCX file, 0.01 MB.

ACKNOWLEDGMENTS

We are grateful to Brian Morgan and Elizabeth Veal for insightful discussions, Mélanie Ikeh for experimental assistance, and Scott Moye-Rowley (University of Iowa) for the gift of the anti-Cap1 antibody.

This work was funded by the NIHR Newcastle Biomedical Research Centre (I.K.), a BBSRC DTG studentship (M.J.P.), the Wellcome Trust (grants 089930 and 097377 to J.Q. and 080088 and 097377 to A.J.P.B.), the BBSRC (grants BB/K016393/1 to J.Q. and BB/F00513X/1 and BB/K017365/1 to A.J.P.B.), the European Research Council (STRIFE Advanced grant ERC-2009-AdG-249793 to A.J.P.B.), the ANR (grant CAN-DIHUB, ANR-14-CE14-0018-01, to C.D.), and the French Government's Investissement d'Avenir program (grant IBEID, ANR-10-LABX-62-IBEID, to C.D.).

FUNDING INFORMATION

This work, including the efforts of Alistair J.P. Brown, was funded by Wellcome Trust (097377 and 080088). This work, including the efforts of Janet Quinn, was funded by Wellcome Trust (097377 and 089930). This work, including the efforts of Alistair J.P. Brown, was funded by EC | European Research Council (ERC) (ERC-2009-AdG-249793). This work, including the efforts of Alistair J.P. Brown, was funded by Biotechnology and Biological Sciences Research Council (BBSRC) (BB/F00513X/1 and BB/K017365/1). This work, including the efforts of Janet Quinn, was funded by Biotechnology and Biological Sciences Research Council (BBSRC) (BB/K016393/1). This work, including the efforts of Christophe d'Enfert, was funded by Agence Nationale de la Recherche (ANR) (ANR-14-CE14-0018-01 and ANR-10-LABX-62-IBEID).

REFERENCES

1. Brown GD, Denning DW, Gow NA, Levitz SM, Netea MG, White TC. 2012. Hidden killers: human fungal infections. *Sci Transl Med* 4:165rv113. <http://dx.doi.org/10.1126/scitranslmed.3004404>.
2. Babior BM. 2004. NADPH oxidase. *Curr Opin Immunol* 16:42–47. <http://dx.doi.org/10.1016/j.co.2003.12.001>.
3. Cohen MS, Ithurz RE, Malech HL, Root RK, Wilfert CM, Gutman L, Buckley RH. 1981. Fungal infection in chronic granulomatous disease: The importance of the phagocyte in defense against fungi. *Am J Med* 71:59–66. [http://dx.doi.org/10.1016/0002-9343\(81\)90259-X](http://dx.doi.org/10.1016/0002-9343(81)90259-X).
4. Hampton MB, Kettle AJ, Winterbourn CC. 1998. Inside the neutrophil phagosome: oxidants, myeloperoxidase, and bacterial killing. *Blood* 92: 3007–3017.
5. Reeves EP, Lu H, Jacobs HL, Messina CG, Bolsover S, Gabella G, Potma EO, Warley A, Roes J, Segal AW. 2002. Killing activity of neutrophils is mediated through activation of proteases by K⁺ flux. *Nature* 416:291–297. <http://dx.doi.org/10.1038/416291a>.
6. Segal AW. 2005. How neutrophils kill microbes. *Annu Rev Immunol* 23: 197–223. <http://dx.doi.org/10.1146/annurev.immunol.23.021704.115653>.
7. Jamieson DJ, Stephen DW, Terrière EC. 1996. Analysis of the adaptive oxidative stress response of *Candida albicans*. *FEMS Microbiol Lett* 138: 83–88. <http://dx.doi.org/10.1111/j.1574-6968.1996.tb08139.x>.
8. Nikolaou E, Agrafioti I, Stumpf M, Quinn J, Stansfield I, Brown AJ. 2009. Phylogenetic diversity of stress signalling pathways in fungi. *BMC Evol Biol* 9:44. <http://dx.doi.org/10.1186/1471-2148-9-44>.
9. Dantas AS, Day A, Ikeh M, Kos I, Achan B, Quinn J. 2015. Oxidative stress responses in the human fungal pathogen, *Candida albicans*. *Biomolecules* 5:142–165. <http://dx.doi.org/10.3390/biom5010142>.
10. Enjalbert B, MacCallum DM, Odds FC, Brown AJ. 2007. Niche-specific activation of the oxidative stress response by the pathogenic fungus *Can-*

dida albicans. Infect Immun 75:2143–2151. <http://dx.doi.org/10.1128/IAI.01680-06>.

11. Enjalbert B, Smith DA, Cornell MJ, Alam I, Nicholls S, Brown AJ, Quinn J. 2006. Role of the Hog1 stress-activated protein kinase in the global transcriptional response to stress in the fungal pathogen *Candida albicans*. Mol Biol Cell 17:1018–1032. <http://dx.doi.org/10.1091/mbc.E05-06-0501>.
12. Fradin C, De Groot P, MacCallum D, Schaller M, Klis F, Odds FC, Hube B. 2005. Granulocytes govern the transcriptional response, morphology and proliferation of *Candida albicans* in human blood. Mol Microbiol 56:397–415. <http://dx.doi.org/10.1111/j.1365-2958.2005.04557.x>.
13. Lorenz MC, Bender JA, Fink GR. 2004. Transcriptional response of *Candida albicans* upon internalization by macrophages. Eukaryot Cell 3:1076–1087. <http://dx.doi.org/10.1128/EC.3.5.1076-1087.2004>.
14. Miramón P, Dunker C, Windecker H, Bohovych IM, Brown AJ, Kurzai O, Hube B. 2012. Cellular responses of *Candida albicans* to phagocytosis and the extracellular activities of neutrophils are critical to counteract carbohydrate starvation, oxidative and nitrosative stress. PLoS One 7:e52850. <http://dx.doi.org/10.1371/journal.pone.0052850>.
15. Kusch H, Engelmann S, Albrecht D, Morschhäuser J, Hecker M. 2007. Proteomic analysis of the oxidative stress response in *Candida albicans*. Proteomics 7:686–697. <http://dx.doi.org/10.1002/pmic.200600575>.
16. Wang Y, Cao YY, Jia XM, Cao YB, Gao PH, Fu XP, Ying K, Chen WS, Jiang YY. 2006. Cap1p is involved in multiple pathways of oxidative stress response in *Candida albicans*. Free Radic Biol Med 40:1201–1209. <http://dx.doi.org/10.1016/j.freeradbiomed.2005.11.019>.
17. Moye-Rowley WS. 2003. Regulation of the transcriptional response to oxidative stress in fungi: similarities and differences. Eukaryot Cell 2:381–389. <http://dx.doi.org/10.1128/EC.2.3.381-389.2003>.
18. Toone WM, Morgan BA, Jones N. 2001. Redox control of AP-1-like factors in yeast and beyond. Oncogene 20:2336–2346. <http://dx.doi.org/10.1038/sj.onc.1204384>.
19. Kuge S, Arita M, Murayama A, Maeta K, Izawa S, Inoue Y, Nomoto A. 2001. Regulation of the yeast Yap1p nuclear export signal is mediated by redox signal-induced reversible disulfide bond formation. Mol Cell Biol 21:6139–6150. <http://dx.doi.org/10.1128/MCB.21.18.6139-6150.2001>.
20. Wood MJ, Storz G, Tjandra N. 2004. Structural basis for redox regulation of Yap1 transcription factor localization. Nature 430:917–921. <http://dx.doi.org/10.1038/nature02790>.
21. Delaunay A, Pflieger D, Barrault MB, Vinh J, Toledano MB. 2002. A thiol peroxidase is an H₂O₂ receptor and redox-transducer in gene activation. Cell 111:471–481. [http://dx.doi.org/10.1016/S0092-8674\(02\)01048-6](http://dx.doi.org/10.1016/S0092-8674(02)01048-6).
22. Znaidi S, Barker KS, Weber S, Alarco AM, Liu TT, Boucher G, Rogers PD, Raymond M. 2009. Identification of the *Candida albicans* Cap1p regulon. Eukaryot Cell 8:806–820. <http://dx.doi.org/10.1128/EC.00002-09>.
23. Alarco AM, Raymond M. 1999. The bZip transcription factor Cap1p is involved in multidrug resistance and oxidative stress response in *Candida albicans*. J Bacteriol 181:700–708.
24. Zhang X, De Michelis M, Coleman ST, Sanglard D, Moye-Rowley WS. 2000. Analysis of the oxidative stress regulation of the *Candida albicans* transcription factor, Cap1p. Mol Microbiol 36:618–629. <http://dx.doi.org/10.1046/j.1365-2958.2000.01877.x>.
25. Jain C, Pastor K, Gonzalez AY, Lorenz MC, Rao RP. 2013. The role of *Candida albicans* AP-1 protein against host derived ROS in vivo models of infection. Virulence 4:67–76. <http://dx.doi.org/10.4161/viru.22700>.
26. Patterson MJ, McKenzie CG, Smith DA, da Silva Dantas A, Sherston S, Veal EA, Morgan BA, MacCallum DM, Erwig LP, Quinn J. 2013. Ybp1 and Gpx3 signaling in *Candida albicans* govern hydrogen peroxide-induced oxidation of the Cap1 transcription factor and macrophage escape. Antioxid Redox Signal 19:2244–2260. <http://dx.doi.org/10.1089/ars.2013.5199>.
27. Kaloriti D, Tillmann A, Cook E, Jacobsen M, You T, Lenardon M, Ames L, Barahona M, Chandrasekaran K, Coghill G, Goodman D, Gow NA, Grebogi C, Ho HL, Ingram P, McDonagh A, de Moura AP, Pang W, Puttnam M, Radmaneshfar E, Romano MC, Silk D, Stark J, Stumpf M, Thiel M, Thorne T, Usher J, Yin Z, Haynes K, Brown AJ. 2012. Combinatorial stresses kill pathogenic Candida species. Med Mycol 50:699–709. <http://dx.doi.org/10.3109/13693786.2012.672770>.
28. Kaloriti D, Jacobsen M, Yin Z, Patterson M, Tillmann A, Smith DA, Cook E, You T, Grimm MJ, Bohovych I, Grebogi C, Segal BH, Gow NA, Haynes K, Quinn J, Brown AJ. 2014. Mechanisms underlying the exqui-
- site sensitivity of *Candida albicans* to combinatorial cationic and oxidative stress that enhances the potent fungicidal activity of phagocytes. mBio 5:e01334-14. <http://dx.doi.org/10.1128/mBio.01334-14>.
29. Okazaki S, Tachibana T, Naganuma A, Mano N, Kuge S. 2007. Multi-step disulfide bond formation in Yap1 is required for sensing and transduction of H₂O₂ stress signal. Mol Cell 27:675–688. <http://dx.doi.org/10.1016/j.molcel.2007.06.035>.
30. Delaunay A, Isnard AD, Toledano MB. 2000. H₂O₂ sensing through oxidation of the Yap1 transcription factor. EMBO J 19:5157–5166. <http://dx.doi.org/10.1093/emboj/19.19.5157>.
31. da Silva Dantas A, Patterson MJ, Smith DA, MacCallum DM, Erwig LP, Morgan BA, Quinn J. 2010. Thioredoxin regulates multiple hydrogen peroxide-induced signaling pathways in *Candida albicans*. Mol Cell Biol 30:4550–4563. <http://dx.doi.org/10.1128/MCB.00313-10>.
32. Urban C, Xiong X, Sohn K, Schröppel K, Brunner H, Rupp S. 2005. The moonlighting protein Tsalp is implicated in oxidative stress response and in cell wall biogenesis in *Candida albicans*. Mol Microbiol 57:1318–1341. <http://dx.doi.org/10.1111/j.1365-2958.2005.04771.x>.
33. Kuge S, Toda T, Iizuka N, Nomoto A. 1998. Crm1 (Xpo1) dependent nuclear export of the budding yeast transcription factor yAP-1 is sensitive to oxidative stress. Genes Cells 3:521–532. <http://dx.doi.org/10.1046/j.1365-2443.1998.00209.x>.
34. Phillips AJ, Sudbery I, Ramsdale M. 2003. Apoptosis induced by environmental stresses and amphotericin B in *Candida albicans*. Proc Natl Acad Sci U S A 100:14327–14332. <http://dx.doi.org/10.1073/pnas.2332326100>.
35. Wood MJ, Andrade EC, Storz G. 2003. The redox domain of the Yap1p transcription factor contains two disulfide bonds. Biochemistry 42:11982–11991. <http://dx.doi.org/10.1021/bi035003d>.
36. Gulshan K, Rovinsky SA, Coleman ST, Moye-Rowley WS. 2005. Oxidant-specific folding of Yap1p regulates both transcriptional activation and nuclear localization. J Biol Chem 280:40524–40533. <http://dx.doi.org/10.1074/jbc.M504716200>.
37. Shenton D, Smirnova JB, Selley JN, Carroll K, Hubbard SJ, Pavitt GD, Ashe MP, Grant CM. 2006. Global translational responses to oxidative stress impact upon multiple levels of protein synthesis. J Biol Chem 281:29011–29021. <http://dx.doi.org/10.1074/jbc.M601545200>.
38. Heidemann M, Hintermair C, Voß K, Eick D. 2013. Dynamic phosphorylation patterns of RNA polymerase II CTD during transcription. Biochim Biophys Acta 1829:55–62. <http://dx.doi.org/10.1016/j.bbagr.2012.08.013>.
39. Alonso-Monge R, Navarro-García F, Molero G, Diez-Orejas R, Gustin M, Pla J, Sánchez M, Nombela C. 1999. Role of the mitogen-activated protein kinase Hog1p in morphogenesis and virulence of *Candida albicans*. J Bacteriol 181:3058–3068.
40. Ferrigno P, Posas F, Koepf D, Saito H, Silver PA. 1998. Regulated nucleo/cytoplasmic exchange of HOG1 MAPK requires the importin beta homologs NMD5 and XPO1. EMBO J 17:5606–5614. <http://dx.doi.org/10.1093/emboj/17.19.5606>.
41. Homann OR, Dea J, Noble SM, Johnson AD. 2009. A phenotypic profile of the *Candida albicans* regulatory network. PLoS Genet 5:e1000783. <http://dx.doi.org/10.1371/journal.pgen.1000783>.
42. Ruiz A, Arino J. 2007. Function and regulation of the *Saccharomyces cerevisiae* ENA sodium ATPase system. Eukaryot Cell 6:2175–2183. <http://dx.doi.org/10.1128/EC.00337-07>.
43. Miramón P, Kasper L, Hube B. 2013. Thriving within the host: *Candida* spp. interactions with phagocytic cells. Med Microbiol Immunol 202:183–195. <http://dx.doi.org/10.1007/s00430-013-0288-z>.
44. Sherman F. 1991. Getting started with yeast. Methods Enzymol 194:3–21. [http://dx.doi.org/10.1016/S0076-6879\(02\)50954-X](http://dx.doi.org/10.1016/S0076-6879(02)50954-X).
45. Noble SM, Johnson AD. 2005. Strains and strategies for large-scale gene deletion studies of the diploid human fungal pathogen *Candida albicans*. Eukaryot Cell 4:298–309. <http://dx.doi.org/10.1128/EC.4.2.298-309.2005>.
46. Barelle CJ, Manson CL, MacCallum DM, Odds FC, Gow NA, Brown AJ. 2004. GFP as a quantitative reporter of gene regulation in *Candida albicans*. Yeast 21:333–340. <http://dx.doi.org/10.1002/yea.1099>.
47. Smith DA, Nicholls S, Morgan BA, Brown AJ, Quinn J. 2004. A conserved stress-activated protein kinase regulates a core stress response in the human pathogen *Candida albicans*. Mol Biol Cell 15:4179–4190. <http://dx.doi.org/10.1091/mbc.E04-03-0181>.
48. Liu TT, Znaidi S, Barker KS, Xu L, Homayouni R, Saidane S, Morschhäuser J, Nantel A, Raymond M, Rogers PD. 2007. Genome-

wide expression and location analyses of the *Candida albicans* Tac1p regulon. *Eukaryot Cell* 6:2122–2138. <http://dx.doi.org/10.1128/EC.00327-07>.

49. Znaidi S, Weber S, Al-Abdin OZ, Bomme P, Saidane S, Drouin S, Lemieux S, De Deken X, Robert F, Raymond M. 2008. Genomewide location analysis of *Candida albicans* Upc2p, a regulator of sterol metabolism and azole drug resistance. *Eukaryot Cell* 7:836–847. <http://dx.doi.org/10.1128/EC.00070-08>.

50. Cabral V, Znaidi S, Walker LA, Martin-Yken H, Dague E, Legrand M, Lee K, Chauvel M, Firon A, Rossignol T, Richard ML, Munro CA, Bachellier-Bassi S, d'Enfert C. 2014. Targeted changes of the cell wall proteome influence *Candida albicans* ability to form single- and multi-strain biofilms. *PLOS Pathog* 10:e1004542. <http://dx.doi.org/10.1371/journal.ppat.1004542>.

51. Livak KJ, Schmittgen TD. 2001. Analysis of relative gene expression data using real-time quantitative PCR and the $2^{-\Delta\Delta CT}$ method. *Methods* 25: 402–408. <http://dx.doi.org/10.1006/meth.2001.1262>.